How the protein antibiotic pyocin S5 kills *Pseudomonas aeruginosa*

By Hannah Michaela Behrens

St. Edmund Hall

A thesis presented for the degree of Doctor of Philosophy at the University of Oxford

Michelmas Term 2019

Supervised by Professor Colin Kleanthous

Declaration

I confirm that the work presented in this thesis, submitted for the degree of Doctor of Philosophy, is my own original work. Work that is not my own is referenced. This thesis has not been previously submitted at this or any other university.

Hannah Behrens

August 2019

Word count including tables, figure legends, appendices and references: 40781

Acknowledgements

I am very thankful for the many people who supported me in this work through their friendship, advice and through collaboration on experiments. I would like to thank the Wellcome Trust for funding this work and all people involved in the Infection, Immunology and Translational Medicine PhD programme, especially Keith Gull, Chris Tang and Dawn Gibbons, for putting in their time and effort.

I would like to thank Colin Kleanthous for the opportunity to do a DPhil in his research group, for his supervision and support. I would like to thank Nick Housden for his ideas, advice, discussions, friendship and sharing his expertise. Many thanks to Ed Lowe who built the backbone of the PyoS5 crystal structure and introduced me to and assisted me with crystallography and SAXS throughout my work. I thank Renata Kaminska for cloning pHB08 and purifying TonB1 and PyoS5ColIa, Mariam Dianat for being an excellent student even though her work did not make it into this thesis, Moritz Weber for purifying several proteins and performing some of the TonB1-related experiments under my supervision, and David Staunton for performing DSC, MS, and SEC-MALs on my samples, and for support with other biophysical methods. Thanks you Connor for answering my bioinformatics questions. Thanks to Joseph Gault from Carol Robinson's group for performing native MS and to Catriona Thompson and Daniel Walker for sharing their PyoS5 knowledge with me. Thanks to Mislin Gaëtan and Isabelle Schalk for providing pyochelin

I am thankful for past and present members of the Kleanthous group, Patrick, Ruth, Nick, Sandip, Renata, Joanna, Jonathan, Soumik, Nathalie, Iva, Gideon, Melissa, Cara, Paul,

Patrice, Connor, Katarina, for help on scientific and social matters, for all the check-reading and for being wonderful colleagues and friends.

I am deeply thankful for the people at Jacobs University, both peers and professors, especially Caroline Hoppe and Prof. Springer, without whom I would not have started this research project.

Outside of work I want to thank a number of friends, especially Ana Ivan, Tim Crothers, Susanna Streubel, Chris Wymant and Laia Alferez, and many others at OUVC who have been a like family to me, Insa Dreyer, Cherrelle Dacon, Richard Morter, Layal Liverpool, Marianne Clements and Lucy Garner. Finally, I would like to thank my parents, Michaela and Joachim Behrens, and my brothers Tim and Michel, for their love, help and support, and Kai Heitmann for encouraging me to go on adventures and supporting me throughout.

Abstract

Antimicrobial resistance is a deadly threat that is on the rise globally. Failure of small molecule antibiotic drug discovery programs and an increasing understanding of the dangers of antibiotic-induced dysbiosis of the microbiome have led to interest in bacteriocins as narrow-spectrum antibiotics. Pyocin S5 (PyoS5), a protein antibiotic against *Pseudomonas aeruginosa*, is the most potent colicin-like bacteriocin known but its structure and molecular mechanism remain poorly understood. This thesis presents the crystal structure of PyoS5, an elongated molecule with three structured domains and an unresolved N-terminal region, which enabled the functional, biochemical and biophysical characterization of this molecule. With its central domain, PyoS5 binds to common polysaccharide antigen (CPA), a lipopolysaccharide (LPS) antigen which acts as a receptor and accumulates the antibiotic on the cell surface. This is followed by binding to the outer membrane protein FptA, a TonB-dependent transporter (TBDT), by the N-terminal domain. A chimeric protein of *Escherichia coli* TonB and *P. aeruginosa* TonB1 allowed us to reconstruct the PyoS5 import process in *E. coli*, an approach that revealed that FptA acts as the translocator and that TonB1 energizes the import process by directly interacting with the N-terminal region of PyoS5. This import process and the structure of PyoS5 show strong similarity with those of PyoS2, which suggests that they are common to several pyocins targeting different TBDTs and delivering different cytotoxic domains into *P. aeruginosa*.

Table of Contents

List of Tables

List of Figures

List of Abbreviations

AF488	Alexa Fluor 488
CCCP	Carbonyl cyanide m-chlorophenyl hydrazone
CD	Circular dichroism
CLB	Colicin-like bacteriocins
CPA	Common polysaccharide antigen
ddH_2O	Double distilled water
DSC	Differential scanning calorimetry
DTT	Dithiothreitol
EDTA	Ethylenediaminetetraacetic acid
ESI	Electrospray ionization
GRAS	Generally recognized as safe
h	hours
ITC	Isothermal titration calorimetry
kDa	Kilo Dalton
kHBD	Kinked helical bundle domain
LIS	lithium diiodosalicylic acid
LPS	Lipopolysaccharide
min	Minutes
MS	Mass spectrometry
MMBL	Monocot mannose-binding lectin
NEB	New England Biolabs
OMP	Outer membrane protein

OSA	O-specific antigen
PCR	Polymerase chain reaction
PMF	Proton motive force
RMSD	Root mean square displacement
SDS	Sodium dodecyl sulphate
SDS-PAGE	Sodium dodecyl sulphate polyacrylamide gel electrophoresis
SEC-MALS	Size exclusion chromatography multiple angle light scattering
SPR	Surface plasmon resonance
TBDT	TonB-dependent transporter
TBE	Tris/Borate/EDTA
TEV	Tobacco etch virus-protease
TLS	Translation-liberation-screw
T_m	Melting temperature
v/v	Volume by volume
w/v	Weight by volume
β-OG	n-octyl-β-d-glucoside

1. General introduction

1.1 The pathogen *Pseudomonas aeruginosa*

P. aeruginosa was recently named one of the three bacteria we most urgently need new antibiotics against by the World Health Organization (WHO, 2017). Due to its double membrane that is devoid of general diffusion porins (Chevalier et al., 2017), *P. aeruginosa* is naturally resistant to many antibiotics and disinfectants, including all first- and second-generation cephalosporins, all macrolides and most penicillins (Koh and Peacock, 2012).

This natural resistance gives *P. aeruginosa* a selective advantage in hospital settings, where it can cause bacteraemia, ventilator-associated pneumonia, catheter-associated urinary tract infections, skin and soft-tissue infections (Koh & Peacock, 2012), and is the most common cause of burn wound infections (Church et al., 2006). In 2013, 51000 hospital-associated infections were caused by *P. aeruginosa* in the US of which 13% were multidrug resistant (CDC, 2013).

In the community, the largest group of people affected by *P. aeruginosa* are those with cystic fibrosis, a genetic condition that leads to mucus not being cleared from the lungs (Koh & Peacock, 2012). As a result, airways are prone to colonization with *P. aeruginosa* as the most common cause, resulting episodes of lung infection (Cystic Fibrosis Trust, 2013). In fact, all CF patients, around 100,000 people world-wide, will suffer from *P. aeruginosa* lung infections during their lifetime of which 80% will be chronically infected (Doring et al., 2011; Folkesson et al., 2012).

In addition to its intrinsic resistance towards many antibiotics, *P. aeruginosa* has also acquired resistances such that 25% of *P. aeruginosa* isolates in the USA (2011 to 2014) and 19% in Europe (2015) were resistant to carbapenem, an antibiotic of last resort (WHO, 2017). The incidence of pan-drug resistant isolates of *P. aeruginosa*, that are resistance to all antibiotics, is rising (Farrell et al., 2013; Hsueh et al., 2005; Souli et al., 2008; Wang et al., 2012). We therefore need to develop new antibiotics against *P. aeruginosa*.

1.2 The Gram-negative cell envelope

The major barrier that antibiotics need to overcome to reach their cellular targets is the bacterium's outer membrane, which is part of the cell envelope. The Gram-negative cell envelope, best studied in *Escherichia coli*, consists of the inner and outer membranes, which enclose the periplasmic space. The cell wall, made of peptidoglycan, is located in the periplasm (Fig. 1-1). A high concentration of proteins within this compartment makes it more viscous than the cytoplasm (Silhavy et al., 2010).

From cryo-transmission electron microscopy it is known that the *Escherichia coli* K-12 outer membrane is 7 nm thick, the inner membrane 6 nm thick, the periplasm 21±3 nm wide, the peptidoglycan 2 nm thick, and the distance between the outer membrane and the peptidoglycan 6 nm (Al-amoudi et al., 2003). Similarly, in *Pseudomonas aeruginosa* PAO1 the outer membrane is 7 nm wide from which up to 40 nm long lipopolysaccharide (LPS) antigens protrude into the extracellular space, the inner membrane is 6 nm thick, the periplasm 24±3 nm wide, and the distance between the outer membrane and the peptidoglycan 5 nm (Al-amoudi et al., 2003).

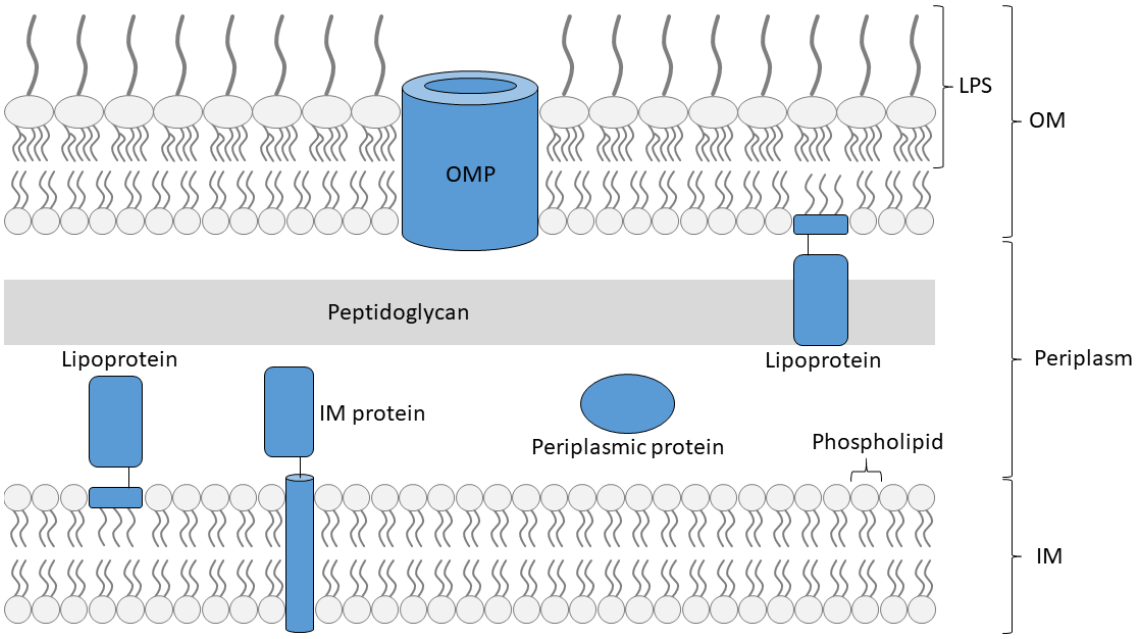

Figure 1-1: The Gram-negative cell envelope.
The different types of proteins found in the cell envelope are shown in blue. IM, inner membrane; OM, outer membrane; LPS, lipopolysaccharide; OMP outer membrane protein. Not drawn to scale.

1.2.1 The outer membrane

The outer membrane, which is specific to Gram-negative bacteria, is asymmetric in its lipid content. It contains glycolipids, mainly LPS, in the outer leaflet of the membrane, which prevent the passage of hydrophobic molecules through the outer membrane. The inner leaflet of the outer membrane is identical to the inner membrane in lipid composition, which is made of phospholipids, primarily phosphatidyl ethanolamine and phosphatidyl glycerol (Silhavy et al., 2010).

LPS consists of lipid A, which is in the outer leaflet of the outer membrane, and core sugars which are linked to lipid A. The core sugars themselves can be linked to O-antigens. *P. aeruginosa* harbours two different types of O-antigen on LPS, common polysaccharide antigen (CPA) and O-specific antigen (OSA). CPA is a homopolymer of D-rhamnose α1 → 3, α1 → 2, α1 → 3 trisaccharide repeats while OSA is a heteropolymer with a repeat unit of three to five sugars. It is the makeup of the OSA repeat unit that

determines *P. aeruginosa* serotypes while the structure of CPA is common to all *P. aeruginosa* strains. In a given *P. aeruginosa* PAO1 cell, a variety of different LPS molecules can be found (Fig. 1-2), including uncapped LPS that has no O-antigen, CPA-capped LPS and OSA-capped LPS with OSA antigens with different numbers of repeat units (Lam et al., 2011). How CPA is linked to the core sugars remains to be determined (Lam et al., 2011). K-12 derived *E. coli* strains, such as the ones used in this study, do not possess O-antigens (Stevenson et al., 1994).

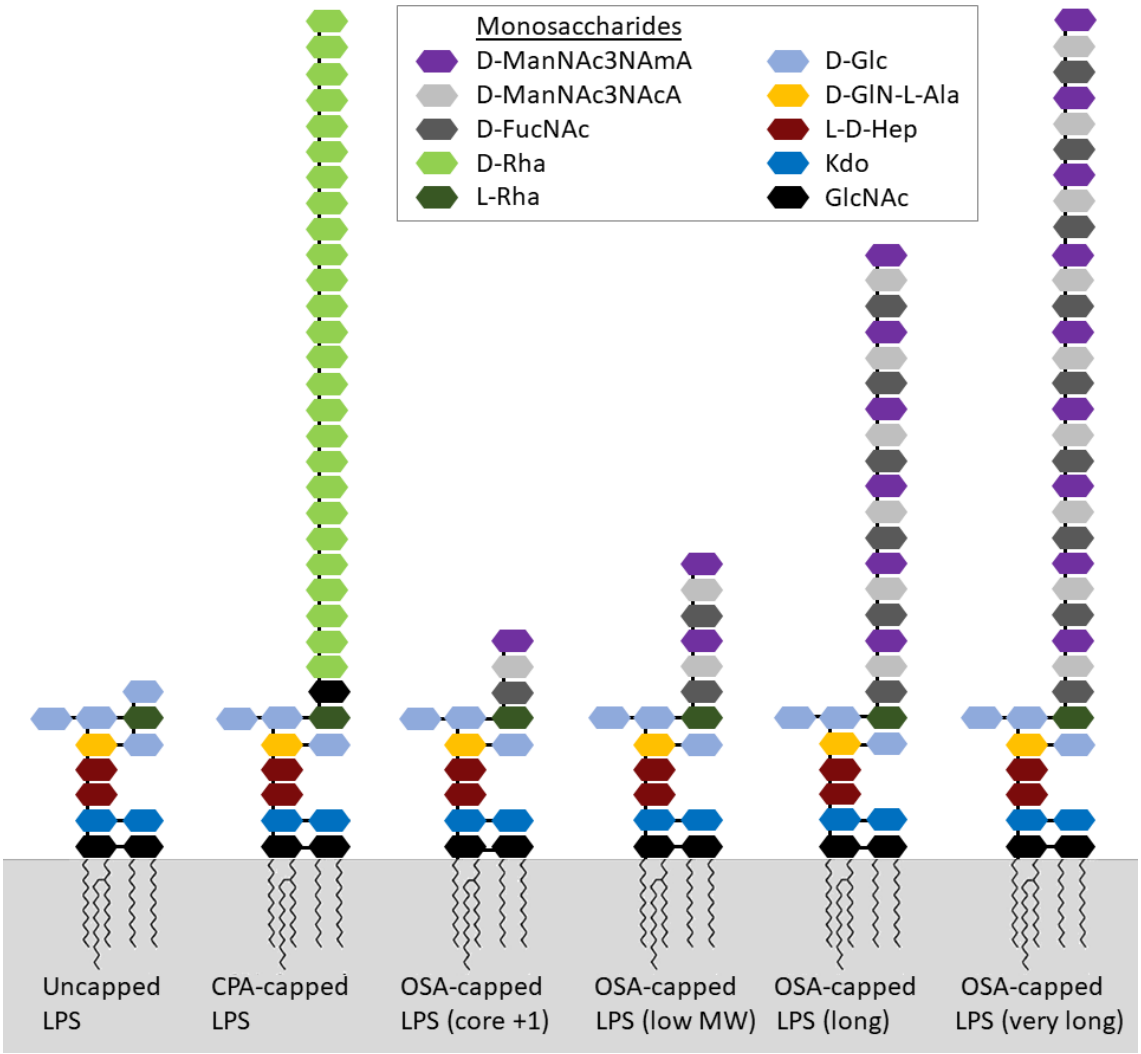

Figure 1-2: Examples of LPS glycoforms present on the surface of a single *P. aeruginosa* cell. The OSA polymer from serotype O5 (e.g. PAO1) is displayed as a representative. CPA polymers are on average 70 D-rhamnose monomers long, OSA are either 12 to 16, 22 to 30, or 40 to 50 repeat units long, depending on the enzyme producing the polymer. Not drawn to scale. Figure adapted from Lam et al. (Lam et al., 2011).

Of the two *P. aeruginosa* O-antigens OSA is more immunogenic, resulting in CPA becoming the dominant antigen in chronic lung infections in cystic fibrosis patients over time (Hancock et al., 1983; Lam et al., 1989). CPA is also required for the formation of robust biofilms (Murphy et al., 2014).

1.2.2 Outer membrane proteins

Proteins in the outer membrane can, with few exceptions, be divided into two classes: β-barrels, which span both leaflets, and lipoproteins which are typically anchored in the inner leaflet of the outer membrane (Silhavy et al., 2010). In *E. coli*, the β-barrels include general diffusion porins and specific nutrient- and siderophore receptors. General diffusion porins, like OmpF and OmpC, allow the passive diffusion of small molecules across the outer membrane (Silhavy et al., 2010), while specific nutrient transporters like Cir and FepA require energy to translocate nutrients across the outer membrane (Noinaj et al., 2010; Skare et al., 1993). These energy dependent transporters are collectively termed TonB-dependent transporters (TBDTs) as their energy is provided by the TonB system (see below). There are nine TBDTs in *E. coli* K12 and up to 18 in other *E. coli* strains (Schauer et al., 2008).

In contrast, *P. aeruginosa* has no general diffusion porins and instead has 26 substrate-specific porins (Chevalier et al., 2017). OprF is the most abundant of these porins and a homolog of *E. coli* OmpA. It can be in an open or closed conformation, and has been shown to enter the open conformation only very briefly, such that just 5% of all OprF molecules are in the open conformation at any time (Hancock, 1998; Nestorovich et al., 2006). It is thought that the lack of general diffusion porins, combined with the low

percentage of open OprF pores, is the reason for the low permeability of the *P. aeruginosa* outer membrane, which is only 8% that of *E. coli* (Hancock, 1998).

In addition to the 26 substrate-specific porins *P. aeruginosa* also has TBDTs. Genes for 26 of them are present in all investigated strains, including *fiuA*, *pirA*, *femA*, *foxA*, *pfeA*, *hasR*, *fecA*, *phuR* and *fptA*, all of which are involved in iron uptake from various sources, and a total of 44 TBDTs in the pan-genome. Each investigated strain has between 30 and 37 TBDTs (Cornelis and Bodilis, 2009). None of the porins or TBDTs is part of the core genome, which is expressed in all growth conditions, however TonB1, the transenvelope energy transduction system for TonB-dependent transporters is, discussed below. (Poulsen et al., 2018).

1.2.3 Energy transduction systems in *E. coli* and *P. aeruginosa*

The outer membrane itself has no access to energy, as no ATP is found in the periplasm. Instead, energised processes at the outer membrane rely on energy transduction systems that transfer energy from the proton motive force (PMF) at the inner membrane to the outer membrane. In *E. coli* these are the Tol-Pal and the Ton system. The Tol-Pal system is important for inner membrane integrity (Lloubès et al., 2001), cell division (Gerding et al., 2007) and has been suggested to be involved in lipid homeostasis (Shrivastava et al., 2017). The Ton system is required for nutrient uptake (Noinaj et al., 2010). Both the Tol-Pal and the Ton systems can be hijacked by phages and toxins like colicin-like bacterions (CLBs) to cross the outer membrane (Cascales et al., 2007).

In *E. coli,* the Ton system consists of three proteins TonB, ExbB and ExbD, encoded by *tonB, exbB, exbD*, respectively (Celia et al., 2016; Postle, 1990). All three proteins are located in the inner membrane (Fig. 1-3).

TonB has an N-terminal domain containing a signal sequence for Sec-dependent export across the inner membrane, which is not cleaved, and thus anchors TonB into the inner membrane (amino acid residues 12 to 32), a proline rich region (residues 66 to 102) and a C-terminal periplasmic domain (residues 103 to 239) (Cascales et al., 2007) as shown in Figure 1-3. The first 140 residues by themselves can undergo a PMF-dependent conformational change (Larsen et al., 1999), while the periplasmic domain by itself can interact with TBDTs, although without transducing energy to them (Howard et al., 2001). Residues 158 to 164 bind to a conserved region of the TBDT called the TonB-box, as observed in crystal structures of the complexes between BtuB and the C-terminal domain of TonB, and FhuA and the C-terminal domain of TonB (Pawlek et al., 2006; Shultis et al., 2006). TonB-boxes consist of 5 to 7 residues which form a β-strand and are located at the N-terminus of TBDTs and CLBs, which are discussed below.

ExbB is made up of seven α-helices, spanning the inner membrane three times (Celia et al., 2016), and forms pentamers or hexamers depending on the pH (Maki-Yonekura et al., 2018). Structures of both oligomers have been solved (Celia et al., 2016; Maki-Yonekura et al., 2018). It is thought that TonB resides outside the channel formed by ExbB and interacts with ExbB through its transmembrane domain (Cobessi et al., 2005; Larsen and Postle, 2001; Maki-Yonekura et al., 2018).

ExbD consists of a transmembrane domain, spanning the inner membrane, and a periplasmic domain. Low resolution density observed inside the channel formed by the ExbB pentamer as well as protein complexes investigated in native mass spectrometry (MS), directly ejected from *E. coli* native membranes, suggest an ExbD monomer inside the channel, while the ExbB hexamer could accommodate three molecules of ExbD (Celia et al., 2016; Chorev et al., 2018; Maki-Yonekura et al., 2018).

Even though the exact mechanism by which the Ton system transduces energy to TBDTs is unknown, it is generally thought that force is transmitted, possibly through a pulling or rotary movement (Hickman et al., 2017; Klebba, 2016; Krewulak and Vogel, 2011; Maki-Yonekura et al., 2018).

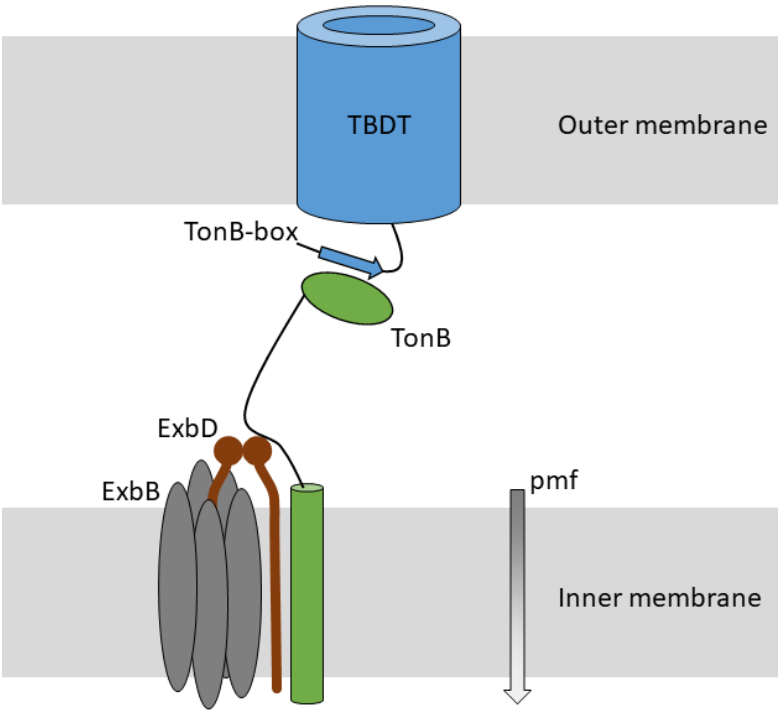

Figure 1-3: The TonB system interacting with a TBDT.
This model of the TonB system is based on studies by Celia et al. and Corev et al. (Celia et al., 2016; Chorev et al., 2018). Other models regarding the arrangement of ExbD and TonB1 in and around the ExbB oligomer exist (Maki-Yonekura et al., 2018; Oeemig et al., 2018). Not drawn to scale.

In *P. aeruginosa,* there are three genes homologous to *tonB*, called *tonB1* (PA5531), *tonB2* (PA0197) and *tonB3* (PA0406). The *exbB* and *exbD* homologs in *P. aeruginosa* are named *exbB1* (PA0198) and *exbD1* (PA0199). TonB1 is involved in iron uptake (Takase et al., 2000) and its deletion can be partially complemented by TonB2, while TonB2 deletion has no effect on iron uptake (Zhao and Poole, 2000). TonB3 is part of the Poc-complex that is required for pilus- and flagellum-mediated movement (Cowles et al., 2013; Huang et al., 2004).

Compared to *E. coli* TonB all three *P. aeruginosa* TonBs have an extended N-terminal domain (Fig. 1-4). TonB1 harbours the longest such extension with an additional 77 residues. The proline-rich region is conserved between *E. coli* TonB, *P. aeruginosa* TonB1, and TonB2, while TonB3 differs notably in this region. Overall, TonB1 is the most similar of the *P. aeruginosa* TonBs to *E. coli* TonB.

Several structures have been solved for various portions of the C-terminal domain of *E. coli* TonB (recently reviewed in Oeemig et al., 2018) as well as one for the C-terminal domain of *P. aeruginosa* TonB1 (Oeemig et al., 2018). These studies suggest similar structures and functions of the *E. coli* TonB and *P. aeruginosa* TonB1 C-terminal domains.

A

```
TonB3  ------------------------------------MRHRLFRPPSADFAPRQ-------- 17
TonB2  ----------------MATPQPV------DARTQPWRE----TPGGDLVALGR------- 27
TonB   ------------------------------------------------------------ 0
TonB1  MSPQPSRSPDRFSLAALAEDHPTAPAQGDESESLPCVNAQRGEPNLRVVDCSGARRDEEV 60


TonB3  PPRSAMNAA-VLKSPSAAAGVRPADRLGFTLFIAAILHVAFILGVGFSMPAPSQISK--- 73
TonB2  PVRQALHLVRHNPAQ---GRVLSRRETILLVLFALTLHGAVIHWLSQQ-RTPALPEVPPQ 83
TonB   -----------------MTLDLPRRFPWPT-LLSVCIHGAVVAGLLYTSVHQ-VIELPAP 41
TonB1  AVEEVLIPYAHGSDPEDVPGEPPKSRWWLSSGAAVAMHVAIIGALVWVMPTPAELNLGHG 120
                                       :  :* *.:  :          .

TonB3  ----TLEITLATFKSDKAPEKADYLAQMNQQGSGT-LEHKAAPKTTEVAP--FQDNQ--V 124
TonB2  V--PPMTIEFTAPA---PPVVE----PPPPEPLPPVVEEPPPPVVDENAVKPPPPKPVPK 134
TonB   A--QPISVTMVTPADLEPPQAV----QPPPE--PVVEPEPE----PEPIPEPPKEAPVVI 89
TonB1  ELPKTMQVNFVQLEKKAEP--------TPQP--PAAAPEPTPPKIEEPKPEPPKPKP--V 168
            : : :.       *                   .       *

TonB3  KKVAPPATPKQARSEEAPKVAVTTTRQRQQKAPS---------KTQAQKAEQVAKPAPHF 175
TonB2  PKPKPKPQPRP---KPAPKA-VEPAP--------------------PAPPQPAAPPAPPA 170
TonB   EKPKPKPKPKPKP---KPVKKV-QEQPK--RDVKPV--------------ESR----PASPF 125
TonB1  EKPKPKPKPKP---KPVENA-IPKAKPKPEPKPKPEPEPSTEASSQPSPSSAAPPPAPTV 224
        *  *   *:    : . :.                                  **

TonB3  DSTQLSAEIASLEADLAKEQQAYAKRPRIHRLSAASTMRDKGAWYKEDWRKKIERIGNLN 235
TonB2  PAAAPAPLTPPSA-----------------------------------NAGYLHNPAPE 194
TonB   ENTAPARLTSS-T------ATAATSK-------------PVT---SVASGPRALSRNQPQ 162
TonB1  GQSTPGAQTAPSG------SQGPAGL-------------PSG--SLNDSDIKPLRMDPPV 263
         :  .

TonB3  YPDEARRQKLYGSLRLLVSINRDGTIYEVQVLESSGEPILDQAAQRIVRLAAPYAPFSGD 295
TonB2  YPALAMRRGWEGTVLLRVHVLASGSPSEIQVQKSSGREALDQAAVK-------------- 240
TonB   YPARAQALRIEGQVKVKFDVTPDGRVDNVQILSAKPANMFEREVKN-------------- 208
TonB1  YPRMAQARGIEGRVKVLFTITSDGRIDDIQVLESVPSRMFDREVRQ-------------- 309
       **  *      * : : . :  .*   ::*: .:     ::: . .

TonB3  LADIDRLEIIRTWRFERGDRLSSK-------------------                  319
TonB2  --------AVKRWSFVPAKRGDKAEDGWVSVPIDFKLN------                  270
TonB   --------AMRRWRYEPGKPGSGIVVNI-----LFKINGTTEIQ                  239
TonB1  --------AMAKWRFEPRVSGGKIVARQATKMFFFKIEKRR---                  342
                :  * :      .
```

B

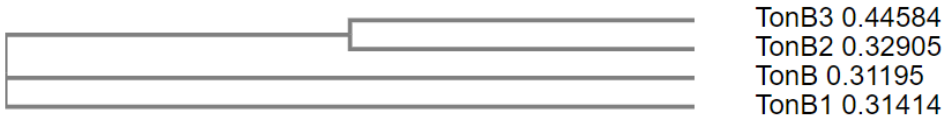

Figure 1-4: Sequence alignment of *E. coli* TonB, *P. aeruginosa* TonB1, TonB2 and TonB3.
(A) Aligned protein sequence with the *E. coli* TonB sequence coloured according to known domains and motifs. N-terminal domain (green), proline-rich region (magenta), periplasmic domain (yellow), residues binding TonB-boxes (blue). (B) Phylogenetic neighbour-joining tree without distance corrections. Branch lengths given in substitutions per site on the right. Alignment was performed in Muscle.

1.3 Protein antibiotics against *P. aeruginosa*

1.3.1 Colicin-like bacteriocins (CLBs) are promising narrow spectrum antibiotics

As a result of the decreased discovery rate of small molecule antibiotics and the increased levels of drug resistance in bacteria, the interest in narrow spectrum antibiotics has risen (Behrens et al., 2017; Brown et al., 2012; Gillor et al., 2005; Kirkup, 2006; Yang et al., 2014). A narrow spectrum of activity has the advantage of not creating selection pressure on any bacteria other than the ones targeted, thereby preventing the development and maintenance of resistances (Isaacs D, 2006). A further advantage is the prevention of dysbiosis, the disruption of the microbiome, which is a serious side effect of broad spectrum antibiotics (Francino, 2016). The first narrow spectrum antibiotic Staphefect, an endolysin against *Staphylococcus aureus*, entered the market in 2016 (Micreos, 2016).

CLBs are narrow spectrum protein antibiotics that have been suggested as therapeutics against Gram-negative bacteria, to tackle drug resistant infections while limiting the increase of antimicrobial resistance (Gillor et al., 2005; Hammami et al., 2013; Karpiński and Szkaradkiewicz, 2013; Yang et al., 2014). They occur in γ-proteobacteria, more specifically in *Enterobacteriaceae* and *Pseudomonadaceae* (Sharp et al., 2017), and are produced to kill closely related strains, while the producing strain protects itself using specific immunity proteins (Cascales et al., 2007). Therefore, CLBs exist against two of the three types of bacteria classed as highest priority for drug research by the WHO: *Enterobacteriaceae* and *P. aeruginosa*.

1.3.2 Mechanisms of CLBs

The best studied CLBs are colicins (Cascales et al., 2007), which kill *E. coli*, followed by pyocins, which kill *P. aeruginosa* (Ghequire and De Mot, 2014). Apart from colicin-like

pyocins, which include S-, M- and L-type pyocins; other phage-like pyocins that have no equivalent in *E. coli* exist and are termed R- and F-type pyocins. The receptors, translocators, transenvelope systems involved in import, and cytotoxic mechanisms are known for all colicins but two (Table 1-1). By contrast, only recently were all these factors determined for some pyocins; PyoS2, PaeM1 and PaeM2 (Latino et al., 2019; White et al., 2017) (Table 1-2).

Most colicins target bacterial cells by binding one of the OMPs, called the receptor. They subsequently bind to a second OMP, known as the translocator, which is employed by the CLB to cross the outer membrane. While the majority of CLBs use two different OMPs there are exceptions. In the case of ColB and ColD, only one OMP, FepA, is known to be involved in reception and translocation (Braun et al., 2002), and ColN utilizes LPS instead of an outer membrane protein as a receptor (Johnson et al., 2014; Sharma et al., 2009). For ColIa, one molecule of the outer membrane protein Cir acts as a receptor and a second Cir molecule acts as the translocator (Jakes and Finkelstein, 2010).

To translocate across the outer membrane, energy is required but the outer membrane neither harbours a membrane potential, nor has access to ATP. Therefore, energy is transduced via one of two transenvelope systems described above, the Ton or the Tol system (Cascales et al., 2007).

Table 1-1: Current knowledge on colicin uptake and cytotoxicity mechanisms.
Mechanisms of colicins from *E. coli* have been extensively reviewed (Cascales et al., 2007). References for more recent findings are given.

Colicin	**Receptor**	**Translocator**	**Cytotoxic activity**	**Transenvelope system employed**
ColA	BtuB	OmpF	Pore-forming	Tol
ColB	FepA		Pore-forming	Ton
ColD	FepA		tRNase	Ton
ColE1	BtuB	TolC	Pore-forming	Tol
ColE2, ColE7-9	BtuB	OmpF	DNase	Tol
ColE3, ColE4, ColE6	BtuB	OmpF	rRNase	Tol
ColE5	BtuB	OmpF	tRNase	Tol
ColIa, ColIb	Cir	Cir[1]	Pore-forming	Ton
ColK	Tsx	OmpF, OmpA	Pore-forming	Tol
ColN	LPS[2]	OmpF	Pore-forming	Tol
ColM	FhuA	TolC	lipid II-hydrolysis	Ton
ColR	OmpA[3]	?	Pore-forming [3]	Tol[3]
ColS4	OmpW[4]	OmpF[4]	Pore-forming [4]	Tol[4]
ColU	OmpA	OmpF	Pore-forming	Tol
ColY	OmpA[5]	?	?	?
Col5,Col10	Tsx	TolC	Pore-forming	Ton

? indicates unknowns. References: Colicin Biology review (Cascales et al., 2007) unless otherwise stated. [1](Jakes and Finkelstein, 2010), [2](Johnson et al., 2014; Sharma et al., 2009), [3](Rendueles et al., 2014), [4](Arnold et al., 2009), [5](Bosák et al., 2016).

Table 1-2: Current knowledge on pyocin uptake and cytotoxicity mechanisms.
Only colicin-like pyocins with demonstrated bactericidal activity are listed.

Pyocin	**Outer membrane molecules known to be involved**	**Cytotoxic activity**	**Transenvelope system employed**
PyoAP41[1]	?	DNase[1]	?
PaeM1[1]	FiuA[2]	lipid II-hydrolysis[1]	TonB1[3]
PaeM2[3]	FiuA[3]	lipid II-hydrolysis[1]	TonB1[3]
PaeM4[4]	HxuC[5]	lipid II-hydrolysis[5]	?
PyoL1[7]	CPA[6], BAM[8]	?	?
PyoL2[7]	BAM[8]	?	?
PyoL3[7]	?	?	?
PyoS1[1]	?	DNase[1]	?
PyoS2[1]	CPA,[9] FpvAI[1,10]	DNase[1]	TonB1[10]
PyoS3[1]	CPA,[9] FpvAII[1]	DNase[1]	?
PyoS4[1]	FpvAI[1]	tRNase[1]	?
PyoS5[1]	CPA,[9] FptA[1]	Pore-forming [1]	?
PyoS6[1]	?	rRNase[1]	?
PyoS8[11]	?	DNase[1]	?
PyoSD1[9]	?	tRNase[1]	?
PyoSD2[9]	CPA,[9] FpvAI[9]	tRNase[1]	?
PyoSD3[9]	CPA,[9] FpvAII[9]	tRNase[1]	?
PyoSN[12]	?	DNase[12]	?

? indicates unknowns. References: [1](Ghequire and De Mot, 2014), [2](Ghequire et al., 2017b), [3](Latino et al., 2019), [4](Paškevičius et al., 2017), [5](Ghequire and Öztürk, 2018), [6](McCaughey et al., 2014), [7](Ghequire et al., 2014), [8](Ghequire et al., 2018), [9](McCaughey et al., 2016a), [10](White et al., 2017), [11](Turano et al., 2017), [12](Sharp et al., 2017).

PyoS5, the pyocin of interest in this thesis, is a pore-forming pyocin. Crystal structures of pore-forming colicins show that out of the ten helices of a pore-forming domain helices 1 to 7 and 10, which are mostly amphiphilic, are arranged around the hydrophobic hairpin formed by helices 8 and 9 (Parker et al., 1992, 1989).

Pore-formation leads to the leakage of ions, mostly protons, from the cytoplasm and therefore depletion of the PMF, yet the mechanistic details of this process remain uncertain. The pore-forming domain first binds to the inner membrane in what is referred to as a closed state before undergoing a rearrangement that opens the pore, leading to the open state.

Two models have been suggested for the closed state, the pen knife model, in which H1+H2 fold away from the remaining helices upon binding to the surface of the inner membrane (Lakey et al., 1993), and the umbrella model, in which the hydrophobic helices H8+H9 are inserted deep into the membrane and the other helices arrange around H8+H9 on the interface between the inner membrane and the periplasm (Parker et al., 1989). A recent study has suggested that pore-forming domains bind the inner membrane in the penknife conformation followed by the insertion of H8 and H9 into the membrane, resulting in the umbrella state and that these two states are can exist in equilibrium (Prieto and Lazaridis, 2011).

There is some evidence that at least ColA, ColB, ColIa and ColN enter a molten globule state in the membrane inserted form. For colicin A and B, which are pH-sensitive, this state is provoked by the low pH of the inner membrane surface (Evans et al., 1996; van der Goot et al., 1991). Colicin I a and N are not pH-sensitive, but treatment with detergent can induce a molten globule state which accelerates insertion (Bullock and Cohen, 1986; Dover et al., 2000).

Positive voltage on the cis-side of the inner membrane leads to opening of the pore, while it closes upon negative voltage (Collarini et al., 1987; Nogueira and Varanda, 1988). In the open state ColIa helices 2 to 5 are exposed on the trans-side of the membrane (Qiu et al., 1996; Slatin et al., 2004). Colicin pores have a high selectivity of protons over other cations but low absolute selectivity (Slatin et al., 2008). In fact, it has not been possible to determine an upper size limit for the pore even though all evidence suggests that they are formed by only some helices of monomeric pore-forming domains (Bullock et al., 1983, 1992; Raymond et al., 1985). Helices 1 to 4 are not needed for the formation of pores with identical-to-native properties (Baty et al., 1990; Nardi et al., 2001). As a result, there is too much pore to be formed by the available protein, a problem that has no satisfactory solution to date.

1.3.3 The antibiotic potential of CLBs *in vivo*

CLBs are active against both planktonic bacteria and biofilms *in vitro* (Brown et al., 2015; Rendueles et al., 2014; Smith et al., 2012; Waite and Curtis, 2009), and in *in vivo* models of infection; mice, pigs and the wax moth *Galleria mellonella* larvae were used to study the potential of CLBs against *P. aeruginosa* and *E. coli* infections. These experiments show great promise for CLBs as therapeutic agents (Behrens et al., 2017). Current efforts focus on delivery to the lungs via inhalation, while delivery and activity in other organs remains to be investigated.

No adverse effects were observed in the hosts, all tested CLBs afforded protection against the respective infection, and showed low levels of immunogenicity and resistance (Table 1-3).

Table 1-3: Effectiveness of pyocins in *in vivo* challenge models.
Prophylactic treatment was given before infection; therapeutic treatment was given after infection. Adapted from Behrens et al. (Behrens et al., 2017).

Model host	Challenge organism	Challenge route	Treatment	Protein	Effective?
Wax moth *G. mellonella* larvae[1]	*P. aeruginosa*	Injection	Therapeutic injection	Pyocin S2	Yes
Mouse[2]	*P. aeruginosa*	Intra nasal	Prophylactic intra nasal	Pyocin S2	Yes
				Pyocin AP41	Yes
				Pyocin S5	Yes
				Pyocin L1	Yes
	P. aeruginosa	Intra nasal	Therapeutic intra nasal	Pyocin S2	Yes
				Pyocin AP41	Yes
				Pyocin S5	Yes
				Pyocin L1	Yes
Pig[3]	*E. coli*	Oral	Prophylactic oral	Colicin E1	Yes

[1](Rendueles et al., 2014), [2](McCaughey et al., 2016b), [3](Cutler et al., 2007).

ColE1 prevented diarrhoea and increased growth and feed efficiency when given in pig feed (Cutler et al., 2007). The tested dose was, however, not sufficient to completely eliminate the targeted pathogenic *E. coli* strain.

PyoS2 was shown to protect wax moth *G. mellonella* larvae against lethal *P. aeruginosa* infections (Walker and Smith, 2015). PyoS2, PyoS5, AP41 and L1 also afforded protection in a murine model of acute lung infection by *P. aeruginosa* when given 6 hours before or 1 hour post infection (McCaughey et al., 2016b). In the latter set, up PyoS5 was

the only treatment that reduced the colony forming units isolated from the lungs to zero in all replicates of the experiment. It was also at least two orders of magnitude more effective than tobramycin, the small molecule antibiotic that is currently used to treat lung infections.

Interestingly, treatment with any of these pyocins did not result in resistance. Solely one AP41-tolerant strain was isolated but infections with this tolerant strain could still be controlled with AP41 *in vivo*. At concentrations that do not kill all bacteria, combinations of pyocins were found to reduce the number of colony forming units further, although the observed differences were not statistically significant (McCaughey et al., 2016b).

Out of all CLBs tested as therapeutic agents against infections *in vivo*, PyoS5 was the most potent (Behrens et al., 2017; McCaughey et al., 2016b). As such, and due to the low immunogenicity and the absence of adverse effect, it is the most promising candidate of all CLBs to be developed into an antibiotic.

1.3.4 Pyocin S5

The *pyoS5* gene (locus tag: PA0985) in the *P. aeruginosa* PAO1 genome was predicted to encode a CLB based on a short sequence similar to PyoS2 and a sequence similarity to the pore-forming domains of colicin Ia and Ib (Parret and De Mot, 2000). Downstream of the PyoS5 gene, on the opposite strand, another open reading frame was identified and predicted to be the corresponding immunity gene (locus tag: PA0984), based on sequence similarity with the colicin Ia and Ib immunity proteins (Parret and De Mot, 2000). Expression of PyoS5 and immunity protein ImS5 resulted in cytotoxicity and immunity, respectively, confirming the predictions (Ling et al., 2010; Rasouliha et al., 2013). The leakage of intracellular molecules as well as electron micrographs of *P. aeruginosa*

treated with PyoS5 agreed with the predicted mechanism of cytotoxicity being through pore formation (Ling et al., 2010).

A transposon insertion screen revealed that the outer membrane protein FptA is required for PyoS5 susceptibility. $PyoS5_{150\text{-}300}$ fused to $PyoS2_{216\text{-}689}$ was cytotoxic against *P. aeruginosa*, while $PyoS5_{1\text{-}150}$ fused to $PyoS2_{216\text{-}689}$ was not (Elfarash et al., 2014). This led the authors to suggest that PyoS5 residues 150 to 300 bind to FptA.

Burkholderia cenocepacia also harbours FptA but is not susceptible to PyoS5 (Elfarash et al., 2014). Expression of a *B. cenocepacia* FptA, which is 63% identical in protein sequence to that of *P. aeruginosa*, in a *P. aeruginosa ΔfptA* mutant did not result in PyoS5 susceptibility. Expression of *P. aeruginosa* FptA in *B. cenocepacia*, however, resulted in low levels of sensitivity to PyoS5, indicating that the protein sequence of FptA is one of the determinants of the PyoS5 specificity (Elfarash et al., 2014). While these experiments show FptA is involved in PyoS5 susceptibility, there is no biochemical evidence showing a protein-protein interaction between PyoS5 and FptA and hence the role of FptA is unclear.

Full length PyoS5 has, however, been shown to bind CPA, one of the *P. aeruginosa* O-antigen,s with a K_D of 1.19±0.75 μM, as determined by isothermal titration calorimetry (ITC) (McCaughey et al., 2016a). A CPA-binding domain has been mapped in PyoS2, another pyocin that binds CPA, and PyoSD2, which has identical sequence in this domain. A region of high sequence similarity exists in PyoS5 but biochemical evidence for an interaction between these residues and CPA is lacking. Furthermore, the effect of CPA-deficiency on PyoS5-susceptibility has not been investigated.

1.3.5 FptA and its siderophore pyochelin

The outer membrane protects Gram-negative bacteria from harmful substances outside the cell, a trade-off with access to nutrients. Iron is essential for bacterial growth and often scarce, because host organisms sequester free iron using proteins like lactoferrin and transferrin. *P. aeruginosa* have several systems to capture iron and transport it across the outer membrane. These include FpvAI, FpvAII, FpvAIII, FpvB, which transport the siderophore ferric pyoverdine, and FptA, PfeA, FoxA, FiuA and HasR, which transport ferric pyochelin, ferric enterobactin, ferrioxamine B, ferrichrome and heme, respectively (de Chial et al., 2003; Dean and Poole, 1993; Ghysels et al., 2004; Heinrichs et al., 1991; Llamas et al., 2006; Ochsner et al., 2000).

FptA is a 22-stranded β-barrel with a structure typical for a TBDT (Fig. 1-5). The crystal structure of FptA bound to ferric pyochelin has shown that the strands of the barrel are connected by short loops or turns on the periplasmic side and longer loops in the extracellular space and the barrel is occluded by an N-terminal plug-domain consisting of a mixed 4-stranded β-sheet (Cobessi et al., 2005). The siderophore pyochelin binds to three residues of the plug domain and four residues of the barrel and is, among other interactions, coordinated by four hydrogen bonds. The pyochelin-binding pocket is hydrophobic, which agrees with the hydrophobic character of pyochelin, and strongly stereospecific (Hoegy et al., 2009; Youard et al., 2007). No electron density was observed for Asp38 to Glu55, which are thought to harbour the TonB-box of FptA, nor for Gln504 to Glu513, which make up loop L7 on the extracellular side (Cobessi et al., 2005).

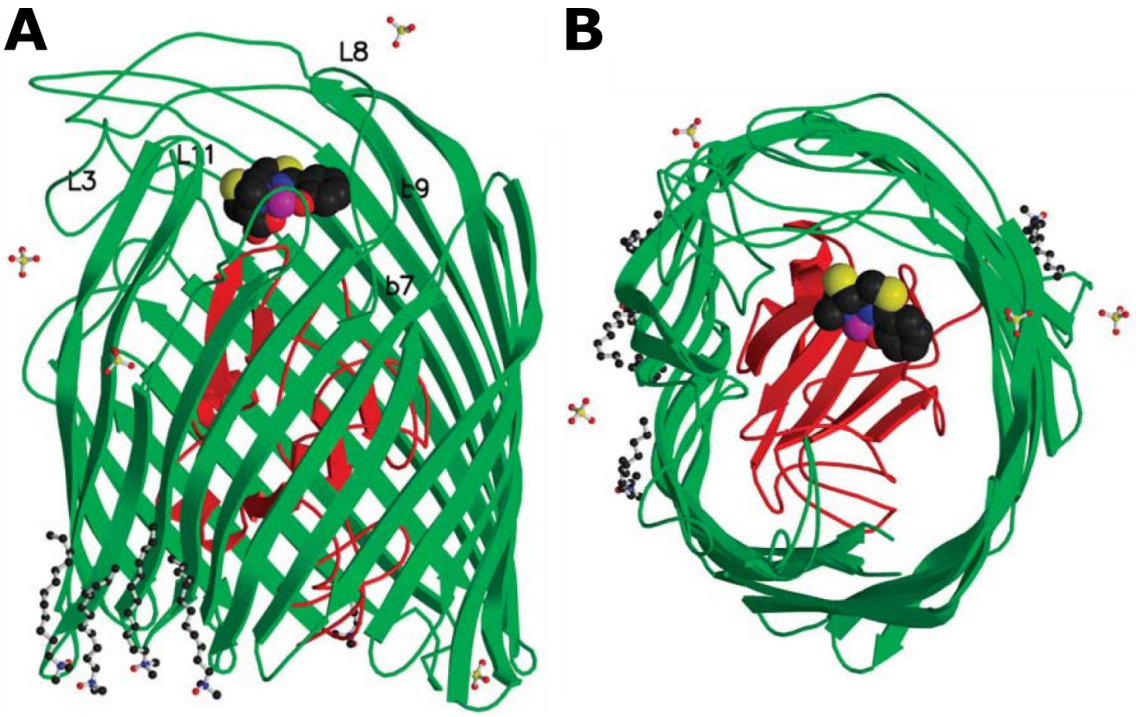

Figure 1-5: Crystal structure of FptA in complex with ferric pyochelin.
Pyochelin is shown as a space-filling representation. The FptA barrel is shown in green and the plug of FptA in red. (A) Side view of FptA with the periplasmic side of FptA oriented towards the bottom. (B) Top view onto FptA from the extracellular space. Figure adapted from Cobessi et al. (Cobessi et al., 2005).

Expression of *fptA*, similar to other genes involved in pyochelin synthesis and uptake, is transcriptionally down-regulated in the presence of iron (Ankenbauer and Quan, 1994) via the regulator PchR (Heinrichs and Poole, 1996; Michel et al., 2007, 2005; Youard et al., 2011). The regulatory impact of PchR is schematically shown in Figure 1-6.

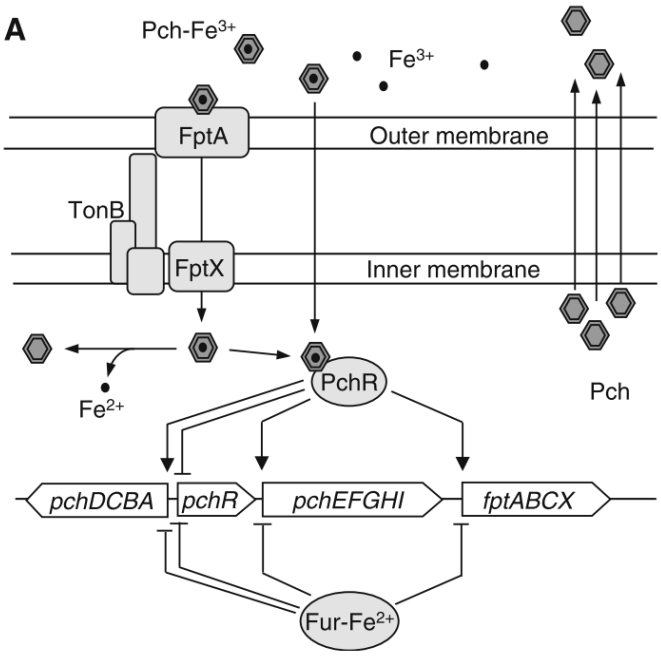

Figure 1-6: Import of pyochelin and regulation of its synthesis and import operons.
Ferric pyochelin crosses the outer membrane using FptA and the IM using FptX, a permease. In the cytoplasm, ferric pyochelin binds to the regulator PchR, which leads to the expression of the pyochelin synthesis operons *pchDCBA* and *pchEFGHI*, and the pyochelin uptake operon *fptABCX*. In iron-replete conditions, the repressor Fur turns off transcription of these three operons and of *pchR*. From Youard et al. (Youard et al., 2011).

Pyochelin, a 324 Da siderophore, is deployed by *P. aeruginosa* and *B. cenocepacia*, two species involved in lung infections in cystic fibrosis (Sokol PA., 1986), and mediates competition in low iron environments (Schiessl et al., 2017). In *P. aeruginosa*, pyochelin is one of the two major siderophores along with pyoverdine (Poole and Mckay, 2003). Pyochelin chelates Fe(III) with 2:1 stochiometry (2 pyochelins to 1 iron) (Ankenbauer et al., 1988; Brandel et al., 2012). The association constant with iron (III) is weak when measured in methanol: $5x10^5$ M^{-1}(Cox and Graham, 1979) but pyochelin-mediated iron uptake is very efficient *in vivo* (Cox, 1980). Pyochelin can bind iron before and after binding to its receptor FptA (Hoegyt et al., 2005) and naturally occurs as two interconvertible stereoisomers (Fig. 1-7) (Zamri and Abdallah, 2000), one of which was observed to be bound to FptA in the crystal structure (Cobessi et al., 2004). The uptake

of pyochelin into the cell requires TonB1 but a direct interaction between TonB1 and FptA has not been shown (Takase et al., 2000).

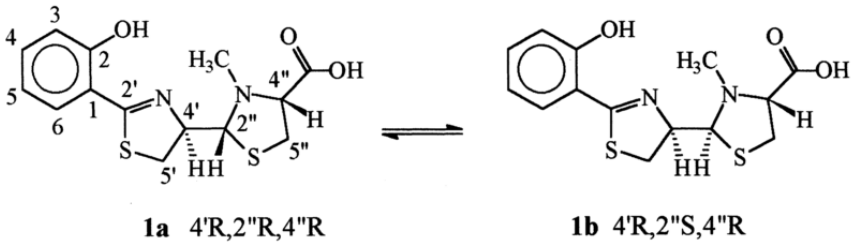

Figure 1-7: The interconvertible stereoisomers 1a and 1b of pyochelin.
Stereoisomer 1a was found bound to FptA in the crystal structure (Cobessi et al., 2005). Figure adapted from Zamri et al. (Zamri and Abdallah, 2000).

1.4 Aims of this study

As presented in this introduction the Gram-negative pathogen *P. aeruginosa* is a severe biomedical threat that we most urgently need new antibiotics against and PyoS5 is the most promising CLB known to act *in vivo* against *P. aeruginosa.* Although there is good evidence for its antibacterial activity *in vivo*, there is a limited understanding of its molecular details, specifically its structure and mechanism for translocating across the outer membrane. It is known that FptA is involved in susceptibility to PyoS5 and that PyoS5 binds to CPA, yet there is no evidence of a direct interaction between FptA and PyoS5 nor is it known whether CPA-deficiency reduces susceptibility to PyoS5. Moreover, it is not known how PyoS5 gains access to energy for translocation across the outer membrane.

This study aims to characterise the structure and the import mechanism of PyoS5 using a multi-disciplinary approach including biophysics, structural biology, microbiology, protein engineering and microscopy. The principal aims were to first characterise the molecule PyoS5 by biophysical and structure-based approaches. Secondly, to investigate

the involvement of FptA and CPA in susceptibility to PyoS5, and finally to determine how its translocation across the outer membrane is energised.

This work is the most complete account of the molecular mechanism of PyoS5, the most potent and most promising CLB antibiotic known to date. This new understanding could have a profound impact on future efforts to employ PyoS5 and PyoS5-derived therapeutics as antibiotics to treat *P. aeruginosa* infections.

2. Materials and methods

All chromatography columns were purchased from GE Healthcare. All chemicals were purchased from Sigma Aldrich or Fischer Scientific, with the exception of n-octyl-β-D-glucopyranoside (β-OG) (Enzo Life Sciences), and DNA restriction enzymes (New England Biolabs (NEB)). Pyochelin was synthesized as described previously (Yang et al., 2011) and provided by Gaëtan Mislin and Isabelle Schalk (University of Strasbourg).

2.1 Strains, media and growth conditions

Table 2-1: Bacterial strains used in this study

Name	Relevant characteristics	Source
E. coli		
NEB5α	*fhuA2 Δ(argF-lacZ)U169 phoA glnV44 Φ80 Δ(lacZ)M15 gyrA96 recA1 relA1 endA1 thi-1 hsdR17*	NEB
BL21 (DE3)	*fhuA2 [lon] ompT gal (λ DE3) [dcm] ΔhsdS λ DE3 = λ sBamHIo ΔEcoRI-B int::(lacI::PlacUV5::T7 gene1) i21 Δnin5*	NEB
TNE012	*ompA−, ompB−, tsx−*	Professor William Cramer (Taylor et al., 1998)
P. aeruginosa		
PAO1	Clinical isolate	Manoil lab Washington mutant library
YHP17	Clinical isolate	Professor Daniel Walker
PAO6609	*met-9011 amiE200 strA pvd-9*	Professor Iain Lamont (Hohnadel et al., 1986)
K1407	*PAO6609 tonB1⁻*	Professor Iain Lamont (Poole et al., 1996; Zhao and Poole, 2000)
K1408	*PAO6609 tonB2⁻*	Professor Iain Lamont (Zhao and Poole, 2000)
MS231	*PAO6609 tonB3⁻*	Professor Iain Lamont (Shirley and Lamont, 2009)
MS233	*PAO6609 tonB2⁻,tonB3⁻*	Professor Iain Lamont (Shirley and Lamont, 2009)
PW8161	*PAO1 fptA⁻*	Manoil lab Washington mutant library
PAO1 *Δrmd*	*CPA deficient*	Professor Cezar Khursigara (Rocchetta et al., 1998)

All bacteria (Table 2-1) were cultured in Miller lysogeny broth (LB) (10 g/L tryptone, 10 g/L NaCl, 5 g/L yeast extract, pH 7.2) at 37 °C at 120 rpm shaking unless otherwise stated. Stocks of bacteria were maintained in 50% LB, 50% glycerol at -80 °C. Liquid cultures were inoculated from single colonies on LB agar (1.5% weight by volume (w/v)) plates. Some experiments required bacteria grown in M9 medium (8.6 mM NaCl, 18.7 mM NH_4Cl, 42.3 mM Na_2HPO_4, 22.0 mM KH_2PO_4) which was supplemented with 0.4% (w/v) glucose, 2 mM $MgSO_4$, and 0.1 mM $CaCl_2$.

2.2 Plasmids

Table 2-2: Expression plasmids used in this study.

Plasmid name	Protein coded by plasmid	Description	Parent vector	Source
pPW18	PyoS5	Encodes PyoS5 with a C-terminal His6-tag cloned into the *Nde*I/*Xho*I sites	pET21a(+)	Daniel Walker (unpublished)
pHB21	$PyoS5_{\Delta 2\text{-}39}$	Derivative of pPW18	pET21a(+)	This study
pHB12	$PyoS5_{\Delta 2\text{-}20}$	Derivative of pPW18	pET21a(+)	This study
pMW02	$PyoS5_{\Delta 2\text{-}9}$	Derivative of pPW18	pET21a(+)	This study, Moritz Weber
pMW08	$PyoS5_{\Delta 10\text{-}13}$	Derivative of pPW18	pET21a(+)	This study, Moritz Weber
pMW10	$PyoS5_{\Delta 16\text{-}20}$	Derivative of pPW18	pET21a(+)	This study, Moritz Weber
pHB18	TR	Encodes $PyoS5_{1\text{-}315}$ with a C-terminal His6-tag cloned into the *Nde*I/*Xho*I sites	pET21a(+)	This study
pHB32	TR-Cys	Derivative of pHB18, encodes $PyoS5_{1\text{-}315}$ with a C-terminal cysteine, followed by a C-terminal His6-tag	pET21a(+)	This study
pHB40	$TR_{\Delta 2\text{-}39}$	Derivative of pHB18	pET21a(+)	This study
pHB39	$TR_{\Delta 2\text{-}20}$	Derivative of pHB18	pET21a(+)	This study
pHB42	$TR_{\Delta 2\text{-}9}$	Derivative of pHB18	pET21a(+)	This study
pHB41	$TR_{\Delta 10\text{-}13}$	Derivative of pHB18	pET21a(+)	This study
pHB43	$TR_{\Delta 16\text{-}20}$	Derivative of pHB18	pET21a(+)	This study
pHB44	$TR_{10\text{-}13A}$	Derivative of pHB18, encodes $TR_{S10A,M10A,V10A,I10A}$	pET21a(+)	This study
pHB46	$TR_{\Delta 10\text{-}13}$-Cys	Derivative of pHB32	pET21a(+)	This study
pHB19	$PyoS5_{1\text{-}196}$	Encodes $PyoS5_{1\text{-}196}$ with a C-terminal His6-tag cloned into the *Nde*I/*Xho*I sites	pET21a(+)	This study

pHB33	PyoS5$_{1-196}$ -Cys	Derivative of pHB19, encodes PyoS5$_{1-196}$ with a C-terminal cysteine followed by a C-terminal His6-tag	pET21a(+)	This study
pHB24	PyoS5$_{194-315}$	Encodes PyoS5$_{194-315}$ with a C-terminal His6-tag cloned into the *Nde*I/*Xho*I sites	pET21a(+)	This study
pHB34	PyoS5$_{194-315}$-Cys	Derivative of pHB24, encodes PyoS5$_{194-315}$ with a C-terminal cysteine followed by a C-terminal His6-tag	pET21a(+)	This study
pHB09	ColBPyoS5	Encodes ColB$_{1-340}$ translationally fused to PyoS5$_{303-498}$ with a C-terminal His6-tag cloned into the *Nde*I/*Xho*I sites	pET21a(+)	This study, Renata Kaminska,
pHB47	PyoS5ColIa	Encodes PyoS5$_{1-315}$ translationally fused to ColIa$_{485-626}$ with a C-terminal His6-tag cloned into the *Nde*I/*Xho*I sites	pET21a(+)	This study
pHB22	ImS5	Encodes ImS5 with a stop codon cloned into the *Nde*I/*Xho*I sites	pACYCDuet-1	This study
pHB04	FptA	Encodes FptA with OmpF signal sequence cloned into the *Nco*I/*Sac*I sites	pBAD/His-MycB	This study
pPW17	TonB1	Encodes TonB1$_{109-342}$ with N-terminal His6-tag followed by TEV cleavage site, cloned into the *Nco*I/*Sac*I sites	pETM11	Paul White (White et al., 2017)
pHB25	TonB-B1 hybrid	Encodes E. coli TonB$_{1-102}$ translationally fused to *P. aeruginosa* TonB1$_{201-342}$ cloned into the *Nde*I/*Xho*I sites	pACYCDuet-1	This study
pNGH131	ColIa	Encodes ColIa with a C-terminal His6-tag cloned into the *Nde*I/*Xho*I sites	pET21a	Nicholas Housden (unpublished)
pNGH243	ImS4	Encodes ImS4-His6 cloned into the *NcoI/HindIII* sites	pET24a	Nicholas Housden (unpublished)
pNGH246	PyoS4-ImS4	Encodes PyoS4-ImS4-His6 cloned into the *NdeI/XhoI* sites	pACYCDuet-1	Nicholas Housden (unpublished)
pPW02	PyoS2-ImS2	Encodes PyoS2-ImS2-His6 cloned into the *NdeI/XhoI* sites	pET21a	Paul White (White et al., 2017)

2.3 Molecular biology techniques

2.3.1 Polymerase chain reaction (PCR)

Genes were obtained from genomic DNA or synthesized (Genewiz). PCR was used to amplify DNA fragments (Table 2-3) and to introduce mutations in plasmids using plasmid mutagenesis PCR (Table 2-4). A PCR reaction mixture contained components as detailed in Table 2-5. The thermal cycler used was an Eppendorf Mastercycler nexus.

Primers (Table 2-6) were purchased from Sigma-Aldrich or Eurofins Genomics. PCR products were analysed by DNA gel electrophoresis (Section 2.3.6). Where necessary, methylated template DNA was removed by incubation with 5 µL CutSmart buffer and 2 µL DpnI restriction enzyme in a reaction volume 50 µL at 37 °C for at least 1 h.

Table 2-3: PCR thermal cycler programme for amplification PCR.

Step	**Temperature [°C]**	**Duration [min:s]**
Denaturation	98	2:00
Denaturation*	98	1:00
Annealing*	50	0:30
Elongation*	72	5:00
Elongation	72	5:00
Hold	14	∞
*Steps repeated for 20 cycles		

Table 2-4: PCR thermal cycler programme for mutagenesis PCR.

Step	**Temperature [°C]**	**Duration [min:s]**
Denaturation	98	2:00
Denaturation*	98	1:00
Annealing*	50	5:00
Elongation*	72	5:00
Elongation	72	5:00
Hold	14	∞
*Steps repeated for 20 cycles		

Table 2-5: PCR reaction.
Reagents purchased from NEB.

Component	**Final concentration**	**Volume [µL]**
5x Reaction Buffer	1x	10
dNTPs	0.2 mM	1
Forward primer	0.2 µM	0.5
Reverse primer	0.2 µM	0.5
DMSO	3% (v/v)	1.5
Template DNA	2 ng/µL	1
Phusion HF DNA Polymerase	1 unit in 50 µL	0.5
Total volume (made up with ddH_2O)		50

Table 2-6: Primers used in this study.

Number	Sequence 5′→3′	Use
HB3	GCGCCATATGAGCTTTAAATACTATTGGG	Amplify *S5I*, encoding ImS5, from the *P. aeruginosa* PAO1 genome followed by ligation into pACYCDuet-1 at the *Nde*I/*Xho*I sites to yield pHB22
HB4	CTTACTCGAGCTACGAGGCCTTTCCATAC	
HB7	GAGATATACATATGAGTGATAATGAAGGTAGTG	HB7 and HB8 to amplify the TR region of *colB*; HB9 and HB10 to amplify the pore-forming region of *pyoS5*; HB7 and HB10 to fuse the products and yield pHB09
HB8	GCGTCGTGTCGTCTCCATGGCGAGCTCATATTCCCCGACTTTG	
HB9	CAAAGTCGGGGAATATGAGCTCGCCATGGAGACGACACGACGC	
HB10	GGTGCTCGAGAATGGATATTACAAG	
HB17	GTCGCACAAGGTCCACATATGCAATACGCATACGAGG	Remove PyoS5 residues 2 to 20 from pPW18 to yield pHB12
HB18	CCTCGTATGCGTATTGCATATGTGGACCTTGGTGCGAC	
HB23	CAGAACGCAAGGCGGCCCTCGAGCAAGCGTTGCAAGATG	Introduces *XhoI* restriction site at PyoS5 residue 316 to remove PyoS5 residues 316-498 by restriction digest to yield TR
HB24	CATCTTGCAACGCTTGCTCGAGGGCCGCCTTGCGTTCTG	
HB25	CAAAAAGCGCTAAAGGAACTCGAGGACCTCTCTCAAC	Introduces *XhoI* restriction site at PyoS5 residue 197 to remove PyoS5 residues 197-498 by restriction digest to yield TR
HB26	GTTGAGAGAGGTCCTCGAGTTCCTTTAGCGCTTTTTG	
HB27	CGGCCGTTGCCGGGAATCATATGGGCGACTTAATTCAAAGAG	Insert *NdeI* site into pPW18 to remove PyoS5 residues 2-39 by digesting with NdeI to create pHB21
HB28	CTCTTTGAATTAAGTCGCCCATATGATTCCCGGCAACGGCCG	
HB29	GAGCTCAACAAGCAAAAACATATGCTAAAGGAAAAAGAGGAC	Insert *NdeI* site into pHB19 to remove PyoS5 residues 2-193 by digesting with NdeI to create pHB24
HB30	GTCCTCTTTTTCCTTTAGCATATGTTTTTGCTTGTTGAGCTC	
HB31	GATATACATATGACCCTTGATTTACCTC	HB31 and HB32 to amplify region encoding *E. coli* $TonB_{1\text{-}102}$; HB33 and HB34 to amplify region encoding $TonB1_{201\text{-}342}$ from *P. aeruginosa* PAO1; HB31 and HB34 to fuse the products and yield pHB25
HB32	GATGCTTCCGTGCTCGGCTCCGGCTTCGGTTTTGGCTTAG	
HB33	CTAAGCCAAAACCGAAGCCGGAGCCGAGCACGGAAGCATC	
HB34	CCAGACTCGAGTCAGCGGCGCTTCTC	
HB35	GACAACGAAGTACCTGGTGCCGCGGCTGCTGTCGCACAAGGTCCAGAC	Mutate residues 10 to 13 of PyoS5 and TR to alanines to yield pHB44
HB36	GTCTGGACCTTGTGCGACAGCAGCCGCGGCACCAGGTACTTCGTTGTC	
HB49	GCAAAAAGCGCTAAAGGAATGCCTCGAGCACCACCACCAC	Add cysteine to the C-terminus of NTD
HB50	GTGGTGGTGGTGCTCGAGGCATTCCTTTAGCGCTTTTTGC	
HB51	GCAGAACGCAAGGCGGCCTGCCTCGAGCACCACCACCAC	Add cysteine to the C-terminus of TR and D2
HB52	GTGGTGGTGGTGCTCGAGCAGGGCCGCCTTGCGTTCTGC	

2.3.2 Restriction enzyme digests

Restriction enzyme digests were performed at 37 °C for 3 hours. Reaction mixtures were prepared as indicated in Table 2-7. Digested DNA was separated using agarose gel electrophoresis and extracted by gel extraction using the QIAquick Gel Extraction Kit (QIAGEN).

Table 2-7: Reaction mixture for restriction enzyme digest.
Reagents were purchased from NEB.

	Preparing fragments for cloning	For analysis only
	Volume [µL]	**Volume [µL]**
10x Cutsmart reaction buffer	2.5	1
DNA	Variable (2 µg)	Variable (0.5 µg)
Enzyme	1	0.2
Total volume made up in ddH_2O	25	10

2.3.3 DNA ligation

DNA ligation reactions were set up as described in Table 2-8, and then incubated at room temperature for at least 1 h.

Table 2-8: Reaction mixture for DNA ligation.
Reagents were purchased from NEB.

	Negative control	Ligation reaction
	Volume [µL]	**Volume [µL]**
Vector	1	1
Insert	0	3
10x ligation buffer	1	1
T4 DNA ligase	1	1
Total volume made up in water	10	10

2.3.4 Preparation of chemically competent cells

Chemically competent *E. coli* NEB5α and BL21 (DE3) were purchased from NEB. These were either used directly or, for transformations that did not require high efficiency, they were propagated to make more competent cells. Competent cells were prepared as follows. Commercially available competent cells were inoculated into 10 mL LB liquid culture and grown at 37 °C overnight. 0.5 mL of this culture was inoculated into 50 mL LB culture and grown until an OD_{600} of 0.3 to 0.6. Cells were harvested by centrifuging 25 mL of the culture at 5000 xg at 4 °C for 10 min. The pellet was resuspended in 20 mL

ice cold 20 mM Tris-HCl pH 8.0, 50 mM $CaCl_2$ and then incubated on ice for 1 h. Cells were centrifuged again at 5000 xg at 4 °C for 10 min. The pellet was resuspended in 2 mL ice-cold 20 mM Tris-HCl pH 8.0, 50 mM $CaCl_2$, 20% volume by volume (v/v) glycerol. 100 µL aliquots were transferred to ice-cold tubes and frozen at -80 °C.

2.3.5 Bacterial heat shock transformation

25 µL to 100 µL competent cells were thawed on ice and mixed with 2.5 µL of DNA. They were incubated on ice for 30 minutes (min) and heat shocked at 42 °C for 30 s, followed by 5 min incubation on ice. Cells were then plated out on 1.5 % LB-agar plates containing ampicillin or where a different antibiotic was used for selection, incubated in 200 µL LB for 45 min at 37 °C and then plated out on LB-agar plates containing the selection antibiotic (Table 2-9). Plates were then incubated at 37 °C for 16 h.

Table 2-9: Antibiotics and their working concentrations used in this study.

Antibiotic	Concentration	Solvent used to make stock
Ampicillin	100 µg/mL	Water
Chloramphenicol	37 µg/mL	Ethanol
Kanamycin	50 µg/mL	Water
Tetracyclin	10 µg/mL	Ethanol
Gentamicin	50 µg/mL	Water

2.3.6 DNA gel electrophoresis

1 % (w/v) agarose gels were prepared by melting agarose in 0.5x Tris/Borate/EDTA (TBE) (44.5 mM Tris-HCl pH 8.3, 44.5 mM boric acid, 1 mM ethylenediaminetetraacetic acid (EDTA)) and mixed with 1x SybrSafe dye. 1 µL sample loading dye (30 % (w/v) glycerol, 6 mM EDTA, 0.4 % (w/v) bromophenol blue) was added to 5 µL sample and loaded onto the gel. Electrophoresis was run at 80 V constant voltage in 0.5x TBE.

2.3.7 Purification and sequencing of plasmid DNA

Plasmid DNA was isolated from NEB5α cultures grown in LB at 37 °C with appropriate antibiotic, using QIAGEN Plasmid Mini- and Plus Midi kits or Monarch Plasmid Miniprep kits and Promega PureYield Plasmid Midiprep kits. Sequencing was done by Source Bioscience or Genewiz.

2.4 Protein Expression and Purification

2.4.1 Expression and purification of bacteriocins

PyoS5 and its derivatives, as well as ColBPyoS5, PyoS5ColIa, PyoS2, PyoS4 and ColIa were expressed heterologously from *E. coli* BL21 (DE3) for 3 hours (h) at 37 °C or overnight at 20 °C while shaking at 120 rpm. For constructs containing the PyoS5 pore forming domain (amino acid residues 315-498), cells were co-transformed with pHB22 which carries the ImS5 immunity protein, for increased yield. Bacteria were harvested at 5050 xg for 15 min at 10 °C, resuspended in binding buffer (0.5 M NaCl, 20 mM Tris-HCl pH 7.5) supplemented with 1 mM PMSF and sonicated on ice at 70% maximum amplitude for 1:30 min in intervals of 3 s on, 7 off (total duration 5 min) using a Misonix S-4000 ultrasonic liquid processor fitted with a 3/8-inch stud probe. They were then centrifuged at 12500 xg for 20 min at 4 °C, filtered through a 0.45 µm syringe filter, loaded onto a 5 mL HisTrap-HP-column equilibrated in binding buffer and eluted by gradient elution using elution buffer (binding buffer + 0.75 M imidazole). The protein was then dialyzed into size exclusion buffer (150 mM NaCl, 20 mM Tris-HCl pH 7.5) using a 12-14 kilo Dalton (kDa) molecular weight cut off membrane (Spectra/Por, Spectrum), filtered through a 0.45 µm syringe filter and applied to a 26/60 Superdex 200 size exclusion chromatography column.

PyoS4 was expressed at 28 °C in the presence of an additional copy of ImS4 provided on plasmid pNGH243, and purified on an S200 16/60 size exclusion chromatography column.

2.4.2 Expression and purification of TonB1 soluble fragments

The TonB1 construct was purified as described previously (White et al., 2017). Briefly TonB1 was expressed, harvested, sonicated, centrifuged and purified by HisTrap-HP-column as described for PyoS5 above. It was then incubated in 300 mM NaCl, 50 mM Tris-HCl pH 7.0 with 0.07 mg/mL 6-His-Tobacco etch virus-protease (TEV) at RT for 4.5 h. TonB1 was then purified by affinity chromatography on a HisTrap-HP column and by size exclusion chromatography on a 26/60 Superdex 200 column equilibrated in 300 mM NaCl, 50 mM Tris-HCl pH 7.5.

2.4.3 Expression and purification of FptA

FptA was expressed heterologously from *E. coli* TNE012 at 37 °C while shaking at 120 rpm in LB, and upon reaching OD_{600} 0.6 induced with 0.15% (w/v) arabinose and supplemented with 0.15% (w/v) glucose. Bacteria were harvested as described for PyoS5 and resuspended in buffer A (10 mM Tris-HCl pH 8.0, 0.25% (w/v) lithium diiodosalicylic acid (LIS)), sonicated as described for PyoS5 and centrifuged at 4000 xg for 20 min at 4 °C. The supernatant was collected, the pellet resuspended in fresh buffer A and centrifuged again. Both supernatants were ultra-centrifuged at 200 000 xg for 45 min at 4 °C. The pellet was homogenized in buffer B (buffer A + 2% (v/v) Triton X-100) and ultra-centrifuged again. The resulting pellet was homogenized in buffer C (10 mM Tris-HCl, pH 8.0) and ultra-centrifuged again. The resulting pellet was homogenized in buffer D (buffer C + 2% (w/v) β-OG, 5 mM EDTA) and ultra-centrifuged again. FptA

was purified from the supernatant by anion exchange chromatography. A 5 mL HiTrap DEAE FF column was equilibrated in buffer E (50 mM Tris-HCl pH 7.5, 1% (w/v) β-OG, 5 mM EDTA) and gradient eluted with buffer F (buffer E + 1 M LiCl). This was followed by 16/60 Sephacryl 300 size exclusion chromatography in buffer E and anion exchange chromatography on a Mono Q 4.6/100 PE column in buffer E, with gradient elution with buffer F.

2.4.4 Sodium dodecyl sulphate polyacrylamide gel electrophoresis (SDS-PAGE)

SDS-PAGE was performed using Hoefer Mighty Small SE250 tanks. 12% bis-acrylamide gels were used for proteins larger than 20 kDa, 15% gels for proteins smaller than 20 kDa. Samples were mixed with 4x loading buffer (200 mM Tris-HCl pH 6.8, 8% w/v sodium dodecyl sulphate (SDS), 0.4% w/v bromophenol blue, 40% glycerol, 400 mM beta-mercaptoethanol) to yield 1x loading buffer. Subsequently, they were heated to 98 °C for 3 min and loaded onto the gel. Gels were run at 30 mA constant current in running buffer (25 mM Tris, 192 mM glycine, 3.5 mM SDS).

2.4.5 Protein quantification

All protein concentrations were measured using absorbance at 280 nm which was converted to concentration using the sequence based predicted molar extinction coefficient (ExPASy ProtParam, Table 2-10). The presence of scattering impurities, like protein aggregates, was checked for by measuring the absorbance at 320 nm. Both absorbances were measured using an Eppendorf Biophotometer with either 10 mm or 2 mm pathlength cuvettes.

Table 2-10: Protein molecular weight and molar extinction coefficients.

Protein	N-term Met?	Molecular weight [Da]	Molar extinction coefficient [$M^{-1}.cm^{-1}$]
PyoS5	No	57007.98	55350
$PyoS5_{\Delta 2-39}$	No	53056.68	52370
$PyoS5_{\Delta 2-20}$	Yes	55214.12	55350
$PyoS5_{\Delta 2-9}$	No	56195.19	55350
$PyoS5_{\Delta 10-13}$	No	56577.42	55350
$PyoS5_{\Delta 16-20}$	No	56495.51	55350
TR	No	37193.13	41370
TR-Cys	No	37296.26	41370
$TR_{\Delta 2-39}$	No	33241.82	38390
$TR_{\Delta 2-20}$	Yes	35399.26	41370
$TR_{\Delta 2-9}$	No	36380.33	41370
$TR_{\Delta 10-13}$	No	36762.56	41370
$TR_{\Delta 16-20}$	No	36680.65	41370
TR_{10-13A}	No	37946.88	41370
$TR_{\Delta 10-13}$-Cys	No	36865.70	41370
$PyoS5_{1-299}$	No	35351.12	41370
$PyoS5_{1-196}$	No	23729.80	32890
$PyoS5_{1-196}$-Cys	No	23832.94	32890
$PyoS5_{194-315}$	Yes	15048.1	8480
$PyoS5_{194-315}$-Cys	Yes	15151.24	8480
ColIa	No	70362.93	59360
PyoS2	No	73722.65	65780
PyoS4	No	80600.64	51800
ColBPyoS5	No	58900.54	54890
PyoS5ColIa	No	56972.98	65320
FptA	Not applicable	76068.27	150120
TonB1	Not applicable	25473	6990

2.4.6 Assessment of protein purity

The purity of isolated proteins was assessed by running 5 mg to 10 mg of each protein on an SDS-PAGE gel which was then stained with Coomassie and evaluated with the programme GeneTools from Syngene using the “lowest slope” method of creating a baseline.

2.5 Pyocin cytotoxicity assays

P. aeruginosa YHP17 cells were grown to OD_{600} 0.6 and 200 µL of the culture mixed with melted, 50 °C warm, soft LB agar (0.75% (w/v) agar) and poured over an LB agar plate. Once the plate had set, 2.5 µL of each bacteriocin concentration were spotted onto the plate. The plates were left to dry and then incubated at 37 °C overnight.

2.6 LPS-derived polysaccharide isolation

LPS-derived polysaccharides were isolated as described before (McCaughey et al., 2016a). Briefly, 1 L of cells were grown for 20 h at 37 °C, pelleted at 6000 xg for 20 min and resuspended in 10 mL 50 mM Tris-HCl pH 7.5, 2 mg/mL lyosozyme, 0.5 mg/mL DNAse I. Cells were lysed by sonication as described for PyoS5 isolation and the lysate incubated for 30 min at RT. 0.2 mM EDTA were added. The lysate was then combined with an equal volume aqueous phenol, heated for 20 min at 70 °C, with mixing. The solution was incubated on ice for 30 min, centrifuged at 7000 xg for 20 min and the aqueous upper layer extracted. 0.05 mg/mL proteinase K was added and the solution dialysed overnight against 5 L dH_2O, followed by dialysis against 5 L fresh dH_2O for 5 h. LPS was pelleted by ultracentrifugation for 1 h at 100,000 xg and the pellet resuspended in 10 mL dH_2O. The suspension was heated at 60 °C for 30 min, then 2% acetic acid was added and the mixture heated at 96 °C for 1.5 h. Lipid A was pelleted by centrifugation at 13 500 xg for 3 min and the supernatant, which contains the polysaccharide, was extracted with 10 mL chloroform. The aqueous phase was then lyophilized.

2.7 Electrospray ionization (ESI) mass spectrometry

Denaturing ESI mass spectrometry was performed on proteins diluted in formic acid by David Staunton, Biophysics Facility, Department of Biochemistry, University of Oxford to determine the masss of intact proteins.

2.8 Assays to investigate protein interactions

2.8.1 Native mass spectrometry

Native mass spectrometry was performed in 100 mM ammonium acetate buffer with exception of TonB1 which was analysed in 200 mM ammonium acetate buffer by Joseph Gault in the Department of Chemistry, University of Oxford.

2.8.2 Analytical size exclusion chromatography

Analytical size exclusion chromatography was performed on a Superdex 200 Increase 10/300 GL column in 150 mM NaCl, 20 mM Tris-HCl pH 7.5, using a 100 µL sample loop which was loaded with 150 µL samples.

2.8.3 Surface plasmon resonance (SPR)

SPR was performed on a Biacore T200 instrument. A Series S Sensor Chip CM5 (GE LifeScience) was docked and primed into HBS-OG buffer (25 mM HEPES pH 7.5, 150 mM NaCl, 1% (w/v) β-OG). This buffer was used as a running buffer for all SPR experiments. For amine-coupling, ligand proteins were desalted into immobilization buffer (25 mM potassium phosphate pH 7.5, 50 mM NaCl) and diluted 10-fold in 10 mM sodium acetate pH 5.0 (GE LifeScience). Amine-coupling was performed using the Amine Coupling kit (GE Healthcare). For thiol-coupling ligand proteins were incubated with 10 mM dithiothreitol (DTT) for 2 h, then desalted into immobilization buffer diluted 10-fold in 10 mM sodium acetate pH 5.0 (GE LifeScience) immediately before immobilization. Ligand thiol-coupling was performed using the Thiol Coupling kit (GE Healthcare). Analyte proteins were desalted into HBS-OG buffer before application. The contact time for SPR was set to 120 s, the dissociation time to 600 s and the flow rate to 30 µL/min. Lower analyte concentrations were applied first. 1:1 binding models were fit

to the equilibrium data in the Biocore software, due to lack of evidence supporting other models, with the following equation

$$R_{eq}=(CR_{max})/(K_D+C)+RI$$

Where C is the concentration, R_{max} is the analyte binding capacity of the surface and RI is the bulk refractive index contribution.

2.8.4 Isothermal titration calorimetry (ITC)

ITC was performed in a MicroCal iTC200 at 25 °C in 0.2 M sodium phosphate buffer pH 7.5. Proteins in the syringe were at 150 µM, polysaccharides in the cell at 7 mg/mL, which estimated to be 30 µM based on an estimated molecular weight of 10 kDa and the estimate that CPA constitutes 5% of the LPS polysaccharides by weight. The data were fit to a one binding site model in Microcal LLC Origin software. As the CPA concentration is estimated, the observed stoichiometry is unlikely to be correct, while ΔH, ΔS and K_D are unaffected by the analyte concentration. Errors reported in the text are standard deviations of the average of two experiments.

2.9 Biophysical Techniques

2.9.1 SAXS

PyoS5 was concentrated to 5.4 mg/mL in HBS buffer (25 mM HEPES pH 7.5, 150 mM NaCl). At the B21 Beamline at Diamond Light Source proteins were subjected to size exclusion chromatography and small-angle scattering data were collected and processed using Scatter and Atsas (Petoukhov et al., 2012; Rambo, 2019). Guinier approximation analysis and P(r) distribitions were determined using Scatter. Dummy atoms were fit using multiple parallel runs of DAMMIF (Franke and Svergun, 2009) and refined using DAMMIN (Svergun, 1999). Bead models were converted to maps using Situs (Wriggers,

2012) and structures fit into the envelopes using Chimera (Pettersen et al., 2004). Data collection and analysis was assisted by Edward Lowe (Crystallization Facility, University of Oxford).

2.9.2 Circular dichroism (CD)

Proteins were analysed at 0.1 mg/mL in 20 mM NaCl, 10 mM potassium phosphate buffer pH 7.5 using a Jasco J-815 Spectropolarimeter. Spectra were measured between 260 nm and 190 nm at a digital integration time of 1 s and a 1 nm band width. Each sample spectrum was measured in quadruplicate and averaged. Molar ellipticity was calculated by subtracting the baseline from sample spectra and dividing by the molecular weight, molar concentration and pathlength (1 mm) in mm.

Melting spectra of proteins were measured at 222 nm between 20 °C and 86 °C at 90 °C/h and 4-parameter sigmoidal melting curves were fit to the equation

$$f = y_0 + a/(1+e^{((x-x0)/b})$$

using non-linear regressions in SigmaPlot to determine the melting temperature (T_m).

2.9.3 Size exclusion chromatography multiple angle light scattering (SEC-MALS)

Proteins were separated in 50 mM Tris pH 7.5, 150 mM NaCl using a Superdex 200 10/300 GL column and detected by a Wyatt Dawn HELEOS-II 8-angle light scattering detector and a Wyatt Optilab rEX refractive index monitor linked to a Shimadzu HPLC system. SEC-MALS was performed by David Staunton, Biophysics Facility, Department of Biochemistry, University of Oxford.

2.9.4 Differential scanning calorimetry (DSC)

Proteins were analysed in 150 mM NaCl, 50 mM Tris-HCl pH 7.5 using a MicroCal VP-Capillary DSC System (Malvern). The scanning speed was 200 °C/h. DSC was performed by David Staunton, Biophysics Facility, Department of Biochemistry, University of Oxford.

2.9.5 X-ray crystallography

Pyocin S5 was concentrated to 16 mg/mL in 25 mL Tris-HCl pH 7.5, 150 mM NaCl using a VivaSpin 20 column with a 30 kDa molecular weight cut off (Sartorius). The crystallisation screens Index (Hampton Research) and PACT, JCSG+ and Morpheus (Molecular Dimensions) were used to screen for crystals. Crystals were grown in a vapour diffusion sitting drop set up in JCSG+ screen (Molecular Dimensions) condition C7 (10% (w/v) PEG 3000, 0.1 M sodium acetate, 0.1 M zinc acetate, pH 4.5) at 18 °C. Drops contained 100 nL protein and 100 nL buffer. The cryoprotectant solution was 25 % glycerol, 10% (w/v) PEG 3000, 0.1 M sodium acetate, 0.1 M zinc acetate, pH 4.5 for cooling the crystals in liquid nitrogen. Diffraction data were collected at beamline ID30A-3 at European Synchrotron Radiation Facility at a wavelength of 0.9679 Å using an EIGER detector. We collected 225 degrees of data with 0.15° oscillation. Transmission was 20% and exposure time 0.010 s.

In a first instance, the raw data were analysed in Dials, revealing a $P2_1$ space group and yielding a 98.8% complete set of indexed diffraction spots but no anomalous signal. Molecular replacement was carried out using ColIa residues 450-624 in Phaser and yielded electron density for the pore-forming domain of PyoS5. Lack of density for the

remainder of the protein indicated that the phases, obtained from ColIa, were not sufficient to build a model for the whole protein.

Improved phases were obtained from anisotropy correction of the same data set using Staraniso in AutoProc, which detected weak anomalous signal from eight metal ions. Based on the type of metal present in the crystallization condition, these were assumed to be Zn^{2+}. The partial model from molecular replacement from Dials and the anomalous data from AutoProc were combined for MR-SAD phasing using Phaser. The result was additional, visible helical density beyond the pore-forming domain.

Iterations of model building into the visible helical density in Coot and refinement against the complete Dials data set in Buster version 2.10.3, resulted in a model of PyoS5. The model building was done by Edward Lowe (Crystallization Facility, University of Oxford) until the whole backbone was built, connected and the sequence docked. Then I took over to refine the structure.

The model was optimized in Coot (Emsley and Cowtan, 2004), followed by one crystallographic refinement in Buster, followed by model optimization in Coot and one refinement in Phenix 1.12 (Adams et al., 2010). Up to then the whole model was treated as one translation-liberation-screw (TLS) group. At this point, four new TLS groups were created based on similar B-factors as determined in Phenix, comprising residues 40 to 212, 213 to 338, 339 to 395 and 395 to 505, respectively. This increased the R_{work} and R_{free} upon refinement indicating that the use of multiple TLS groups made the model worse. The refinement process was therefore continued with the whole model treated as one TLS group.

At the end of the model optimization and refinement, R_{work} was 0.212 and the R_{free} 0.272. MolProbitiy, (Chen et al., 2010), was used to validate the structure and assess its quality, resulting in a Molprobity score of 2.76. At the end of this validation process the R_{work} was 0.225 and the R_{free} 0.275. Figures of the crystal structure were created using PyMOL (Delano, 2002). Homology models were created using SwissModel (Benkert et al., 2011; Waterhouse et al., 2018).

2.10 Fluorescence microscopy

2.10.1 Fluorescent labelling of proteins

Bacteriocins were fluorescently labelled using Alexa Fluor 488 C5 maleimide (AF488) labels via an engineered C-terminal cysteine. To reduce the cysteine, the protein was mixed with DTT to yield a concentration of 10 mM DTT and incubated for 2 h at RT. To remove aggregates, it was centrifuged at 16000 xg for 1.5 min and the supernatant transferred to a new tube. The supernatant was then applied to a 5 mL HiTrap desalting column and desalted into 25 mM Tris-HCl pH 7.5, 100 mM NaCl, 1% (w/v) β-OG. The protein concentration was measured and immediately maleimide AF488 was added in 3-fold molar excess. The reaction was allowed to proceed for 1 h while mixing by rotary inversion in the dark at RT. The reaction was then quenched by adding DTT to a final concentration of 5 mM. The solution was centrifuged and desalted as before. The absorbance was measured at 280 nm and 494 nm using a V-550 UV-Visible Spectrophotometer (Jasco). Labelling efficiency was determined as described in the manufacturers protocol (Molecular Probes Inc, 2006). All fluorescently labelled proteins used for microscopy were labelled with greater than 95% efficiency.

2.10.2 Coverslip preparation

Coverslips were cleaned by water bath sonication at 50 °C for 15 min in 2% Neutracon (Decon) solution. Subsequently, the coverslips were washed in double-distilled water (ddH_2O) and air dried.

2.10.3 Fluorescent labelling of bacteria

Bacteria were grown overnight in LB medium. 1 mL of this overnight culture were pelleted and resuspended in 10 mL supplemented M9 medium and grown until an OD_{600} of 0.6. 600 µL of this culture were used per condition. All pelleting steps were performed at 7000 xg for 3 min at RT.

For treatment with carbonyl cyanide m-chlorophenyl hydrazine (CCCP), CCCP was added to a final concentration of 100 µM (10 mM stock in DMSO) to the bacteria before addition of the fluorescently labelled protein. The bacteria were incubated with CCCP while mixing by rotary inversion at RT for 5 min, while all other samples were incubated without CCCP for the same time.

Fluorescently labelled protein was added to a concentration of 1 µM to the bacteria and incubated in the dark while mixing by rotary inversion for 20 min at RT.

For trypsin treatment, trypsin was added to a final concentration of 0.1 mg/mL immediately after the incubation with the fluorophore-labelled pyocin. The bacteria were incubated with or without trypsin at 30 °C for 1 hour at 120 rpm.

Subsequently, bacteria were washed three times in supplemented M9, where each wash consisted of pelleting the bacteria, removing the supernatant, resuspending the pellet in 50 µL by pipetting up and down 10 times with a P20 pipette, transferring the 50 µL to a new tube with 450 µL supplemented M9, and vortexing. The bacteria were resuspended in a final volume of 30 µL. 3 µL were applied to an agar pad for microscopic analysis. Agar pads were prepared using Geneframes (Thermo Scientific) as follows. A 1% (w/v) supplemented M9 agar was prepared and 190 µL were pipetted into the Geneframe. Using a coverslip, the surface was flattened and excess agar removed. Once the agar solidified the cover slip was removed, the bacterial suspension added and a new coverslip attached to the adhesive side of the Geneframe.

2.10.4 Image collection

All images were collected on an Oxford Nanoimager S microscope at 100 ms exposure. For every image, 200 frames were collected and averaged. Green fluorescence was measured at 35% laser power.

2.10.5 Data analysis

In ImageJ, the 200 collected frames per image were merged using the command "Z project". Bacterial cells and background were identified in trans-illumination images using "Trainable Weka Classifier". Regions of interest were transferred to green fluorescence images and the mean fluorescence of cells, "signal", and background "noise" quantified. Each image contained a minimum of 15 bacterial cells. For each repeat a minimum of six images were collected per sample and three independent experiments were performed for each experiment. As a result, a minimum of 270 bacterial

cells were quantified for each sample. Students t-tests were performed to determine p-values.

2.11 Sequence and structure comparisons

Sequences were compared using NCBI BLASTn and BLASTp (Altschul et al., 1990), MUSCLE (Madeira et al., 2019), and jackhmmer (Potter et al., 2018). Similar structures were searched for using NCBI VAST (Madej et al., 2014) in June 2019 and PDBeFold v2.59 (Krissinel and Henrick, 2004) in August 2019.

3. Protein purification and preliminary characterization

3.1 Introduction

It is of utmost importance for biochemical studies to know that proteins of interest were expressed correctly and are pure. In this chapter, all purification protocols used in this work, both newly developed and existing ones, are assessed for their quality.

PyoS5, FptA and TonB1, the proteins central to this research, have previously been isolated and studied but existing protocols for PyoS5 and FptA purification were not fit for the purpose of this study for reasons explained below, so that new purification protocols had to be developed. Currently, the best method to purify PyoS5 for therapeutic purposes, is plant-based expression (Paškevičius et al., 2017). This method is however too slow for laboratory studies that aim to use many different constructs. Here, a new His6-tag-based purification protocol for PyoS5 was developed and validated.

FptA has previously been purified from *P. aeruginosa.* However, crystallographic studies showed that it co-purified with pyochelin, its native siderophore ligand (Cobessi et al., 2005). To purify FptA without ligands - a requirement in this study - I developed a heterogeneous expression and purification protocol for *P. aeruginosa* FptA.

While PyoS2 and the cytoplasmic domain of TonB1 have previously been purified by the same protocol that was also used here, the quality of the purified protein has not been assessed to date (White et al., 2017). Additionally, the quality of PyoS4 and ColIa, which are used as in this study was assessed.

This chapter aims to validate the protocols used in this study for purification of PyoS5 and constructs derived from it, FptA, TonB1 and other bacteriocins employed in this study. To achieve this, I assessed their purity and oligomeric state using size exclusion chromatography, SDS-PAGE combined with Coomassie staining, ESI-MS and SEC-MALS. Further, I assessed the activity of PyoS5 against a susceptible *P. aeruginosa* strain and the ability of FptA to bind its native ligand pyochelin.

3.2 Results

3.2.1 PyoS5 and PyoS5-derived constructs

PyoS5 was expressed in *E. coli* BL21 (DE3) cells. I found that the yield of PyoS5 increased from 4 mg to 19 mg per litre of *E. coli* culture when the immunity protein ImS5 was co-expressed in the same cells.

PyoS5 was purified by affinity chromatography using a HisTrap-HP-column followed by size exclusion chromatography on a 26/60 Superdex 200 column (Fig. 3-1). During its purification (Section 2.4.1), PyoS5 eluted from the 26/60 S200 size exclusion chromatography column at a volume between 180 mL and 200 mL (Fig. 3-1). The isolated protein resulting from this final purification step was 97 % pure, as determined by GeneTools from SynGene (Section 2.4.6) (Fig. 3-2).

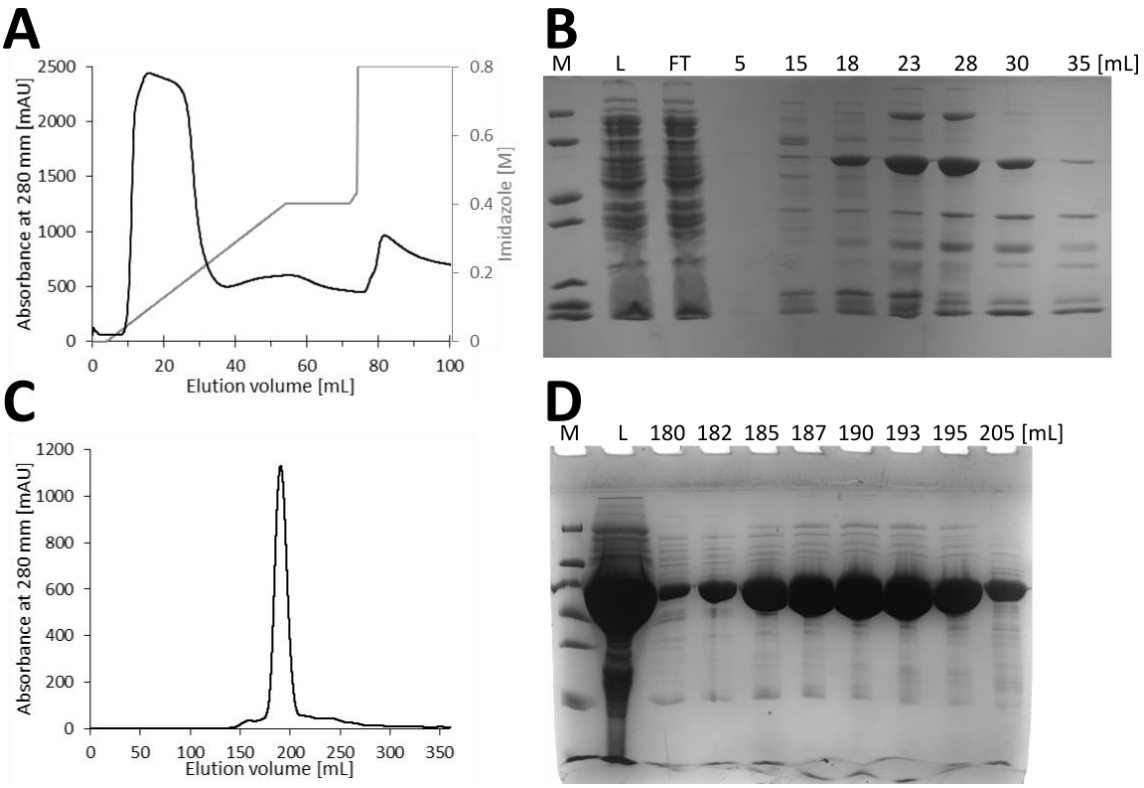

Figure 3-1: Purification of PyoS5.
(A) PyoS5 was loaded onto a 5 mL HisTrap-HP-column equilibrated in binding buffer (0.5 M NaCl, 20 mM Tris-HCl pH 7.5) and eluted by binding buffer supplemented with 0.75 M imidazole at a flow rate of 2.5 mL/min. (B) Marker (M), loaded bacterial lysate (L), flow through (FT), and 15 µL of fractions from 5 mL, 15 mL, 18 mL, 23 mL, 28 mL, 30 mL and 35 mL elution volume were analysed by SDS-PAGE. The dominant band in fractions 18 to 30 contains PyoS5. The marker (M) bands from highest to lowest mass are 116 kDa, 66 kDa, 45 kDa, 35 kDa, 25 kDa, 18.8 kDa and 14.4 kDa. (C) PyoS5 eluted between 180 mL and 200 mL from a 26/60 Superdex 200 column equilibrated in 150 mM NaCl, 20 mM Tris-HCl pH 7.5. Additional peaks contained impurities or aggregates. (D) Marker (M), loaded pooled fractions from affinity chromatography (L), and 15 µL of fractions from 180 mL, 182 mL, 185 mL, 187 mL, 190 mL, 193 mL, 195 mL and 205 mL elution volume were analysed by SDS-PAGE. The dominant band is PyoS5. Marker as in (B).

The oligomeric state of PyoS5 was investigated by SEC-MALS and found to be monomeric, with an estimated mass of 49 kDa (Fig. 3-3). Indeed, SEC-MALS was performed at concentrations ranging from 0.062 mg/mL to 9.5 mg/mL and PyoS5 was found to be monomeric at all these concentrations. The exact mass of PyoS5 was determined by ESI-MS to be 57008.00 Da, which is just 0.02 Da higher than its expected mass (Table 3-1).

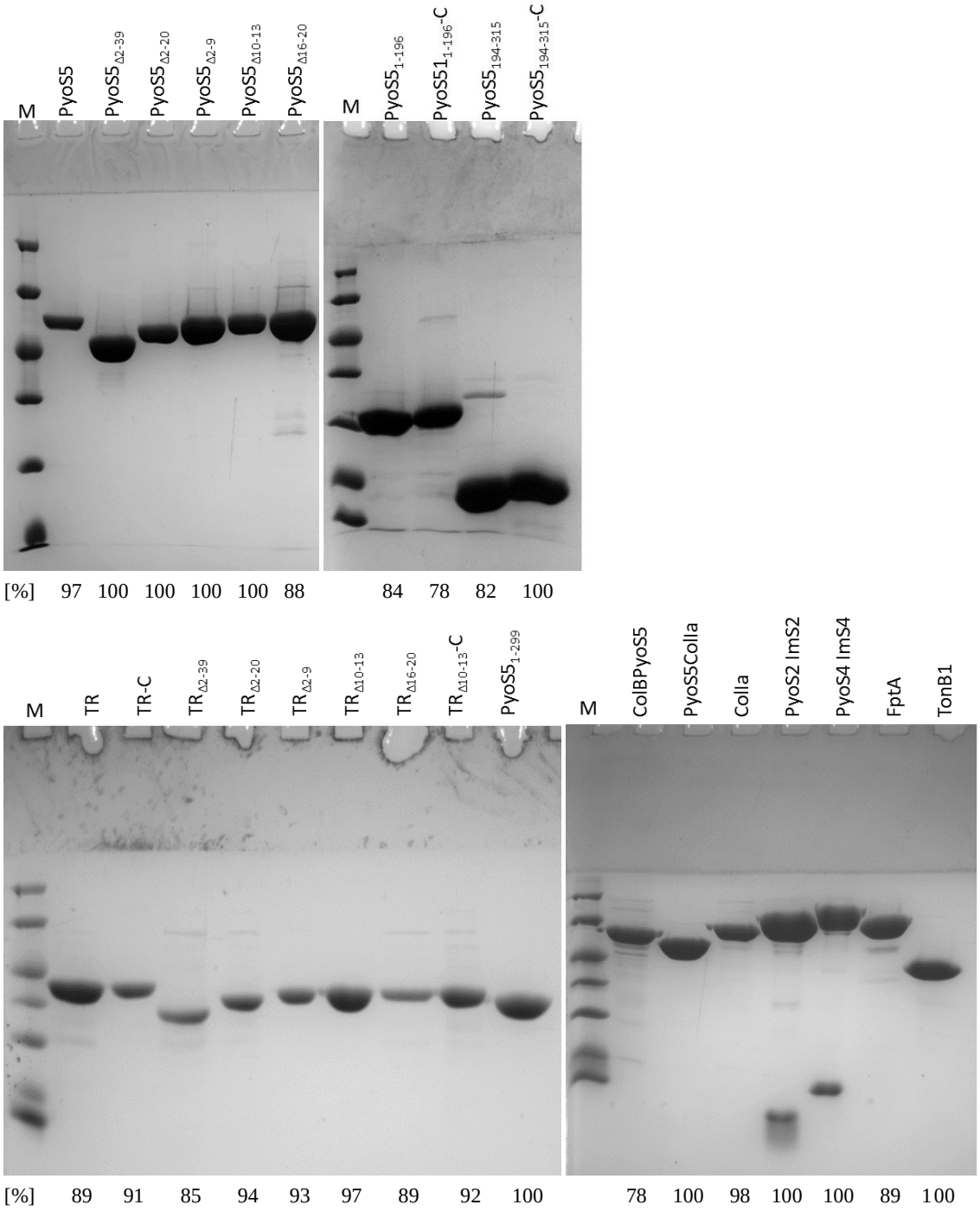

Figure 3-2: Coomassie stained SDS-PAGE of all purified proteins.
The marker (M) bands from highest to lowest mass are 116 kDa, 66 kDa, 45 kDa, 35 kDa, 25 kDa, 18.8 kDa and 14.4 kDa. 5 mg to 10 mg of each protein was loaded. Protein purity was determined (Section 2.4.6) and is given in percent. For PyoS2-ImS2 and PyoS4-ImS4 purity of the complex is given.

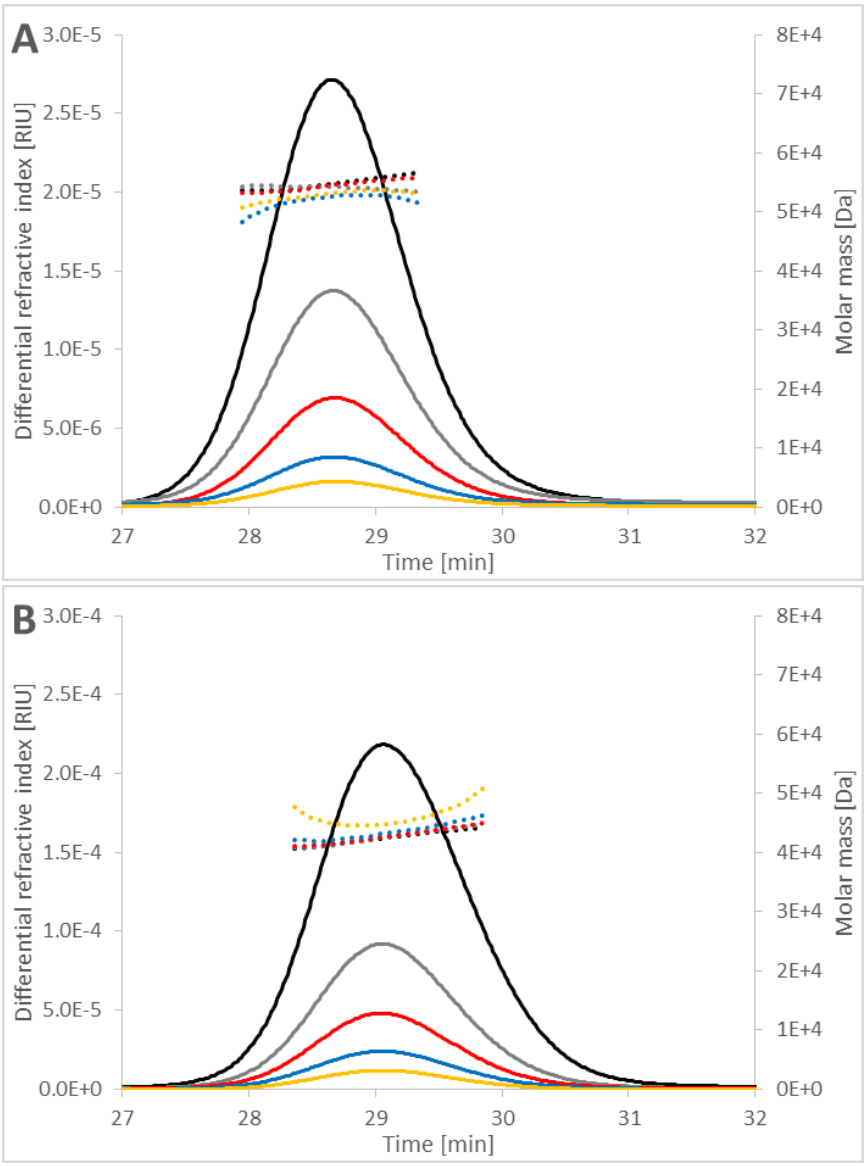

Figure 3-3: SEC-MALS shows PyoS5 is monomeric.
PyoS5 is investigated by SEC-MALS at concentrations of (A) 1 mg/mL (black), 0.5 mg/mL (grey), 0.25 mg/mL (red), 0.125 mg/mL (blue), 0.063 mg/mL (orange) and (B) 9.5 mg/mL (black), 4.75 mg/mL (grey), 2.38 mg/mL (red), 1.12 mg/mL (blue), and 0.59 mg/mL (orange). (A) and (B) are independent experiments performed on separate Superdex 200 10/300 GL columns. Solid lines show differential refractive index, dotted lines show molar mass.

Table 3-1: Masses determined by ESI-MS or native MS of all proteins used in this study.

Protein	N-terminal methionine present	Calculated MW [Da]	Observed MW [Da]	Difference [Da]
PyoS5	No	57007.98	57008.00	0.02
$PyoS5_{\Delta 2-39}$	No	53056.68	53056.60	0.08
$PyoS5_{\Delta 2-20}$	Yes	55214.12	55213.28	0.84
$PyoS5_{\Delta 2-9}$	No	56195.19	56196.06	0.84
$PyoS5_{\Delta 10-13}$	No	56577.42	56578.16	0.74
$PyoS5_{\Delta 16-20}$	No	56495.51	56496.05	0.54
TR	No	37193.13	37193.98	0.85
TR-Cys	No	37296.26	37297.71	1.45
$TR_{\Delta 2-39}$	No	33241.82	33242.08	0.26
$TR_{\Delta 2-20}$	Yes	35399.26	35398.43	0.83
$TR_{\Delta 2-9}$	No	36380.33	36380.39	0.06
$TR_{\Delta 10-13}$	No	36762.56	36762.29	0.27
$TR_{\Delta 16-20}$	No	36680.65	36680.57	0.08
$TR_{\Delta 10-13}$-Cys	No	36865.70	36864.20	1.50
$PyoS5_{1-299}$	No	35351.12	35350.92	0.20
$PyoS5_{1-196}$	No	23729.80	23729.74	0.06
$PyoS5_{1-196}$-Cys	No	23832.94	23832.79	0.15
$PyoS5_{194-315}$	Yes	15048.1	15048.22	0.12
$PyoS5_{194-315}$-Cys	Yes	15151.24	15150.35	0.89
ColIa	No	70362.93	70365.01	2.08
PyoS2	No	73722.65	73725.09	2.44
PyoS4	No	80600.64	80603.24	2.60
ColBPyoS5	No	59231.93	59232.06	0.13
PyoS5ColIa	No	56972.98	56972.47	0.52
FptA	Not applicable	76068.27	76066.1	2.17
TonB1	Not applicable	25473.4	25473	0

The activity of PyoS5 was assessed using plate-based growth inhibition assays. PyoS5 was found to be active against clinical isolate *P. aeruginosa* YHP17 both shortly after purification and after 36 months of storage at -20 °C (Fig. 3-4). The purification protocol employed here to purify PyoS5 was considered successful in all tested aspects and suitable for this study.

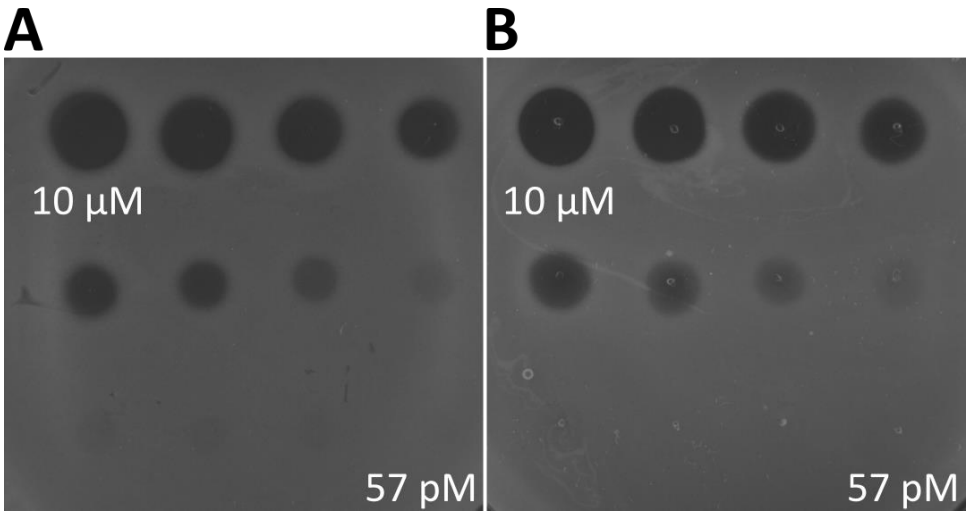

Figure 3-4: PyoS5 is active over 36 months.
Killing assays with (A) fresh PyoS5 and (B) PyoS5 stored at -20 °C for 36 months. 3-fold serial dilution starting at 10 µM going down to 57 pM spotted onto the soft agar containing *P. aeruginosa* YHP17 from top left to bottom right.

PyoS5$_{\Delta 2\text{-}39}$, PyoS5$_{\Delta 2\text{-}20}$, PyoS5$_{\Delta 2\text{-}9}$, PyoS5$_{\Delta 10\text{-}16}$ and PyoS5$_{\Delta 16\text{-}20}$ were purified to 88 % to 100 % purity by the same protocol as PyoS5 (Section 2.4.1) (Fig. 3-2). These constructs differed from PyoS5 by up to 38 residues and eluted from the size exclusion column in the same volume as PyoS5, between 180 and 200 mL. This indicated they have the same oligomeric state as PyoS5 and are therefore monomeric (Fig. 3-5).

To determine the exact masses of the PyoS5 derivatives (PyoS5$_{\Delta 2\text{-}39}$, PyoS5$_{\Delta 2\text{-}20}$, PyoS5$_{\Delta 2\text{-}9}$, PyoS5$_{\Delta 10\text{-}16}$ and PyoS5$_{\Delta 16\text{-}20}$) ESI-MS was performed (Table 3-1) and showed that each construct was within one Da of its expected mass. For all of these constructs apart from PyoS5$_{\Delta 2\text{-}20}$ the observed mass corresponded to the N-terminal methionine being cleaved.

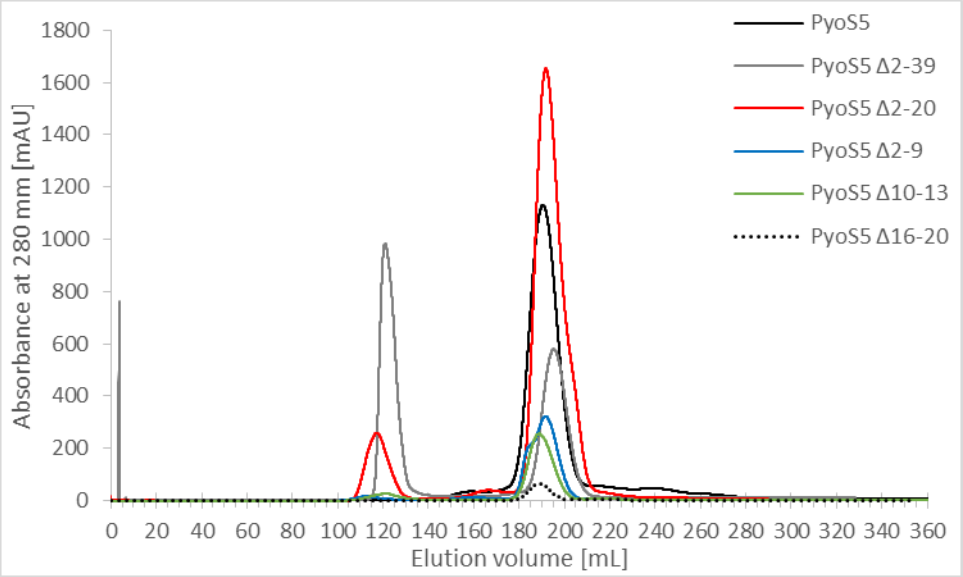

Figure 3-5: Size exclusion chromatography of PyoS5 and related constructs.
PyoS5 and constructs that differed by up to 38 residues eluted between 180 mL and 200 mL at a flow rate of 2.6 mL/min from a 26/60 Superdex 200 column equilibrated in 150 mM NaCl, 20 mM Tris-HCl pH 7.5. Additional peaks contained impurities or aggregates. Size exclusion chromatography of PyoS5$_{\Delta 2\text{-}39}$, PyoS5$_{\Delta 2\text{-}20}$, PyoS5$_{\Delta 2\text{-}9}$, PyoS5$_{\Delta 10\text{-}13}$ and PyoS5$_{\Delta 16\text{-}20}$ was performed by Moritz Weber under supervision of Hannah Behrens.

Further constructs were designed based on the crystal structure of PyoS5, which will be described in chapter 4. One of these, PyoS5$_{1\text{-}315}$ was expressed and termed TR. TR, as well as the constructs differing from it by up to 19 residues: TR-Cys, TR$_{\Delta 2\text{-}20}$, TR$_{\Delta 2\text{-}9}$, TR$_{\Delta 10\text{-}13}$, TR$_{\Delta 16\text{-}20}$, TR$_{\Delta 10\text{-}13}$-Cys and PyoS5$_{1\text{-}299}$ were expressed without co-expression of ImS5 and then purified by His6-tag affinity chromatography and size exclusion chromatography by the same protocol as PyoS5 (Section 2.4.1). The resulting proteins were of 85 % to 100% purity (Fig. 3-2). During the purification they eluted from the size exclusion chromatography column at a volume of 210 mL to 220 mL. This indicated that they were all of equivalent oligomeric state (Fig. 3-6). SEC-MALS revealed that TR was monomeric, with an estimated mass of 39 kDa (Fig. 3-7).

The masses of TR, TR-Cys, TR$_{\Delta 2\text{-}20}$, TR$_{\Delta 2\text{-}9}$, TR$_{\Delta 10\text{-}13}$, TR$_{\Delta 16\text{-}20}$, TR$_{\Delta 10\text{-}13}$-Cys and PyoS5$_{1\text{-}299}$ were observed through ESI-MS and differed by no more than 1.45 Da from

the calculated masses based on amino acid sequence (Table 3-1). Analogous to the observation that the N-terminal methionine of PyoS5$_{\Delta 2\text{-}20}$ was not cleaved, the N-terminal methionine of TR$_{\Delta 2\text{-}20}$ was not cleaved either. The masses of all other TR-derived proteins were in agreement with a cleaved N-terminal methionine.

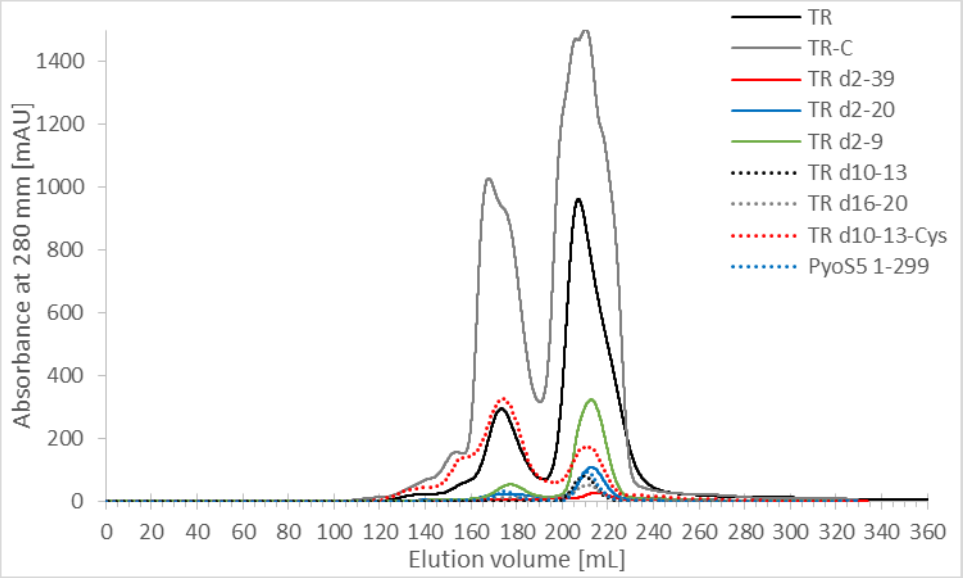

Figure 3-6: Size exclusion chromatography of TR and related constructs.
TR and constructs that differed from it by up to 19 residues eluted between 200 mL and 220 mL at a flow rate of 2.6 mL/min from a 26/60 Superdex 200 column equilibrated in 150 mM NaCl, 20 mM Tris-HCl pH 7.5. Additional peaks contained impurities or aggregates.

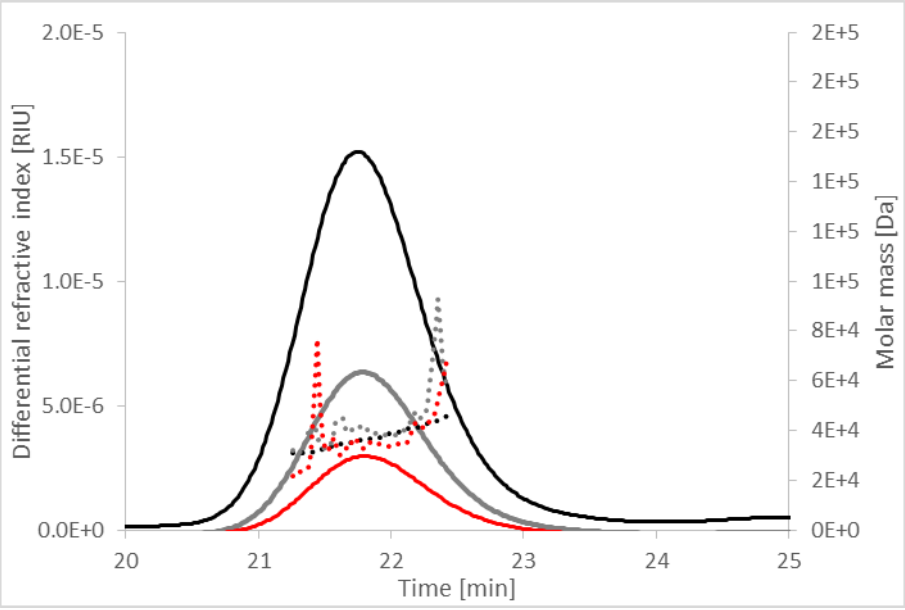

Figure 3-7: SEC-MALS shows TR is monomeric.
TR is investigated by SEC-MALS at concentrations of 1 mg/mL (black), 0.5 mg/mL (grey), and 0.25 mg/mL (red) on a Superdex 200 10/300 GL column. Solid lines show differential refractive index, dotted lines show molar mass.

PyoS5$_{1-196}$ and PyoS5$_{1-196}$-Cys were another two constructs based on the PyoS5 crystal structure. They were expressed and purified by affinity and size exclusion chromatography, like TR (Section 2.4.1), leading to 84 % and 78 % purity, respectively (Fig. 3-2). During the purification they eluted between 200 mL and 220 mL from the size exclusion chromatography column (Fig. 3-8) and PyoS5$_{1-196}$ was found to be monomeric by SEC-MALS with an estimated mass of 23 kDa (Fig. 3-9). The exact mass of both proteins was determined by ESI-MS and found to be within one Da of the expected mass based on amino acid residues and a cleaved N-terminal methionine (Table 3-1).

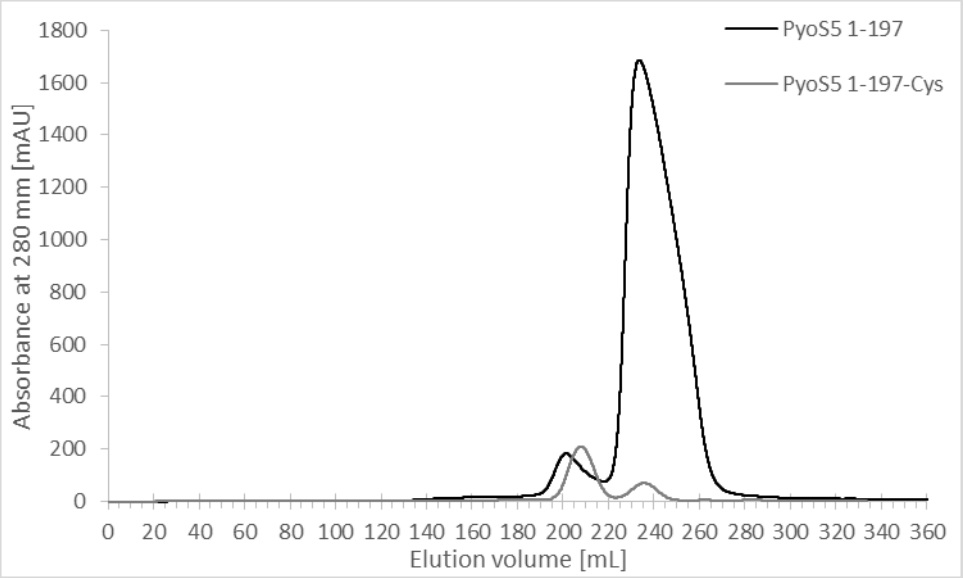

Figure 3-8: Size exclusion chromatography of PyoS5$_{1-196}$ and PyoS5$_{1-196}$-Cys.
PyoS5$_{1-315}$ (black) and PyoS5$_{1-315}$-Cys (grey) eluted between 220 mL and 260 mL at a flow rate of 2.6 mL/min from a 26/60 Superdex 200 column equilibrated in 150 mM NaCl, 20 mM Tris-HCl pH 7.5. Additional peaks contained impurities or aggregates.

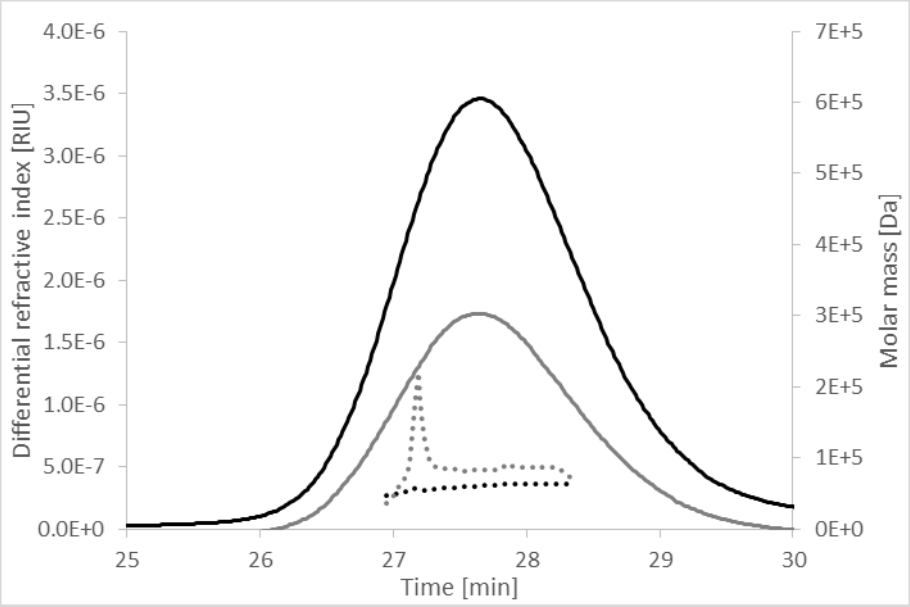

Figure 3-9: SEC-MALS shows PyoS5$_{1-196}$ is monomeric.
PyoS5$_{1-196}$ is investigated by SEC-MALS at concentrations of 1 mg/mL (black), and 0.5 mg/mL (grey) on a Superdex 200 10/300 GL column. Solid lines show differential refractive index, dotted lines show molar mass.

The final constructs derived from the PyoS5 crystal structure were PyoS5$_{194-315}$ and PyoS5$_{194-315}$-Cys. They were purified like TR (Section 2.4.1) resulting in 82 % and 100 % purity, respectively, (Fig. 3-2), and eluted from the size exclusion chromatography column between 230 mL and 250 mL during this purification (Fig. 3-10). SEC-MALS showed PyoS5$_{194-315}$ was monomeric with a mass of 13 kDa (Fig. 3-11). The exact masses of PyoS5$_{194-315}$ and PyoS5$_{194-315}$-Cys, as determined by ESI-MS, differed less than one Da from the expected mass (Table 3-1). Both proteins retained their N-terminal methionine.

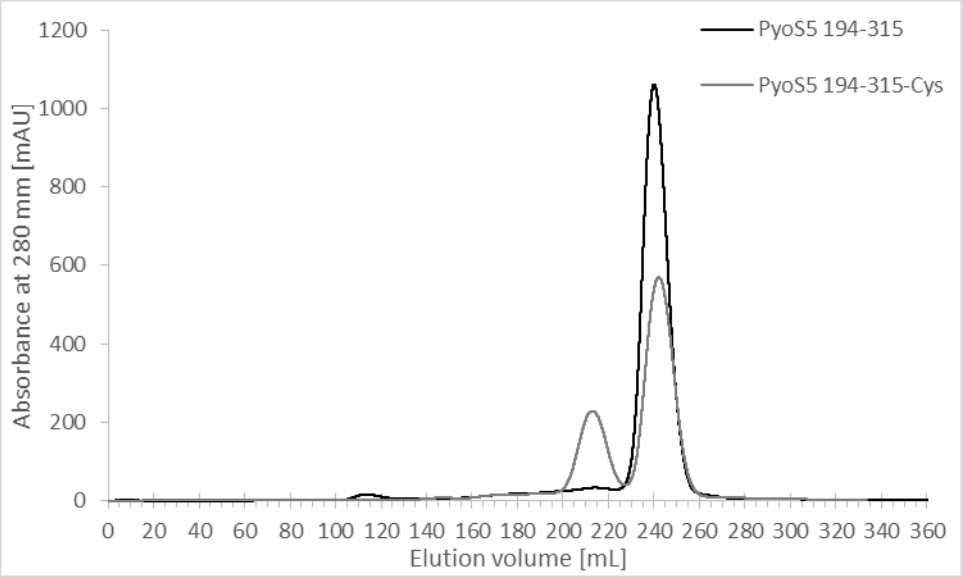

Figure 3-10: Size exclusion chromatography of PyoS5$_{194-315}$ and PyoS5$_{194-315}$-Cys.
PyoS5$_{194-315}$ (black) and PyoS5$_{194-315}$-Cys (grey) eluted between 230 mL and 250 mL at a flow rate of 2.6 mL/min from a 26/60 Superdex 200 column equilibrated in 150 mM NaCl, 20 mM Tris-HCl pH 7.5. Additional peaks contained impurities or aggregates.

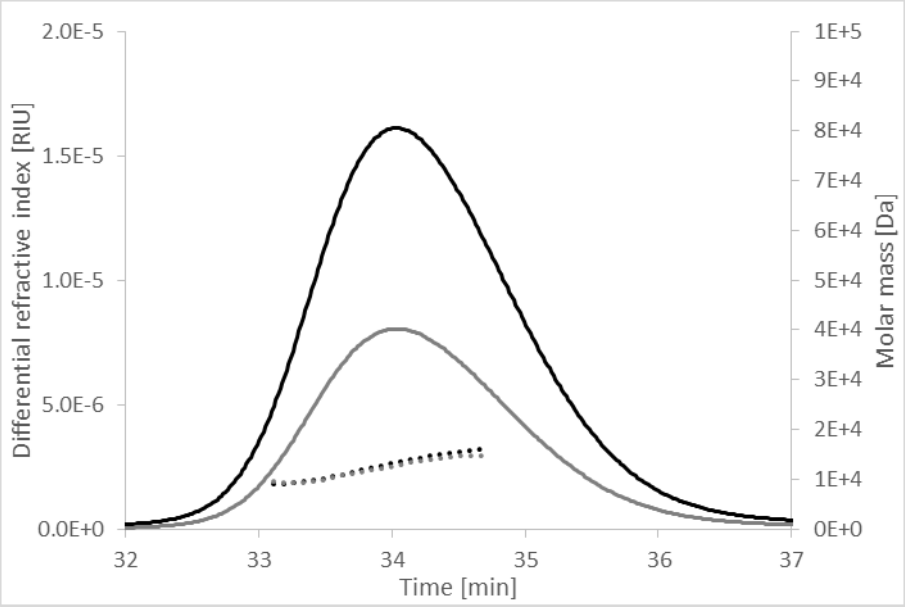

Figure 3-11: SEC-MALS shows PyoS5$_{194-315}$ is monomeric.
PyoS5$_{194-315}$ is investigated by SEC-MALS at concentrations of 1 mg/mL (black), and 0.5 mg/mL (grey) on a Superdex 200 10/300 GL column. Solid lines show differential refractive index, dotted lines show molar mass.

3.2.2 Chimeric bacteriocins

ColBPyoS5 is a chimeric protein comprising of the first 340 amino acids of ColB and the last 186 of PyoS5. PyoS5ColIa is another chimeric bacteriocin that harbours the

N-terminal 315 amino acid residues of PyoS5 fused to the pore-forming domain of ColIa, consisting of amino acid residues 485 to 626. Both were purified by the same protocol as PyoS5 (Section 2.4.1), including His6-tag affinity chromatography followed by size exclusion chromatography, resulting in 78 % and 100 % pure protein respectively (Fig. 3-2). During the purification both eluted from the size exclusion chromatography column between 180 mL and 200 mL (Fig. 3-12).

Both were found to be monomeric based on SEC-MALS with an approximate mass of 56 kDa for ColBPyoS5 (Fig. 3-13) and 52 kDa for PyoS5ColIa (Fig. 3-14). The exact mass of ColBPyoS5 was determined by ESI-MS to be 59232.06 Da which is only 0.12 Da different from the mass calculated for ColBPyoS5 without the N-terminal methionine (Table 3-1). The exact mass of PyoS5ColIa was also determined and found to be within 1 Da of the expected mass for PyoS5ColIa without its N-terminal methionine (Table 3-1).

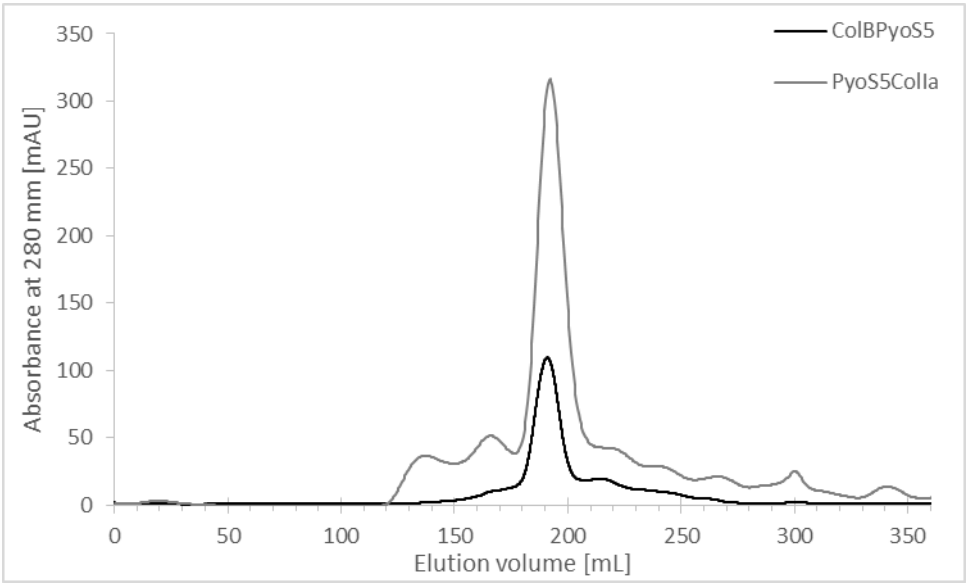

Figure 3-12: Size exclusion chromatography of ColBPyoS5 and PyoS5ColIa.
ColBPyoS5 and PyoS5ColIa eluted between 180 mL and 200 mL at a flow rate of 2.6 mL/min from a 26/60 Superdex 200 column equilibrated in 150 mM NaCl, 20 mM Tris-HCl pH 7.5. Additional peaks contained impurities or aggregates.

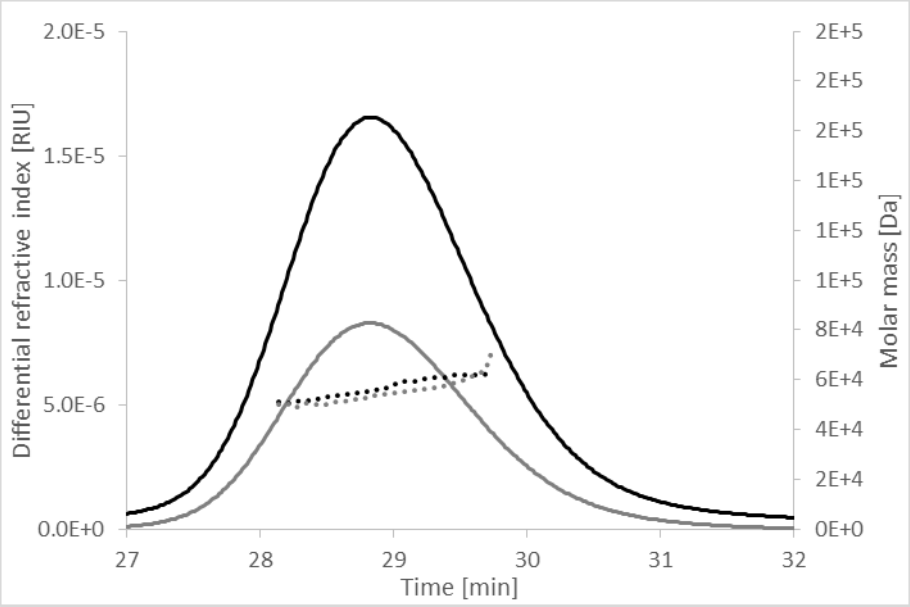

Figure 3-13: SEC-MALS shows ColBPyoS5 is monomeric.
ColBPyoS5 is investigated by SEC-MALS at concentrations of 1 mg/mL (black), and 0.5 mg/mL (grey) on a Superdex 200 10/300 GL column. Solid lines show differential refractive index, dotted lines show molar mass.

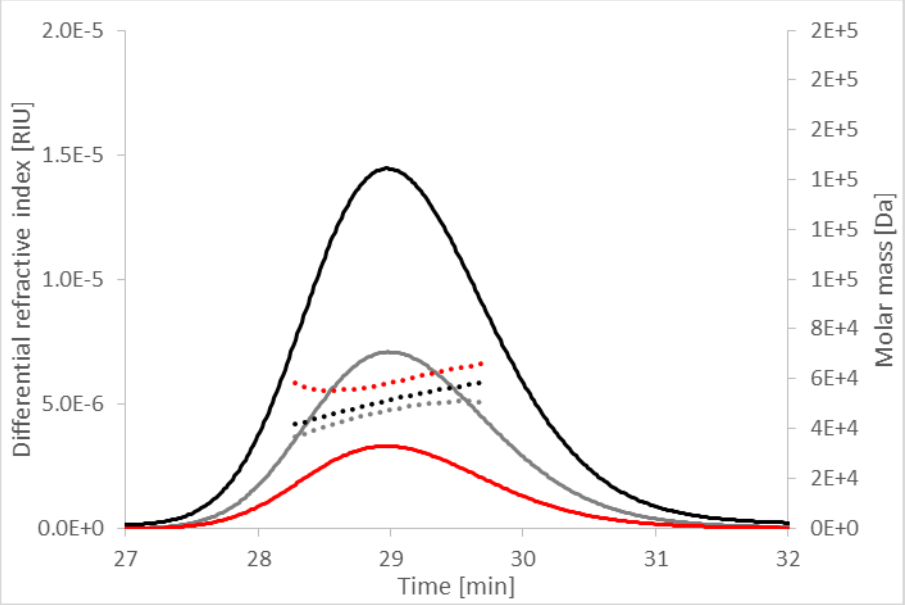

Figure 3-14: SEC-MALS shows PyoS5ColIa is monomeric.
PyoS5ColIa is investigated by SEC-MALS at concentrations of 1 mg/mL (black), 0.5 mg/mL (grey) and 0.25 mg/mL (red) on a Superdex 200 10/300 GL column. Solid lines show differential refractive index, dotted lines show molar mass.

3.2.3 Other bacteriocins

ColIa was purified like PyoS5 by affinity and size exclusion chromatography (Section 2.4.1) (Fig. 3-15) to 98 % purity (Fig. 3-2). Through SEC-MALS it was found to be monomeric in solution with an estimated mass of 74 kDa (Fig. 3-16). Its exact mass was found to be 70365.01 Da which is within 3 Da of the expected mass for ColIa without its N-terminal methionine.

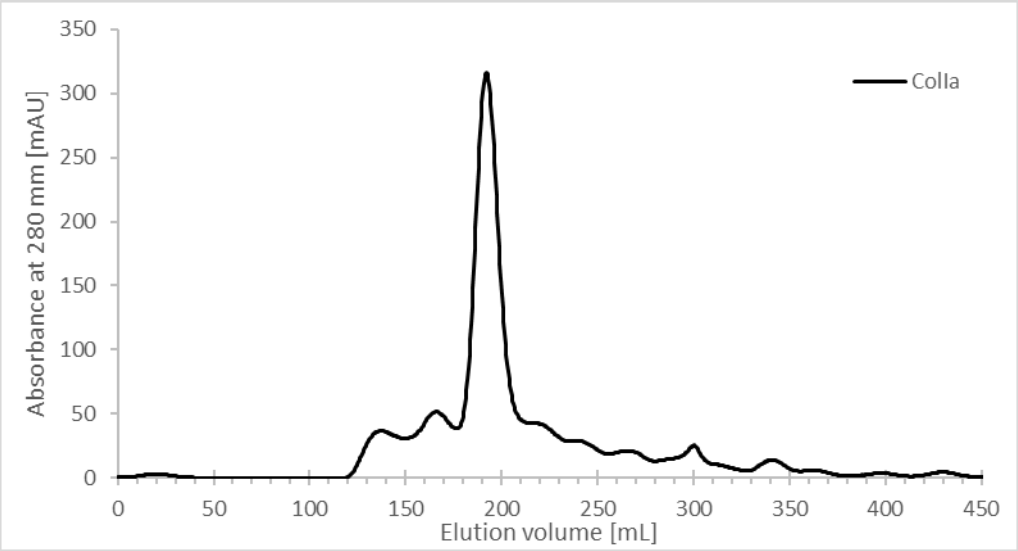

Figure 3-15: Size exclusion chromatography of ColIa.
ColIa eluted between 180 mL and 210 mL at a flow rate of 2.6 mL/min from a 26/60 Superdex 200 column equilibrated in 150 mM NaCl, 20 mM Tris-HCl pH 7.5. Additional peaks contained impurities or aggregates. Size exclusion chromatography was performed by Nicholas Housden.

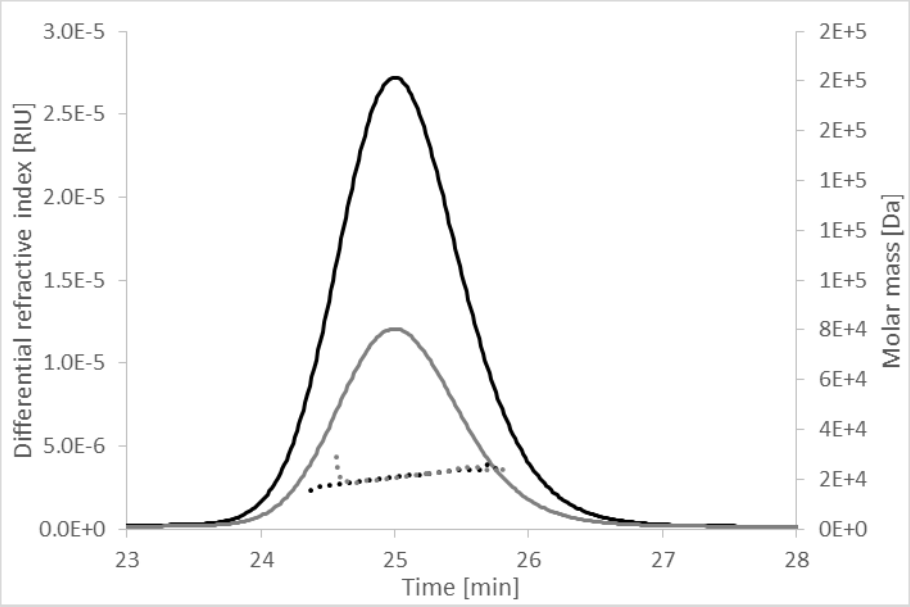

Figure 3-16: SEC-MALS shows ColIa is monomeric.
ColIa is investigated by SEC-MALS at concentrations of 1 mg/mL (black), and 0.5 mg/mL (grey) on a Superdex 200 10/300 GL column. Solid lines show differential refractive index, dotted lines show molar mass.

PyoS2-ImS5 (Fig. 3-17) and PyoS4-ImS4 (Fig. 3-18) were expressed and purified in complex with their respective immunity proteins by His6-tag affinity and size exclusion chromatography (Section 2.4.1) resulting in 100 % purity (Fig. 3-2). Their approximate masses, as determined by SEC-MALS, were 74 kDa and 97 kDa, respectively, indicating monomeric proteins. Their exact masses were within three Da of the masses calculated based on the amino acid sequence that lacks the N-terminal methionine.

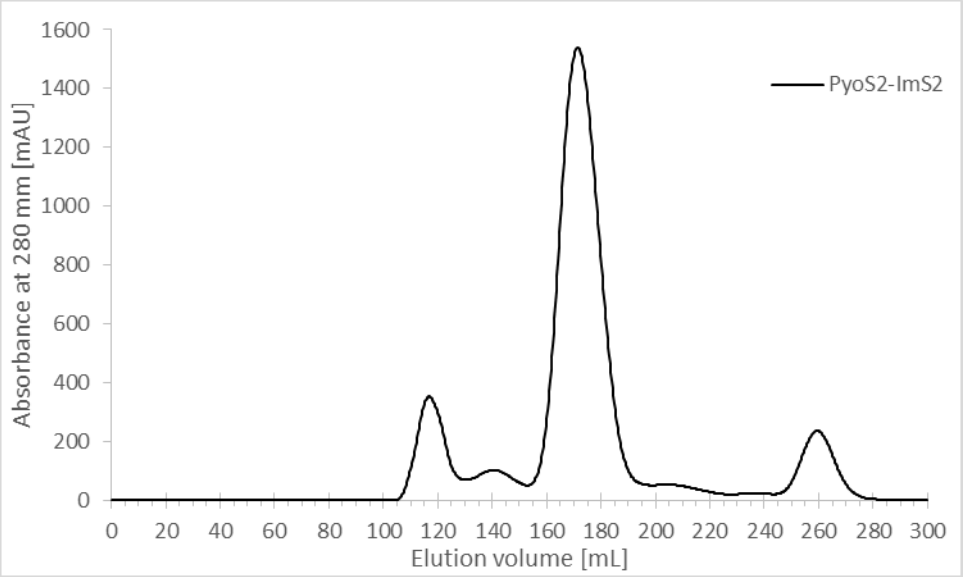

Figure 3-17: Size exclusion chromatography of PyoS2-ImS2.
PyoS2-ImS2 eluted between 160 mL and 190 mL at a flow rate of 2.6 mL/min from a 26/60 Superdex 200 column equilibrated in 150 mM NaCl, 20 mM Tris-HCl pH 7.5. Additional peaks contained impurities or aggregates. Size exclusion chromatography was performed by Paul White.

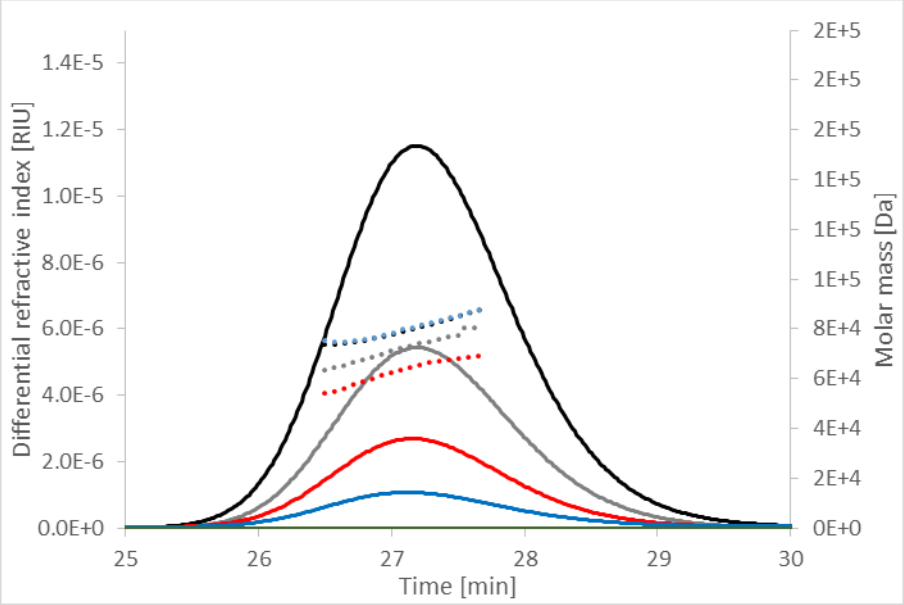

Figure 3-18: SEC-MALS shows PyoS2-ImS2 is monomeric.
PyoS2-ImS2 is investigated by SEC-MALS at concentrations of 1 mg/mL (black), 0.5 mg/mL (grey), 0.25 mg/mL (red), and 0.125 mg/mL (blue) on a Superdex 200 10/300 GL column. Solid lines show differential refractive index, dotted lines show molar mass.

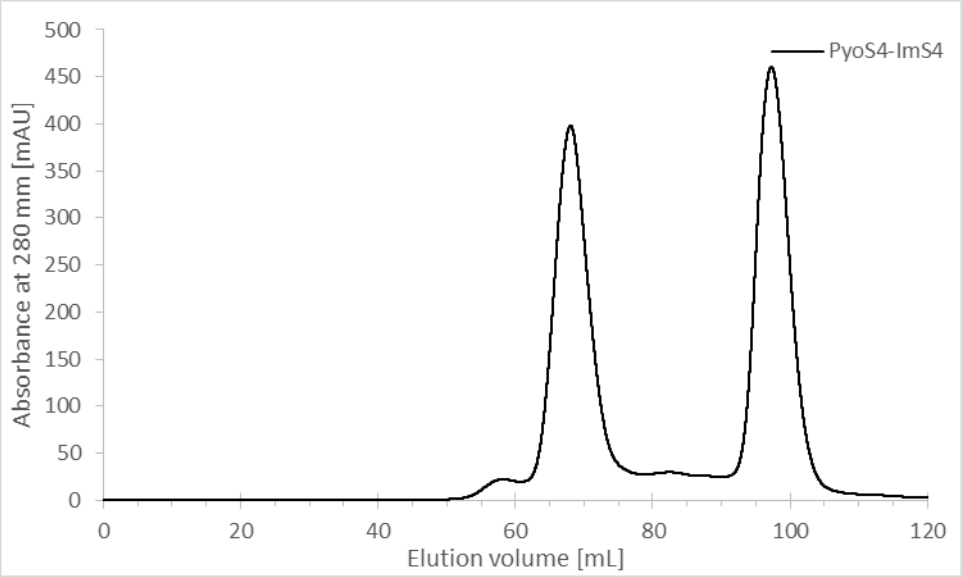

Figure 3-19: Size exclusion chromatography of PyoS4-ImS4.
PyoS4-ImS4 eluted between 60 mL and 75 mL at 1 mL/min from a 16/60 Superdex 200 column equilibrated in 150 mM NaCl, 20 mM Tris-HCl pH 7.5. Additional peaks contained impurities including excess immunity protein or aggregates. Size exclusion chromatography was performed by Nicholas Housden.

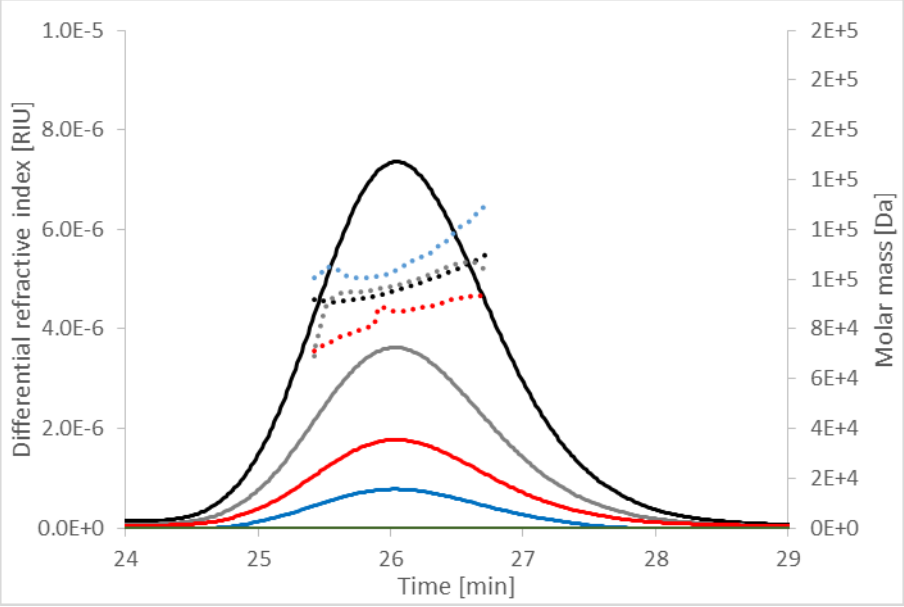

Figure 3-20: SEC-MALS shows PyoS4-ImS4 is monomeric.
PyoS4-ImS4 is investigated by SEC-MALS at concentrations of 1 mg/mL (black), 0.5 mg/mL (grey), 0.25 mg/mL (red), and 0.125 mg/mL (blue) on a Superdex 200 10/300 GL column. Solid lines show differential refractive index, dotted lines show molar mass.

3.2.4 FptA

FptA was extracted from isolated outer membranes using β-OG and purified (Section 2.4.3) by anion exchange chromatography on a HiTrap DEAE FF column, followed by size exclusion chromatography on a 16/60 Sephacryl 300 column and anion exchange chromatography on a Mono Q 4.6/100 PE column (Fig. 3-21) resulting in 89 % pure protein (Fig. 3-2).

The yield was between 0.2 mg and 2 mg per litre of FptA-expressing *E. coli* culture. Native MS revealed a mass of 76066 Da which is within two Da of the mass expected for FptA (Table 3-1) and shows FptA is monomeric. When mixed with ferric pyochelin a complex corresponding to FptA bound to pyochelin-Fe^{III} was observed showing that the isolated FptA was functional in binding its native ligand (Fig. 3-22).

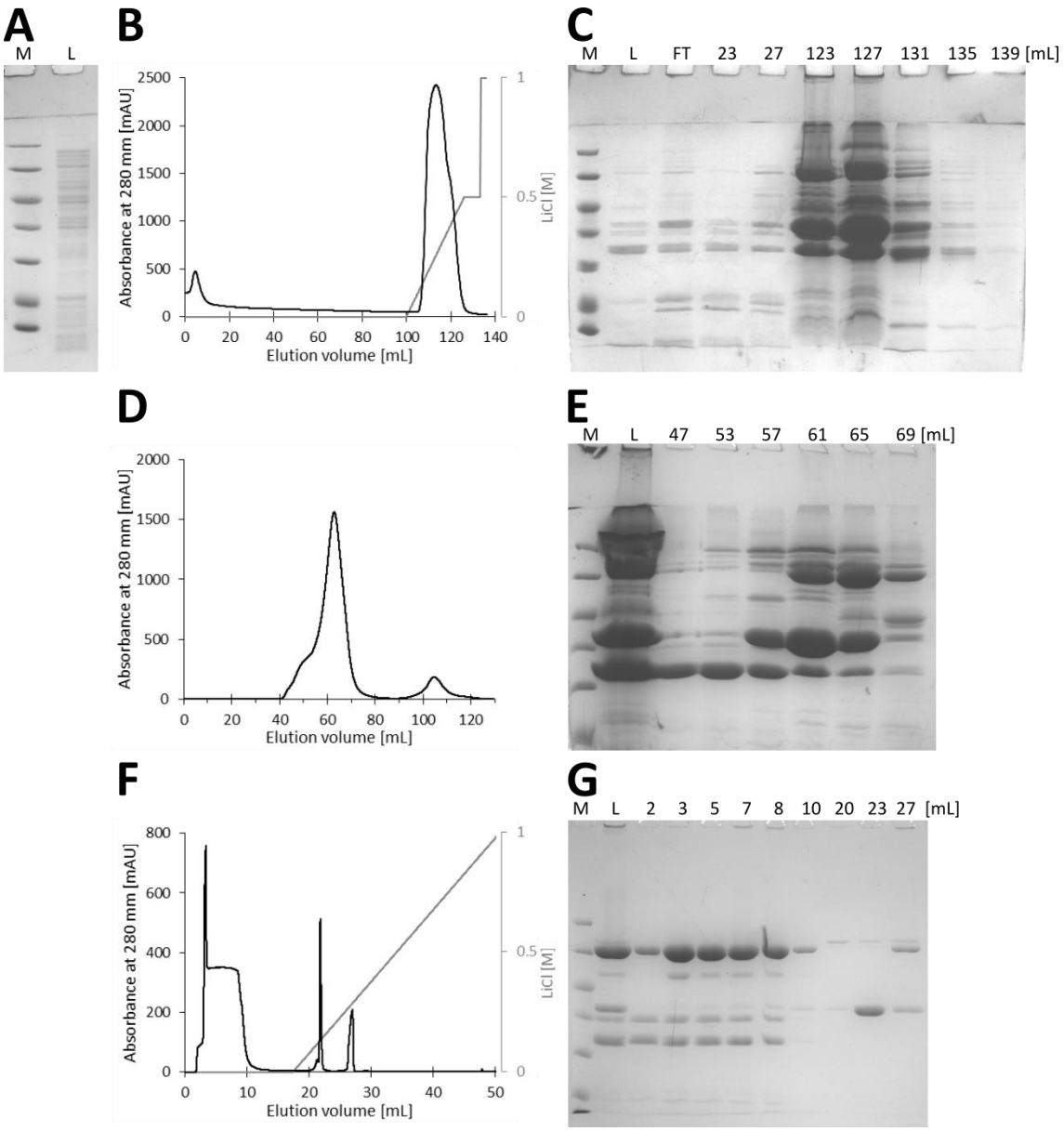

Figure 3-21: Purification of FptA.

(A) Marker (M) and lysate (L) of *E. coli* BL21 (DE3) cells expressing FptA. (B) Anion exchange chromatography on a DEAE column equilibrated in buffer E (50 mM Tris-HCl pH 7.5, 1% (w/v) β-OG, 5 mM EDTA) and eluted by increasing the concentration of LiCl. (C) Marker (M), loaded protein extracted from purified outer membranes (L), flow through (FT), and 15 µL of fractions from 23 mL, 27 mL, 123 mL, 127 mL, 131 mL, 135 mL and 139 mL elution volume from DEAE anion exchange chromatography were analysed by SDS-PAGE. (D) Size exclusion chromatography on pooled fractions containing FptA from DEAE anion exchange chromatography on a 16/60 Sephacryl 300 column equilibrated in buffer E. FptA eluted between 55 mL and 75 mL. Additional peaks contained impurities or aggregates. (E) Marker (M), loaded pooled fractions containing FptA from DEAE anion exchange chromatography (L) and 15 µL of fractions from 47 mL, 53 mL, 57 mL, 61 mL, 65 mL and 69 mL elution volume from size exclusion chromatography were analysed by SDS-PAGE. (F) Anion exchange chromatography on a Mono Q 4.6/100 PE column equilibrated in buffer E and eluted with by increasing the concentration of LiCl. (G) Marker (M), loaded pooled fractions containing FptA from size exclusion chromatography (L) and 15 µL of fractions from 2 mL, 3 mL, 5 mL, 7 mL, 8 mL, 10 mL, 20 mL, 23 mL and 27 mL elution volume from Mono Q anion exchange chromatography were analysed by SDS-PAGE. The dominant band eluting between 2 mL and 10 mL contained FptA. (A,C,E,G) The marker bands from highest to lowest mass are 116 kDa, 66 kDa, 45 kDa, 35 kDa, 25 kDa, 18.8 kDa and 14.4 kDa.

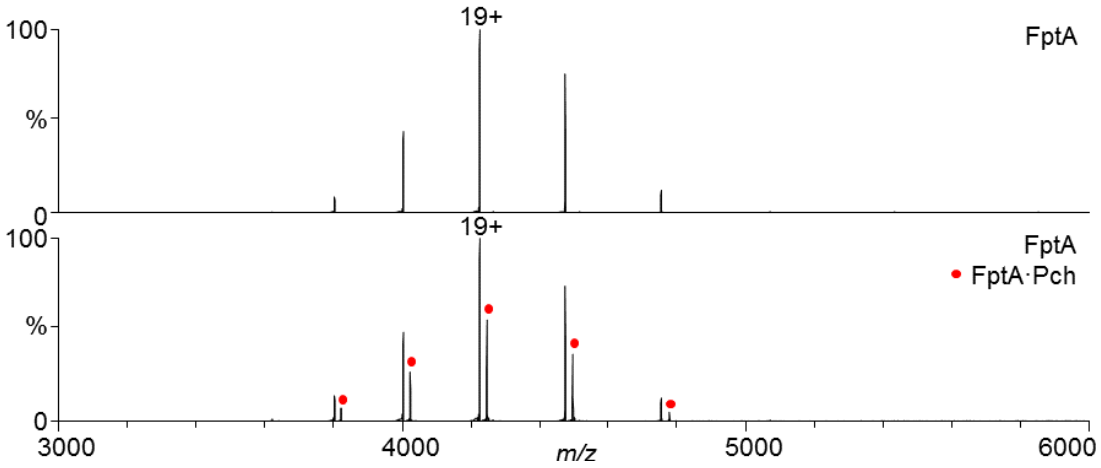

Figure 3-22: Purified FptA binds to its native ligand pyochelin.
FptA was incubated with a 4-fold excess of ferric pyochelin for 45 min, then excess pyochelin was removed by desalting. The native mass spectrum of FptA alone showed a 76066.1 ± 0.3 Da species. 10 µM FptA in the presence of ferric pyochelin gave peaks for FptA at 76066.0 ± 0.2 Da and a complex at 76443.4 ± 0.3 Da, which corresponds to FptA and the 377.4 Da pyochelin-Fe^{III} (expected mass 377.3 Da). The y-axis shows relative abundance in percent.

3.2.5 TonB1

The cytoplasmic domain of TonB1 was purified as described previously (White et al., 2017) by His6-tag affinity chromatography followed by TEV-cleavage of the His6-tag, negative selection by His6-tag affinity chromatography and size exclusion chromatography (Section 2.4.2). The resulting protein eluted as one peak from size exclusion chromatography (Fig. 3-23) and was 100 % pure (Fig. 3-2).

Previously, constructs derived from *E. coli* TonB where found to dimerize. To investigate whether this was also true for the TonB1 construct used in this study, it was analysed by SEC-MALS and found to be monomeric based on an approximate mass of 17 kDa (Fig. 3-24). The exact mass of the cytoplasmic domain of TonB1 was determined to be 25473 Da by native MS, just like expected based on the amino acid sequence (Table 3-1), which further confirmed that it was monomeric.

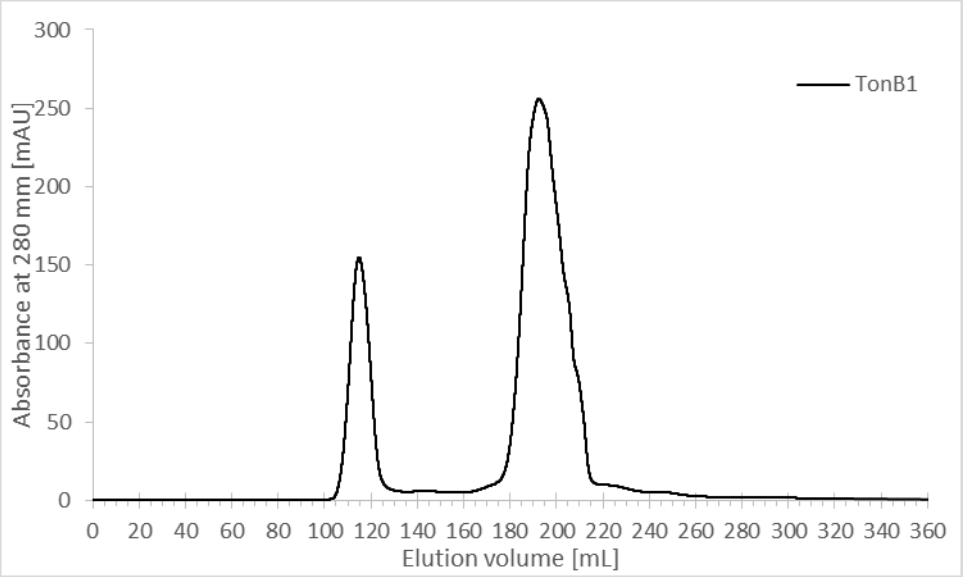

Figure 3-23: Size exclusion chromatography of the TonB1 cytoplasmic domain.
The TonB1 cytoplasmic domain eluted between 180 mL and 210 mL at a flow rate of 2.6 mL/min from a 26/60 Superdex 200 column equilibrated in 300 mM NaCl, 50 mM Tris-HCl pH 7.5. The additional peak contained impurities. Experiment was performed by Renata Kaminska (Department of Biochemistry, University of Oxford).

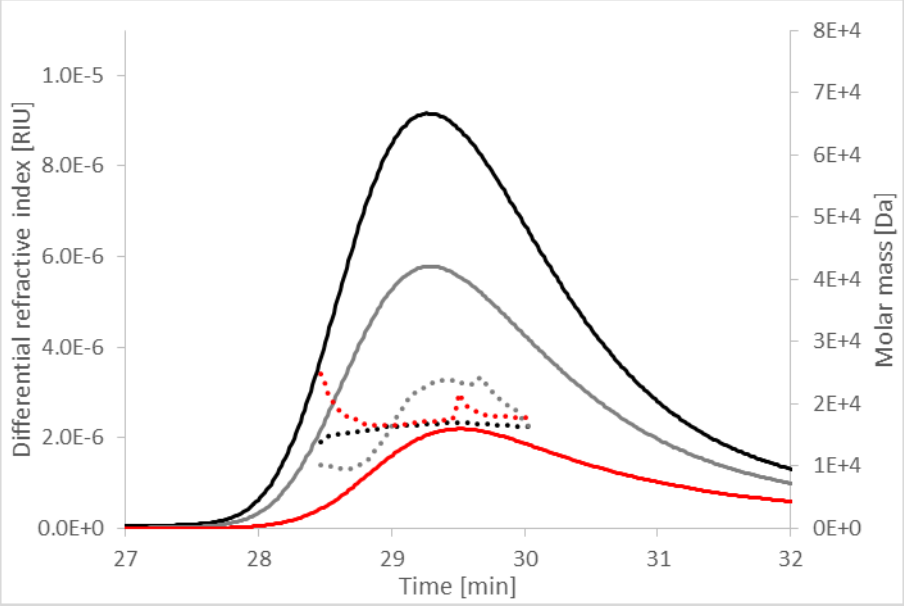

Figure 3-24: SEC-MALS shows TonB1 is monomeric.
TonB1 is investigated by SEC-MALS at concentrations of 1 mg/mL (black), 0.5 mg/mL (grey), and 0.25 mg/mL (red) on a Superdex 200 10/300 GL column. Solid lines show differential refractive index, dotted lines show molar mass.

3.3 Discussion

The new His6-tag based purification protocol for PyoS5 performed well. Co-expression of ImS5 did not lead to co-purification and yielded pure, monomeric, correctly sized and active PyoS5. Therefore, His6-tagged PyoS5 from co-expression with ImS5 was used throughout this study.

The other proteins derived from parts of the PyoS5 sequence as well as PyoS5-based chimera and other bacteriocins were of similarly high quality.

The heterologous purification protocol for FptA achieves for the first time purification without the 324 Da native ligand pyochelin and thus is suitable for the purpose of this study. The yield was sufficient for this study but future efforts might focus on improving it, considering that 10-fold higher yields have been achieved for other TBDTs (Buchanan et al., 2007).

The TonB1 periplasmic domain and PyoS2-ImS2 have previously been purified by the protocols used here and shown to be functional in binding each other (White et al., 2017). Here, it was observed that the TonB1 cytoplasmic domain is monomeric in solution. Structures of *E. coli* TonB periplasmic domain constructs have shown both monomers and dimers (Chang et al., 2001; Ködding et al., 2005; Koedding et al., 2004; Sean Peacock et al., 2005), while the only structure available for the *P. aeruginosa* TonB1 periplasmic domain reveals a monomer (Oeemig et al., 2018). Structures of complexes between the *E. coli* TonB cytoplasmic domain and TBDTs revealed that TonB binds the TBDT in its monomeric form (Pawlek et al., 2006; Shultis et al., 2006). The results presented here add to the previous evidence confirming that *P. aeruginosa* TonB1 is monomeric.

4. Biophysical characterization and crystal structure of PyoS5

4.1 Introduction

In vivo experiments have shown that PyoS5 is the most promising CLB as an antibiotic, but *in vitro* analysis of this protein is lacking. As a result, neither the domain architecture, structure or its mechanism of translocating across the outer membrane are known, all of which would be useful for the development of improved antibiotics.

Most CLBs consist of several domains that each confer a specific function such as receptor-binding, translocation and cytotoxicity which can be combined to yield different bacteriocins. For example, the receptor-binding and translocation domains of PyoS2 and PyoSD2, are conserved but they deliver different cytotoxic domains into the target bacterium (McCaughey et al., 2016a). Very similar cytotoxic domains can be delivered by many different receptor-binding and translocation domains, as for example in the case of pore-forming CLBs like ColE1 and ColIa (Elkins et al., 1997; Wiener et al., 1997). Based on sequence similarity PyoS5 seems to harbour a pore-forming domain most similar to that of ColIa and ColIb.

Generally, CLBs, like the well-characterized ColE9 (Klein et al., 2016), have an unstructured N-terminal region, translocation domain, receptor-binding domain, and cytotoxic domain, however, a variety of other architectures also exist. Some bacteriocins have fewer domains, like ColN and ColB, which have an unstructured region, a pore-forming domain and only one structured domain for interacting with outer membrane components (Hilsenbeck et al., 2004; Vetter et al., 1998). Others CLBs have additional

domains; PyoS2, for example, has an unstructured region and four domains, an N-terminal domain for binding FpvAI, followed by a CPA-binding domain, a Pyocin S domain, presumably for crossing the inner membrane, and a cytotoxic DNase domain (Sano et al., 1993a). Colicin S4 harbours two copies of its receptor-binding domain also resulting in a total of four domains (Arnold et al., 2009), while PmnH from *Pseudomonas synxantha* harbours two different cytotoxic domains, a ColM-like and a ColN-like domain, even though only the latter is active (Ghequire et al., 2017a). The domain architecture of PyoS5 is currently unknown and is not predictable from its sequence making it an interesting target for further investigation.

Previously, chimeric CLBs have been constructed in order to identify domain boundaries and functions (Benedetti et al., 1991; Elfarash et al., 2014; Kageyama et al., 1996; Sano et al., 1993a; White et al., 2017). Parts of CLBs have also been combined with parts of other proteins to create improved therapeutics with custom species-specificity or cytotoxic modes of action, allowing them to overcome naturally occurring immunity of target bacteria (Jakes et al., 1988; Qiu et al., 2003). Instead of combining CLBs with other proteins, it seems a good strategy to return to chimeric proteins made from different CLBs only, with the objective of creating therapeutics with desired characteristics. This approach has the advantage that all parts of the final product have evolved to cross the Gram-negative outer membrane, as opposed to strategies where CLBs are combined with other molecules, like phage proteins and pheromones. Chimeric CLBs based on PyoS5 could expand the use of this potent pyocin as a therapeutic by overcoming immunity conferred by ImS5 and by expanding the range of target species. In order for this to be done precise information on domain boundaries is needed.

This chapter describes the biophysical properties and crystal structure of PyoS5, showing it has three domains and assigns the parts responsible for import into and killing of target cells, respectively. This knowledge is then used to design chimeric CLBs that can overcome native immunity.

4.2 Results

4.2.1 Structure of PyoS5 in solution

In order to investigate the secondary structure of PyoS5, CD was performed (Section 2.9.2) which revealed a spectrum characteristic for α-helices with differential absorbance troughs at 208 nm and 222 nm (Fig. 4-1). A melting temperature of 57 °C was determined by monitoring thermal melting between 20 °C and 86 °C (Fig. 4-2). The transition from folded protein to unfolded protein was broad which led us to hypothesise that several unfolding events were contributing to this overall melting curve.

To investigate this hypothesis, DSC was used to attain PyoS5 unfolding data with greater resolution (Fig. 4-3) (Section 2.9.4). The DSC spectrum shows an asymmetric peak, made up of a shoulder and a main peak, and one symmetric peak. This confirms that there are at least three independent unfolding events, which suggests that PyoS5 is comprised of three separate domains (Figure 4-3).

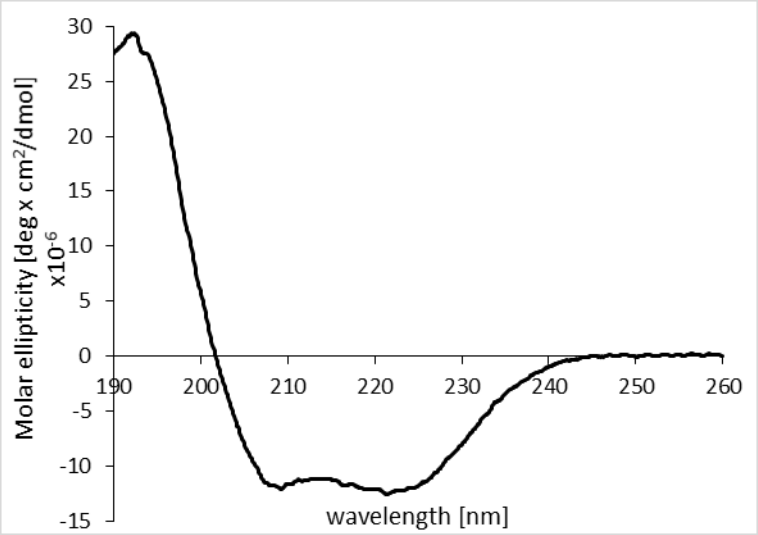

Figure 4-1: CD shows PyoS5 is folded and predominantly α-helical.
CD spectrum of 0.1 mg/mL PyoS5 at room temperature in 20 mM NaCl, 10 mM potassium phosphate buffer pH 7.5.

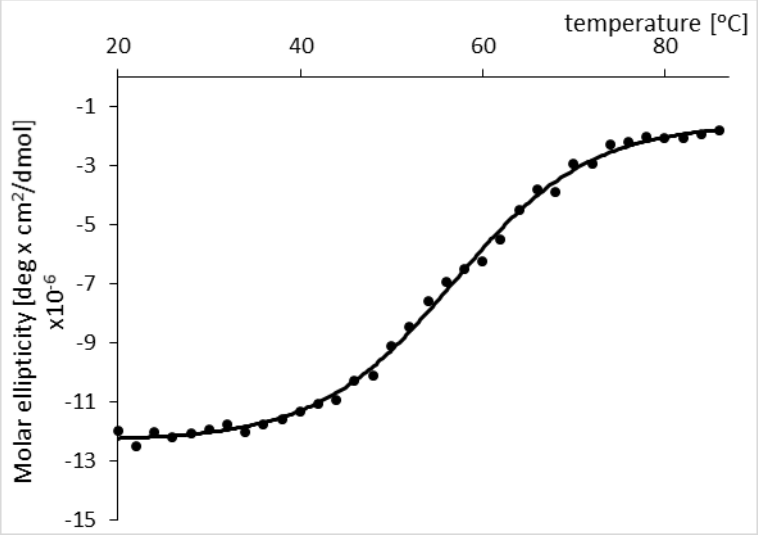

Figure 4-2: The T_m of PyoS5 is 57.3 °C.
A CD thermal melt of 0.1 mg/mL PyoS5 was performed in 20 mM NaCl, 10 mM potassium phosphate buffer pH 7.5 in duplicate and a 4-parameter sigmoidal curve fit to each melting curve. The T_m was calculated to be 57.3±0.7 °C. One repeat is shown and represented as solid circles with associated fit indicated by a solid line.

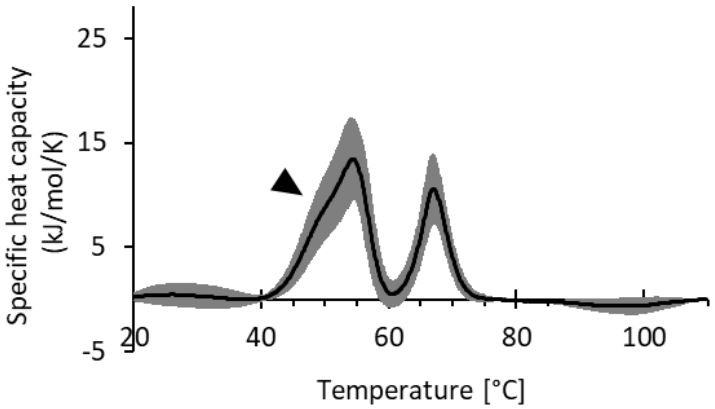

Figure 4-3: PyoS5 has three thermodynamically independent domains.
DSC was performed on PyoS5 in 150 mM NaCl, 50 mM Tris-HCl pH 7.5 and three unfolding events observed, with a shoulder around 50 °C (black arrow head) and peaks at 54.7±0.6 °C and 76.1±0.3 °C. Shown is the mean of three repeats with the standard deviation in grey.

To further investigate how the domains are arranged relative to each other SAXS was employed to determine a low resolution envelope of PyoS5 (Section 2.9.1). Previously a concentration range of PyoS5 had been tested for SAXS (Catriona Thompson, personal communication). Scattering data were collected at the suitable concentration of 5.4 mg/mL of PyoS5 and are consistent with a monodisperse species (Fig. 4-4A). Envelope calculations were performed with no constraints and revealed that PyoS5 is an elongated protein with a length of 197 Å (Fig. 4-4B+C). Along the X-axis of the envelope are several globular partitions consistent with separate domains. Taken together with DSC data it is likely that PyoS5 is comprised of at least three independent domains.

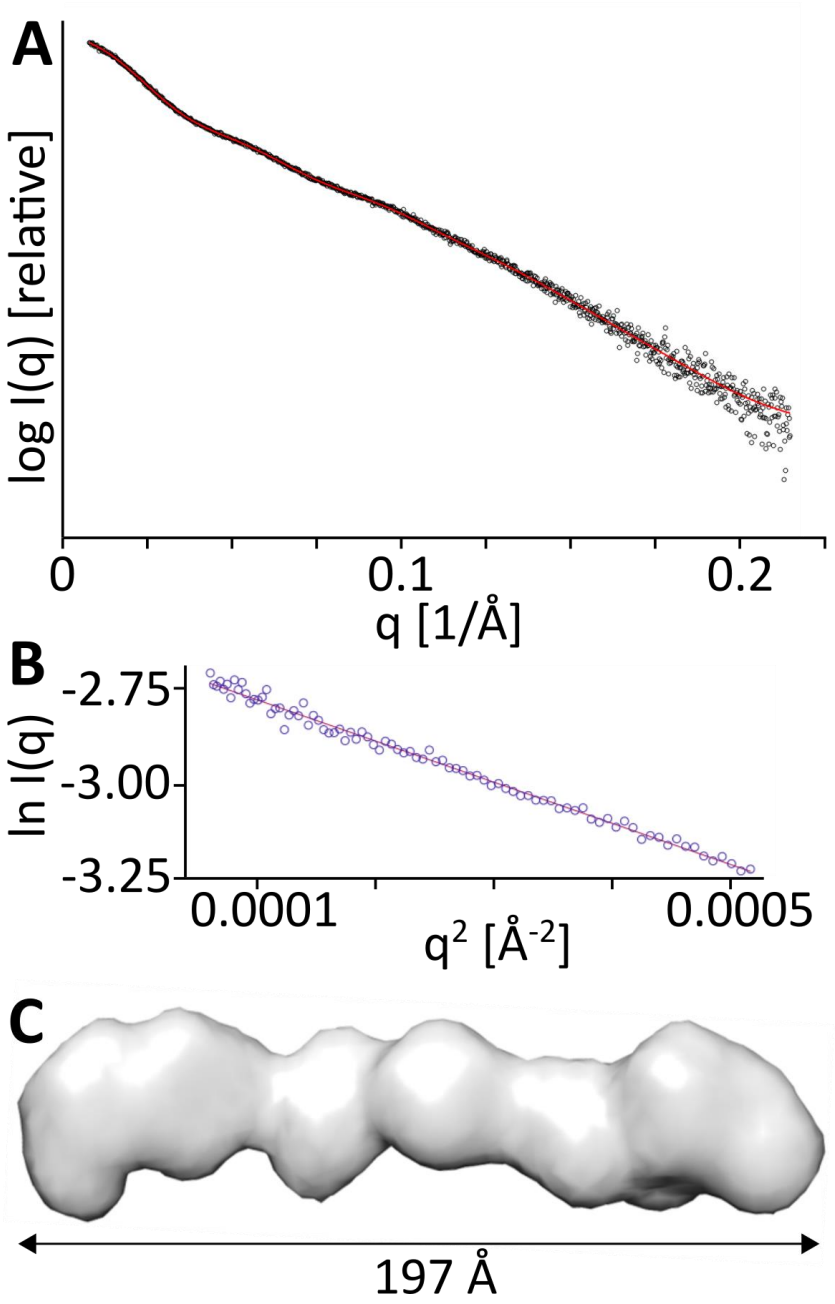

Figure 4-4: SAXS envelope of PyoS5.
(A) SAXS data (black) of PyoS5 at 5.4 mg/mL in HBS buffer pH 7.5 at room temperature with fit of the average DAMMIN model (red). The model fits the data well with a X^2 of 1.114 (B) Guinier fit (red) fitted to the experimental data (blue). (C) SAXS envelopes of the PyoS5 were generated using DAMMIF and refined using DAMMIN. The envelope at a threshold of 1 shows PyoS5 has an elongated conformation. Distinct globular features can be observed within the envelope.

4.2.2 Determination of the PyoS5 structure by X-ray crystallography

To further understand the domain organisation of PyoS5 the atomic structure was solved using X-ray crystallography (Section 2.9.5). From multiple crystal screens the best crystals were obtained in a condition with 10% w/v PEG 3000, 0.1 M sodium acetate,

and 0.1 M zinc acetate, pH 4.5 at 18 °C. Crystals were cryo-protected and frozen in liquid nitrogen prior to mounting and data collection. To identify the area of each crystal with the highest resolution, diffraction grid scanning was employed. Crystals were assigned to the P 1 2_1 1 space group with the unit cell parameters a=50.246, b=53.878, c=104.807, α=90°, β=95.16° and γ=90° (Table 4-1).

Table 4-1: X-ray data processing, refinement and validation statistics for PyoS5.

Data Processing	
X-ray wavelength	0.9679 Å
Space group	P 1 2_1 1
Cell dimensions	a = 50.246 Å, b = 52.878 Å, c = 104.807 Å
Cell angles	α = 90°, β = 95.16°, γ = 90°
Resolution	53.88-2.20 Å (2.27-2.20 Å)
Unique reflections	28285 (2473)
Completeness	98.8 % (99.8 %)
Multiplicity	4.4 (4.6)
CC(1/2)	0.996 (0.728)
R_{meas}	0.179 (2.52)
Refinement	
R_{work}/R_{free}	0.225/0.275
Number of protein atoms	3633
Number of Zn^{2+} atoms	8
Average B-factor	63.91 $Å^2$
Validation	
RMS bonds	0.0096 Å
RMS angles	1.05°
Ramachandran favoured	98.49%
Ramachandran allowed	1.51%
Ramachandran outliers	0%
MolProbity Clashscore	2.76

Values in parenthesis denote highest resolution shell.

Molecular replacement with the pore-forming domain of ColIa was attempted but sufficient phases could not be determined using this model. Staraniso, a feature of AutoProc, allowed the detection of a weak anisotropic signal from Zn^{2+} ions in the original dataset from crystals of native PyoS5. By combining these data with the partial molecular replacement solution it was possible to solve the structure to 2.2 Å (Figure

4-5). There was one copy of PyoS5 in the asymmetric unit and continuous density was observed from residue 40 to the C-terminus.

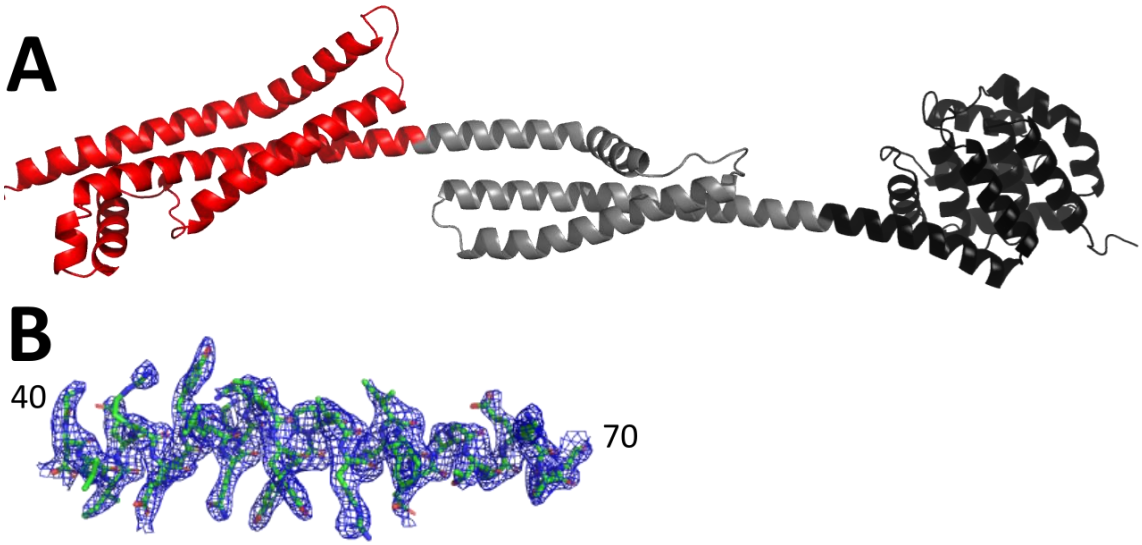

Figure 4-5: Crystal structure of PyoS5.
(A) The 2.2 Å crystal structure of PyoS5 with residues 40 to 195 (red), 196 to 315 (grey) and 315 to 505 (black). Residues 2 to 39 are not resolved in the structure. (B) Electron density (blue) shown at 1.0 σ for PyoS5 residues 40 to 70 (green), the first 31 residues from the N-terminus that were resolved.

Analysis of the structure showed that PyoS5 is comprised of 17 helices making up a very elongated molecule of 194.5 Å in length. The first 39 amino acids from the N-terminus are not resolved in the crystal structure suggesting that this region might be unstructured or flexible.

4.2.3 Analysis of pore-forming domains

Alignment of PyoS5 to the structures of colicin pore-forming domains showed the C-terminal residues 315 to 498 of PyoS5 are organized in the canonical ten helix bundle that is found for pore-forming colicins (Fig. 4-6). Among the six known structures of colicin pore-forming domains, ColIa is most similar to that of PyoS5 with a Root-mean-square deviation (RMSD) of 1.5 Å for the alignment. This is consistent with the high

degree of protein sequence identity between PyoS5 and ColIa (46 %) compared to other CLB pore-forming domains.

Bacteria producing CLBs with pore-forming domains protect themselves from the effect of their toxin with immunity proteins. The immunity proteins of ColE1, ColIa, ColIb, Col5, Col10 and ColK pass the inner membrane three times and are termed E1-type immunity proteins, while the immunity proteins of ColA, ColB, ColN and ColU belong to the A-type and pass the inner membrane four times (Fig. 4-6) (Cascales et al., 2007; Geli et al., 1989; Nilsson and von Heijne, 1990; Song and Cramer, 1991). The structure of PyoS5 provides a third structure of a pore-forming domain with an E1-type immunity protein and allows a comparison of pore-forming domains with immunity proteins of the A-type and E1-type. I find that the different immunity protein topologies between A-type and E1-type CLBs are reflected in the sequence and structure of their pore-forming domains (Fig. 4-6). The main difference between the two groups is the positioning of helices 1 and 5 with respect to each other; in A-type pores helix 1 is positioned close to the centre of the pore-forming domain, pushing out helix 5, while in E1-type pores helix 5 is located closer to the centre (Fig. 4-7).

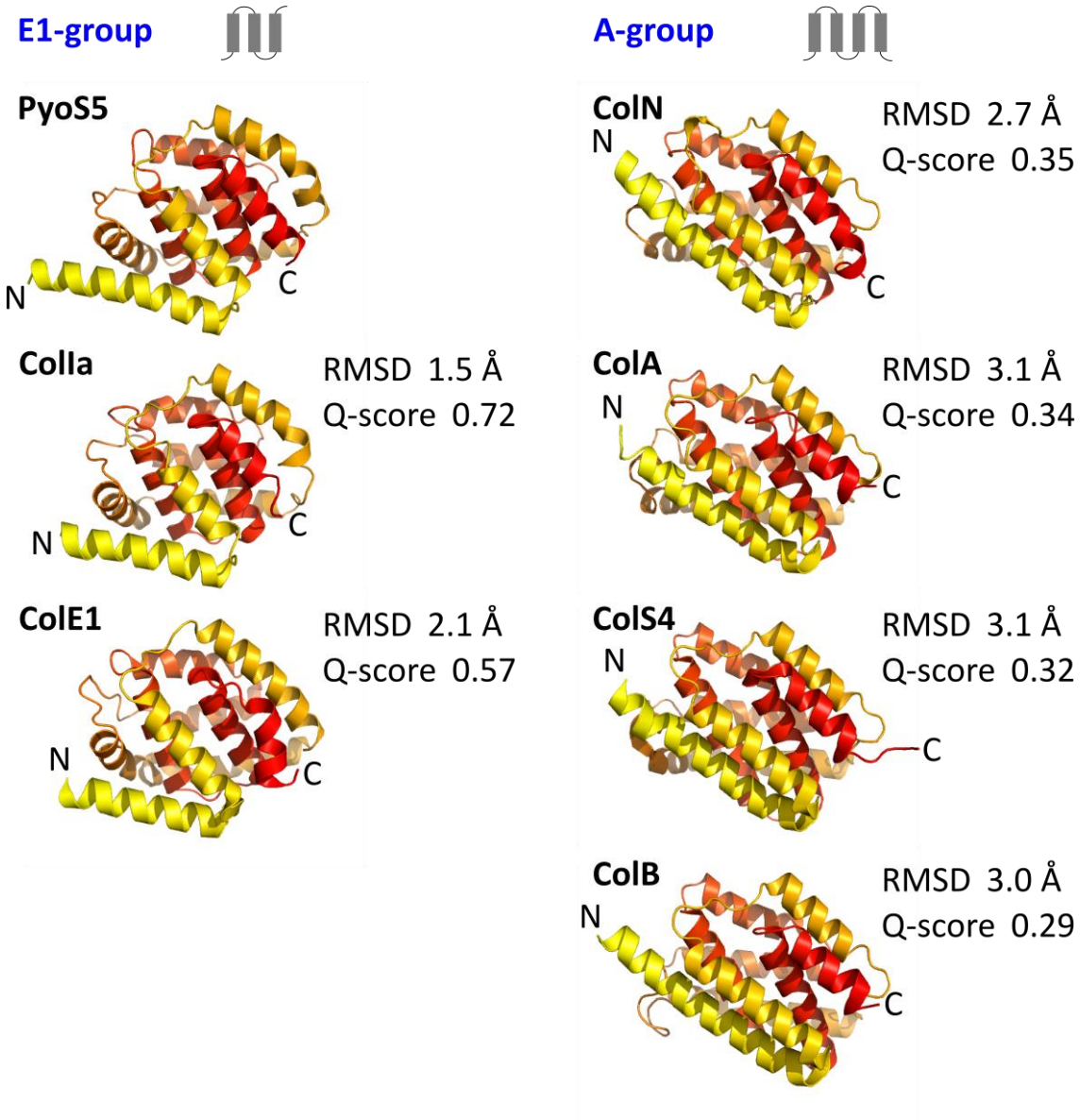

Figure 4-6: Comparison of pore forming domains of CLBs.
All the available structures of CLB pore-forming domains were aligned and coloured in a gradient from yellow (N-terminus) to red (C-terminus). The pores are shown in order of decreasing alignment quality score. All pores in the left column have immunity proteins (Im) that pass the membrane three times, those in the right column have immunity proteins that pass the membrane four times. RMSDs, Q-scores, and immunity protein topologies are shown. The following residues were aligned to PyoS5 residues 315 to 498: ColIa 448 to 624 (PDB 1CII), ColE1 345 to 522 (PDB 2I88), ColN 188 to 486 (PDB 1A87), ColA 393 to 591 (PDB 1COL), ColS4 299 to 499 (PDB 3FEW) and ColB 312 to 511 (PDB 1RH1).

A "jackhmmer" search (Potter et al., 2018) starting with the sequences of the pore-forming domains with known structures (Fig. 4-6), was used to identified more pore-forming domains and highlight the conserved residues (Section 2.11). The sequence e-value cut-offs for the searches were chosen to be 10^{-23} for A-type and 10^{-32} for E1-type

pore-forming domains in order to exclude annotated proteins of the opposite type. 193 sequences of A-type and 730 of E1-type pore-forming domains were identified, suggesting that E1-type pore-forming domains are more common. Conserved residues were identified for each type and mapped onto the structures of PyoS5 and ColA, respectively (Fig. 4-7). PyoS5 residues G339, G355, W435, P437, F459, G468 and G471 were conserved among all pore-forming domains from both types.

In A-type pore-forming domains helix 1 is packed close to the centre of the pore. This is possible because of glycine residues that are conserved in A-type domains (Fig. 4-7A). In contrast, helix 1 in E1-type pore-forming domains is pushed away from the centre of the pore by conserved aromatic residues, interacting between helixes 1, 2, 5 and 8 (Fig. 4-7B). Possible implications of these conserved features and differences between the pore types will be discussed in Section 4.3.

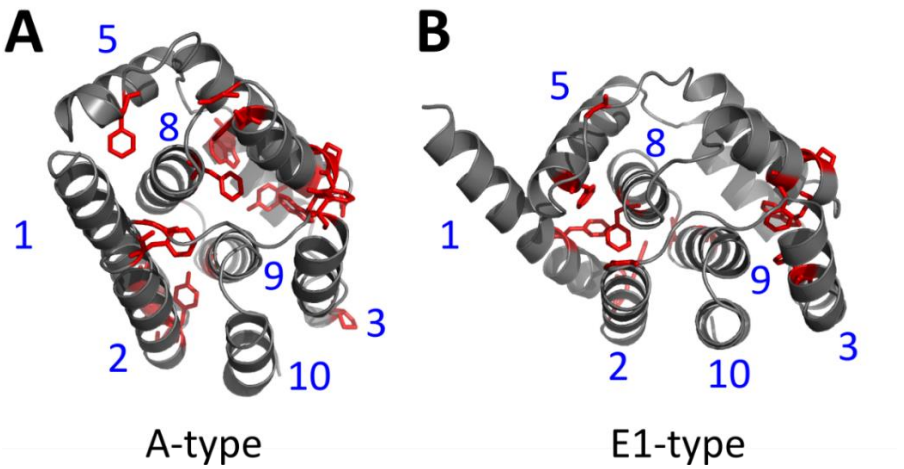

Figure 4-7: Conserved residues in A- and E1-type pore-forming domains.
(A) ColA pore-forming domain with residues conserved among A-type pore-forming domains represented as sticks (red). (B) PyoS5 pore-forming domain with residues conserved among E1-type pore-forming domains highlighted as sticks (red). Helices number denoted in blue with numbering starting from the N-terminus. Conserved residues were identified using the "jackhammer" search algorithm.

4.2.4 PyoS5 contains two similar domains

Next, the N-terminal half of PyoS5 was inspected and revealed two domains with similar fold. The two domains only had 12.4 % amino acid identity but an alignment of the structures of PyoS5 residues 40 to 196 to PyoS5 residues 197 to 315 confirmed that the two domains had a highly similar domain fold with an RMSD of 2.5 Å (Fig. 4-8). The fold is a helical bundle in which a kinked helix (HαI) is connected to a straight helix (HαII) by a loop. HαII packs against both Hα1 and a third straight helix (HαIII) within the bundle. The connection between HαII and HαIII varies between the two copies of the fold. In the N-terminal domain (residues 40-196) HαII is connected to HαIII by a helical turn induced by 3 short helices. In contrast, in the central domain (residues 194-315) HαII and HαIII are connected by a loop sequence. The two copies of this kinked helical bundle domain (kHBD) are connected as the last helix of the N-terminal domain continues to become the kinked helix of the second copy of the fold (Fig. 4-5).

In order to unravel the function of the N-terminal half of PyoS5 I aimed to find proteins with similar domains. PDBefold was used to search for structures with similarity to PyoS5 residues 1 to 315, 1 to 197 and 194 to 315. The top five hits of each search were inspected but no structure showed a helical bundle consisting of a kinked helix followed by two straight helices which was observed in PyoS5.

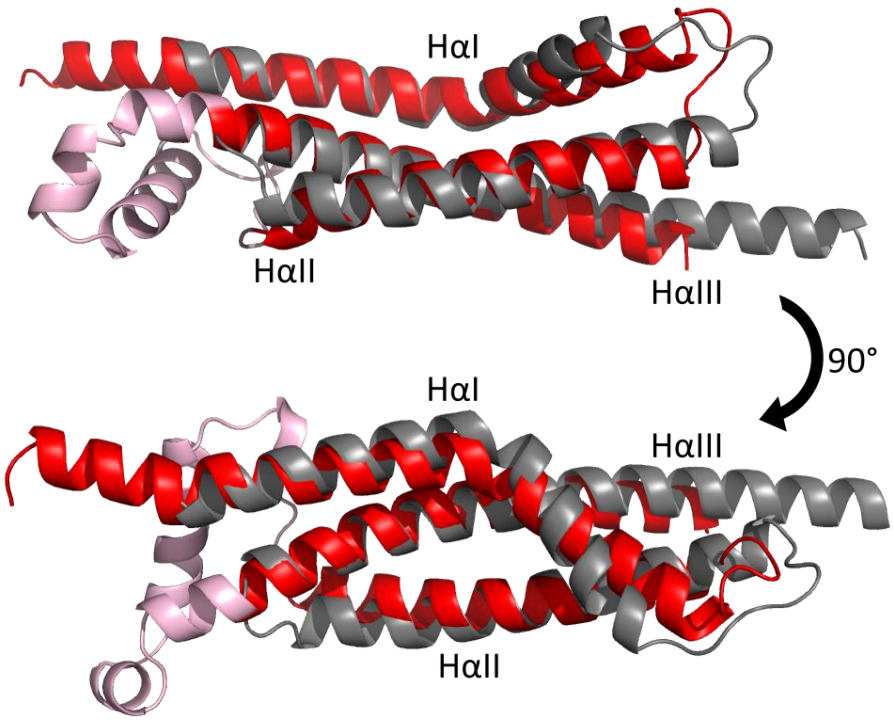

Figure 4-8: Alignment of PyoS5$_{40-196}$ and PyoS5$_{194-315}$.
The overlay shows PyoS5$_{40-196}$ (red) aligned to PyoS5$_{194-315}$ (grey) with an RMSD of 2.51. The lower view is rotated by 90° around the x-axis. The additional helical turn present in PyoS5$_{40-196}$, consisting of residues 123-162 (pink), was excluded from the alignment.

An equivalent search was also performed using NCBI VAST. No structures with similarity to PyoS5 residues 1 to 315, six structures with similarity to PyoS5 residues 1 to 197 and four structures with similarity to PyoS5 residues 194 to 315 were found. These structures were inspected and again none of them showed the topology of a kinked helix followed by two straight helices arranged into an α-helical bundle. In conclusion, no structures similar to the N-terminal half of PyoS5 were found, suggesting the kHBD may be a novel fold.

4.2.5 Comparison of solution data with the PyoS5 crystal structure

To determine if the crystal structure of PyoS5 is consistent with the structure in solution, it was fit into the SAXS-derived envelope (Fig. 4-9). Alignment parameters confirm that 93 % of the crystal structure's residues fit inside the envelope. Based on this and visual inspection of the fit, it was concluded that the structure determined for PyoS5 using X-

ray crystallography is not a crystal packing artefact and is in fact representative of the structure observed in solution by SAXS.

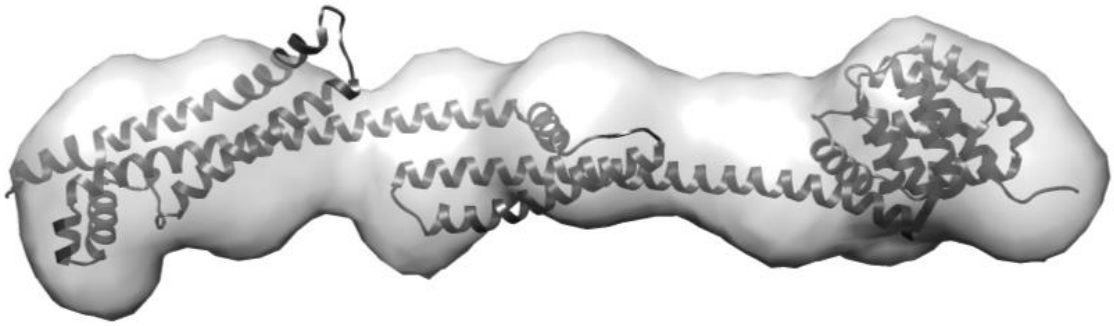

Figure 4-9: The PyoS5 crystal structure is consistent with SAXS envelope density.
PyoS5 docked into the SAXS envelope set at a threshold of 1 in Chimera, results in 93 % of the atoms of the crystal structure inside the envelope.

I inspected the crystal structure of PyoS5 and hypothesized that the three domains observed in DSC corresponded to residues 1 to 195, 195 to 315, which are the two copies of the kHBD, and 315 to 498, which is similar to the ColIa pore-forming domain. The constructs $PyoS5_{1\text{-}315}$, $PyoS5_{1\text{-}196}$, and $PyoS5_{194\text{-}315}$ were purified and investigated by CD and DSC to interrogate this hypothesis. The construct $PyoS5_{1\text{-}315}$ was termed TR as it only lacks the pore-forming domain and based on domain arrangement in other CLBs is likely to harbour the translocation and receptor-binding activity of PyoS5.

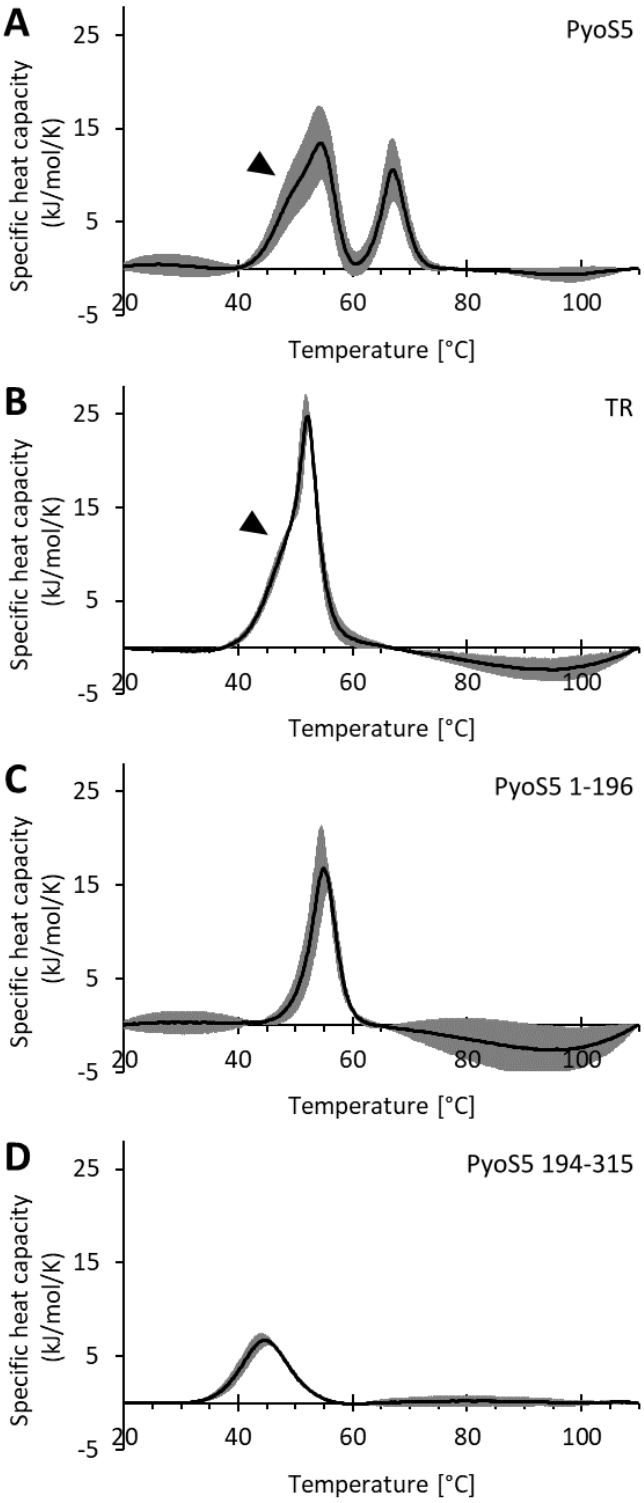

Figure 4-10: Thermal unfolding of individual PyoS5 domains.
Average DSC spectra of (A) PyoS5, (B) TR, (C) PyoS51-196 and (D) PyoS5194-315 in 150 mM NaCl 50 mM Tris-HCl pH 7.5 from three repeats with one standard deviation shown (grey). TR shows a shoulder centred around 47 °C and a peak at 52.1 ±0.4 °C, PyoS51-196 shows a peak at 55.1 ±0.7 °C and PyoS5194-315 at 44.7 ±0.8 °C.

The DSC spectrum of the TR construct showed the peaks similar to the two lower temperature transitions observed for full length PyoS5. The first transition occurred at around 47 °C compared to approximately 50 °C in PyoS5 and the second transition occurred at 52 °C instead of 55 °C, suggesting that the C-terminal pore-forming domain stabilized the other domains (Fig. 4-10A). The spectra of PyoS5$_{1\text{-}196}$ and PyoS5$_{194\text{-}315}$ showed only a single peak each, suggesting that they each contain only one domain (Fig. 4-10B+C). The transition observed for PyoS5$_{194\text{-}315}$ occurred at lower temperatures and peaked at 45 °C; the transition observed for PyoS5$_{1\text{-}196}$ was at 55 °C. Mapping these transitions onto those of full length PyoS5 leads to the assignment of PyoS5$_{194\text{-}315}$ to the first transition peak observed, PyoS5$_{1\text{-}196}$ to the second and the pore-forming domain from residues 315 to 498 to the third.

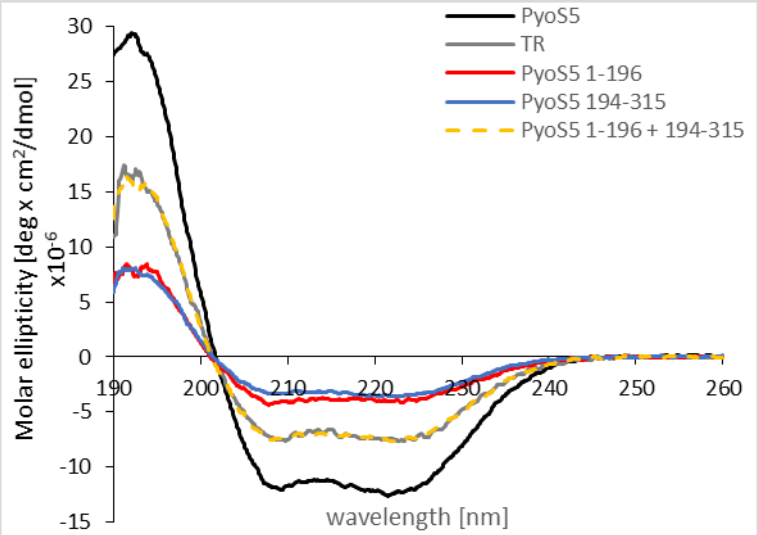

Figure 4-11: CD of PyoS5 domains.
CD spectra of 0.1 mg/mL PyoS5 (black), TR (grey), PyoS5$_{1\text{-}196}$ (red) and PyoS5$_{194\text{-}315}$ (blue) at RT in 20 mM NaCl, 10 mM potassium phosphate buffer pH 7.5 show PyoS5 and its domains are helical and folded. The sum of the molar ellipticity from PyoS5$_{1\text{-}196}$ and PyoS5$_{194\text{-}315}$ (dashed yellow) shows both constructs are fully folded compared to TR.

The CD spectra of all constructs, PyoS5, TR, PyoS5$_{1\text{-}196}$ and PyoS5$_{194\text{-}315}$, revealed predominantly helical secondary structure which is in accordance with the structure observed by crystallography which shows 87 % of all residues forming α-helices (Fig. 4-

11). Addition of the curves generated by PyoS5$_{1\text{-}196}$ and PyoS5$_{194\text{-}315}$ results in a curve identical to that generated by TR (Fig. 4-11). Furthermore, CD thermal melts showed narrower transitions for PyoS5$_{1\text{-}196}$ and PyoS5$_{194\text{-}315}$ than for TR, which was itself narrower than the transition observed for full length PyoS5 (Fig. 4-12). This confirmed that the transition observed in thermal melt data for PyoS5 was broad because several domain-unfolding events were contributing to it. The T_m values extracted from CD thermal melts also agreed with those determined by DSC.

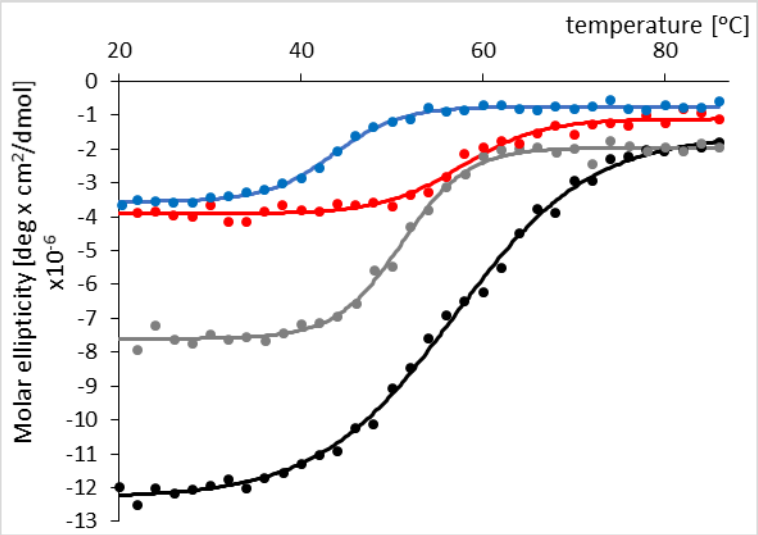

Figure 4-12: PyoS5 domains have different T_ms.
CD thermal melts of 0.1 mg/mL PyoS5 (black) T_m 57.3 ±0.7 °C, TR (grey) T_m 51.0 ±0.1 °C, PyoS5$_{1\text{-}196}$ (red) T_m 57.5 ±0.0 °C, and PyoS5$_{194\text{-}315}$ (blue) T_m 43.7 ±0.3 °C in 20 mM NaCl, 10 mM potassium phosphate buffer pH 7.5. Two repeats were performed; one is shown as circles with their fits as lines.

4.2.6 Translocation and pore-formation

Based on the structure and sequence similarity of residues 315 to 498 of PyoS5 with other pore forming domains I assigned this as the cytotoxic domain. If this hypothesis was correct then removal of this domain might result in a non-toxic protein, which retains its ability to translocate into *P. aeruginosa* cells. Application of TR to *P. aeruginosa* YHP17, which are susceptible to PyoS5, did not result in any zones of clearance,

consistent with cytotoxic activity residing in a domain spanning residues 315 to 498 (Fig. 4-13).

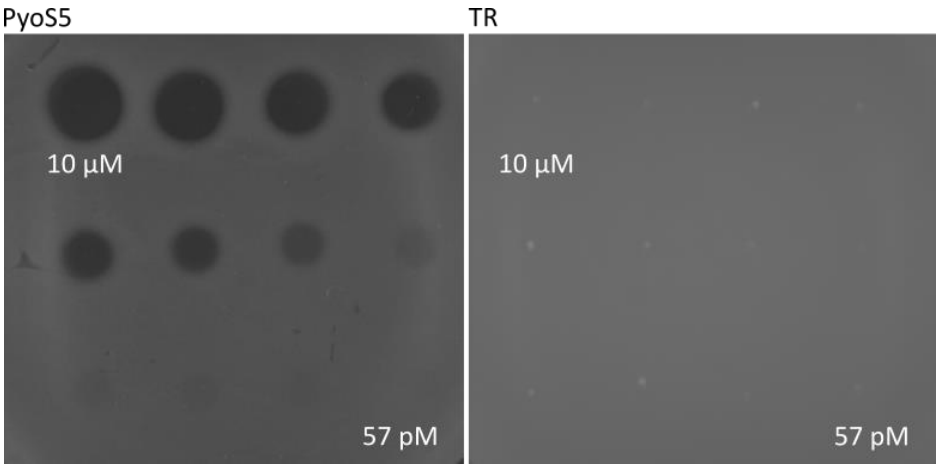

Figure 4-13: TR does not inhibit *P. aeruginosa* YHP17.
A 3-fold serial dilution of purified PyoS5 (left) or TR (right) starting at 10 µM, spotted onto the soft agar containing *P. aeruginosa* YHP17. No zones of clearance from TR were observed.

To test whether TR alone could cross the outer membrane, a AF488 label was chemically attached to a C-terminal cysteine engineered onto TR (Section 2.10.1), the labelled TR protein TR-AF488 was incubated with live *P. aeruginosa* cells and after 20 min excess protein was washed away (Section 2.10.3). Fluorescence microscopy imaging of the cells showed that these cells were labelled with AF488 (Fig. 4-14). To determine whether the fluorescent TR construct had crossed the outer membrane or was bound to the cell surface, the labelled cells were treated with trypsin to remove any surface exposed protein. This resulted in reduced fluorescence intensity suggesting that the majority of the signal was surface bound, but also that TR was capable of translocation through the outer membrane (Fig. 4-14).

To test if this was an energy dependent translocation mechanism, the cells were treated with PMF inhibitor CCCP, prior to labelling with TR. CCCP treated cells showed a reduced total fluorescence per cell and after trypsin cleavage no fluorescent signal was

observed. This suggested that energy from the PMF is required for the translocation of the TR domain across the outer membrane but not for binding to the cell surface (Fig. 4-14). The requirement of energy for translocation was the first indication that the import of PyoS5 is an active transport process mediated by an outer membrane translocator.

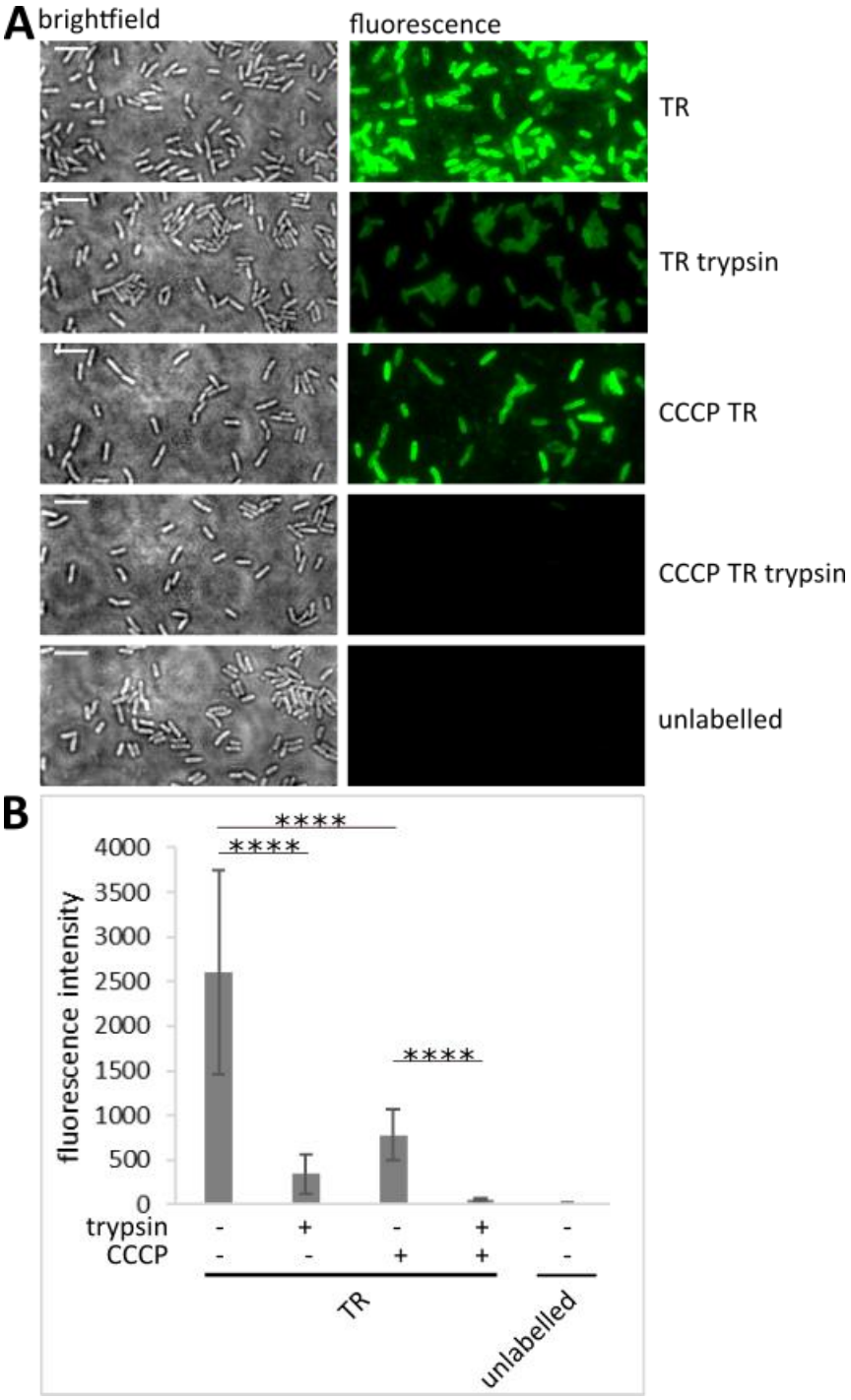

Figure 4-14: TR translocates across the *P. aeruginosa* outer membrane.
(A) Fluorescent labelling of live *P. aeruginosa* PAO1 cells with TR-AF488. Additionally, the effects of depleting the PMF with CCCP before incubation with TF-AF488 and of trypsin treatment to remove surface exposed TR-AF488 after incubation with TR-AF488 were examined. Scale bars 5 µm. (B) Quantification of the average cell fluorescence observed under different conditions tested in A. **** indicates a p-value below 0.0001 in Student's t-test.

If PyoS5 uptake and toxicity was limited by receptor availability, an excess of isolated TR might prevent or reduce cytotoxicity. This was confirmed in a liquid killing assay

when culture of *P. aeruginosa* YHP17 in LB medium was incubated with PyoS5 and a 100-fold excess of TR and compared with a control in the absence of TR (Fig. 4-15). However, no protective effect was observed for the individual domains $PyoS5_{1\text{-}196}$ and $PyoS5_{194\text{-}315}$ (Fig. 4-15).

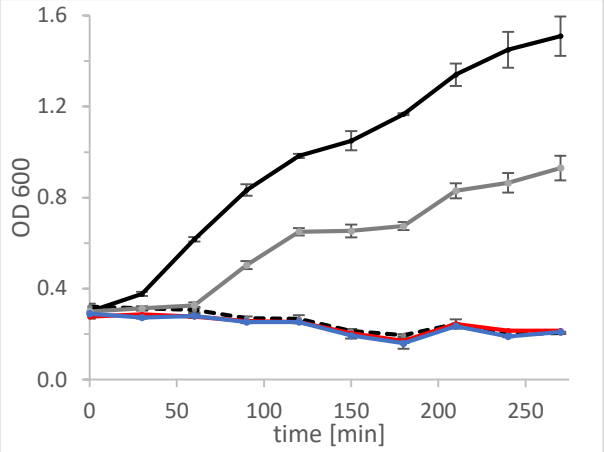

Figure 4-15: In liquid culture killing competition TR inhibits PyoS5 activity.
P. aeruginosa YHP17 grown to OD 0.3 in LB medium. Growth was monitored under the following conditions; no pyocin (black), 20 µM PyoS5 (black dashed), 20 µM PyoS5 plus 2 mM TR (grey), 20 µM PyoS5 plus 2 mM $PyoS5_{1\text{-}196}$ (red), and 20 µM PyoS5 plus 2 mM $PyoS5_{194\text{-}315}$ (blue).

4.2.7 Chimera to overcome immunity and target new species

With the knowledge that TR is able to cross the outer membrane of *P. aeruginosa* while the pore-forming domain harbours the cytotoxic activity, I sought to design chimeras that could target other species and overcome the native immunity conveyed by ImS5, for example to strain *P. aeruginosa* PAO1.

First, I aimed to construct a chimeric bacteriocin against *E. coil*, because colicins are well characterized and *E. coli* is a member of the *Enterobacteriaceae* family which is also among the three pathogens of highest priority for antibiotic development (WHO, 2017). A chimera of ColB residues 1 to 340, providing the receptor-binding and translocation activity required for crossing the *E.coli* outer membrane, and PyoS5 residues 303 to 498

providing pore-forming cytotoxic activity, was constructed. A plate killing assay where ColBPyoS5 was spotted on to *E. coli* BL21 (DE3) found the chimera to inhibit growth of *E. coli* down to the lowest tested concentration of 57 pM (Fig. 4-16). As expected this chimera was not capable of killing *P. aeruginosa* (Fig. 6-1).

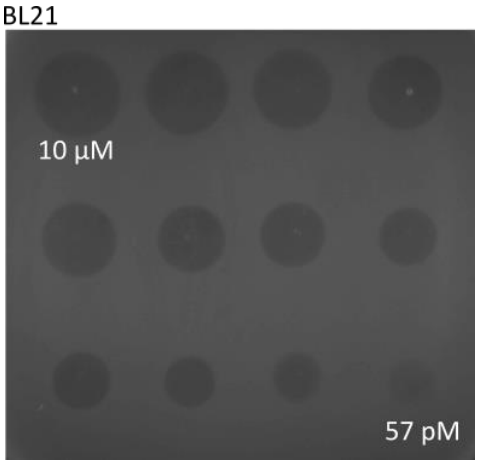

Figure 4-16: ColBS5 kills *E. coli*.
ColBPyoS5 was spotted onto *E. coli* BL21 (DE3) grown in LB-agar in three-fold dilutions starting at 10 µM. Clearance zones were observed down to the lowest concentration of 56 pM.

Next, I wanted to overcome the native immunity against PyoS5 that is present in some *P. aeruginosa* strains, such as PAO1, and is conveyed by immunity proteins expressed from genes downstream of the respective bacteriocin. I hypothesized that exchanging the PyoS5 pore-forming domain for one from another CLB which *P. aeruginosa* PAO1 is not immune against would yield an antibiotic that overcomes the native immunity to PyoS5. It is unknown if immunity proteins against pore-forming CLBs can cross-protect against cytotoxic domains similar to their own. Therefore, I expressed the PyoS5 immunity protein, ImS5, in *E. coli* to test whether it would protect against ColIa toxicity, which has the pore-forming domain most similar to PyoS5. Plate killing assays revealed that expression of ImS5 in *E. coli* did not provide protection against ColIa killing (Fig. 4-17). At the same time, killing of *E. coli* by ColBPyoS5 was inhibited by the expression of ImS5, showing that heterogeneously expressed ImS5 was functional in *E. coli* and

ImS5 is specific to the pore-forming domain of PyoS5 (Fig. 4-17). The ColIa pore-forming domain was therefore determined to be a suitable candidate to overcome PyoS5 immunity.

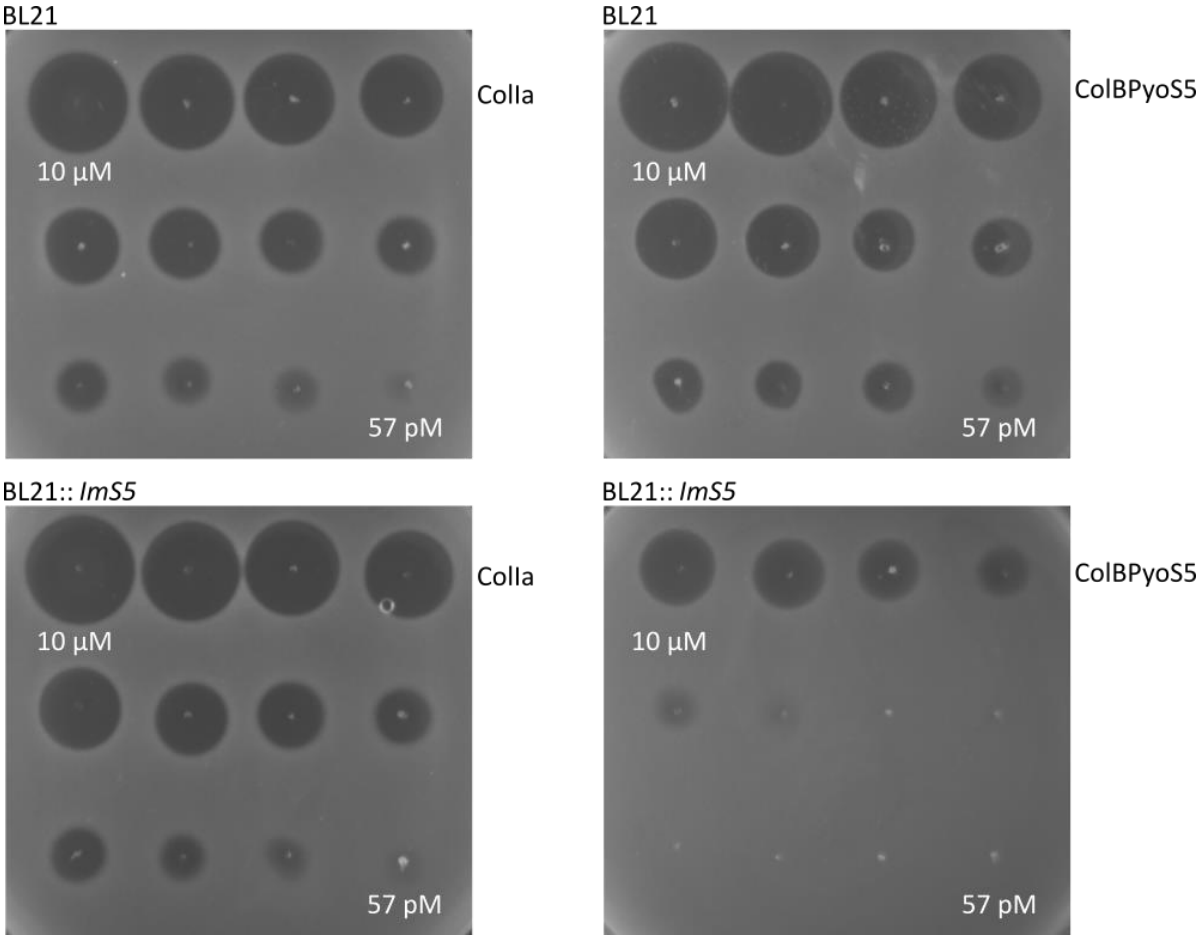

Figure 4-17: ColIa is not inhibited by ImS5.
ColIa and ColBPyoS5 were spotted onto *E. coli* BL21 (DE3) and *E. coli* BL21 (DE3) expressing ImS5, grown in LB-agar in three-fold dilutions starting at 10 µM.

I next constructed a chimera made from PyoS5 residues 1 to 315 and ColIa residues 485 to 626. Plate killing assays showed that the PyoS5ColIa chimera inhibited *P. aeruginosa* PAO1 under conditions were PyoS5 did not (Fig. 4-18). Against *P. aeruginosa* YHP17, a strain susceptible to PyoS5, inhibition by PyoS5ColIa was observed (Fig. 4-19), however, the clearance zones were weaker when compared with those from PyoS5 and the lowest inhibiting concentration was 18-fold higher than for PyoS5 (Fig. 3-4). This

suggests that PyoS5 is more potent than PyoS5ColIa while PyoS5ColIa can overcome native immunity conveyed to some *P. aeruginosa* strains by ImS5.

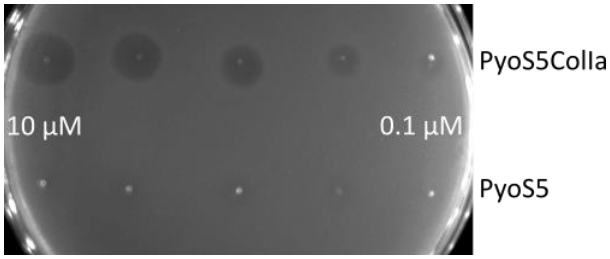

Figure 4-18: *P. aeruginosa* PAO1 is susceptible to PyoS5ColIa but not to PyoS5.
PyoS5ColIa and PyoS5 were spotted onto *P. aeruginosa* PAO1 grown in M9-agar in three-fold dilutions starting at 10 µM.

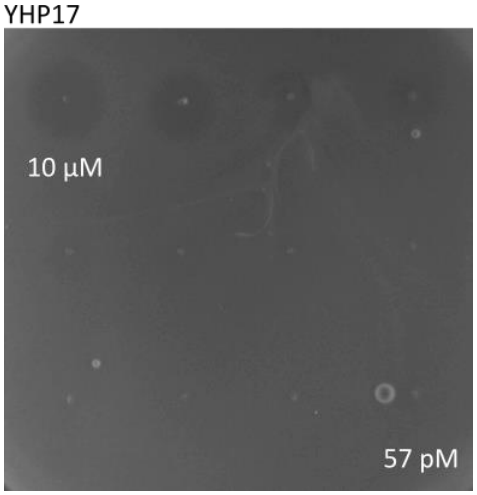

Figure 4-19: *P. aeruginosa* YHP17 is moderately susceptible to PyoS5ColIa.
PyoS5ColIa was spotted onto *P. aeruginosa* YHP17 grown in LB-agar in three-fold dilutions starting at 10 µM.

4.3 Discussion

The structural and biophysical data presented here show that PyoS5 has three folded and functional domains and an unstructured or flexible N-terminal region. The function of the C-terminal domain from residues 315 to 498 was confirmed to harbour the cytotoxic activity, which had been previously identified as pore-forming (Ling et al., 2010; Parret and De Mot, 2000). The N-terminal region and the remaining two N-terminal domains

were found to be involved in cell surface binding and translocation, however, the details of this remain to be elucidated in the chapters to come.

PyoS5 is the second example of a CLB with a duplicated domain fold. The first example was ColS4, which harbours two copies of its receptor-binding domain (Arnold et al., 2009). With 61 % amino acid sequence identity and an RMSD of 0.7 Å they have much higher similarity to each other than the two kHBDs in PyoS5 and the domain duplication in ColS4 was identified based on sequence similarity before structural information was available. In agreement with the high similarity is the conserved function of the ColS4 receptor-binding domain. Both bind to OmpW by the same conserved residues and only one copy is required to be active for ColS4 cytotoxicity (Arnold et al., 2009).

A comparison of the PyoS5 pore-forming domain with structures of pore-forming domains from other CLBs, revealed that differences in the topology of immunity proteins correlate with differences in the sequence and structure of the pore-forming domains. Previously E1-type immunity proteins were found to interact with helices 6 and 7 of the pore-forming domains, while A-type immunity proteins were found to interact with helices 8 and 9 (Lin et al., 2005; Pilsl and Braun, 1995; Zhang and Cramerz, 1993). Surprisingly, these helices do not carry many of the residues conserved within each group that I identify here. It is therefore possible that the conserved residues identified are important for the cytotoxic activity of the pore-forming domain rather than for the interaction with the immunity proteins. Mutating the conserved residues has the potential to clarify if their role is in correct folding, immunity protein binding or cytotoxicity. Such mutations could yield inactive-cytotoxic domains, that can be exploited for the study of

pore-forming CLBs or an active pore-forming domain that cannot be recognized by its immunity protein which might be useful as a therapeutic (Pilsl et al., 1998).

Previous attempts to engineer bacteriocins to yield better antibiotics have focussed on chimera between bacteriocins and other proteins including T4 lysozyme (Lukacik et al., 2012), phage proteins (Jakes et al., 1988), pheromones (Qiu et al., 2003), antibodies or ligands (Qiu, 2006). An easier approach is to combine bacteriocin domains from different species as was used here. ColBPyoS5 and PyoS5ColIa have demonstrated for the first time cytotoxic activity of a pyocin pore-forming domain against *E. coli* and of a colicin pore-forming domain against *P. aeruginosa*. I also show here for the first time that a pore-forming pyocin's immunity protein can be functional in *E. coli*. In conclusion, all features required for insertion of the pore-forming domain and the immunity protein into the inner membrane are conserved between *E. coli* and *P. aeruginosa*.

The exchangeability of pore-forming domains between *E. coli* and *P. aeruginosa* opens up the possibility of chimeric bacteriocins that overcome native immunity in different strains. This is exemplified in this chapter where it has been shown that the ColIa pore-forming domain can overcome PyoS5 immunity and it will be interesting to see in the future whether the opposite is also true.

5. Identification of CPA- and FptA-binding domains

5.1 Introduction

All CLBs interact with outer membrane components to overcome the barrier of the outer membrane. As described in Chapter 1, each Tol-dependent colicin first attaches to a specific TBDT, which acts as a receptor, (with exception of ColN which binds to LPS) and then translocates through another outer membrane protein, the translocator. Ton-dependent colicins are more diverse in their import mechanisms (reviewed in Section 1.3.2). ColM, Col5 and Col10 use a TBDT as a receptor and TolC as a translocator; FepA acts as a translocator and possibly also as a receptor for ColB and ColD; ColIa uses one copy of Cir as a receptor and a second copy as a translocator (Table 1-1). Among pyocins, PaeM1, PaeM2, PaeM4, PyoL2 and PyoS4 are known to depend on one outer membrane protein, but it is not clear whether additional outer membrane components are involved (Table 1-2). PyoL1, PyoS2, PyoS3, PyoS5, PyoSD2 and PyoSD3 all depend on an outer membrane protein for their cytotoxicity and also bind CPA, a polysaccharides antigen that caps LPS molecules (Table 1-2).

As opposed to O-specific antigen that determines the strain's serogroup, CPA is common to all *P. aeruginosa* strains and exclusively occurs in this species. In PyoS2, which also binds CPA, the CPA-binding capacity has been shown to reside with residues 217 to 318 (McCaughey et al., 2016a). PyoS5 residues 216 to 318 show 76% amino acid identity to this region and were therefore hypothesized to bind CPA. However, given that these residues are also part of the domain fold that occurs twice in PyoS5, the idea of two CPA-binding sites within PyoS5 is also feasible. While it is known that susceptibility to SD2 is reduced in CPA deficient strains (McCaughey et al., 2016a), it is not known whether CPA influences PyoS5 susceptibility.

Transposon insertions into the *fptA* gene, which encodes the siderophore receptor FptA, were found to abolish PyoS5-susceptibility (Elfarash et al., 2014). FptA is therefore a strong candidate for the PyoS5 translocator but direct interaction between FptA and PyoS5 has not been shown.

Chapter 4 showed that the first 315 residues of PyoS5 are sufficient to translocate across the outer membrane of *P. aeruginosa*. Chapter 5 aims to delineate how the individual domains in this region interact with outer membrane components and how this contributes to the translocation of PyoS5. Considering the TR region consists of two copies of the kHBD fold it will be interesting to see whether both copies serve the same function or whether the fold has been conserved while the function diverged.

5.2 Results

5.2.1 PyoS5$_{194\text{-}315}$ binds CPA

ITC was used to confirm the previously observed binding between CPA and PyoS5 (McCaughey et al., 2016a) and to narrow down the CPA-binding site of PyoS5 (Section 2.8.4). Saturating heats, which are indicative of binding, were observed when the PyoS5 TR construct was titrated into *P. aeruginosa* PAO1 LPS-derived polysaccharides containing CPA and a K_D of 0.6 µM was obtained for the interaction (Fig. 5-1A). Saturating heats of binding were also observed when PyoS5$_{194\text{-}315}$ was titrated into *P. aeruginosa* PAO1 polysaccharides yielding a K_D of 0.3 µM (Fig. 5-1C) which is not significantly ($p=0.28$) different from that observed for TR or from the previously published K_D of 1.19 µM ($p=0.23$) for full length PyoS5 (McCaughey et al., 2016a).

A titration of PyoS5$_{1\text{-}196}$ into *P. aeruginosa* PAO1 LPS-derived polysaccharides did not yield any saturating heats (Fig. 5-1B). Titration of PyoS5$_{194\text{-}315}$, which did bind *P. aeruginosa* PAO1 polysaccharides, did not yield saturating heats when titrated into LPS polysaccharides derived from *P. aeruginosa* PAO1 Δ*rmd*, a strain that produces O-antigen but not CPA (Fig. 5-1C) (Rocchetta et al., 1998).

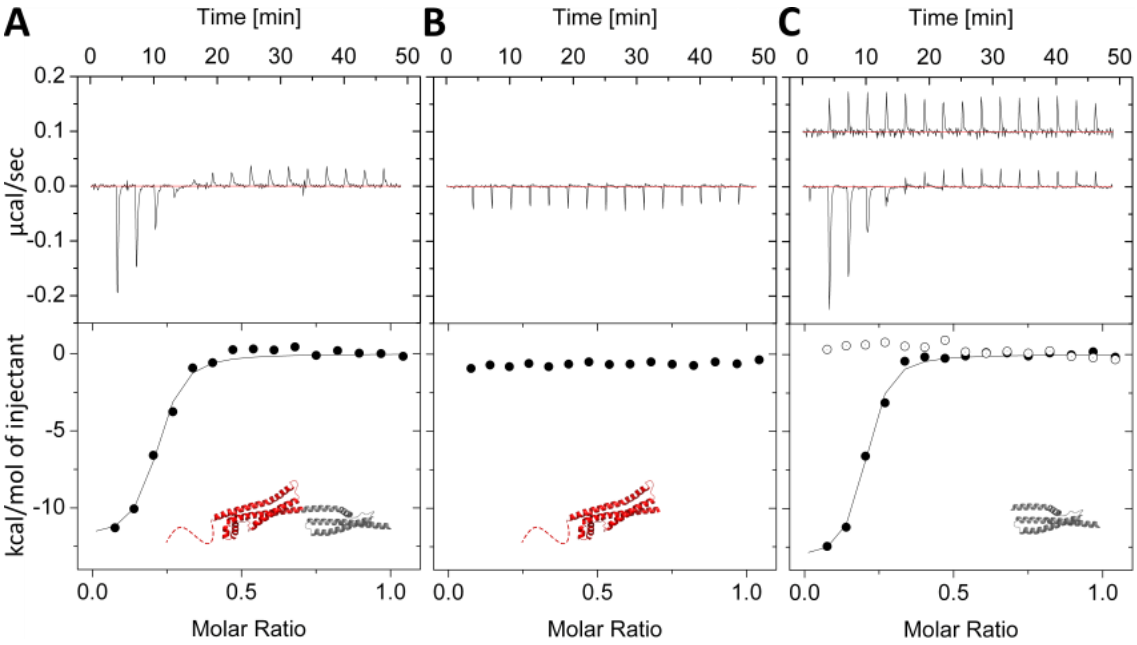

Figure 5-1: TR binds LPS-derived polysaccharides from *P. aeruginosa* PAO1.
(A) ITC data of 150 µM TR titrated into 7 mg/mL *P. aeruginosa* PAO1 LPS-derived polysaccharide containing CPA and OSA. Binding occurred with a K_D of 612 ±332 nM, ΔH of -18 ±6 kcal/mol, ΔS of -32 ±22 cal/mol/K and N of 0.16 ±0.04. (B) ITC data of 150 µM PyoS5$_{1\text{-}196}$ titrated into 7 mg/mL *P. aeruginosa* PAO1 LPS-derived polysaccharide containing CPA and OSA. No binding was observed. (C) ITC data of 150 µM PyoS5$_{194\text{-}315}$ titrated into 7 mg/mL *P. aeruginosa* PAO1 LPS-derived polysaccharide containing CPA and OSA (closed circles). Binding occurred with a K_D of 269 ±44 nM, ΔH of -14 ±0.3 kcal/mol, ΔS of -16 ±1 cal/mol/K and N of 0.56 ±0.36. ITC data of 150 µM PyoS5$_{194\text{-}315}$ titrated into 7 mg/mL *P. aeruginosa* Δ*rmd* LPS-derived polysaccharide containing OSA only (open circles). No binding was observed. All ITC reactions were performed in duplicate in 0.2 M Na-phosphate buffer pH 7.5 at 25 °C and one repeat is shown. Data were corrected for heats of dilution by subtracting the average of the last five injections and fit to a model of single-site binding.

Together, these results indicated that full CPA-binding activity of PyoS5 resides within residues 194 to 315, and that the PyoS5$_{194\text{-}315}$ construct retained full CPA-binding activity

compared to the TR construct. The results also suggest that the CPA-binding domain ($PyoS5_{194-315}$) might bind CPA tighter than the full length PyoS5.

5.2.2 Distribution and conservation of CPA-binding domains

PyoS2 and PyoSD3 have been shown to bind CPA and harbour domains homologous to the PyoS5 CPA-binding domain with protein sequence identities of 76 % (S2 to S5) and 49 % (SD3 to S5), and homologous to each other with 54% identity (S2 to SD3). The PyoS5 crystal structure contained the first structural information on these CPA-binding domains and was thus used as a template to build homology models of the equivalent domains of PyoS2 and PyoSD3 (Fig. 5-2).

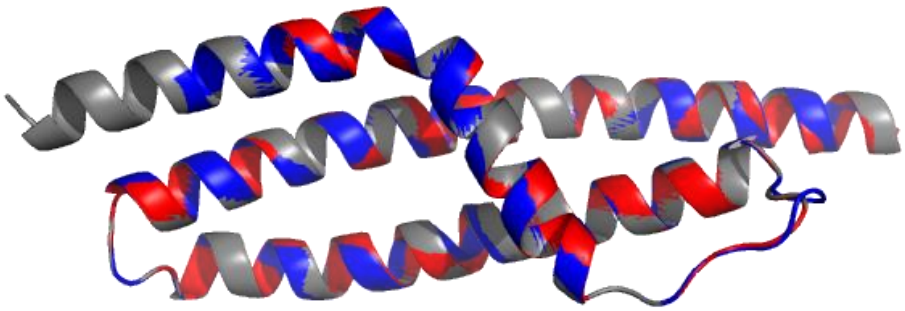

Figure 5-2: Homology models of the PyoS2 and PyoSD3 CPA-binding domains.
SwissModel homology models of PyoS2 (red) and PyoSD3 (blue) CPA-binding domains were built using PyoS5 (grey) residues 194 to 315 as a template. The model quality was good with a QMEAN score of 0.49 and an RMSD of 0.30 Å over 104 residues for PyoS2 and a QMEAN score of 1.04 and an RMSD of 0.72 Å over 112 residues for PyoSD3.

Across the three CPA-binding domains of PyoS2, PyoSD3 and PyoS5, there is 39 % sequence identity. Of these 45 residues, 28 form the surface of a groove that runs perpendicular to the long axis of PyoS5 and the remainder of the conserved residues is distributed along the long axis of PyoS5 (Fig. 5-3).

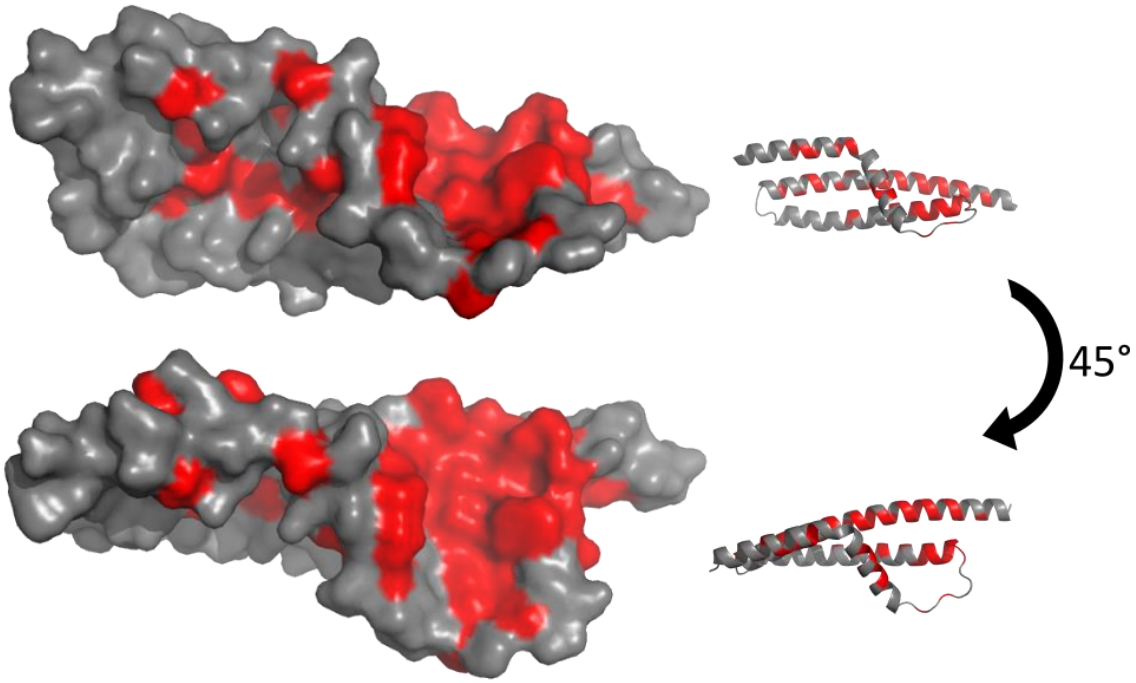

Figure 5-3: Conserved residues between PyoS2, PyoSD3 and PyoS5 CPA-binding domains. Residues identical in all three CPA-binding domains (red) are mapped onto the PyoS5 CPA-binding domain (grey). Surface and cartoon representation are shown at two different angles.

5.2.3 CPA binding accumulates PyoS5 on the cell surface

It was clear from ITC experiments that PyoS5 residues 194 to 315 bind CPA but how and whether this binding is relevant to the import and function of PyoS5 remained unresolved. To understand whether CPA influences PyoS5-susceptibility, a cytotoxicity assay was performed on the CPA-deficient strain *P. aeruginosa* PAO1 Δ*rmd*. As this strain is a derivative of *P. aeruginosa* PAO1, it is not susceptible PyoS5, therefore PyoS5ColIa was used to overcome the immunity of both *P. aeruginosa* PAO1 and *P. aeruginosa* PAO1 Δ*rmd*. CPA-deficient *P. aeruginosa* had 9-fold reduced susceptibility compared to the parent strain but was not completely resistant (Fig. 5-4).

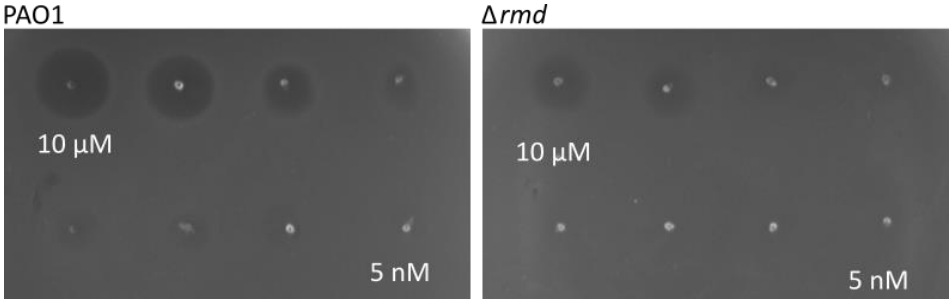

Figure 5-4: CPA increases susceptibility to PyoS5ColIa.
3-fold serial dilution starting at 10 µM spotted onto the soft agar containing *P. aeruginosa* PAO1 or *P. aeruginosa* PAO1 Δ*rmd* from top left to bottom right. In the CPA-deficient Δ*rmd* strain a 9-fold reduction in susceptibility but not complete resistance is observed.

Considering CPA increases but is not essential for PyoS5-susceptibility, it was not clear whether CPA influences translocation of PyoS5 across the outer membrane. Live cell microscopy was used to observe whether the CPA-binding domain could translocate across the outer membrane and how CPA-deficiency would impact translocation.

Both PyoS5$_{1\text{-}196}$-AF488 and PyoS5$_{194\text{-}315}$-AF488 lead to significantly reduced fluorescence on the surface of the *P. aeruginosa* cells compared with TR-AF488 and the sum of the fluorescent signals was also lower than the signal observed for TR-AF488 (Fig. 5-5). This indicated that the effects of the two domains making up TR was cooperative. While all of PyoS5$_{1\text{-}196}$-AF488 appeared to be translocated across the outer membrane, all of PyoS5$_{194\text{-}315}$-AF488 was found on the cell surface. In conclusion, PyoS5$_{194\text{-}315}$-AF488 alone did not cross the outer membrane but bound to the cell surface, and PyoS5$_{1\text{-}196}$-AF488 translocated but did so more efficiently in conjunction with PyoS5$_{194\text{-}315}$, as was seen for TR (Fig. 5-5).

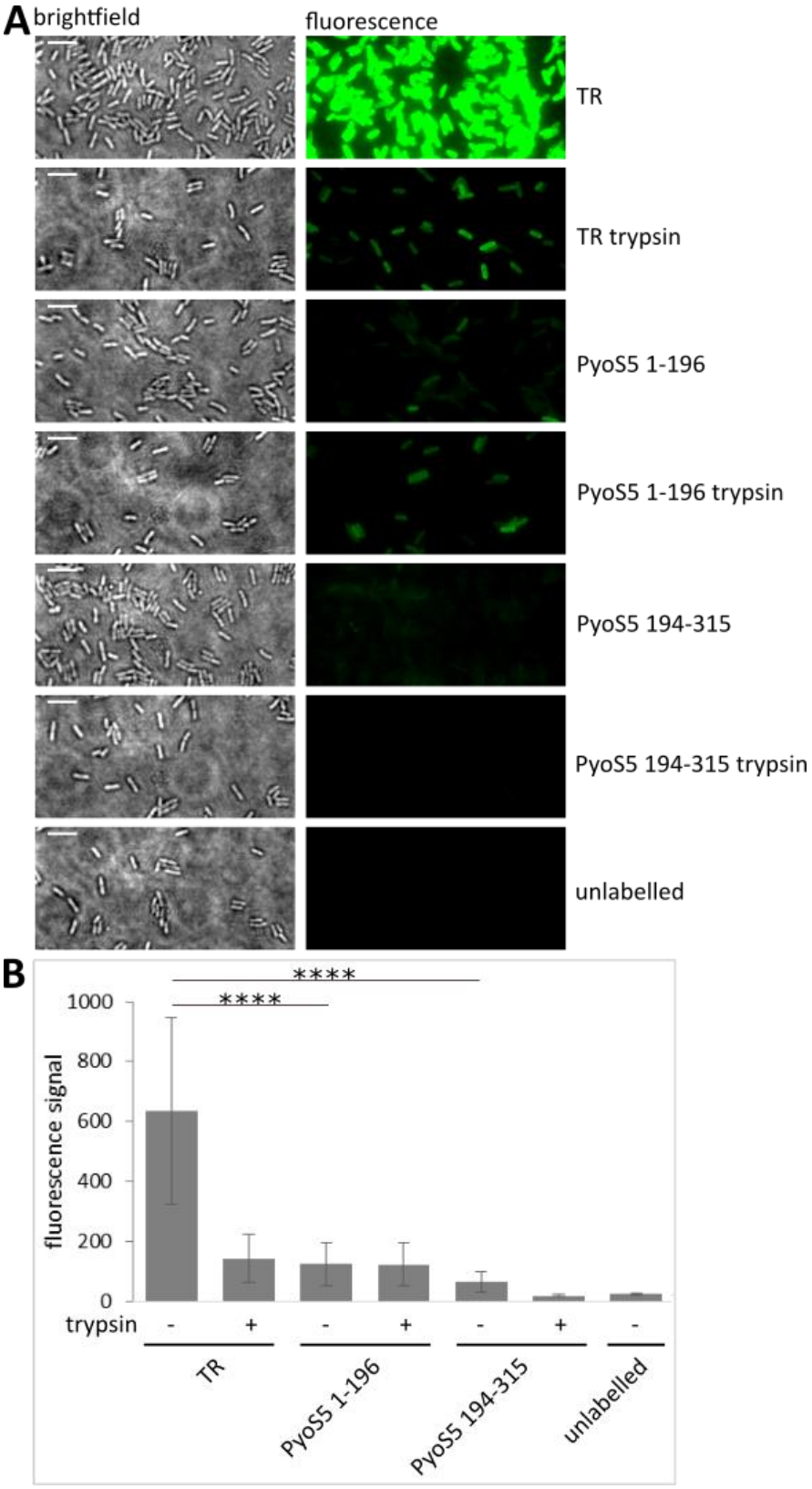

Figure 5-5: CPA leads to PyoS5 accumulation on the cell surface.
(A) Fluorescent labelling of live *P. aeruginosa* PAO1 using TR-AF488, PyoS5$_{1-196}$-AF488 and PyoS5$_{194-315}$-AF488 with and without trypsin treatment. Scale bars, 5 µm. (B) Quantification of the average cell fluorescence observed under different conditions tested in A. **** indicates a p-value below 0.0001 in Student's t-test.

In CPA-deficient *P. aeruginosa*, the amount of TR-AF488 on the surface is lower than in *P. aeruginosa* PAO1, suggesting that CPA is necessary for accumulation of PyoS5 on the surface of *P. aeruginosa* (Fig. 5-6). This was supported by the lack of fluorescent signal from cells labelled with the CPA-binding domain PyoS5$_{194-315}$-AF488 (Fig. 5-6). These results show that the interaction between CPA and PyoS5$_{194-315}$-AF488 leads to CPA accumulation on the cell surface but not to translocation, consistent with CPA being the receptor for PyoS5.

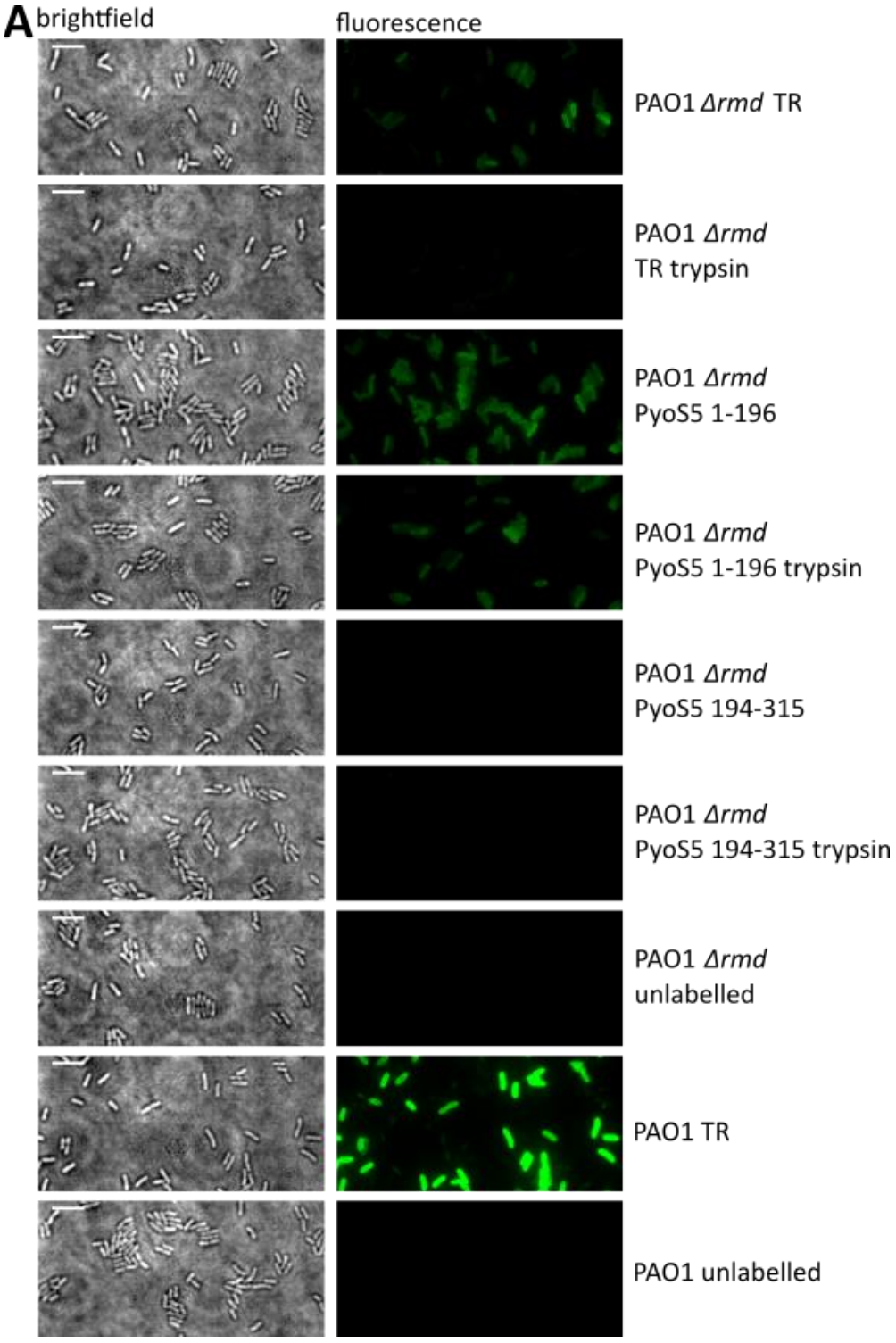

Figure legend after part B.

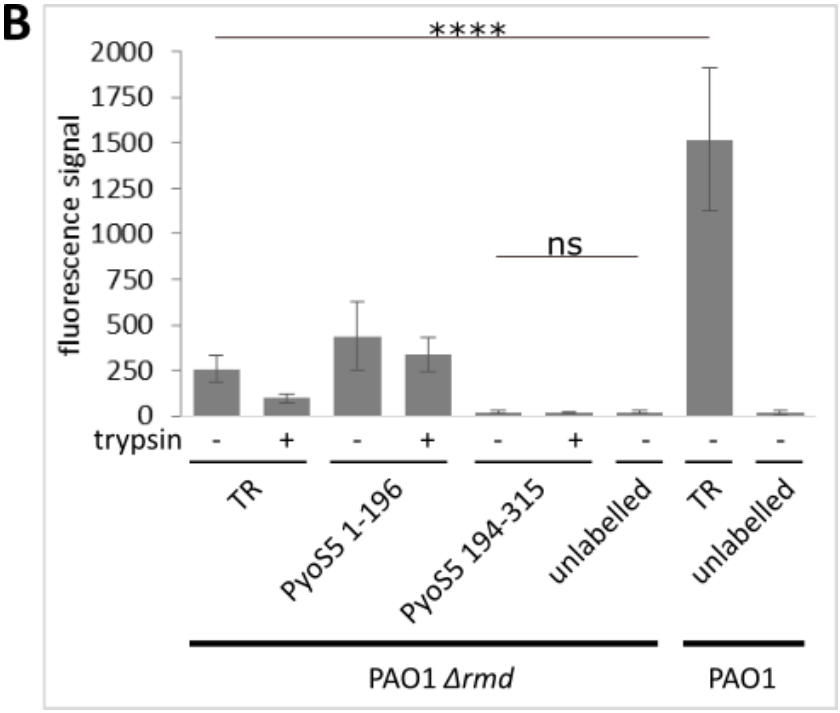

Figure 5-6: CPA-deficiency reduces PyoS5 accumulation on the cell surface and translocation.
(A) Fluorescent labelling of live *P. aeruginosa* PAO1 Δ*rmd* and PAO1 using TR-AF488, PyoS5$_{1\text{-}196}$-AF488 and PyoS5$_{194\text{-}315}$-AF488 with or without trypsin treatment. Scale bars, 5 μm. (B) Quantification of the average cell fluorescence observed under different conditions tested in A. **** indicates a p-value below 0.0001 in Student's t-test.

5.2.4 PyoS5 directly interacts with FptA

As opposed to PyoS5$_{194\text{-}315}$, PyoS5$_{1\text{-}196}$ was able to translocate across the outer membrane in the presence and absence of CPA (Fig. 5-5 and 5-6). I hypothesized that FptA was involved in the translocation process.

In a cytotoxicity assay PyoS5ColIa, which was used to overcome native immunity to PyoS5, was spotted onto the FptA-deficient strain *P. aeruginosa* PW8161. The FptA-deficient bacteria were found to be resistant to PyoS5ColIa, confirming that FptA is essential for PyoS5 import (Fig. 5-7). To investigate whether this is due to a direct interaction between purified PyoS5 and FptA or an indirect effect, size exclusion chromatography was used (Section 2.8.2), where a peak shift, indicative of complex formation, was observed (Fig. 5-8).

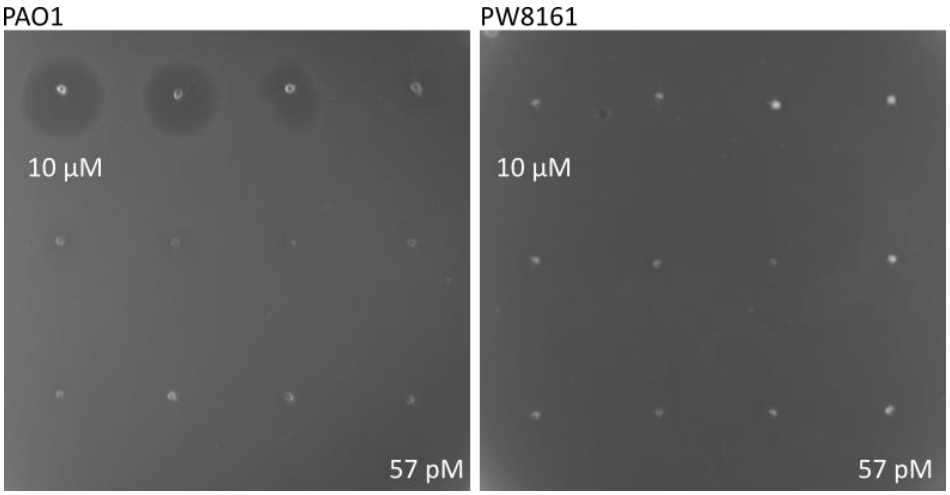

Figure 5-7: FptA-deficient cells are PyoS5ColIa-resistant.
PyoS5ColIa was spotted onto wild type *P. aeruginosa* PAO1 (left) and FptA-deficient *P. aeruginosa* PW8161 (right), grown on M9-agar, in three-fold dilutions staring at 10 µM. No zones of clearance are observed.

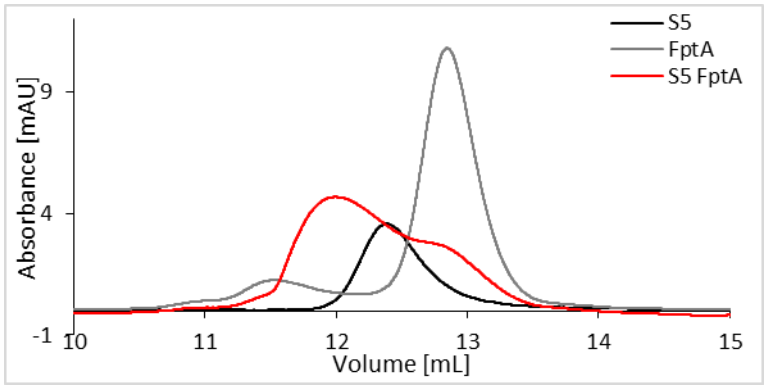

Figure 5-8: PyoS5 and FptA form a complex.
PyoS5 (black), FptA (grey), and a mixture of both (red) were injected onto a 10/300 S200 size exclusion chromatography column equilibrated in 150 mM NaCl, 20 mM Tris-HCl pH 7.5, 1 % β-OG. The elution profile of the mixture shows an additional earlier peak, indicative of complex formation.

I had previously found that PyoS5 residues 316 to 498 were not required for translocation and therefore hypothesized that TR would bind FptA. Native MS and SPR (Section 2.8.3) confirmed this hypothesis and a K_D of 6 µM was determined by SPR (Fig. 5-9).

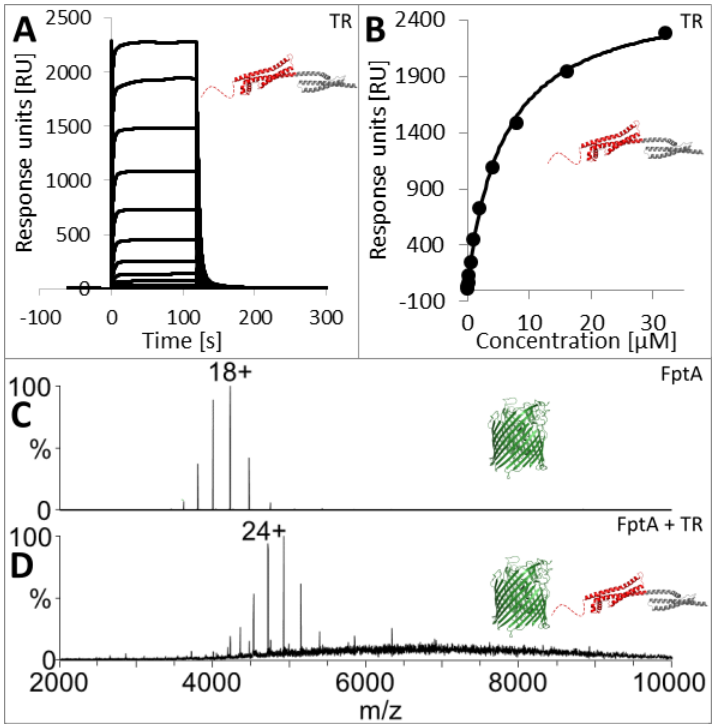

Figure 5-9: TR binds FptA.
(A) SPR sensorgram shows FptA (0.03-32 µM) binding to TR immobilized by amine-coupling in HBS-OG buffer at 25 °C. One of three repeats is shown. (B) Sensorgram data were extracted and fit with a 1:1 binding model which gave a K_D of 6.5 ±0.4 µM. (C) Native MS spectrum of FptA at 10 µM, 76,066 Da (expected mass 76,068.27 Da), disappears upon the addition of 17.3 µM TR, to yield a complex of 113,259 Da (expected mass 113,261.40 Da).

To determine whether the method of immobilizing TR influenced the affinity measured for the interaction with FptA, I also immobilized TR-C by thiol coupling. As opposed to the previously used amine coupling, which immobilizes TR in random orientations, thiol coupling leads to directional immobilization, with the C-terminal cysteine of TR-C being attached to the chip. The K_D measured with both methods in parallel did not differ significantly (Fig. 5-10).

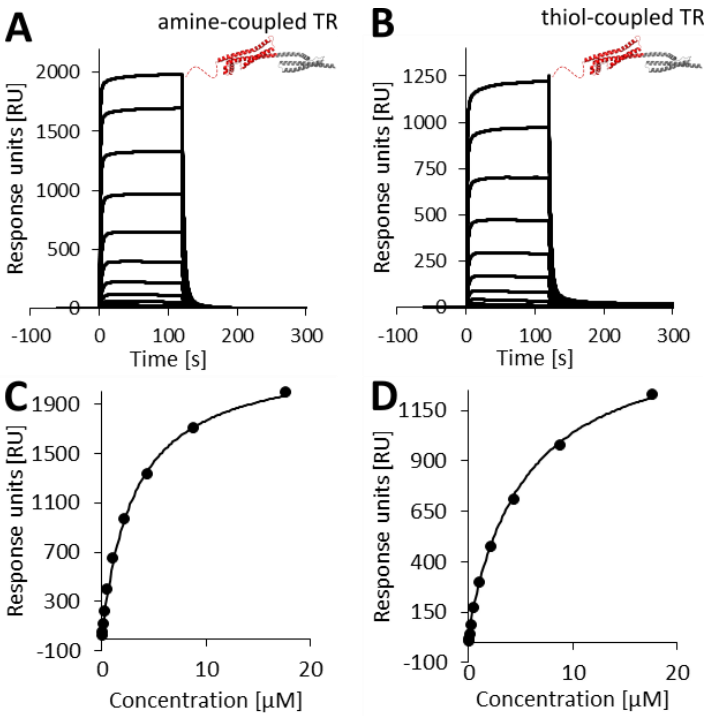

Figure 5-10: Immobilization method does not influence binding.
SPR sensorgram shows FptA (0.03-17 µM) binding to (A) TR immobilized by amine-coupling and (B) TR-C immobilized by thiol-coupling in HBS-OG buffer at 25 °C. One of two repeats is shown. (C) Sensorgram data from amine-coupled TR were extracted and fit with a 1:1 binding model which gave a K_D of 4.4 ±0.8 µM. (D) Sensorgram data from thiol-coupled TR-C were extracted and fit with a 1:1 binding model which gave a K_D of 3.3 ±0.2 µM.

5.2.5 PyoS5 competes for FptA-binding with the native ligand pyochelin

The native ligand of FptA is the iron siderophore pyochelin which binds to the plug and parts of the barrel on the extracellular side of FptA (Cobessi et al., 2005). To determine whether PyoS5 binding to FptA was competitive to that of pyochelin, a native MS experiment was conducted (Section 2.8.1). I observed complexes of FptA and pyochelin, and of FptA and PyoS5 but never of all three together, showing that binding of these two ligands appears mutually exclusive (Fig. 5-11). I then showed by SPR that PyoS5 and pyochelin compete for FptA binding (Fig. 5-12).

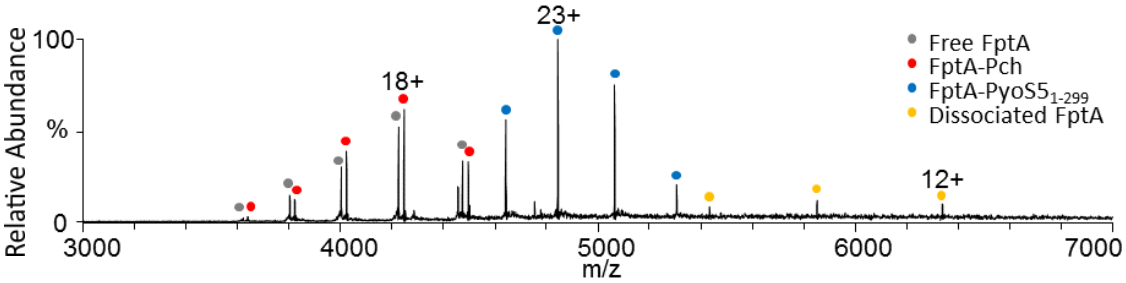

Figure 5-11: FptA binds either PyoS5 or pyochelin but not both simultaneously.
FptA was incubated with a 4-fold excess of ferric pyochelin for 45 min, then excess pyochelin was removed by desalting. The native mass spectrum of 19 µM FptA with pre-bound pyochelin, and 19 µM PyoS5$_{1-299}$ shows free FptA (grey) at 76,067 Da (expected mass 76,068 Da), FptA-pyochelin (Pch) complex (red) at 76,463 Da (expected mass 76463 Da), FptA-PyoS5$_{1-299}$ complex (blue) at 111,419 Da (expected mass 113,261 Da) and dissociated FptA (yellow) at 76,067 Da (expected mass 76,068 Da) which is characterized by a lower mass to charge ratio. No complex of FptA, PyoS5$_{1-299}$ and pyochelin is observed. The y-axis shows relative abundance in percent. Experiments were performed by Joseph Gault (Department of Chemistry, University of Oxford).

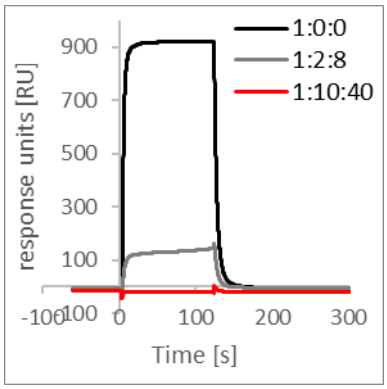

Figure 5-12: Pyochelin and PyoS5 compete for FptA binding.
SPR in HBS-OG buffer at 25 °C shows 3.4 µM FptA binding to TR immobilized by amine-coupling in the presence of pre-mixed pyochelin and $FeCl_3$ at ratios of 1:0:0 (black), 1:2:8 (grey) and 1:10:40 (red) FptA to pyochelin to $FeCl_3$. At 10-fold excess of pyochelin no binding of FptA to TR is observed.

5.2.6 The FptA-binding domain is PyoS5$_{1-196}$

To further narrow down the FptA-binding domain of PyoS5, constructs of the first and second repeat of the domain duplication in PyoS5 were used. By SPR I found that PyoS5$_{1-196}$ but not PyoS5$_{194-315}$ bound FptA (Fig. 5-13). The K_D of the interaction between PyoS5$_{1-196}$ and FptA was 7 µM and not significantly different from the K_D observed for the interaction between TR and FptA (Fig. 5-10). This suggested that FptA-binding capacity observed for TR resides with residues 1 to 196 and when expressed separately the construct retains full activity.

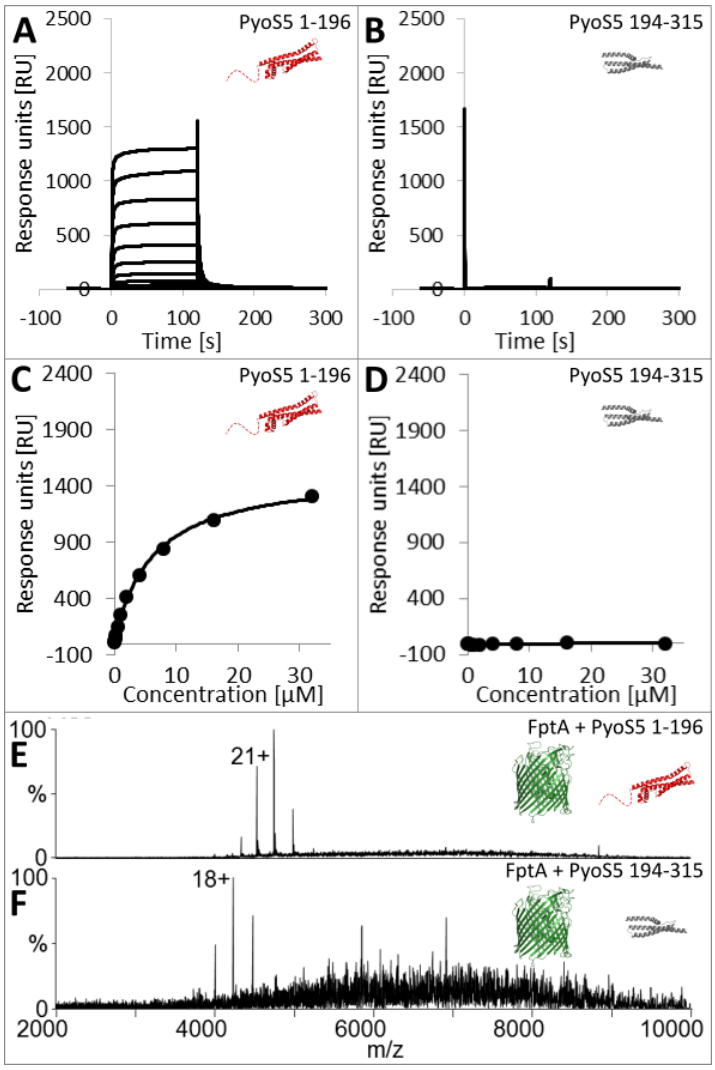

Figure 5-13: PyoS5$_{1\text{-}196}$ but not PyoS5$_{194\text{-}315}$ binds FptA.
(A) SPR sensorgram shows FptA (0.03-32 µM) binding to PyoS5$_{1\text{-}196}$ immobilized by amine-coupling in HBS-OG buffer at 25 °C. One of three repeats is shown. (B) No binding is observed for the same concentrations of FptA to PyoS5$_{194\text{-}315}$ immobilized by amine-coupling. One of three repeats is shown. (C) Sensorgram data from A were extracted and fit with a 1:1 binding model which gave a K_D of 7.1 ±0.7 µM. (D) Sensorgram data from B were extracted and no binding was observed. (E) Native MS spectrum of 5 µM FptA mixed with 7.5 µM PyoS5$_{1\text{-}194}$ shows formation of a 99796 Da complex (expected mass 99797.97 Da). (F) Native mass spectrum of 10 µM FptA mixed with 7 µM PyoS5$_{194\text{-}315}$ shows 76066 Da unbound FptA (expected mass 76068.27 Da) and was obtained by Joseph Gault (Department of Chemistry, University of Oxford).

5.2.7 PyoS5 Translocation is FptA-dependent

If PyoS5$_{1\text{-}196}$ mediates the translocation of PyoS5 through FptA as suggested by microscopy (Fig. 5-5), then no translocation into FptA-deficient *P. aeruginosa* should occur. This was found to be the case as neither TR-AF488 nor PyoS5$_{1\text{-}196}$-AF488 reached the inside of the cell, which is trypsin-protected, while labelling with the CPA-binding domain PyoS5$_{194\text{-}315}$ was not affected by the presence or absence of FptA (Fig. 5-5 and Fig. 5-6). The CPA-binding capacity of TR also resulted in the presence of fluorescence on the cell surface but this was reduced approximately 3-fold in the FptA-deficient strain compared to the parent strain (Fig. 5-14). All these observations are consistent with PyoS5$_{1\text{-}196}$ binding to and translocating using FptA, while PyoS5$_{194\text{-}315}$ is responsible for binding to CPA.

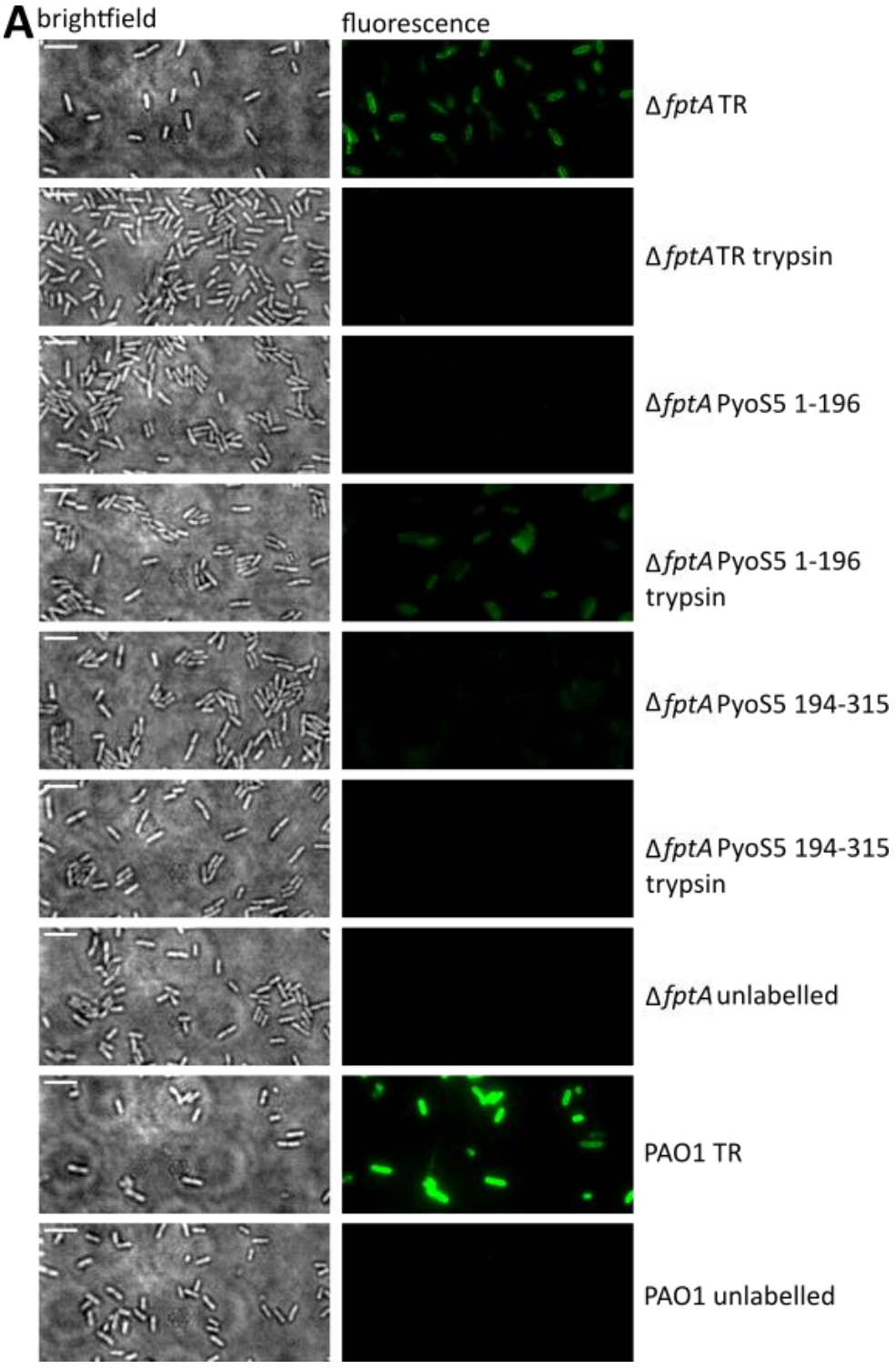

Figure legend after part B

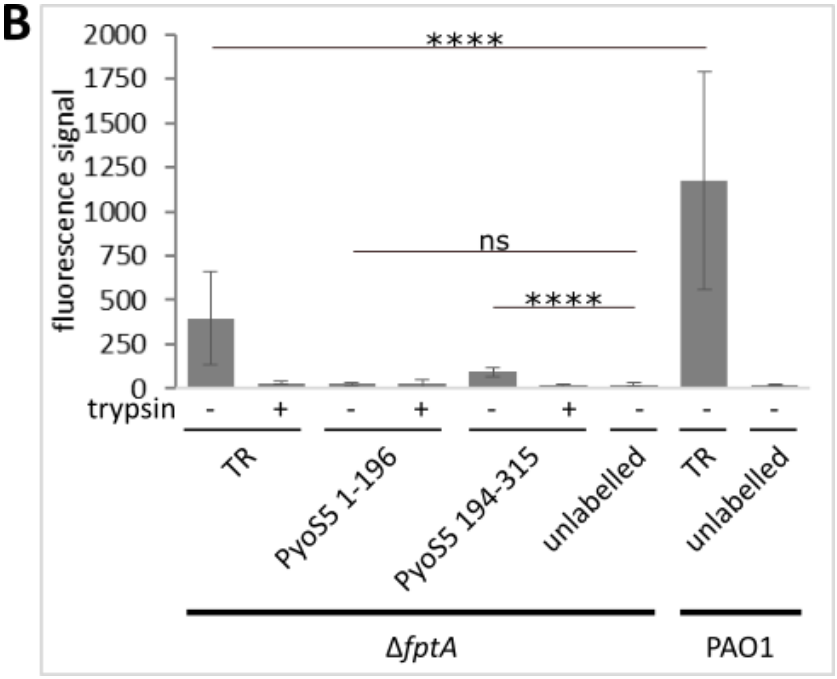

Figure 5-14: FptA-deficiency prevents translocation.
(A) Fluorescent labelling of live *P. aeruginosa* PW8161 (Δ*fptA*) and *P. aeruginosa* PAO1 using TR-AF488, $PyoS5_{1-196}$-AF488 and $PyoS5_{194-315}$-AF488 with and without trypsin treatment. Scale bars, 5 μm. (B) Quantification of the average cell fluorescence observed under different conditions tested in A. **** indicates a p-value below 0.0001 in Student's t-test.

5.2.8 Similarity with PyoS2

The import mechanism of PyoS5, by accumulation by CPA and translocation by iron siderophore receptor FptA, showed strong parallels to the import mechanism of PyoS2, which also binds CPA and is translocated by the iron siderophore receptor FpvAI (McCaughey et al., 2016a; White et al., 2017). Manual inspection of the crystal structure of PyoS2 residues 11 to 205 bound to its translocator FpvAI, showed strong similarities in structure. To our surprise these similarities had not been detected in an NCBI VAST or PDBeFold search of the newly solved PyoS5 structure. Alignment of the structure of PyoS5 to PyoS2 residues 11 to 205 gave an RMSD of 4.9 Å over 152 residues (Fig. 5-15A). Combined with the homology model of the CPA-binding domain which covers PyoS2 residues 207 to 315 it became apparent that PyoS2 is very similar to the PyoS5 TR region in structure (Fig. 5-15A).

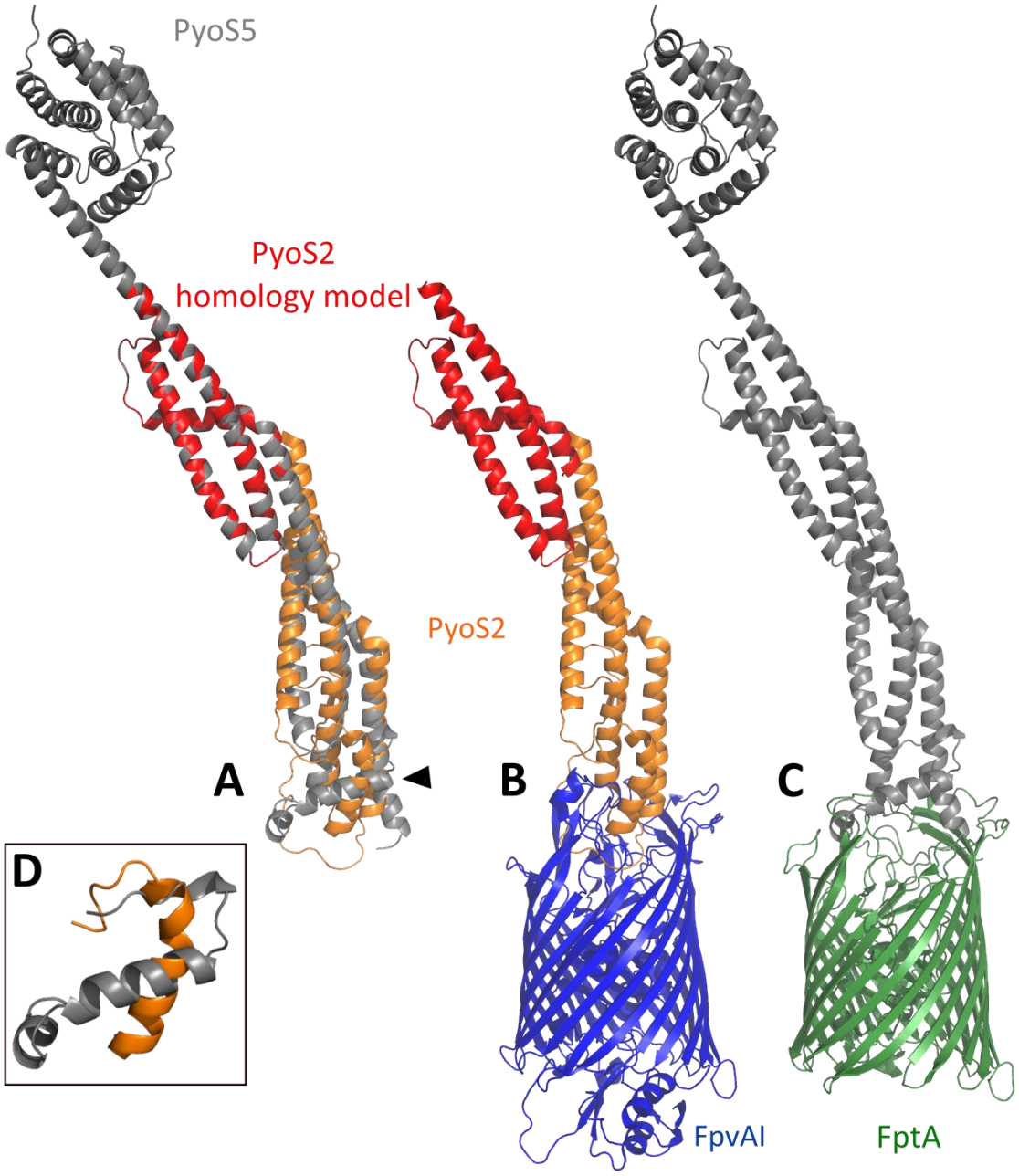

Figure 5-15: Similarity between PyoS5 and PyoS2.
(A) PyoS2 residues 11 to 205 (orange, PDB 5ODW), and the homology model of the PyoS2 CPA binding domain covering residues 207 to 315 (red) aligned to PyoS5 (grey). (B) PyoS2 residues 11 to 205 (orange) bound to FpvAI (blue) (PDB 5ODW) and the PyoS2 homology model aligned to PyoS5, which was aligned to PyoS2. (C) PyoS5 (grey) and FptA (green, PDB 1XKW) aligned to PyoS2 and FpvAI (PDB 5ODW) respectively. (D) Magnified detail of (A), indicated by a black arrowhead: differently oriented short helixes of PyoS5 residues 123 to 156 (grey) and PyoS2 residues 126 to 150 (orange).

Structures of two more pyocins are available, the full length structure of PyoL1 and the DNase domain of AP41 (Joshi et al., 2015; McCaughey et al., 2014). The nuclease domain consists of short alpha helices and a beta sheet composed of three short beta

strands and has no similarity to PyoS5 with its kHBDs and long helices. PyoL1 is radically different from PyoS5 in that it is constructed entirely of beta strands.

While PyoS5 provided information about the structure of the CPA-binding domain of PyoS2, the resolved N-terminal flexible region of PyoS2 improved our understanding of the unresolved flexible N-terminal region of PyoS5. PyoS2 residues 11 to 205 were solved in complex with the PyoS2 translocator FpvAI, which is similar to FptA with an RMSD of 3.0 Å. The flexible N-terminal loop of PyoS2 contacts the extracellular side of the FpvAI plug and β-barrel, and orients PyoS2 vertically onto the outer membrane protein (Fig. 5-15B). An alignment of PyoS5 to PyoS2 and of FptA to FpvAI suggested how PyoS5 might bind to FptA: vertically onto the receptor by means of the unresolved N-terminal residues (Fig. 5-15C). I tested this hypothesis by removing the unresolved residues 2 to 39 from TR, which abolished binding to FptA, confirming that these residues are part of the FptA-binding site (Fig. 5-16). One main difference between the PyoS2 and PyoS5 N-terminal domains is the orientation of their short helices (Fig. 5-15D). In PyoS2 the helix is involved in binding to FpvAI (White et al., 2017) but the equivalent helix in PyoS5 clashes with the barrel of FptA when both molecules are aligned to the crystal structure of the complex of PyoS2 and FpvAI. Whether the different orientation of the short helices is an inherent difference between the two pyocins or a conformational change occurring upon receptor binding is unclear. Sequence similarities of domains in PyoAP41, PyoS1, PyoSD1, PyoSD2, PyoS3, PyoSD3, PyoS4 and PyoSN to one of the kHBDs that were crystallized in PyoS5 and PyoS2 suggest that kHBDs are common among pyocins.

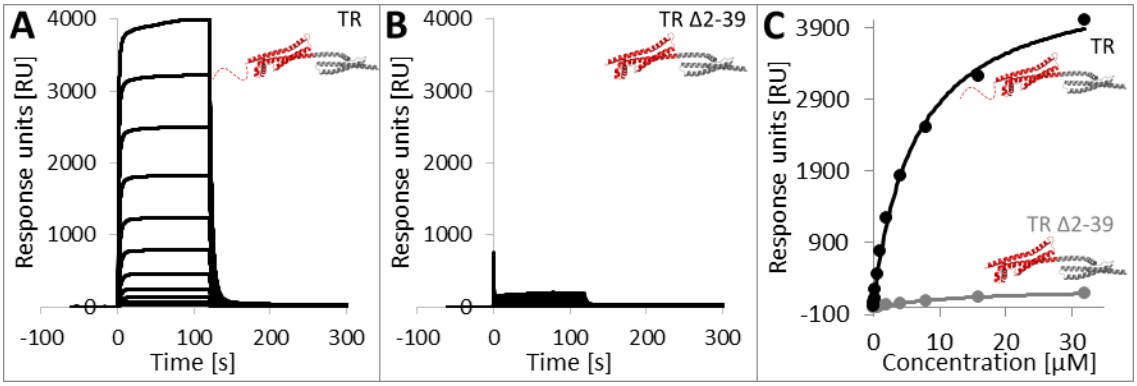

Figure 5-16: $TR_{\Delta 2-39}$ does not bind FptA.
SPR sensorgram shows FptA (0.03-32 µM) binding to (A) TR and (B) $TR_{\Delta 2-39}$ immobilized by amine-coupling in HBS-OG buffer at 25 °C. (C) Sensorgram data were extracted and fit with a 1:1 binding model giving a K_D of 6.5 ±0.0 µM for TR (black) and while no binding was observed for $TR_{\Delta 2-39}$ (grey). One of three repeats is shown.

5.3 Discussion

This chapter shows that the two PyoS5 domains of conserved fold in the TR region serve different functions and interact with different outer membrane components. $PyoS5_{194-315}$ binds CPA and leads to accumulation of PyoS5 on the surface of *P. aeruginosa* cells – a non-essential step. $PyoS5_{1-196}$ on the other hand binds to FptA and competes with the native ligand pyochelin to do so. Cytotoxicity and translocation are FptA-dependent and the FptA-binding domain was able to translocate by itself. Hence, while the fold is conserved, the function differs between the two copies of the kHBD.

Analysis of conserved residues among CPA-binding proteins revealed a potential CPA-binding groove (Fig. 5-3). CPA might bind to this groove as a linear polysaccharide, or it might be flexible and wrap around the CPA-binding domain. It is also conceivable that CPA adopts a rigid non-linear conformation which is recognized by PyoS5 and other CPA-binding pyocins.

The stoichiometries of PyoS5 binding to CPA obtained in ITC experiments suggested 0.16 CPA molecules bound each molecule of TR and 0.56 each molecule of D2. These

numbers are inaccurate because the concentration of CPA had to be estimated based on an average molecular weight and estimated purity of the preparation. Nonetheless, it is clear from the observed stoichiometries that PyoS5 does not bind to each tri-rhamnose repeat unit, as there are on average 70 per CPA molecule. It seems more likely that the true stoichiometry is 1:1 or even fewer than one CPA molecule per PyoS5. A 1:1 stoichiometry would be possible if PyoS5 bound to unique features in the CPA molecule, such as the first or last tri-rhamnose repeat. If CPA multimerized, an even lower stoichiometry would be the result. Future work will be needed on the structure of the CPA-PyoS5 complex to determine how CPA binds to the identified CPA-binding domains.

It is likely that CPA has the same role in other pyocins like PyoSD3 as it has in PyoS2 and PyoS5. However, confirming this role is beyond the scope of this work.

5.3.1 Complete translocation into the periplasm

One hypothesis on the import of pore-forming CLBs was that some CLB domains remain at the surface while the pore-forming domain is inserted in the inner membrane (Bénédetti et al., 1992). This dates back to experiments on ColA in 1992, which found that extracellular addition of trypsin stops the ColA-induced release of K^+ from cells (Bénédetti et al., 1992). The initial interpretation was that some colicin domains remain at the surface during pore formation and that their degradation closes the pore. This was termed the alternative model (Cramer et al., 2018) and was applied to other types of CLBs including ColE1 (Fig. 5-17). This model was supported by the observation that helices 1 and 2 (green in Fig. 5-17) of the pore-forming domains are located further away from the remainder of the helices in the closed state of the pore, which led to the hypothesis that

they might form a linker to the outer membrane (Bénédetti et al., 1992). A more recent experiment showed that despite being further away from the other helices, helices 1 and 2 are still located at the inner membrane-periplasm interface (Pulagam and Steinhoff, 2013).

A second interpretation was that the degradation of ColA molecules, which have not translocated into the periplasm yet, stops the release of K+ from additional cells rather than closing the already existing pores (Ridley et al., 2010). This explanation is supported by the fact that isolated pore-forming domains can form pores independent of the other domains, as long as access to the periplasmic side of the inner membrane is provided (Duché, 2002). The degradation of N-terminal CLB domains is therefore unlikely to influence pore stability in the inner membrane. This second explanations is compatible with the total thread model (Fig. 5-17), which suggests that the full CLB is imported into the cytoplasm. Further support of this model comes from experiments which suggested complete translocation through the outer membrane for pore-forming colicin ColN (El Kouhen and Pagès, 1996).

The work presented in this chapter shows that no PyoS5 extracellular domains coexist with the pore-forming domain of the same molecule inserted in the inner membrane. Both the N-terminal kHBD with a fluorophore in position 197 as well as the PyoS5 TR with a fluorophore in position 316 are protected from extracellular trypsin in an FptA-dependent manner (Fig. 5-5 and Fig. 5-6). Helixes 3 to 10 of the pore-forming domain are in close proximity to each other (Duché et al., 1994b; Lakey et al., 1993, 1991; Luo et al., 2005) and helices 5 to 10 involved in the formation of the pore (Baty et al., 1990; Nardi et al., 2001). The remaining amino acids that have neither been shown to have entered the

periplasm (residue 317 onwards) and nor to be required at the inner membrane for pore-formation (up to residue 380) could span a maximum length of 22 nm when fully extended. For any part of PyoS5 to be exposed at the surface, while residues 1 to 315 are protected from trypsin in the periplasm and the pore-forming domain is inserted in the inner membrane, requires the available residues to span the outer membrane (7 nm) and the periplasm (24 nm) at least once. The available residues are therefore too few to span this distance which means that no part of a PyoS5 molecule can be present at the cell surface while the pore-forming domain is inserted in the inner membrane. This study therefore shows that the fishing pole model cannot hold true for PyoS5 and therefore proposes the total thread model for the import of PyoS5 into the periplasm.

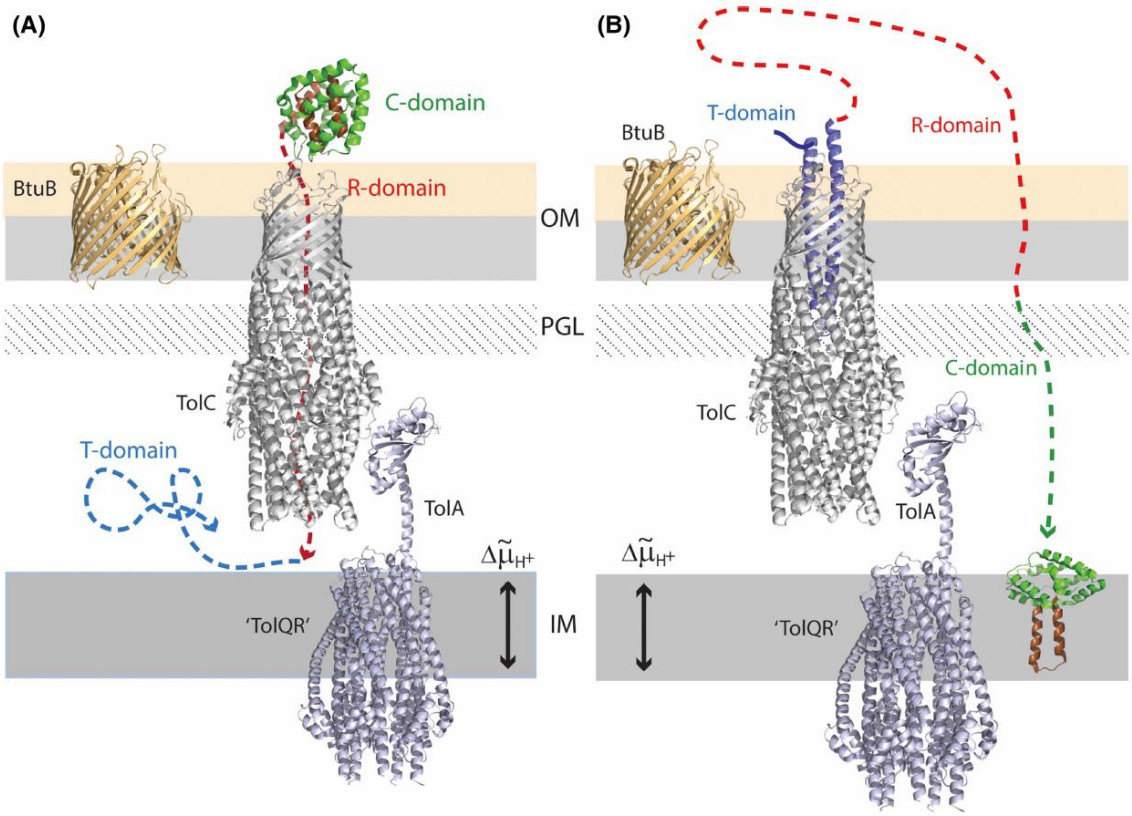

Figure 5-17: Total thread and alternative models of CLB translocation.
(A) The total thread model of ColE1 translocation suggests the whole protein translocates through its translocator in an unfolded state. (B) The alternative model suggests the E1 translocator-binding domain is anchored in the translocator, presenting part of the sequence at the cell surface while the cytoplasmic domain gains access to the periplasm by crossing the outer membrane (OM) independently. This allows

the pore-forming domain to insert in the inner membrane (IM) while part of the CLB sequence remains at the surface. Peptidoglycan (PGL). Figure replicated from Cramer et al. (Cramer et al., 2018).

5.3.2 The PyoS5:FptA complex

Further, this chapter revealed the similarities between PyoS5 and PyoS2 and comparison of the available data added to our understanding of both pyocins. The structural data on PyoS5 allowed us to build a homology model for the CPA-binding domains of PyoS2, while the receptor bound structure of PyoS2 suggested that the unresolved residues of PyoS5 might be involved in FptA binding – a hypothesis that was confirmed experimentally. It remains unclear whether structural differences observed between them reflect their bound and unbound state or inherent differences of the pyocins. Initial attempts to crystallize a complex of FptA bound to PyoS5 or to the TR of PyoS5 were not successful, yet future structural studies of the FptA:PyoS5 complex or of PyoS2 in an unbound state may provide an answer to this question.

This chapter suggests based on the similarity between the two pyocins that PyoS5 binds to FptA in an orientation similar to that of PyoS2 to FpvAI (Fig. 5-15). This orientation is nearly perpendicular to the outer membrane and different than that observed in colicin-receptor complexes (Fig. 5-18). Structures of two such complexes have been solved, that of the ColE3 receptor-binding domain bound to BtuB and that of the ColIa receptor binding domain bound to Cir (Buchanan et al., 2007; Kurisu et al., 2003). Both ColE3 and ColIa are long, mostly helical proteins, just like PyoS2 and PyoS5. Yet they bind to their receptors at a 45° angle to the outer membrane such that their translocation domains can interact with the respective translocators (Fig. 5-18). Section 7.1.2 will discuss how

vertical binding of PyoS2 and PyoS5 to their receptors can be integrated with CPA binding and what implications this has for the import mechanism of these pyocins.

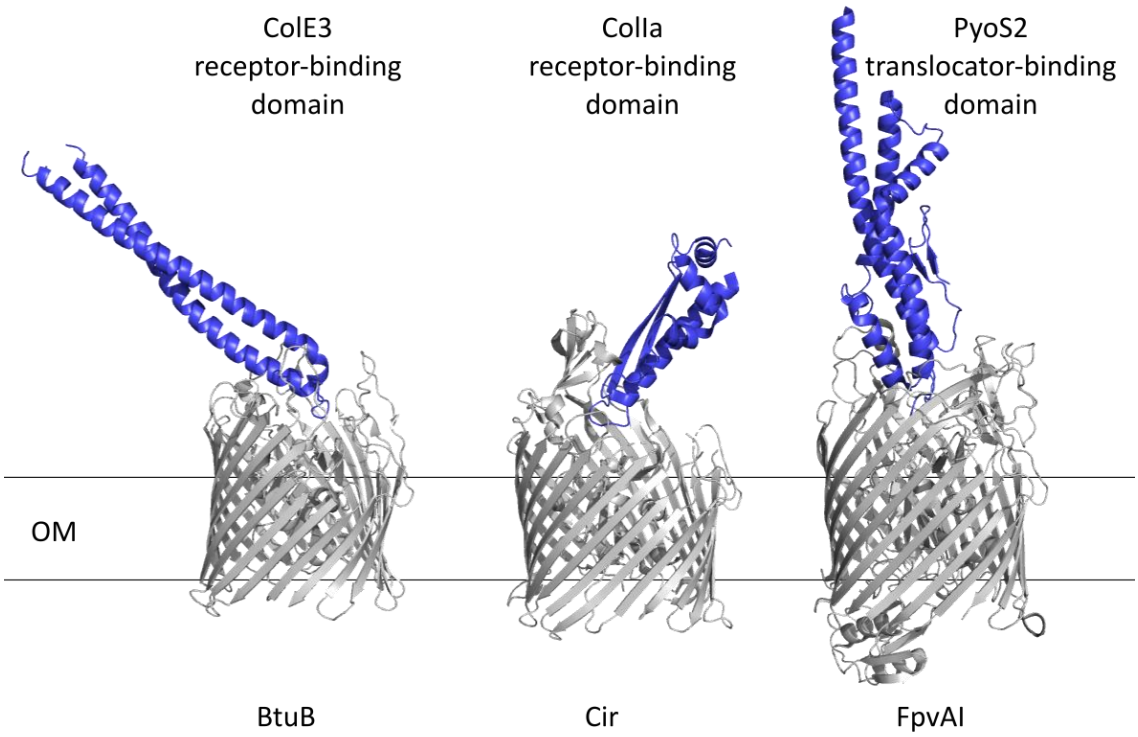

Figure 5-18: Comparison of three CLB-receptor complexes.
Crystal structures of the ColE3 receptor-binding domain bound to BtuB (PDB 1UJW), the ColIa receptor-binding domain bound to Cir (2HDI), and the PyoS2 translocator-binding domain bound to FpvAI (PDB 5ODW).

Previous work using photoactivated cross-linking showed that PyoS2 translocates through the barrel of FpvAI (White et al., 2017). Given the similarity between PyoS2 and PyoS5 it is likely that PyoS5 also crosses the outer membrane by translocating through the barrel of FptA.

PyoS2 mimics pyoverdin, the native ligand of its translocator FpvAI (White et al., 2017), which begs the question whether PyoS5 also mimics its translocator's natural ligand pyochelin. Interestingly, a similar motif to the PyoS2 residues that bind FpvAI and mimic pyoverdine occurs in PyoS5 (Fig. 5-19) but is located in the CPA-binding domain, which

was shown not to bind FptA. The CPA-binding domain did not bind FpvAI or any other outer membrane protein, which is known because fluorescent PyoS5$_{194\text{-}315}$ does not label CPA-deficient *P. aeruginosa.* Within this domain the motif is also in a different position with respect to the kHBD fold and is part of the CPA binding groove. This suggests that the motif is not conserved but convergently evolved to form binding sites in pyocins. The rigidity resulting from the prolines may provide needed stability in loops involved in interactions with outer membrane components. No equivalent proline-rich region is present in the N-terminal domain of PyoS5. Again, structural studies on the complex between PyoS5 and FptA will elucidate how these two proteins interact.

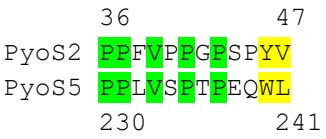

Figure 5-19: A sequence similar to the FpvAI-binding motif in PyoS2 occurs in PyoS5
42% identity was detected in this region using NCBI blastp. Identical residues are highlighted in green, similar residues in yellow. Residues Pro41 and Pro43 of PyoS2 interact with the plug of FpvAI (White et al., 2017).

The final results chapter will investigate whether *fptA* is the only gene essential for PyoS5 susceptibility and aims to define the minimal system required for a cell to become susceptible to PyoS5.

6. Energy for translocation of PyoS5

6.1 Introduction

In the previous chapters, I determined the crystal structure of PyoS5, identified three domains and assigned their functions as FptA-binding, CPA-binding and pore-forming. This chapter uses a minimal system approach to determine whether all essential parts of the PyoS5 translocon have been identified. Based on previously published work on CLBs one might expect an energy transduction system, like the Ton- or Tol systems, to be involved.

Here, I show that FptA alone is not sufficient to make bacteria susceptible to PyoS5; TonB1 is also essential. The contribution of TonB1 is realized by a direct interaction with PyoS5 via a TonB-box in the N-terminal domain of PyoS5. The minimal system approach was then validated using the well-studied PyoS2 system and applied to PyoS4 to find that, like PyoS2 and PyoS5, it is dependent on TonB1 for import. Finally, this chapter shows that TonB1 binds to FptA and suggests that two sequential TonB1 binding events are needed for PyoS5 import.

6.2 Results

6.2.1 The minimal system for PyoS5 susceptibility

E. coli are not susceptible to pyocins, including PyoS5 (Fig. 6-1A), even though the PyoS5 pore-forming domain is cytotoxic when transported into *E. coli* by the ColB translocation domain (Fig. 6-1A). *E. coli* is therefore a suitable organism to test which components are needed to make a bacterium susceptible to a pyocin. To test whether FptA is not only essential but also sufficient for susceptibility to PyoS5, FptA was

expressed in *E. coli* BL21 (DE3). These bacteria were not susceptible to PyoS5 therefore at least one other component is involved in PyoS5 susceptibility (Fig. 6-1B).

As discussed in Chapter 1, all well-characterized CLBs were found to rely on the Tol system or Ton system. I hypothesised that PyoS5 relies on one of the Ton systems present in *P. aeruginosa* because it employs FptA, which is predicted to be a TonB-dependent transporter. To test this hypothesis, knockouts of one or several of the three TonBs present in *P. aeruginosa*, TonB1, TonB2 and TonB3, were obtained. Their parent strain *P. aeruginosa* PAO6609, is a derivative of *P. aeruginosa* PAO1 and as such is immune to PyoS5 because it harbours the ImS5 immunity gene, which is why PyoS5ColIa was used to test susceptibility of *P. aeruginosa* PAO6609 and the TonB-knockouts. The absence of TonB2, TonB3, or both did not change susceptibility to PyoS5ColIa (Fig. 6-2). Unfortunately, it was not possible to test the susceptibility of any strains lacking TonB1 because the high levels of iron needed for their growth diminished susceptibility in the parent strain, possibly due to iron-dependent down-regulation of FptA (Fig. 6-3).

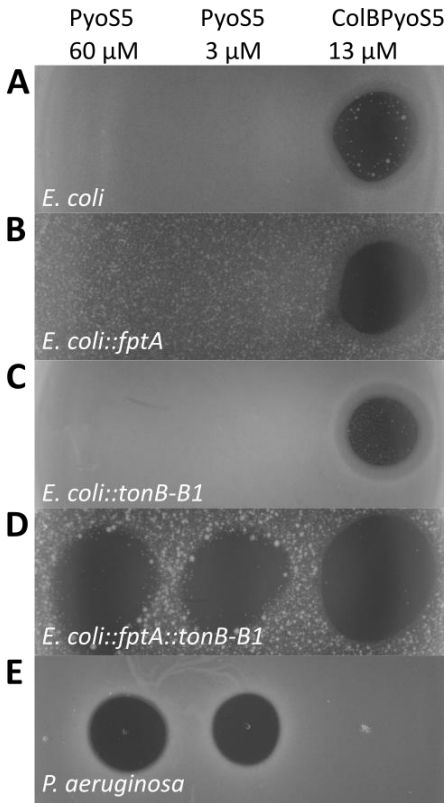

Figure 6-1: FptA and TonB1 constitute the minimal system for PyoS5-susceptibility in *E. coli*.
Susceptibility to PyoS5 (3 and 60 µM) was assessed for *E. coli* BL21 (DE3) cells (A), *E. coli* BL21 expressing FptA from pHB04 (B), *E. coli* BL21 (DE3) expressing TonB-B1 from pHB25 (C), *E. coli* BL21 (DE3) expressing FptA from pHB04 and TonB-B1 from pHB25 (D), and *P. aeruginosa* YHP17 (E). Zones of clearance are observed in all *E. coli* samples for ColBPyoS5 (13 µM) control (A-D) and for both concentrations of PyoS5 in *E. coli* expressing FptA and TonB-B1 (D). In the *P. aeruginosa* control clearance zones were observed for PyoS5 (E). This experiment was performed by Moritz Weber under supervision of Hannah Behrens.

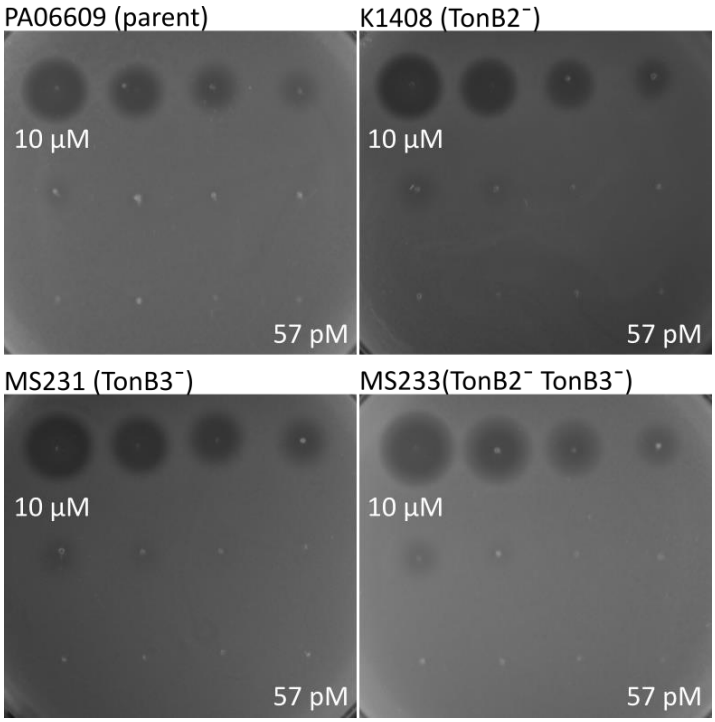

Figure 6-2: TonB2 and TonB3 do not influence PyoS5ColIa-susceptibility.
Susceptibility to PyoS5ColIa did not differ between parent strain PA6609, TonB2-deficient strain K1408, TonB3-deficient strain MS231, and TonB2- and TonB3-deficient strain MS233. 3-fold dilution series starting at 10 µM PyoS5ColIa added to strains grown on LB agar.

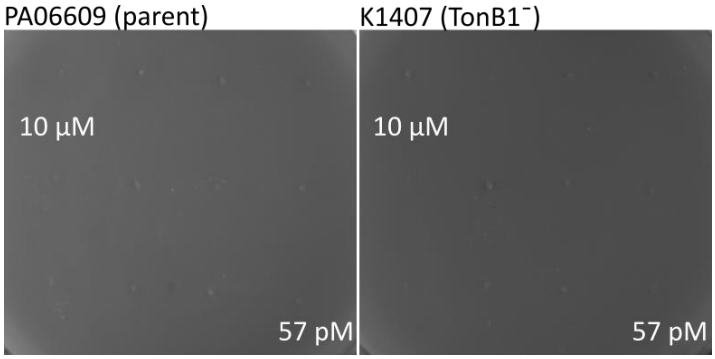

Figure 6-3: TonB1-deficient strain is not suitable to test PyoS5ColIa-susceptibility.
TonB1-deficient strain K1407 requires the addition of 100 µM $FeCl_3$ to grow in LB (Poole et al., 1996). Under these conditions neither its parent strain PA00609 nor K1407 is susceptible to PyoS5ColIa.

Because neither TonB2 nor TonB3 was essential for susceptibility I tested whether TonB1 could make *E. coli* susceptible. A TonB-B1 hybrid consisting of the *E. coli* transmembrane region of TonB (residues 1 to 102), responsible for interaction with ExbB and ExbD and accessing the PMF, and the cytoplasmic region of *P. aeruginosa* TonB1 (residues 201 to 342), responsible for interaction with substrates, was constructed and

expressed in *E. coli* BL21 (DE3). This construct alone did not result in susceptibility to PyoS5ColIa, but co-expression with FptA did (Fig. 6-1C+D). In conclusion the components needed to make *E. coli* susceptible to PyoS5 are FptA and TonB1.

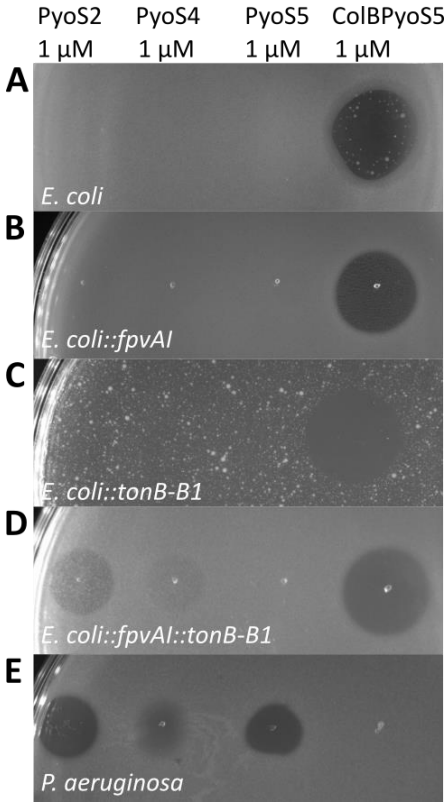

Figure 6-4: FpvAI and TonB1 constitute the minimal system for PyoS2- and PyoS4-susceptibility. Susceptibility to 1 µM PyoS2, PyoS4, PyoS5 and ColBPyoS5 was assessed for (A) *E. coli* BL21 (DE3) cells, (B) *E. coli* BL21 (DE3) expressing FpvAI from pNGH183, (C) *E. coli* BL21(DE3) expressing TonB-B1 from pHB25, (D) *E. coli* BL21 (DE3) expressing FpvAI from pNGH183 and TonB-B1 from pHB25, and (E) *P. aeruginosa* YHP17. Zones of clearance are observed for all *E. coli* conditions tested when ColBPyoS5 was applied (A-D). Similarly, *E. coli* expressing FpvAI and TonB-B1 were susceptible to both PyoS2 and PyoS4, as was the *P. aeruginosa* control (E). Zones of clearance for PyoS5 were only observed in *P. aeruginosa*.

To validate the approach of a minimal susceptibility system in *E. coli*, the components known to be involved in PyoS2 uptake were transformed into *E. coli* BL21 (DE3). Again, the individual components FpvAI and the TonB-TonB1 hybrid did not lead to susceptibility but both together did (Fig. 6-4). The approach was then applied to PyoS4, which is known to also parasitize FpvAI, and revealed that PyoS4 is also TonB1 dependent (Fig. 6-4).

6.2.2 TonB1 binding

PyoS2 binds directly to the cytoplasmic domain of TonB1 (henceforth called TonB1) begging the question whether PyoS5 does the same (White et al., 2017). Native MS showed that PyoS5$_{1\text{-}299}$ binds TonB1 (Fig. 6-5); SPR confirmed this and revealed a K_D of 241 ±9 nM for this interaction (Fig. 6-6). PyoS5$_{1\text{-}196}$ bound to TonB1 while PyoS5$_{194\text{-}315}$ did not, which showed that the TonB1-binding site, the so-called TonB-box, lies within the first 196 residues of PyoS5 (Fig. 6-6).

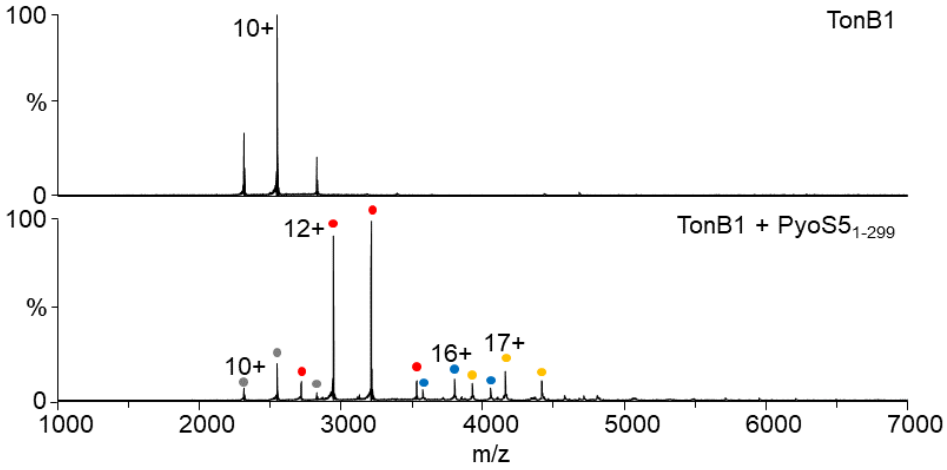

Figure 6-5: PyoS5 binds to TonB1.
Native mass spectra of 12 µM TonB1 with an observed mass of 25473 Da (expected mass 25473.4 Da), and of 12 µM TonB1 mixed with 2.9 µM PyoS5$_{1\text{-}299}$ which yields a complex with an observed mass of 60822 Da (expected mass 60824.4). Free TonB1 (•grey), free S5 (•red), S5-TonB1 (•blue), S5 dimer (•yellow). The y-axis shows relative abundance in %. Experiments were performed by Joseph Gault (Department of Chemistry, University of Oxford).

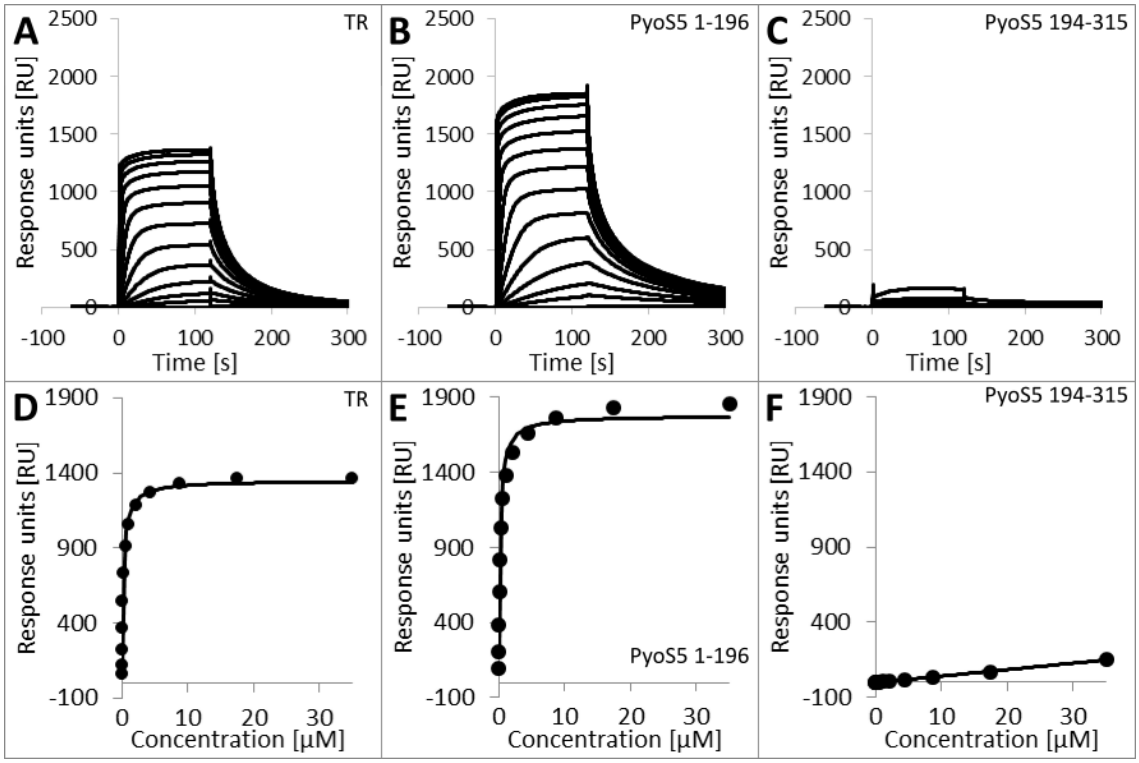

Figure 6-6: PyoS5$_{1-196}$ binds to TonB1.
(A) SPR sensorgram shows TonB1 (0.009-35 µM) binding to TR, (B) PyoS5$_{1-196}$ and (C) PyoS5$_{194-315}$ immobilized by amine-coupling in HBS-OG buffer at 25 °C. (D) Sensorgram data from A were extracted and fit with a 1:1 binding model which gave a K_D of 241 ±9 nM. (E) Sensorgram data from B were extracted and fit with a 1:1 binding model which gave a K_D of 231 ±2 nM. (F) Sensorgram data from C were extracted and no binding was observed.

PyoS2 is the only pyocin in which a TonB-box has been experimentally confirmed. Comparison of the first 196 amino acid residues of PyoS5 and PyoS2 reveals a region of 75 % identity (Fig. 6-7), including PyoS2 residues 11 to 15 (MVITH) which have been identified as the TonB-box of PyoS2 (White et al., 2017).

Three PyoS5 constructs lacking residues 2 to 9, 10 to 13, and 16 to 20, respectively, were tested for cytotoxicity against *P. aeruginosa* (Fig. 6-8). Deletion of residues 10 to 13 completely abolished cytotoxicity while the absence of residues 2 to 9 had no effect and the lack of residues 16 to 20 led only to a 3-fold decrease in cytotoxicity. Based on the similarity to the PyoS2 TonB-box it is likely that residues 10 to 13 are essential residues of the TonB-box and hence bind TonB1.

```
             1   5      10   15   20
PyoS2        MAVNDYE-PGSMVITHVQGGG
PyoS5        MS-NDNEVPGSMVIVAQGPDD
             1    5     10   15   20
```

Figure 6-7: Alignment of PyoS2 and PyoS5 TonB boxes.
Region of similarity between PyoS2 and PyoS5 identified by BlastP in the first 196 amino acid residues of each protein. Identical residues are highlighted in green.

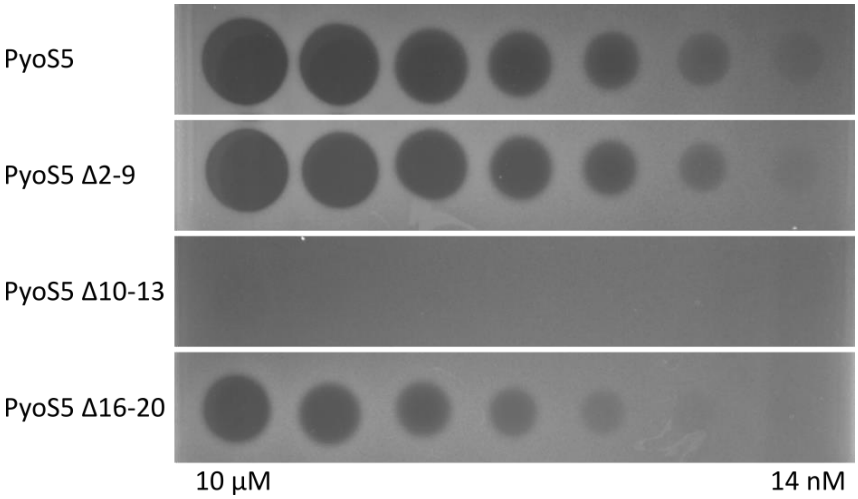

Figure 6-8: PyoS5 residues 10 to 13 are essential for cytotoxicity.
PyoS5, PyoS5$_{\Delta 2\text{-}9}$, PyoS5$_{\Delta 10\text{-}13}$, and PyoS5$_{\Delta 16\text{-}20}$ were applied to *P. aeruginosa* YHP17, grown on LB agar, in 3-fold dilutions starting at 10 µM. Zones of clearance were observed for PyoS5, PyoS5$_{\Delta 2\text{-}9}$ and PyoS5$_{\Delta 16\text{-}20}$, but not PyoS5$_{\Delta 10\text{-}13}$. Susceptibility of PyoS5$_{\Delta 16\text{-}20}$ was reduced 3-fold compared to PyoS5. This experiment was performed by Moritz Weber under supervision by Hannah Behrens.

To test this hypothesis, binding to TonB1 was compared between the TR$_{\Delta 2\text{-}9}$, TR$_{\Delta 10\text{-}13}$ and TR$_{\Delta 16\text{-}20}$ constructs. Analogous to the results of the cytotoxicity assays TR$_{\Delta 10\text{-}13}$ showed no binding to TonB1, while TR$_{\Delta 2\text{-}9}$ and TR$_{\Delta 16\text{-}20}$ bound to TonB1 with 6.5-fold and 1.3-fold increased K_Ds compared to TR, respectively (Fig. 6-9). To make sure the differences observed were directly due to the deletions of residues and not due to indirect effects like altered folding, binding to FptA was tested as a measure of functionality. All three constructs, TR$_{\Delta 2\text{-}9}$, TR$_{\Delta 10\text{-}13}$ and TR$_{\Delta 16\text{-}20}$ bound to FptA but the binding observed for TR$_{\Delta 16\text{-}20}$ was weaker than expected (Fig. 6-9). Nonetheless, it was concluded that TR$_{\Delta 10\text{-}13}$ bound FptA and therefore that the lack of binding to TonB1 was directly due to the deleted residues 10 to 13.

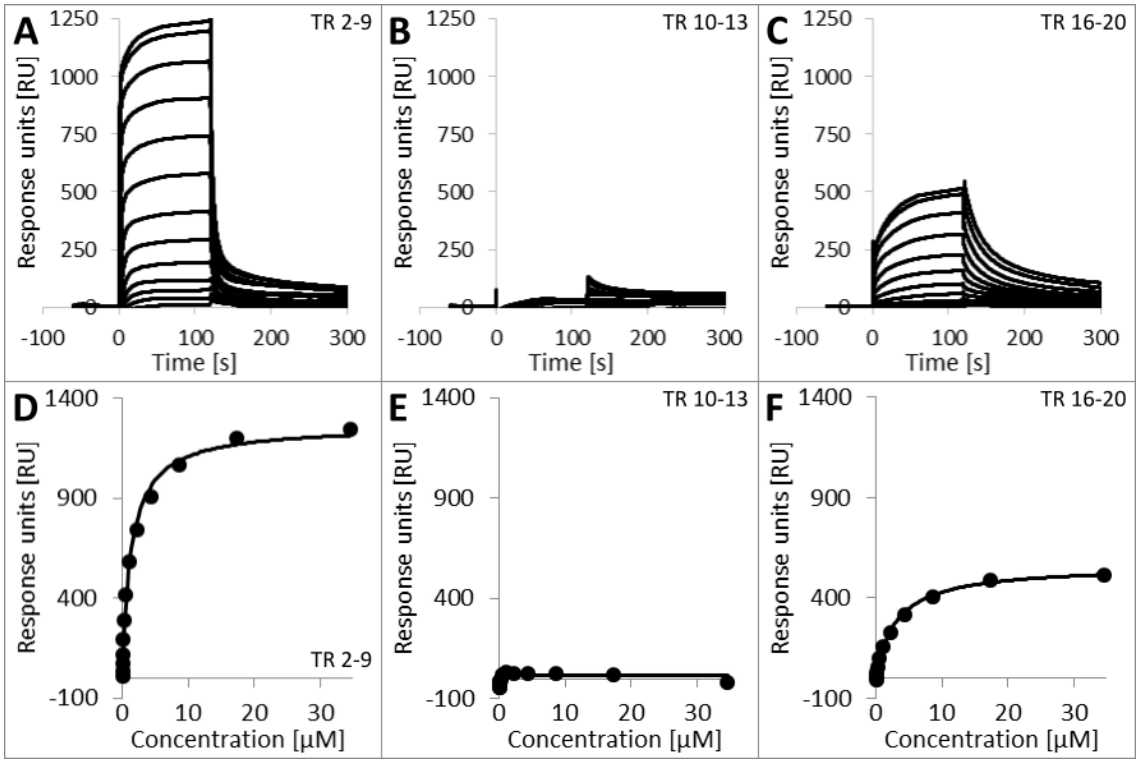

Figure 6-9: Residues 10 to 13 are needed for TonB1-binding.
SPR sensorgram shows TonB1 (0.008-34.7 µM) binding to (A) $TR_{\Delta 2\text{-}9}$, (B) $TR_{\Delta 10\text{-}13}$ and (C) $TR_{\Delta 16\text{-}20}$ immobilized by amine-coupling in HBS-OG buffer at 25 °C. (D) Sensorgram data from A were extracted and fit with a 1:1 binding model with a K_D of 1.57 ±0.09 µM. (E) Sensorgram data from B were extracted and no binding was observed. (F) Sensorgram data from C were extracted and fit with a 1:1 binding model with a KD of 3.12 ±0.05 µM.

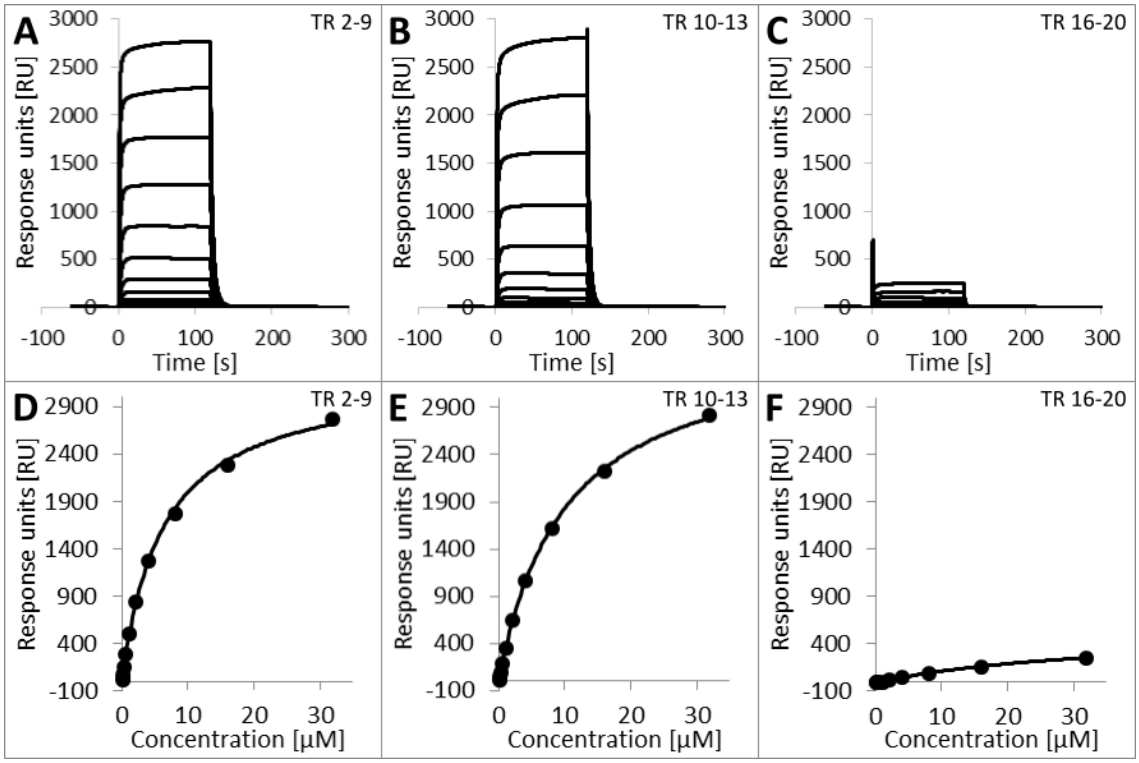

Figure 6-10: Truncation of the TonB-box does not impair FptA-binding.
SPR sensorgram shows FptA (0.03-32 µM) binding to (A) $TR_{\Delta 2\text{-}9}$, (B) $TR_{\Delta 10\text{-}13}$ and (C) $TR_{\Delta 16\text{-}20}$ immobilized by amine-coupling in HBS-OG buffer at 25 °C. (D) Sensorgram data from A were extracted and fit with a 1:1 binding model with a K_D of 6.53 ±0.13 µM. (E) Sensorgram data from B were extracted and fit with a 1:1 binding model with a KD of 10.07 ±0.19 nM. (F)Sensorgram data from C were extracted and fit to a 1:1 binding model with a K_D of 36.2 ±4.9 µM, which is well outside the reliably measured range but indicates a reduction in affinity.

It was then hypothesized that the interaction between TonB1 and PyoS5 allows the transfer of energy from the PMF for the translocation of PyoS5. If this was the case, a TonB-box-deletion should give the same phenotype in microscopy as the addition of CCCP (Fig. 4-14) which depletes the PMF. Indeed, this was the case; cells labelled with $TR_{\Delta 10\text{-}13}$ had lower fluorescence levels than TR-labelled cells but higher levels than cells labelled with TR and treated with trypsin (Fig. 6-11). No fluorescence was observed when cells were labelled with $TR_{\Delta 10\text{-}13}$ and treated with trypsin, showing the identified TonB-box is critical for translocation.

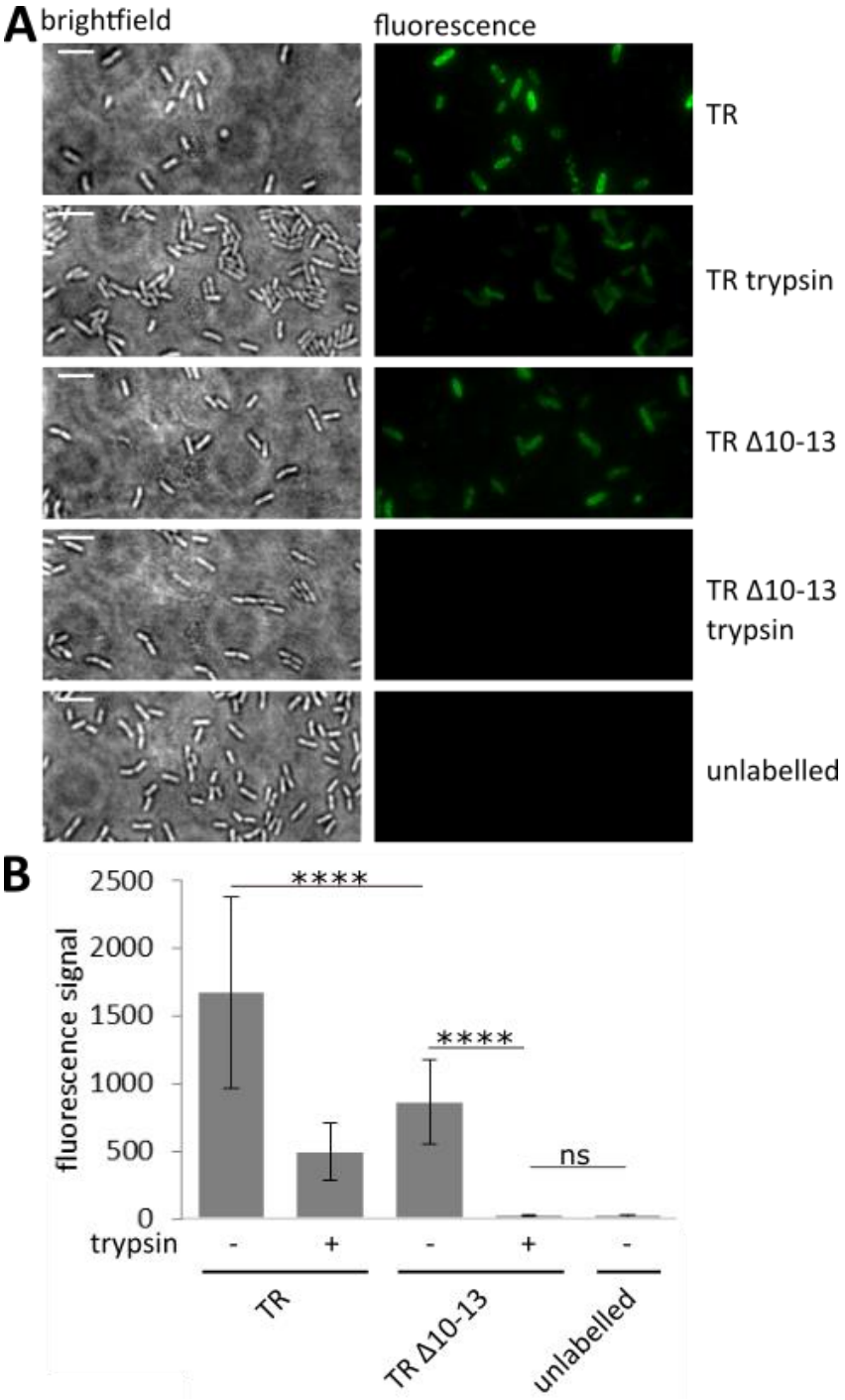

Figure 6-11: TonB-box-deletion prevents translocation.
(A) Fluorescent labelling of live *P. aeruginosa* PAO1 using TR-AF488 and $TR_{\Delta 10\text{-}13}$-AF488 with and without trypsin treatment. Scale bars, 5 μm. (B) Quantification of the average cell fluorescence observed under different conditions tested in A. **** indicates a p-value below 0.0001 in Student's t-test, ns indicates p-value above 0.05.

The interaction between TonB1 and PyoS5 is needed for PyoS5 translocation and cytotoxicity. However, FptA might also bind TonB1, as it is predicted to be a TBDT, has an N-terminal sequence that is thought to be a TonB-box and because TonB1 was shown

to be required for the import of pyochelin (Cobessi et al., 2005; Takase et al., 2000). To probe a potential interaction between TonB1 and FptA native MS was performed on a mixture of TonB1, FptA and PyoS5$_{1-299}$ and revealed complexes between FptA and PyoS5$_{1-299}$, FptA and TonB1, and a 1:1:1 complex between FptA, TonB1 and PyoS5$_{1-299}$ (Fig. 6-12). This shows for the first time that FptA interacts with TonB1. The absence of complexes between TonB1 and PyoS5 suggests that FptA has a higher affinity for TonB1 than PyoS5.

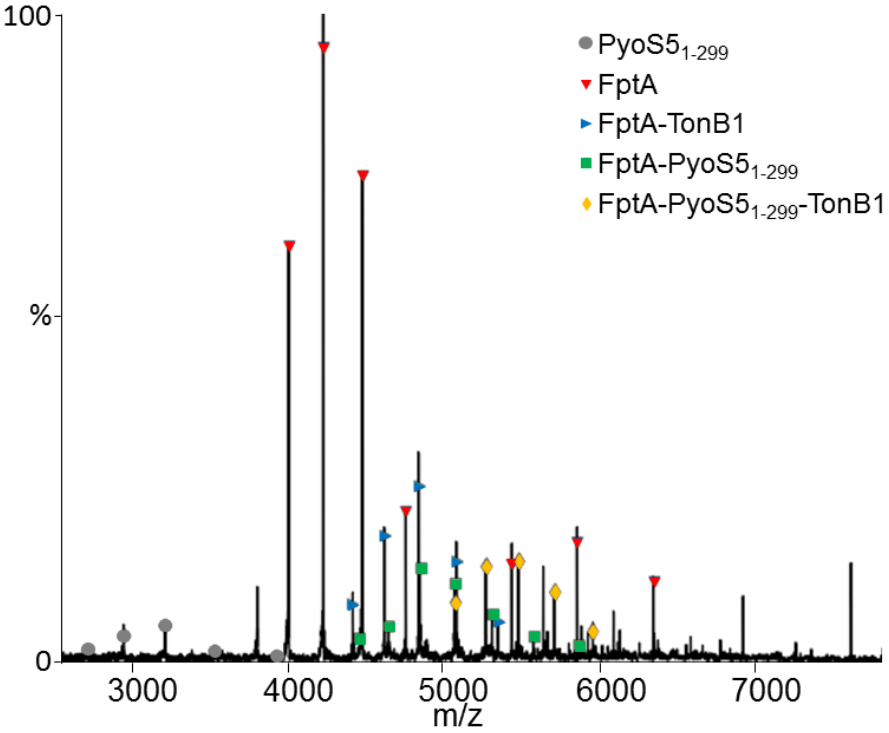

Figure 6-12: TonB1 preferentially interacts with isolated FptA.
Native mass spectrum of mixture containing purified FptA (3.3 µM), PyoS5$_{1-299}$ (6 µM) and TonB1 (8 µM). Species observed are PyoS5$_{1-299}$ at 35347 ±3 Da (expected mass 35351.12 Da), FptA at 76063 ±100 Da (expected mass 76068 Da), a complex of FptA and TonB1 at 101544 ±23 Da (expected mass 101541.67 Da), a complex of FptA and PyoS5$_{1-299}$ at 111420 ±11 Da (expected mass 111419.12 Da), and a complex containing one copy each of FptA, PyoS5$_{1-299}$ and TonB1 at 136901 ±11 Da (expected mass 136892.52 Da). Complexes of PyoS5$_{1-299}$ and TonB1 and of FptA, PyoS5$_{1-299}$ and two copies of TonB1 are absent. Experiment was performed by Joseph Gault (Department of Chemistry, University of Oxford).

6.3 Discussion

6.3.1 TonB-B1 as a tool

This chapter introduced the *E. coli-P. aeruginosa* TonB-B1 construct as a tool to find and confirm translocon components of pyocins. Here, the TonB-B1 construct was used to show that TonB1 is essential for the translocation of PyoS5 and PyoS4 but in the future it could be used to identify receptors of pyocins that are known or suspected to be TonB1-dependent.

It is worth keeping in mind that even though *E. coli* are not susceptible to PyoS5 nor any other pyocin that has been tested, some *E. coli* components might contribute to the import of PyoS5 into *E. coli* expressing FptA and TonB1. The TonB-TonB1 fusion was designed to interact with *E. coli* ExbB and ExbD and will likely also rely on the PMF and therefore relies indirectly on any component contributing to the maintenance of the PMF.

In *P. aeruginosa*, CPA accumulates PyoS5 on the cell surface, but it is unlikely that an equivalent step takes place in *E. coli* as the BL21 (DE3) strain used here lacks O-antigens and does not harbour the *P. aeruginosa*-specific antigen CPA.

The use of the TonB-B1 construct and a suitable receptor allowed pyocin-mediated killing of *E. coli* for the first time, showing that both the pyocin translocation and cytotoxic mechanism are conserved enough to be transferred between bacterial orders, those of Enterobacteriales and Pseudomonadales. While modification of bacteria to achieve susceptibility is not useful as a therapeutic treatment, it might inform future drug design. One can imagine engineered TonB-boxes and swapped receptor- and

translocator-binding domains to design drugs to target species from different orders of bacteria and to overcome native immunity to CLBs.

6.3.2 TonB1 as a translocon component

All well-characterized CLBs fall into two groups, group A CLBs that rely on the Tol-system and group B CLBs that rely on a Ton system. The dependence on TonB1, which was observed in this chapter, places PyoS5 and PyoS4 in group B. So far, all five pyocins for which the group has been determined: PyoS2 (White et al., 2017), PaeM1 and PaeM2 (Latino et al., 2019), and in this study PyoS5 and PyoS4, all belong to group B and use TonB1.

Interestingly, the three-way complex between FptA, PyoS5$_{1\text{-}299}$ and TonB1 has a 1:1:1 stoichiometry (Fig. 6-12) and no complex of FptA, S5 and two copies of TonB1 (1:1:2 stoichiometry) was observed, even though both FptA and PyoS5$_{1\text{-}299}$ bound TonB1 by themselves. In this three-way complex TonB1 was most likely to be bound to FptA as this interaction seemed to be favoured over the interaction between TonB1 and PyoS5$_{1\text{-}299}$. This and the fact that the interaction between TonB1 and PyoS5 was essential for cytotoxicity suggest that TonB1 interacts first with FptA and in a second event binds to PyoS5. It is conceivable that the TonB1-FptA interaction leads to a conformational change of the FptA plug, akin to the change that occurs when pyochelin binds FptA, which consequently exposes the TonB-box of PyoS5 to the cytoplasm. Similar conformational changes have been observed for BtuB and FpvAI (Hickman et al., 2017; White et al., 2017).

Future work might be able to uncover the role of the interaction between TonB1 and FptA, whether it is needed for PyoS5 cytotoxicity, receptor binding, translocation, and the formation of a three-way complex like that observed by native MS.

7. Discussion

7.1 General Discussion

7.1.1 A model for PyoS5 import

The recognition of antimicrobial resistance as a global problem has led to calls for new and better antibiotics, with *P. aeruginosa* identified as one of the priority pathogens (WHO, 2017, 2014). Bacteriocins have been suggested as candidates for new antibiotics and three recent developments have made CLBs especially attractive. First, CLB expression in plants was found to be an economically feasible and safe way of production and led to the approval of generally recognized as safe (GRAS) status of several CLBs in the United States (Hahn-Löbmann et al., 2019; Paškevičius et al., 2017; Schneider et al., 2018; Schulz et al., 2015). Second, CLBs have shown great potential as therapeutics in models of infection *in vivo* (Behrens et al., 2017; Cutler et al., 2007; Elfarash et al., 2014; McCaughey et al., 2016b). Finally, more than 3000 naturally occurring nuclease bacteriocins have been identified *in silico* (Sharp et al., 2017). Despite these advances fewer than 100 CLBs have been expressed and purified, and even fewer have been biochemically and functionally characterized.

Previously, PyoS5 was identified *in silico* and expressed to confirm its function and binding to CPA, the common polysaccharide antigen on the LPS of *P. aeruginosa* (Ling et al., 2010; McCaughey et al., 2016b; Parret and De Mot, 2000). A study by Elfarash et al. discovered that FptA is required for susceptibility to PyoS5, and suggested it functioned as a receptor for PyoS5 (Elfarash et al., 2014). However, the role of CPA binding was not clear, no direct interaction between FptA and PyoS5 was observed, the domain boundaries were not mapped, and no information on the structure of PyoS5 was

available. This study presents the crystal structure of PyoS5 which enabled the characterization of the PyoS5 import mechanism (Fig. 7-1).

Fluorescence microscopy showed for the first time that binding to CPA leads to accumulation of a pyocin on the cell surface, but not to translocation (Fig. 7-1). PyoS5 binds CPA with its CPA-binding domain, comprised of residues 194 to 315; this step is non-essential but increases susceptibility nine-fold. This is consistent with the decreased killing efficiency of PyoSD2, which harbours a homologous CPA binding domain, towards strains lacking CPA (McCaughey et al., 2016a).

After binding CPA, PyoS5 binds to FptA with its N-terminal domain, consisting of residues 1 to 196, of which residues 14 to 39 are essential for FptA-binding. Subsequently, it translocates using FptA with the help of TonB1 which provides energy from the PMF for import by means of a TonB-box, made up of PyoS5 residues 10 to 13 (Fig. 7-1). These processes are similar to those observed for PyoS2. PyoS2 also binds to an iron-siderophore receptor, FpvAI, followed by TonB1-dependent translocation through FpvAI (White et al., 2017) and like PyoS5, PyoS2 has an N-terminal TonB-box. The data presented in this thesis, together with those presented by White et al., suggest that the import mechanism presented here (Fig. 7-1) is a mechanism used by several pyocins including PyoS5, PyoS2 and PyoSD2.

It had previously been speculated that two copies of TonB1 bind consecutively during the import process of PyoS2, one to FpvAI and one to PyoS2, yet there was no data in support of this hypothesis (White et al., 2017). This study uses native MS data to show

for the first time that the un-energized PyoS5 FptA complex only binds one copy of TonB1, which suggests that the two interactions with TonB1 must be consecutive (Fig. 7-1) and that TonB1 and FptA directly interact to form a complex. This is in agreement with previous functional data showing that TonB1 is required for the uptake of pyochelin (Takase et al., 2000).

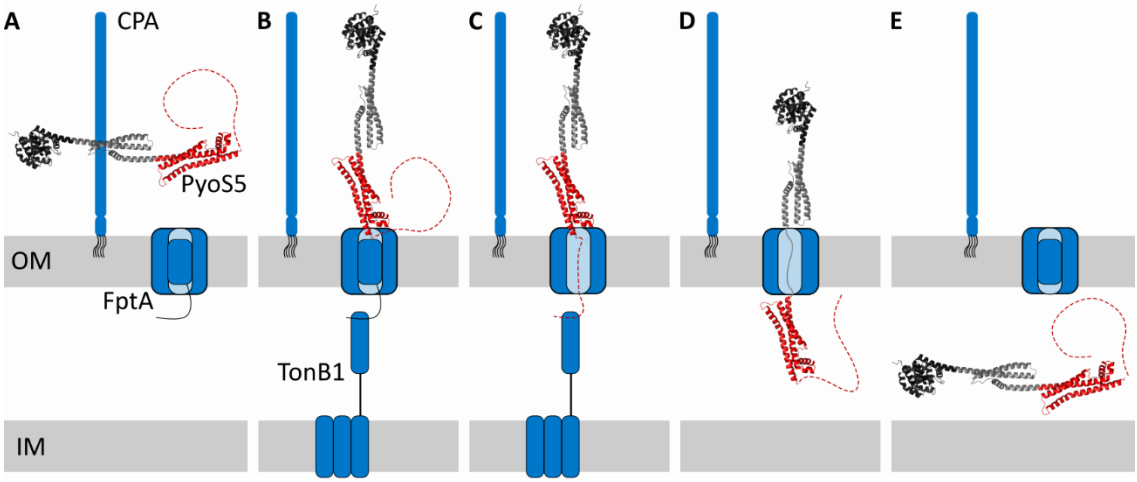

Figure 7-1: Model of PyoS5 translocation across the Gram-negative outer membrane.
(A) PyoS5 accumulates on the cell surface by binding to CPA. CPA is shown in linear conformation for clarity. (B) Surface bound PyoS5 can then associate with its outer membrane receptor, FptA which is in turn in contact with TonB1 in the periplasm. Interactions between FptA and TonB1 likely induce movement of the receptor plug domain, allowing the unstructured N-terminus of PyoS5 to thread through the translocator and access the periplasm. (C) Following entry into the periplasm the N-terminus of PyoS5 binds to TonB1 with its TonB-box motif. The formation of the PyoS5-TonB1 complex enables transduction of energy from the PMF that facilitates translocation of PyoS5 through the outer membrane, (D) possibly by a chain reaction of unfolding and refolding. (E) This results in PyoS5 inside the periplasm. Model not drawn to scale.

7.1.2 Interaction with CPA

The conserved CPA-binding groove identified in the second kHBDs of PyoS5, and also PyoS2 and PyoSD3, runs perpendicular to the long axis of the pyocin. This suggests two possibilities for the interaction of PyoS5 with CPA and FptA. If CPA is rigid and linear then two distinct binding events need to occur: first PyoS5 binds to CPA while being parallel to the membrane, then it unbinds CPA and binds FptA in a vertical orientation. This scenario is depicted in Figure 7-1. However, I do not know whether CPA is rigid

and linear and studies on LPS from *E. coli* suggest it is flexible (Schneck et al., 2009). If this is not the case, PyoS5 might be binding to both CPA and FptA simultaneously. The same is true for PyoS2 binding to CPA and FpvAI. In favour of this scenario is the cooperativity of binding of the two kHBDs observed in microscopy (Fig. 5-5) and liquid culture killing competition (Fig. 4-15). The same effect could, however, also stem from a local concentration effect that prevents washing away of the pyocin upon unbinding from FptA by rebinding to one of the many CPAs in the vicinity.

By accumulating pyocins at the outer membrane, CPA acts as a receptor that enables efficient translocator binding, a function analogous to the outer membrane proteins serving as receptors for some colicins in *E. coli*. ColA, ColE2 and ColE3, for example, bind to vitamin B12 transporter BtuB before translocating through the porin OmpF (Cascales et al., 2007). As in the case of CPA, BtuB increases susceptibility of *E. coli* to these colicins but is not essential for cytotoxicity (Benedetti et al., 1989). Previously the outer membrane proteins upon which pyocins depend were termed receptors (Ghequire and De Mot, 2014; Michel-Briand and Baysse, 2002; Sano et al., 1993b; White et al., 2017). However, for consistency with colicin nomenclature it is more appropriate to name them translocators. The table summarizing current knowledge on colicin-like pyocins (Table 2-1) has been updated accordingly, also including the finding that TonB1 is used by PyoS4 and PyoS5 (Table 7-1). For some of the pyocins with no known receptor, a receptor may not be required, as is the case for ColB and ColD (Cascales et al., 2007).

Table 7-1: Updated knowledge on pyocin uptake and cytotoxicity mechanisms.
Only colicin-like pyocins with demonstrated bactericidal activity are listed.

Pyocin	**Receptor**	**Translocator**	**Cytotoxic activity**	**Transenvelope system employed**
PyoAP41[1]	?	?	DNase[1]	?
PaeM1[1]	?	FiuA[2]	lipid II-hydrolysis[1]	TonB1[3]
PaeM2[3]	?	FiuA[3]	lipid II-hydrolysis[1]	TonB1[3]
PaeM4[4]	?	HxuC[5]	lipid II-hydrolysis[5]	?
PyoL1[7]	CPA[6]	BAM[8]	?	?
PyoL2[7]	?	BAM[8]	?	?
PyoL3[7]	?	?	?	?
PyoS1[1]	?	?	DNase[1]	?
PyoS2[1]	CPA[9]	FpvAI[1,10]	DNase[1]	TonB1[10]
PyoS3[1]	CPA[9]	FpvAII[1]	DNase[1]	?
PyoS4[1]	?	FpvAI[1]	tRNase[1]	TonB1 (this study)
PyoS5[1]	CPA[9]*	FptA[1]*	Pore-forming [1]	TonB1 (this study)
PyoS6[1]	?	?	rRNase[1]	?
PyoS8[11]	?	?	DNase[1]	?
PyoSD1[9]	?	?	tRNase[1]	?
PyoSD2[9]	CPA[9]	FpvAI[9]	tRNase[1]	?
PyoSD3[9]	CPA[9]	FpvAII[9]	tRNase[1]	?
PyoSN[12]	?	?	DNase[12]	?

? indicates unknowns. References: [1](Ghequire and De Mot, 2014), [2](Ghequire et al., 2017b), [3](Latino et al., 2019), [4](Paškevičius et al., 2017), [5](Ghequire and Öztürk, 2018), [6](McCaughey et al., 2014), [7](Ghequire et al., 2014), [8](Ghequire et al., 2018), [9](McCaughey et al., 2016a), [10](White et al., 2017), [11](Turano et al., 2017), [12](Sharp et al., 2017), *roles uncovered in this study.

Compared with most CLB receptors, CPA is different in that it is an LPS antigen rather than a protein. Apart from CPA-binding pyocins, the only other CLB known to use LPS as a receptor is ColN, which binds to the inner core and first residue of the outer core of *E. coli* LPS (Johnson et al., 2014; Sharma et al., 2009). As opposed to the protein receptors used by colicins, CPA and *E. coli* LPS are likely more abundant than the respective translocators. At several hundred to a few thousand copies per cell, receptor BtuB is approximately 50 times less abundant than translocator OmpF, which is the most abundant protein in the *E. coli* outer membrane at 60 000 to 90 000 copies (Li et al., 2014). The ratio of FptA to CPA is not known but it seems likely that FptA, which is one of the many outer membrane proteins (26 porins and 30 to 37 TBDTs per strain) and not among the four most abundant ones, is less abundant than CPA (Choi et al., 2011). The different ratios of receptor to translocator in *E. coli* and *P. aeruginosa* might reflect different ways of pre-concentrating the CLB on the cell surface to increase the chance of translocator binding. In *E. coli*, the protein receptors are used for high affinity binding with low nanomolar K_Ds to concentrate the bacteriocin onto the cell surface, whereas the pyocins use a high abundance of receptor to which they bind with medium affinity (high nanomolar to low micromolar K_Ds).

The role of colicin receptors, including LPS for ColN, is to orient the colicin correctly to bind the translocator (Housden et al., 2013, 2005; Johnson et al., 2014). Whether CPA also has a role in orienting pyocins for optimized binding to their receptors remains to be shown.

In *E. coli*, O-antigen presented on LPS prevents colicins and phages from binding to their receptors and thereby can cause insensitivity (Hoa Tran et al., 2014; Knirel et al., 2015;

Sharp et al., 2019; Van Der Ley et al., 1986). Another reason for pyocins to bind CPA, and in the case of bacteriophage A7 to degrade it, might be to overcome potential protective effects of LPS (Rivera et al., 1992). Whether the different LPS antigens and lack of antigens influence sensitivity to pyocins, and whether the CPA-binding domains present an advantage under such conditions, remains to be investigated.

This study presents the first structure of a kinked helical bundle CPA-binding domain, which is common to PyoS2, PyoSD3 and PyoS5. The structure of the PyoS5 CPA-binding domain is radically different than the monocot mannose-binding lectin (MMBL) domain in PyoL1 that binds CPA (McCaughey et al., 2014). The MMBL-fold consists of a three-sided β-prism with the conserved motif QxDxNxVxY to bind sugars on each face. It shows no similarity to the domain found in PyoS5, which consists of an α-helix bundle made up of one kinked and two straight helices.

The structure of the PyoS5 CPA-binding domain allowed us to build homology models for the CPA binding domains of PyoS2 and PyoSD3, which help to better understand these pyocins and might allow the phasing of future crystallographic data. Furthermore, the structure of the CPA-binding domain revealed that its fold is conserved with the N-terminal TBDT-binding domains of PyoS2 and PyoS5, suggesting that the kinked helical bundle fold is well-suited for the environments and processes pyocins are involved in. No other examples of the kinked helical bundle domains were found in the PDB using PDBefold (September 2017) or NCBI VAST (June 2019). This might be because structural similarity was not detected by the search algorithms, as in the case of PyoS2, or because other proteins harbouring this domain have not been crystallized yet. Among the better characterized pyocins, weak amino acid sequence similarity suggested that

kHBDs are common. It remains to be determined whether this is the case across the whole spectrum of CLBs, or is limited to group VIII bacteriocins as identified by Sharp et al., which include PyoAP41, PyoS1, PyoS2, PyoS3, PyoS4 and PyoSN (Sharp et al., 2017).

7.1.3 Interactions with FptA

Compared with other interactions between CLBs and their receptors and translocators, the interaction between PyoS5 and FptA is surprisingly weak, with a K_D of 6.5 µM. Yet PyoS5 is known to be a very potent pyocin *in vivo*. The interaction between PyoS2 and its translocator FpvAI is in the pM range, just like that of native ligand pyoverdine (Clément et al., 2004; Schalk et al., 2001; White et al., 2017). The interaction between ColE3 and BtuB has a K_D around 1 nM, which is similar to that of natural ligand vitamin B12 binding to BtuB with a K_D of 0.5 nM (Kurisu et al., 2003; White et al., 1973). Ferric pyochelin binds to FptA with a K_D of 2.5 nM (Hoegy et al., 2009); it is therefore surprising that PyoS5, which competes for the same receptor, binds with a K_D three orders of magnitude higher. In fact, the affinity of the PyoS5:FptA interaction is more similar to interactions between CLBs and receptors or translocators that do not have natural ligands. Examples of these include OmpF to which ColN and ColE9 bind with low micromolar K_D, LPS to which ColN binds with a ~2 µM K_D, and CPA to which several S-type pyocins bind with K_Ds between 0.2 and 1.5 µM (Housden et al., 2010; Johnson et al., 2014; McCaughey et al., 2016a).

It is possible that the discrepancy between the affinities of pyochelin and PyoS5 for FptA is due to the different experimental conditions: FptA was in *P. aeruginosa* membranes at 0 °C for studies on pychelin, compared with detergent-solubilized FptA at 25 °C in this study (Hoegy et al., 2009). In favour of this explanation is the K_D for the interaction

between FptA and Tb-bound pyochelin which was determined to be 4.6 μM under conditions similar to the ones in this study, with detergent solubilized FptA at RT (Yang et al., 2011). However, it is again not clear whether the difference between ferric and Tb-bound pyochelin is due to the different metal or the different experimental conditions. An alternative explanation is that the competition of PyoS5 and pyochelin is not a limitation *in vivo*, for example because the abundance of pyochelin is low or the rate limiting step is translocation, not translocator binding. If this is the case, a tight interaction to compete with the native ligand is not necessary and a micromolar K_D would be sufficient, just like it is for interactions of CLBs with outer membrane components that have no natural ligands.

In 2014 Elfarash et al. aimed to further characterize PyoS5 by domain swaps with PyoS2, yet the lack of information about the PyoS5 domain boundaries and the functions of PyoS2 domains limited this effort. The advantage of the study presented here is the crystal structure that allowed us to map the domains of PyoS5, and thereby paved the way for in-depth characterization of the PyoS5 import mechanism. I showed by fluorescence microscopy and SPR that PyoS5 binds to FptA with residues 1 to 315, and narrowed down the essential residues to 14 to 39. These findings disagree with the domain-swap characterization by Elfarash et al. who had inferred residues 150 to 300 would interact with FptA. Interestingly, Elfarash et al. observed cytotoxic activity by a construct consisting of PyoS5 residues 150 to 300 translationally fused to PyoS2 residues 216 to 689 when 10 μL at 15 mg/mL were spotted onto a plate with a bacterial cell layer, an amount equivalent to 763.2 μM in our assays. This is surprising not only because I find no role of PyoS5 residues 150 to 300 in FptA-binding, but also because neither the PyoS5 nor the PyoS2 portion of the fusion-construct contain a TonB-box yet both PyoS5 and

PyoS2 have been shown to lose their cytotoxic activity when the TonB-box is removed (White et al., 2017).

7.1.4 Interaction with TonB1

The present study showed that PyoS4 and PyoS5 use TonB1 to cross the outer membrane. This means that TonB1 is used by all five colicin-like pyocins that have been investigated with respect to their energy requirements: PaeM1, PaeM2, PyoS2, PyoS4 and PyoS5 (Latino et al., 2019; White et al., 2017). In *E. coli* all TolA-dependent colicins use general diffusion porins like OmpF as translocators, which have no equivalent in *P. aeruginosa* (Chevalier et al., 2017). It is therefore conceivable that there are no Tol-dependent colicin-like pyocins and that many, if not all, colicin-like pyocins use TonB1.

To show that PyoS4 and PyoS5 used TonB1 I modelled *P. aeruginosa* in *E. coli* by supplying a TonB-TonB1 hybrid and the respective translocator. A similar approach, where translocator YiuR and TonB from *Yersinia kristensenii* were expressed in *E. coli*, was used to determine the role of TonB in colicin FY import (Bosák et al., 2012). Beyond confirming the role of TonB1 in CLB import, the TonB-TonB1 hybrid will also be a useful addition to the tools available to study translocators (Atanaskovic and Kleanthous, 2019). It will allow us to determine translocators of those pyocins that are TonB1-dependent (which might be all of them, as discussed above), and to distinguish translocators from receptors.

The interaction of TonB1 with PyoS5 is required for the translocation of PyoS5 across the outer membrane. It is likely that TonB1 provided energy to unfold PyoS5 to be pulled through the barrel of FptA as an unfolded polypeptide chain (Fig. 7-1). While there is no

direct evidence for the unfolding of PyoS5 for translocation, it is known that the N-terminal kHBD domain of PyoS2 unfolds during translocation through FpvAI (White et al., 2017) and that several colicin domains unfold during translocation, including the receptor-binding and DNase domains of ColE9 and the pore-forming domains of ColA and ColN (Baboolal et al., 2008; Duché et al., 1994b, 1994a; Penfold et al., 2004; Vankemmelbeke et al., 2013). TonB1-driven unfolding and partial or complete refolding in the periplasm therefore seems a plausible mechanism for PyoS5 translocation through FptA

7.1.5 Conserved domains in PyoS2 and PyoS5

This study describes similarities in the import mechanism and structures of the N-terminal domains of PyoS2 and PyoS5, and predicts similarities in the structures of their CPA-binding domain. While the similarity of the CPA-binding domains is expected based on similarities in protein sequence, no such similarities were apparent in the N-terminal domains. The similarity between the two pyocins in structure and function and in parts of their sequences suggests a common vertical evolutionary origin of PyoS2 and PyoS5. However, their different C-terminal halves including different cytotoxic mechanisms suggest an event of horizontal gene transfer or recombination later on. While PyoS5 and PyoS2 markedly differ in sequence even in the regions with conserved fold and function, PyoSD2 has a nearly identical sequence to PyoS2 in these two domains. The different cytotoxic domains of PyoS2 and PyoSD2 suggest yet another event of recombination. I conclude that both vertical and horizontal evolution shaped the development of S-type pyocins.

7.1.6 PyoS5 as a therapeutic

The strong potency of PyoS5 in *in vivo* models of infection motivated the present study. The new details on biophysical properties of PyoS5 I report are promising for future therapeutic applications. These properties include its long-term stability at -20 °C, its T_m of 57 °C (far above room temperature and common outdoor temperatures), and its monomeric state at high concentrations.

Once considered a disadvantage for therapeutics, the narrow spectrum of CLBs is now recognized as beneficial because it allows us to precisely target pathogens with minimal disruption to host microbiota, and therefore with reduced risk of antibiotic-induced dysbiosis. For narrow-spectrum antibiotics like PyoS5 to be useful in the clinic, improved diagnostics or the use of several narrow-spectrum antibiotics in a cocktail (or both) are needed. The presence of *P. aeruginosa* in wound infections can already be detected at the point of care by a hand-held device detecting autofluorescence (DaCosta et al., 2015). Understanding the minimal components that make a cell susceptible, for example to PyoS5, might allow us to predict susceptibility based on sequences of relevant loci. PCR- and sequencing-based diagnostic methods can gather this information within a few hours; current procedures of culturing bacteria in the presence of antibiotics, by contrast, cannot be done within the same day (Charalampous et al., 2019; Dinc et al., 2016; Song and Gyarmati, 2019). Alternatively, the fluorescent probes developed in this study by modifying PyoS5 domains with AF488 could be used to predict the susceptibility of *P. aeruginosa* from clinical samples to PyoS5 before treatment: the probes bind to susceptible bacteria which become fluorescent and can be detected in a portable device. A similar approach using a ColS4-GFP fusion has already been developed to detect if water is contaminated with *E. coli* (Gutiérrez-del-Río et al., 2018).

The reconstitution of PyoS5-import in *E. coli* has shown that FptA and TonB1 determine the spectrum of bacteria against which PyoS5 is active. Outside of *P. aeruginosa*, *fptA* occurs in other *Pseudomonas* species, *Burkholderia* species and in *Serratia marcescens*, with amino acid sequence identities to *P. aeruginosa fptA* of 99.7 % to 74.5 %, 62.9 % to 64.0 % and 64.8 % to 65.0 %, respectively. A *B. cenocepia fptA*, with 63% amino acid sequence identity to *P. aeruginosa fptA*, has previously been shown not to complement a knockout of *P. aeruginosa fptA* with respect to PyoS5 susceptibility (Elfarash et al., 2014). It will be interesting to see whether *fptA*s with higher sequence similarities can complement an *fptA* knockout in *P. aeruginosa*, and whether strains harbouring such similar FptA are susceptible to PyoS5.

TonB1 is the second component required for *P. aeruginosa* specificity, and its C-terminal domain which was expressed in *E. coli* in this study exclusively occurs in the genus *Pseudomonas*, based on a cut-off of 50 % sequence identity. To the best of our knowledge, PyoS5 therefore specifically targets only *Pseudomonas* strains without effects on other bacteria, and would therefore cause minimal disruption to the microbiome when used as a therapeutic.

Where altered target specificity is desired, for example to different TBDTs in *P. aeruginosa* or to different species and where native immunity needs to be overcome, chimeric CLBs can be used, as has been demonstrated in this study. Naturally occurring bacteriocins can more easily find their way to application due to easier approval pathways, such as GRAS. Nonetheless, the use of therapeutics optimized based on

naturally occurring substances is well established, for example among small molecule antibiotics (Walsh and Wencewicz, 2014).

7.2 Future work

The last piece of the puzzle concerning the translocation of PyoS2 and PyoS5 across outer membranes is the influence of the interaction of their respective translocators, FpvAI and FptA, with TonB1. This question might be solved in the future by mutating the predicted TonB-box of FptA to see whether translocation of PyoS5 or killing by PyoS5 are affected, and whether the absence of the PyoS5 TonB-box or FptA TonB-box influences the formation of the TonB1 complex with FptA and PyoS5 *in vitro*. Equivalent experiments could be performed with PyoS2.

Structural studies on the interactions characterized in this work, CPA:PyoS5, PyoS5:FptA, PyoS5:TonB1 and FptA:TonB1, might be able to improve the level of detail in which I understand these interactions. By using cryo-electron microscopy it might even be possible to structurally characterize the whole PyoS5 translocon.

This study presents two new chimeric CLBs that alter the targeted species-specifity compared to PyoS5 and overcome native immunity. The design of chimeric CLBs is therefore a promising path to new antibiotics with custom targets. These experiments also showed that the cytotoxic domains of ColIa and PyoS5 are active against *P. aeruginosa* and *E. coli*, bacteria from different phylogenetic orders. It is therefore likely that all bacteria in these orders and possibly all Gammaproteobacteria are susceptible to CLB pore-forming domains. The challenge will be the translocation of these domains across the outer membrane of different bacterial species.

To further inform the design of chimeric and engineered CLBs, the TonB-boxes of pyocins could be engineered to make use of TonBs from different species. For example, the TonB-box of PyoS5 could be exchanged for that of ColB, and to test whether this altered TonB-box is functional, cytotoxic activity against *E. coli* expressing FptA can be tested. To change the translocator a CLB uses, domains can be swapped or alternatively new translocator-binding domains can be designed. The high structural similarity of PyoS5 and PyoS2 suggests that the common protein architecture is well-suited for pyocins and is suitable for targeting and translocating through different *P. aeruginosa* TBDTs. Directed evolution combined with repertoire selection technologies such as phage display (Sioud, 2019) could be used to further develop pyocins against other TBDTs in *P. aeruginosa* and potentially even other bacteria.

It would also be useful to determine whether *Pseudomonas* strains other than *P. aeruginosa* are targeted by naturally occurring translocation domains such as those of PyoS2 and PyoS5.

Apart from the outer membrane, native immunity can present a problem to treatment with CLBs. It was shown in this study that immunity to PyoS5 can be overcome by the most similar CLB pore-forming domain, that of ColIa. If the cytotoxic domain of PyoS5 can also overcome the immunity of ColIa, then a mixture of CLBs with just these two cytotoxic domains should be able to kill all strains, because immunity to ColIa does not occur in *P. aeruginosa* and ImS5 immunity to PyoS5 does not occur outside of *P. aeruginosa*.

7.3 Conclusions

In summary, this thesis used a multidisciplinary approach to uncover the structure and import mechanism of PyoS5, a potent protein antibiotic. This began by biophysically characterizing PyoS5 and solving its crystal structure. Microbiological approaches and fluorescence microscopy then identified the roles of outer membrane components CPA and FptA and inner membrane protein TonB1 in PyoS5 import. Binding assays determined binding sites for each of these components on PyoS5, and this knowledge was used to design new chimeric CLBs which overcame native immunity and had altered target specificity. A new approach was developed to mimic *P. aeruginosa* susceptibility but using *E. coli*, which was used to show that the minimal components needed for PyoS5 import are FptA and TonB1. Finally, homology modelling and structure comparisons revealed conserved folds between PyoS2 and PyoS5 which match similarities in the import mechanisms of the two pyocins.

Combined, these data describe a multi-step molecular mechanism of PyoS5 translocation across the outer membrane of *P. aeruginosa*. PyoS5 is first accumulated by its receptor CPA on the cell surface where it can efficiently locate its translocator FptA. PyoS5 then binds to FptA, which triggers energy transfer from the PMF to FptA via TonB1 and leads to a conformational change that allows PyoS5 to expose its N-terminal TonB-box to the periplasm. There PyoS5 interacts with TonB1 which provides energy to drive translocation, probably by successive unfolding and re-folding of domains.

This work reveals a common structure and import mechanism of two CLBs, PyoS2 and PyoS5, and showed how such knowledge can be used to design novel antibiotics with

custom characteristics. I hope this study aids and inspires the design of more and better antibiotics, so urgently needed in the race against antimicrobial resistance.

8. Appendix

8.1 Protein sequences

8.1.1 PyoS5

MSNDNEVPGSMVIVAQGPDDQYAYEVPPIDSAAVAGNMFGDLIQREIYLQKNIYYPVRSIFEQGTKEKKEI
NKKVSDQVDGLLKQITQGKREATRQERVDVMSAVLHKMESDLEGYKKTFTKGPFIDYEKQSSLSIYEAWVKI
WEKNSWEERKKYPFQQLVRDELERAVAYYKQDSLSEAVKVLRQELNKQKALKEKEDLSQLERDYRTRKANL
QMKVQSELDQAGSALPPLVSPTPEQWLERATRLVTQAIADKKQLQTTNNTLIKNSPTPLEKQKAIYNGELLV
DEIASLQARLVKLNAETTRRRTEAERKAAEEQALQDAIKFTADFYKEVTEKFGARTSEMARQLAEGARGKNI
RSSAEAIKSFEKHKDALNKKLSLKDRQAIAKAFDSLDKQMMAKSLEKFSKGFGVVGKAIDAASLYQEFKISTE
TGDWKPFFVKIETLAAGAAASWLVGIAFATATATPIGILGFALVMAVTGAMIDEDLLEKANNLVISILEHHH
HHH

8.1.2 **ColBPyoS5:** ColB residues 1-340 and PyoS5 residues 303-498

MSDNEGSVPTEGIDYGDTMVVWPSTGRIPGGDVKPGGSSGLAPSMPPGWGDYSPQGIALVQSVLFPGIIR
RIILDKELEEGDWSGWSVSVHSPWGNEKVSAARTVLENGLRGGLPEPSRPAAVSFARLEPASGNEQKIIRL
MVTQQLEQVTDIPASQLPAAGNNVPVKYRLTDLMQNGTQYMAIIGGIPMTVPVVDAVPVPDRSRPGTNI
KDVYSAPVSPNLPDLVLSVGQMNTPVRSNPEIQEDGVISETGNYVEAGYTMSSNNHDVIVRFPEGSGVSPL
YISAVEILDSNSLSQRQEAENNAKDDFRVKKEQENDEKTVLTKTSEVIISVGDKVGEYEL
TTRRRTEAERKAAEEQALQDAIKFTADFYKEVTEKFGARTSEMARQLAEGARGKNIRSSAEAIKSFEKHKDAL
NKKLSLKDRQAIAKAFDSLDKQMMAKSLEKFSKGFGVVGKAIDAASLYQEFKISTETGDWKPFFVKIETLAA
GAAASWLVGIAFATATATPIGILGFALVMAVTGAMIDEDLLEKANNLVISILEHHHHHH

8.1.3 **PyoS5ColIa:** PyoS5 residues 1-315 and ColIa residues 485-626

MSNDNEVPGSMVIVAQGPDDQYAYEVPPIDSAAVAGNMFGDLIQREIYLQKNIYYPVRSIFEQGTKEKKEI
NKKVSDQVDGLLKQITQGKREATRQERVDVMSAVLHKMESDLEGYKKTFTKGPFIDYEKQSSLSIYEAWVKI
WEKNSWEERKKYPFQQLVRDELERAVAYYKQDSLSEAVKVLRQELNKQKALKEKEDLSQLERDYRTRKANL
QMKVQSELDQAGSALPPLVSPTPEQWLERATRLVTQAIADKKQLQTTNNTLIKNSPTPLEKQKAIYNGELLV
DEIASLQARLVKLNAETTRRRTEAERKAAELKATKDAINFTTEFLKSVSEKYGAKAEQLAREMAGQAKGKKIR
NVEEALKTYEKYRADINKKINAKDRAAIAAALESVKLSDISSNLNRFSRGLGYAGKFTSLADWITEFGKAVRTE
NWRPLFVKTETIIAGNAATALVALVFSILTGSALGIIGYGLLMAVTGALIDESLVEKANKFWGILEHHHHHH

8.1.4 ImS5

MSFKYYWAKFFWGAFFFVLVAWKGSVFPSLASVNPLVVAGLSTILFPFSVKLVEDFALKYTEREFWVTGFFS
ETPAKTGLYAVFYLSCYLFSIPLGMVFLFYKYGKAS

8.1.5 **FptA:** *E. coli* OmpF signal sequence residues 1-23 and FptA residues 39-720

MVKRNILAVIVPALLVAGTANAA
DARKDGETELPDMVISGESTSATQPPGVTTLGKVPLKPRELPQSASVIDHERLEQQNLFSLDEAMQQATGV
TVQPFQLLTTAYYVRGFKVDSFELDGVPALLGNTASSPQDMAIYERVEILRGSNGLLHGTGNPAATVNLVRK
RPQREFAASTTLSAGRWDRYRAEVDVGGPLSASGNVRGRAVAAYEDRDYFYDVADQGTRLLYGVTEFDLS
PDTLLTVGAQYQHIDSITNMAGVPMAKDGSNLGLSRDTYLDVDWDRFKWDTYRAFGSLEQQLGGGWKG
KVSAEYQEADSRLRYAGSFGAIDPQTGDGGQLMGAAYKFKSIQRSLDANLNGPVRLFGLTHELLGGVTYAQ
GETRQDTARFLNLPNTPVNVYRWDPHGVPRPQIGQYTSPGTTTTTQKGLYALGRIKLAEPLTLVVGGRESW
WDQDTPATRFKPGRQFTPYGGLIWDFARDWSWYVSYAEVYQPQADRQTWNSEPLSPVEGKTYETGIKGE
LADGRLNLSLAAFRIDLENNPQEDPDHPGPPNNPFYISGGKVRSQGFELEGTGYLTPYWSLSAGYTYTSTEYL
KDSQNDSGTRYSTFTPRHLLRLWSNYDLPWQDRRWSVGGGLQAQSDYSVDYRGVSMRQGGYALVNMR
LGYKIDEHWTAAVNVNNLFDRTYYQSLSNPNWNNRYGEPRSFNVSLRGAF*

8.1.6 **TonB1:** Residues 109-342

GAMATPAELNLGHGELPKTMQVNFVQLEKKAEPTPQPPAAAPEPTPPKIEEPKPEPPKPKPVEKPKPKPKP
KPKPVENAIPKAKPKPEPKPKPEPEPSTEASSQPSPSSAAPPPAPTVGQSTPGAQTAPSGSQGPAGLPSGSL
NDSDIKPLRMDPPVYPRMAQARGIEGRVKVLFTITSDGRIDDIQVLESVPSRMFDREVRQAMAKWRFEPR
VSGGKIVARQATKMFFFKIEKRR

8.1.7 **TonB-B1 hybrid:** TonB residues 109-342 and TonB1 residues 201-342

MTLDLPRRFPWPTLLSVCIHGAVVAGLLYTSVHQVIELPAPAQPISVTMVTPADLEPPQAVQPPPEPVVEPE
PEPEPIPEPPKEAPVVIEKPKPKPKPKPKP
EPSTEASSQPSPSSAAPPPAPTVGQSTPGAQTAPSGSQGPAGLPSGSLNDSDIKPLRMDPPVYPRMAQAR
GIEGRVKVLFTITSDGRIDDIQVLESVPSRMFDREVRQAMAKWRFEPRVSGGKIVARQATKMFFFKIEKRR

8.1.8 **ColIa**

MSDPVRITNPGAESLGYDSDGHEIMAVDIYVNPPRVDVFHGTPPAWSSFGNKTIWGGNEWVDDSPTRSD
IEKRDKEITAYKNTLSAQQKENENKRTEAGKRLSAAIAAREKDENTLKTLRAGNADAADITRQEFRLLQAELR
EYGFRTEIAGYDALRLHTESRMLFADADSLRISPREARSLIEQAEKRQKDAQNADKKAADMLAEYERRKGIL
DTRLSELEKNGGAALAVLDAQQARLLGQQTRNDRAISEARNKLSSVTESLNTARNALTRAEQQLTQQKNTP
DGKTIVSPEKFPGRSSTNHSIVVSGDPRFAGTIKITTSAVIDNRANLNYLLSHSGLDYKRNILNDRNPVVTEDV
EGDKKIYNAEVAEWDKLRQRLLDARNKITSAESAVNSARNNLSARTNEQKHANDALNALLKEKENIRNQLS
GINQKIAEEKRKQDELKATKDAINFTTEFLKSVSEKYGAKAEQLAREMAGQAKGKKIRNVEEALKTYEKYRAD
INKKINAKDRAAIAAALESVKLSDISSNLNRFSRGLGYAGKFTSLADWITEFGKAVRTENWRPLFVKTETIIAG
NAATALVALVFSILTGSALGIIGYGLLMAVTGALIDESLVEKANKFWGILEHHHHHH

8.1.9 PyoS4

MTNNSAPPLVVTRGNDNGYEPGSMVITHVQASGLDIIQYIPGRSSYGTPPFVPPGPSPYVGPGMQEYRRLR
DTLDKSNSELKKNLKNKTLKEVDELKSEAGLPVKAVSANDIRDEKSIVDALMDAKAKSLKAIEDRPANLYTAS
DFPQKSEAMYQNQLLASRKFYGEFLDRHMSELAKAYSADIYKAQIAILKQTSQELESKARSMEAQAQQVTQ
QLGADFNAITTPTATKVQQRVKAVDASLSQVSTQVSGAVASATQAVQVKTAQAQQQANSQISSSQNLISA
AFRNQIALAAQASGEAQVTAFNTQVKQIVNEATAFSTARKQALAQFAANAAAEVETEVNRLTAQVKASPT
KAASQAAQATLRQFTESTYAKVNTYAQQTEAELQAKAKEVSAAVAEAQRAATNDLQKTADVVPGQIIQAA
NTLAMPATSTPLVSVAGFGSAAVETARLAASLTNAVNRLVQIAGSGPGAYVATFAVLSLYSDQAGKDSDKV
PAGVRNALALEASALGLPGTADLQSVAKAGGTVDMPVRLTSAAQESPSGKSQIAAMLTNGATVPKGVPVR
AATLNAATGRYEVTVPAKSTVPNTPPLILTWTPATPPGSQNPSSTTPVVPQPVPVYEGATITPVQAEPESYP
GVPLDLDDLIVIFPVGSGVKPIYIMFNHNPHDVVIDDKIREQIPIRGWTEVEVRDVIGKGATGSSSDKRRPNK
TIDGLGRNDSATVYGSPPNGYIVVNDRTGEIIQIADRNDSAWAVDGRIIWRNK

8.1.10 ImS4

MVNPNSVEIVDNGLDFFSKEGNGKMWLTTKATLEVVSLATKKGLAISKIEGFIWHKDVGRFEARLDAIFEGL
VNPVKVPDVVNNNNARAKESTEEDASLGHDAFIVTIASRKLEHHHHHH

8.1.11 PyoS2

MAVNDYEPGSMVITHVQGGGRDIIQYIPARSSYGTPPFVPPGPSPYVGTGMQEYRKLRSTLDKSHSELKKN
LKNETLKEVDELKSEAGLPGKAVSANDIRDEKSIVDALMDAKAKSLKAIEDRPANLYTASDFPQKSESMYQS
QLLASRKFYGEFLDRHMSELAKAYSADIYKAQIAILKQTSQELENKARSLEAEAQRAAAEVEADYKARKANVE
KKVQSELDQAGNALPQLTNPTPEQWLERATQLVTQAIANKKKLQTANNALIAKAPNALEKQKATYNADLL
VDEIASLQARLDKLNAETARRKEIARQAAIRAANTYAMPANGSVVATAAGRGLIQVAQGAASLAQAISDAI
AVLGRVLASAPSVMAVGFASLTYSSRTAEQWQDQTPDSVRYALGMDAAKLGLPPSVNLNAVAKASGTVD
LPMRLTNEARGNTTTLSVVSTDGVSVPKAVPVRMAAYNATTGLYEVTVPSTTAEAPPLILTWTPASPPGNQ
NPSSTTPVVPKPVPVYEGATLTPVKATPETYPGVITLPEDLIIGFPADSGIKPIYVMFRDPRDVPGAATGKGQP
VSGNWLGAASQGEGAPIPSQIADKLRGKTFKNWRDFREQFWIAVANDPELSKQFNPGSLAVMRDGGAPY
VRESEQAGGRIKIEIHHKVRIADGGGVYNMGNLVAVTPKRHIEIHKGGK

8.1.12 ImS2

MKSKISEYTEKEFLEFVKDIYTNNKKKFPTEESHIQAVLEFKKLTEHPSGSDLLYYPNENREDSPAGVVKEVKE
WRASKGLPGFKAGLEHHHHHH

8.2 The therapeutic potential of bacteriocins as protein antibiotics

Emerging Topics in Life Sciences (2017) **1** 65–74
DOI: 10.1042/ETLS20160016

PORTLAND PRESS

Review Article

The therapeutic potential of bacteriocins as protein antibiotics

Hannah M. Behrens[1,*], Anne Six[2,*], Daniel Walker[2] and Colin Kleanthous[1]

[1]Department of Biochemistry, University of Oxford, South Parks Road, Oxford OX1 3QU, U.K. and [2]Institute of Infection, Immunity and Inflammation, College of Medical, Veterinary and Life Sciences, University of Glasgow, Glasgow G12 8QQ, U.K.

Correspondence: Daniel Walker (daniel.walker@glasgow.ac.uk) or Colin Kleanthous (colin.kleanthous@bioch.ox.ac.uk)

OPEN ACCESS

The growing incidence of antibiotic-resistant Gram-negative bacterial infections poses a serious threat to public health. Molecules that have yet to be exploited as antibiotics are potent protein toxins called bacteriocins that are produced by Gram-negative bacteria during competition for ecological niches. This review discusses the state of the art regarding the use for therapeutic purposes of two types of Gram-negative bacteriocins: colicin-like bacteriocins (CLBs) and tailocins. In addition to *in vitro* data, the potency of eight identified CLBs or tailocins has been demonstrated in diverse animal models of infection with no adverse effects for the host. Although the characteristics of bacteriocins will need further study, results obtained thus far regarding their *in vivo* potency, immunogenicity and low levels of resistance are encouraging. This leads the way for the development of novel treatments using bacteriocins as protein antibiotics.

Introduction

Antibiotic resistance has increased at an alarming rate worldwide, yet at the same time the discovery of new antibiotics is stalling. Of particular concern are infections caused by Gram-negative bacteria, which possess a highly impermeable outer membrane that limits the entry of multiple classes of antibiotics, leaving limited therapeutic options that are increasingly less efficacious as resistance spreads [1–4]. Foremost among the Gram-negative pathogens are *Pseudomonas aeruginosa*, *Escherichia coli*, *Klebsiella pneumoniae* and *Acinetobacter baumannii*, all of which pose serious threats to global healthcare and patient safety; in 2008, US intensive care units reported 17, 13, 13 and 74%, respectively, of clinical isolates of these species as multidrug-resistant [5]. Among these pathogens, *E. coli* and *K. pneumoniae* are well-known producers of extended-spectrum β-lactamases and carbapenemases that render producing bacteria resistant to β-lactams including cephalosporins and carbapenems, which are considered to be antibiotics of last resort [2,6,7]. In addition, chronic biofilm-mediated infections, such as *P. aeruginosa* lung infections in cystic fibrosis patients and *E. coli* urinary tract infections, are relatively poorly treated with existing antibiotics [8–10]. Consequently, treatment options for infections caused by Gram-negative bacteria are limited and patient outcome is increasingly poor [8–10].

Bacteriocins offer a potential alternative therapeutic strategy to treat both multidrug-resistant and chronic bacterial infections. These antimicrobial peptides or proteins are diverse and widespread among Gram-positive and Gram-negative bacteria [11]. It is becoming evident that they are linked to pathogenesis as they play a role in displacing bacterial flora, enhancing colonization and therefore infection ([11–13] and Sharp et al. unpublished data). In fact, protein bacteriocin-encoding genes can be found in the genomes of most Gram-negative pathogens, including *P. aeruginosa*, *E. coli* and *K. pneumoniae* ([14] and Sharp et al. unpublished data). Importantly, they are highly specific antibacterials that kill only bacteria closely related to the producer and are deployed during the fight for resources with competitor strains [14–16]. This specificity makes them attractive as therapeutics as they offer a more targeted approach. Indeed, one major issue with conventional antibiotics is the dysbiosis induced by broad-range killing of bacteria [17]. While the narrow killing spectrum of

*These authors contributed equally to this work.

Received: 23 February 2017
Revised: 14 March 2017
Accepted: 16 March 2017

Version of Record published: 21 April 2017

PORTLAND PRESS

Emerging Topics in Life Sciences (2017) 1 65–74
DOI: 10.1042/ETLS20160016

bacteriocins means that the bacteria responsible for the infection have to be identified prior to treatment, it gives the advantage of being able to specifically target one species, or even one strain of bacteria, leaving the normal healthy microflora intact [17]. The narrow killing spectrum also reduces the selective pressure for resistance on bystander microorganisms [18].

Gram-negative bacteriocins can be classified into three groups: peptide bacteriocins, which have been reviewed elsewhere [19,20], colicin-like bacteriocins (CLBs) and tailocins. The potential of the latter two, CLBs and tailocins, to treat bacterial infections is reviewed here. Previous reviews have discussed Gram-positive bacteriocins as antibiotics [11,21,22] and the *in vitro* potential of bacteriocins against Gram-negative bacteria [11,23–25]. Our aim is to focus on the potential ability of CLBs and tailocins to treat Gram-negative infections and give an exhaustive report of the results available from *in vivo* models of infection to date. We will not discuss data from probiotic applications of bacteriocins as the role of bacteriocins in probiotics is complex and only beginning to be understood [26], and although recent progress has been made in understanding the role of peptide bacteriocins in *E. coli*, equivalent investigations for CLBs and tailocins are still lacking [27].

In vitro studies have demonstrated the activity of bacteriocins against both planktonic and biofilm-embedded bacteria [28–31] and, interestingly, Rendueles et al. demonstrated that colicin R preferentially targets bacteria growing in the biofilm state. As a result, there is renewed interest in investigating the efficacy of bacteriocins in animal models. The use of animal models of infection to test antibacterial compounds is a long-established practice and acknowledged as a useful tool in predicting if translation into the treatment of human infections is likely to be successful. While there is no such thing as a standard animal model, new models have been developed to more closely resemble specific human infections (acute or chronic infections, sepsis and meningitis), giving improved insights into host–pathogen interactions during antibiotic treatment (reviewed in ref. [32] for *P. aeruginosa*). Since their discovery, bacteriocins have been tested in a variety of animal models, with a range of modes of administration and dosing regimens. Here, we summarize the results of these investigations and discuss factors that will ultimately determine the success of bacteriocins as therapeutic agents. Although further research is required, bacteriocins have key properties such as high potency *in vivo* and exquisite specificity that suggest they may be excellent candidates for further therapeutic development.

In vivo activity of bacteriocins

Colicin-like bacteriocins

Colicins are 40–70 kDa toxins that specifically target *E. coli*. Given the fact that these molecules were the first to be discovered and have been the best studied to date [33], we refer to similar molecules produced by other Gram-negative bacteria as CLBs. CLBs target strains closely related to the producing strain, typically of the same species, and have species-specific names: colicins from *E. coli*, klebicins from *Klebsiella* and pesticins from *Yersinia pestis*. *Pseudomonas* CLBs are named S-type pyocins (named after *P. pyocyanea*) [34] and are produced by >70% of strains [35]. CLBs are protease-susceptible, modular proteins with domains involved in receptor binding, translocation and cytotoxicity.

Using their receptor-binding domain, CLBs bind to bacterial outer membrane proteins before translocation through either the Ton or Tol systems of Gram-negative bacteria [36]. Many CLBs exploit TonB-dependent transporters to enter the cell, the physiological role of which is to import siderophores or vitamins. Although less well understood, the Tol system is also required for the entry of some CLBs. Several CLBs, such as colicin N and pyocin L1, have also been shown to interact with lipopolysaccharides (LPSs) on the cell surface [37,38]. The cytotoxic domains of CLBs are commonly pore-forming ionophores or nucleases, but some also have lipid II- or peptidoglycan-degrading activity (Figure 1) [39]. For the producing organism to be protected from its own bacteriocin, it produces an immunity protein that, at least in the case of the nuclease CLBs, binds the cytotoxic domain and neutralizes its activity [15].

Although data are currently limited, the efficacy of both the colicins and S-type pyocins has been tested *in vivo*. Indeed, a previous study showed that colicin E1 in pig feed can prevent diarrhoea and increase growth and feed efficiency; however, the dose was not sufficient to completely eradicate the targeted pathogenic strain of *E. coli* [40]. Pyocin S2 was shown to protect against a lethal *P. aeruginosa* infection in the greater wax moth *Galleria mellonella* larvae, a model of *P. aeruginosa* infections [41], and in murine lung infections when given 1 h post-infection [42]. The latter effect was also observed with pyocins AP41, S5 and L1, with pyocin S5 being particularly potent. Indeed, pyocin S5 was at least two orders of magnitude more potent than tobramycin in this model (Table 1) [42]. Similarly, all four pyocins were protective when given 6 h before infection.

Emerging Topics in Life Sciences (2017) 1 65–74
DOI: 10.1042/ETLS20160016

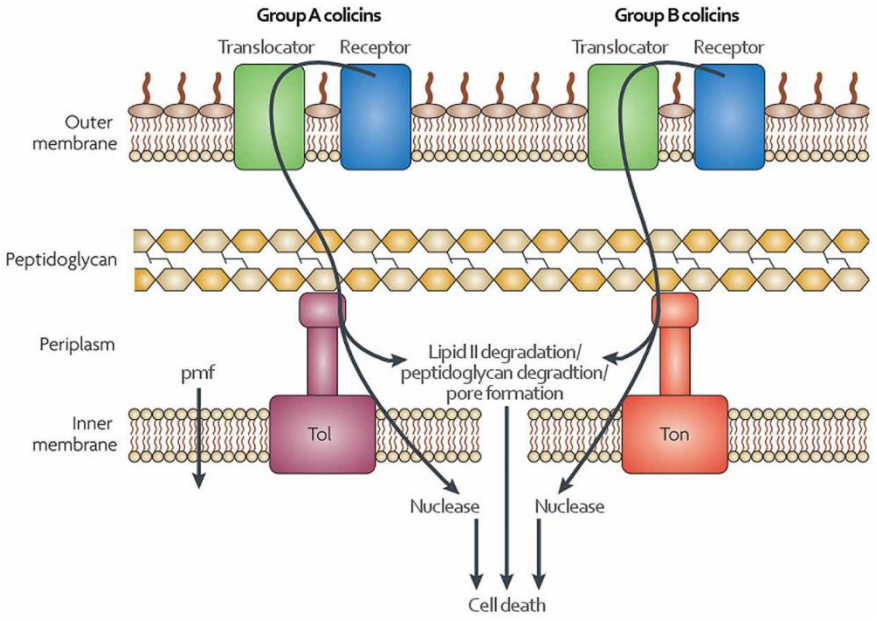

Figure 1. Import of colicin-like bacteriocins.

Specificity of CLBs is mediated by binding a receptor in the outer membrane of a target cell. An adjacent translocator will then mediate transport into the periplasm. Energy for this transport is provided by either the Tol system for group A CLBs or by the Ton system for group B CLBs. Pore-forming colicin-like bacteriocins then insert into the inner membrane to disrupt the proton motive force (pmf) while nucleases translocate into the cytoplasm. Adapted from ref. [36].

Interestingly, none of the bacteria isolated after pyocin treatment were resistant to the pyocins used, one isolate displaying increased tolerance to pyocin AP41. However, infection with this pyocin AP41-tolerant strain could still be controlled with this pyocin *in vivo*. Combinations of pyocins were also tested *in vivo* and were found to reduce colony forming units counts further, although not significantly [42].

Tailocins

Tailocins, also called high molecular mass bacteriocins, resemble the tail structures of bacteriophages from the Myoviridae and Siphoviridae families [39]. Although they are thought to be derived from phages, they are not simply defective phages, but are adapted specifically to their function as bacteriocins [43]. Tailocin gene clusters are found in the genomes of many Gram-negative and Gram-positive bacteria [44,45]. The best studied tailocins are the R- and F-type pyocins of *P. aeruginosa*. R-type pyocins are morphologically and genetically similar to the contractile tail of P2-like temperate enterophages [46]. They consist of a core and sheath, and are contractile (Figure 2). F-type pyocins resemble λ phage, have no sheath and are flexible (Figure 2) [39]. Tailocin specificity is modulated by tail fibres, which have been demonstrated to bind to LPSs, with different residues involved depending on the tailocin [47,48]. Upon contact with the receptor, the tailocin undergoes conformational changes that result in lethal membrane damage, detected as the depletion of the proton motive force. As opposed to CLBs, tailocins are not protease-susceptible and no immunity proteins have been described [39]. Very little is known about the mechanisms of resistance to tailocins; however, it is suggested to be mediated by an alteration of cell surface receptors recognized by the tailocin [47].

Studies of tailocins in animal models have shown that, like CLBs, they show strong efficacy against Gram-negative infections. Scholl and Martin [43] conducted a thorough study of pyocin R2 efficacy in a murine peritonitis model. They determined the time window after infection in which treatment is possible and

PORTLAND PRESS

Emerging Topics in Life Sciences (2017) 1 65–74
DOI: 10.1042/ETLS20160016

Table 1 Effectiveness of protein antibiotics in *in vivo* challenge models

Model host	Protein	Treatment route	Challenge organism	Challenge route	Prophylactic (P) or therapeutic (T)?*	Effective?	
	Colicin-like bacteriocins						
Wax moth *G. mellonella* larvae	Pyocin S2	Injection	*P. aeruguinosa*	Injection	T	Yes	[29]
Mouse	Pyocin S2	IN	*P. aeruguinosa*	IN	P	Yes	[42]
	Pyocin AP41					Yes	
	Pyocin S5					Yes	
	Pyocin L1					Yes	
	Pyocin S2				T	Yes	[42]
	Pyocin AP41					Yes	
	Pyocin S5					Yes	
	Pyocin L1					Yes	
Pig	Colicin E1	Oral	*E. coli*	Oral	P	Yes	[40]
	Tailocins						
Mouse	Pyocin R2	IP	*P. aeruginosa*	IP	T	Yes	[43]
		IV			T	Yes	
Mouse	Enterocoliticin	Oral	*Yersinia enterocolitica*	Oral	T	Yes	[49]
	Engineered tailocins						
Rabbit	AvR2-V10.3	Orogastrically	*E. coli*	Orogastrically	T	Yes	[63]
	Unknown and unidentified bacteriocins						
Mouse	Unknown pyocin (s) P10	IP	*P. aeruginosa*	IP	P	Yes	[52]
		IP		IP	T	No	
Chick embryo	Unknown pyocin	Allantoic cavity	*P. aeruginosa*	Allantoic cavity	P	Yes	[50]
Mouse	Pyocin H108 (S-type)	IP	*P. aeruginosa*	IP	P	No	[54]
					T	No	
Mouse	Colicin 'wash'	'Bladder wash'	?	'Established UTI'	T	Yes	[53]
Mouse	Unknown pyocin 78-C2	IV	*P. aeruginosa*	IV	P	Yes	[51]
		IP				No	
Mouse	Pyocin 1577 (R-type)	IP	*P. aeruginosa*	IP	P	Yes	[54]
					T	No	
	Pyocin 5882 (F-type)				P	Yes	
					T	No	
	Pyocin 1577 (R-type)	Topical		Topical on burn	T	No	
		IV			T	No	
	Pyocin 5882 (F-type)	Topical		Topical on burn	T	Minimal	

Detailed description of studies with known and identified bacteriocins can be found in the text. Abbreviations: IV, intravenous; IP, intraperitoneal; IN, intranasal; UTI, urinary tract infection. *Bacteriocin given at the same time as the challenge is considered prophylactic.

the dose necessary for adequate treatment. Protection via immune system stimulation was ruled out and pyocin R2 was found to be an effective therapeutic up to 4 h after infection in an aggressive infection model. Their results suggest that higher or repeated doses would allow for later treatment. The treatment of a second infection was less effective due to protective antibodies that had formed. They also found that the effective dose of pyocin R2 to treat the intraperitoneal (IP) challenge was lower when delivered through IP injection than through intravenous (IV) injection, suggesting that site-specific delivery of this pyocin can improve its efficacy (Table 1) [43].

Enterocoliticin, an R-type tailocin from *Yersinia enterocolitica*, was found to be effective for the treatment of mice orally infected with *Y. enterocolitica* when given orally [49]. The tailocin was only found to be active

Emerging Topics in Life Sciences (2017) 1 65–74
DOI: 10.1042/ETLS20160016

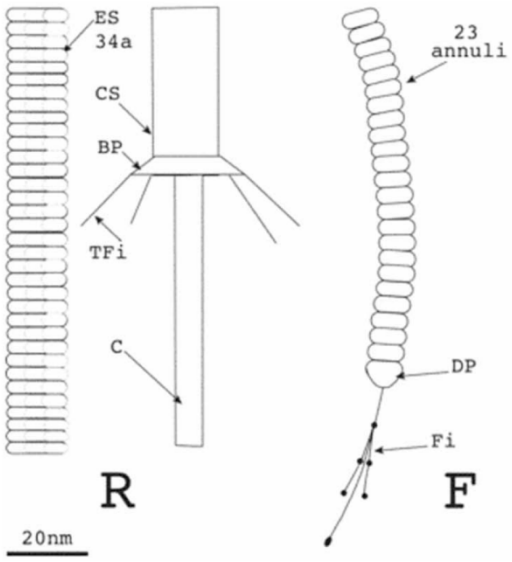

Figure 2. R-type tailocins consist of an inner core (C) and sheath, which can be contracted (CS) or extended (ES).
Upon binding a target cell with tail fibres (TFi), attached to the sheath via the base plate (BP), the sheath contracts and inserts the core into the inner membrane of a target cell, consequently depleting the proton motive force. F-type tailocins consist of a flexible rod, made from 23 annuli, to which fibres (Fi) with some globular structures are attached via a distal part (DP). Taken from ref. [46].

in vivo for 5 h; however, doses were given up to 24 h apart. Taking this into consideration, only those mice that received enterocoliticin 1 h after infection and were analyzed 5 h later can inform on the effect of the tailocin, and these mice did indeed show significantly reduced bacterial numbers (Table 1) [49].

Unfortunately, many CLBs and tailocins that were shown to be active *in vivo* [50–55] cannot be identified today, due to incoherent naming and lack of identification of the active molecules (Table 1).

Engineered bacteriocins

An important aspect of bacteriocin structure and function is their organization into domains that can be engineered to generate chimeric bacteriocins. Indeed, domains from different CLBs can be combined to customize their features. These include the target specificity via change of the receptor recognition domain, the immunity profile via change of immunogenic domains, mode of action via change of the cytotoxic domain and stability via change of structure, length or amino acid composition.

A combination of receptor binding and translocation domains of the CLB pesticin and bacteriophage T4 lysozyme was shown to be active against *Y. pestis* in mice [56]. The cytotoxic domain of CLBs can be combined with other pathogen-targeting proteins or domains, such as phage proteins [57], pheromones [58,59], antibodies or parts thereof, or ligands [60]. Combinations of the colicin Ia killing domain with pheromones, PMC-SA [58] against Gram-positive *Staphylococcus aureus* and PMC-EF [61] against Gram-positive *Enterococcus faecalis*, have been tested *in vivo* and were found to be effective.

Tailocin chimeras can be created by combining tailocins with parts of other tailocins or phages [62,63]. As the specificity of the tailocin is mediated by tail fibres, replacing them can enable the complex to recognize new targets [46]. AvR2-V10.3, an R-type pyocin with tail fibres engineered to target *E. coli* O157:H7, was shown to be effective in a diarrhoea model in rabbits, even when given after the onset of diarrhoea [63].

PORTLAND PRESS

Emerging Topics in Life Sciences (2017) 1 65–74
DOI: 10.1042/ETLS20160016

Bacteriocins as protein antibiotics

While data on the use of bacteriocins as protein antibiotics obtained in the last few years from *in vivo* experiments are encouraging, there are key questions related to their suitability as therapeutics that remain to be addressed. First, only preliminary data on the effect of bacteriocins on the host in terms of toxicity or immune response are available. However, the limited data that are available in the majority of cases report no adverse or toxic effects against the host organism (Table 2). There is one exception to this: Bird and Grieble [50] observed 11% mortality in pyocin-treated chick embryos, while in the control group 6% mortality occurred from injection alone, although it is not clear whether this pyocin preparation was free of endotoxin. In addition, more research is required on dosing regimens and in particular the timing of bacteriocin administration pre- or post-infection. To address this, testing in well-defined infection models and detailed pharmacokinetic studies are required.

What about immunogenicity? One might assume that bacteriocins and phage proteins are not immunogenic as they have been employed in bacterial and viral warfare within our bodies for millennia. Nonetheless, some groups have found low levels of antibodies against these proteins [42,43]. Repeated exposure to high doses of pyocin S5 via the IP route in mice did not lead to the development of pyocin S5-specific IgA or IgG, whereas exposure via the intranasal route led to low levels of S5-specific IgG, which did not interfere with pyocin S5 treatment of subsequent infection [42]. Conversely, another study demonstrated that a single IV exposure of

Table 2 Adverse effects of protein antibiotics *in vivo*

Model host	Protein	Treatment route	Adverse effect	
Colicin-like bacteriocins				
Pig	Colicin E1	Oral	None	[40]
G. mellonella caterpillar	Pyocin S2	Injection	None	[41]
Mouse	Pyocin S2 Pyocin AP41 Pyocin S5 Pyocin L1	IN	None None None None	[42]
Tailocins				
–	–	–	–	–
Unknown and unidentified bacteriocins				
Mouse	Unknown pyocin 78-C2	IV IP	None None	[51]
Mouse	Unknown pyocin(s) P10	IP	None	[52]
Chick embryo	Unknown pyocin	Allantoic cavity	11% mortality after pyocin treatment and 6% mortality in controls	[50]
Mouse	Pyocin H108 (S-type)	IP	None	[54]
Mouse	Pyocin 1577 (R-type) Pyocin 5882 (F-type) Pyocin 1577 (R-type) Pyocin 5882 (F-type)	IP Topical 	None None None None	[54]
Mouse Rabbit	Unknown pyocin (tailocin)	IP SC	None None	[55]

Abbreviations: IV, intravenous; IP, intraperitoneal; IN, intranasal; SC, subcutaneous.

Emerging Topics in Life Sciences (2017) 1 65–74
DOI: 10.1042/ETLS20160016

pyocin R2 to mice induced the production of neutralizing antibodies, consequently making a second treatment ineffective in 90% of mice. Four of five mice that died in the second treatment round had formed neutralizing antibodies [43]. Overall, immunogenicity has barely been investigated and more research is required.

Comparison of the potency of bacteriocins with that of conventional antibiotics has elicited encouraging results. Indeed, pyocin S5 is at least 100-fold more potent than tobramycin in a murine lung infection model, making pyocin S5 a promising replacement for traditional antibiotics to target *P. aeruginosa* [42]. The same study demonstrated that pyocins are stable and active *in vivo* for at least 24 h [42]. However, most protein antibiotic candidates are not as stable as traditional antibiotics and may need to be applied in higher doses and with shorter dosing intervals between repeated doses. While this may be perceived as a disadvantage, low stability can also reduce whole-body and environmental exposure to the antibiotic, which may minimize the selective pressure for the development of resistance [64].

Finally, at the origin of the antibiotic crisis, we are currently facing is the emergence of resistance to conventional antibiotics. While emergence of resistance to conventional antibiotics is widely documented, little is known about how resistance to bacteriocins might arise and evolve *in vivo*. Several studies have shown resistance to bacteriocins in environmental settings and that resistance to bacteriocins can occur through modification of cell surface receptors *in vitro*. Recent results suggest that mechanisms of resistance are dependent on environmental factors and that resistance may be reduced *in vivo* [17,65]. It is interesting to note that while resistance is possible, many bacteria remain sensitive to a certain level to the bacteriocin, suggesting that complete resistance is hard to evolve or comes at a great cost for the bacteria [66].

Immunity, as opposed to resistance, is mediated by immunity proteins that specifically bind CLBs. The natural immunity of bacteriocin-producing strains could prove to be a drawback to the use of bacteriocins as protein antibiotics. However, it has recently been shown that immunity, too, comes at a great cost, as immune strains are outcompeted by non-immune strains under non-selective conditions [67]. Moreover, while some bacteriocins share killing mechanisms or have identical cytotoxic domains that could lead to cross-immunity between bacterial strains, it is to be noted that many different killing mechanisms exist. These varied mechanisms limit the emergence of cross-resistance and immunity among protein antibiotics. It is also interesting to note that most bacterial strains do not express CLBs and among those that do, the majority produce only one CLB (Sharp et al. unpublished data). This suggests that most strains will either be susceptible to bacteriocins or be immune to a limited number of them. Therefore, it is expected that the use of a cocktail of bacteriocins will be able to circumvent individual immunity. Interestingly, in rare cases, *in vitro* susceptibility of strains to protein antibiotics did not correspond to *in vivo* susceptibility [51,68].

Conclusions

Commercial interest in bacteriocins comes from many sides. Farming industries, such as the poultry industry [21,69] and aquaculture industry [70], look for more efficient ways to treat their stock. Interest in human applications comes from scientists and companies that realize the global health and economic potential of bacteriocin therapeutics. As early as 1986, a potential application of colicin E1 was patented [71]. Many researchers have since patented applications of CLBs to treat infections [41,60,68,72,73]. Two patents focus on the delivery of CLBs to specific organs [68,74]. Scientists at Avid-Biotics Corporation have been engineering tailocin tail fibres for over a decade, resulting in five patents [75–79] with either diagnostic or therapeutic aims.

Eventually, application of probiotic bacteria-producing bacteriocins rather than application of purified bacteriocins might be more cost-effective. Recently, production of bacteriocins in plants has been achieved at costs that may encourage commercialization [80]. However, interactions between pathogenic and probiotic species in the setting of an *in vivo* microbiome are not yet understood well enough to predict their success [27].

This review provides an overview of *in vivo* studies undertaken to date. However, the lack of systematic identification and naming of bacteriocins have rendered the results of *in vivo* studies, e.g. that of Rosamund Williams [54], useless for posterity, highlighting the need for a uniform nomenclature accessible and used by all. While databases on bacteriocins exist (BACTIBASE, BAGEL), they mostly focus on Gram-positive peptide-type bacteriocins, leaving a big gap to be filled for Gram-negative bacteria, which also use protein bacteriocins.

Recently, over 2000 protein bacteriocins were identified across a range of Gram-negative bacteria including the important pathogens *P. aeruginosa*, *E. coli* and *K. pneumoniae* (Sharp et al. unpublished data). Less than 100 of these have been studied *in vitro* [15] and only eight of them have been studied *in vivo*. More preclinical studies are required to better characterize bacteriocins, especially their immunogenicity and the emergence of resistance *in vivo*. However, the results of the reviewed *in vivo* experiments, as well as the use of bacteriocins

PORTLAND PRESS

Emerging Topics in Life Sciences (2017) **1** 65–74
DOI: 10.1042/ETLS20160016

against Gram-positive bacteria such as nisin as a food preservative and topical antibiotic in humans [81], are encouraging. They showcase the potential that might be hidden among the thousands of unstudied bacteriocins in terms of therapeutics and indicate promise for the use of bacteriocins as protein antibiotics.

Summary

- Bacteriocins have been shown to be effective in a range of acute infection models and offer the potential for highly targeted antibiotic therapy.
- There is a lack of key data on issues such as the ability of bacteria to develop resistance to bacteriocins *in vivo* and the toxicity and immunogenicity of bacteriocins on repeat administration.
- High quality preclinical data that address these key questions are required to support the development of bacteriocins as therapeutic protein antibiotics.

Abbreviations

CLBs, colicin-like bacteriocins; IP, intraperitoneal; IV, intravenous; LPSs, lipopolysaccharides; UTI, urinary tract infection.

Competing Interests

The University of Glasgow has filed patents on the use of the protein antibiotics (colicins and pyocins) as therapeutics with DW listed as an inventor. The University of Oxford has filed a patent on methods for the discovery and engineering of bacteriocins with CK listed as an inventor. The authors have no other conflicts of interest.

References

1 Fair, R.J. and Tor, Y. (2014) Antibiotics and bacterial resistance in the 21st century. *Perspect. Med. Chem.*, **6**, 25–64 doi:10.4137/PMC.S14459
2 Cadman, H. and Marinez, L. (eds) (2014) *Antimicrobial Resistance Global Report on Surveillance*, World Health Organization, pp. 1–42
3 Tommasi, R., Brown, D.G., Walkup, G.K., Manchester, J.I. and Miller, A.A. (2015) ESKAPEing the labyrinth of antibacterial discovery. *Nat. Rev. Drug Discov.* **14**, 529–542 doi:10.1038/nrd4572
4 European Centre for Disease Prevention and Control (ECDC) (2015) *Antimicrobial resistance surveillance in Europe 2014*. Annual Report of the European Antimicrobial Resistance Surveillance Network (EARS-Net), ECDC, Stockholm, pp. 1–118
5 Center for Disease Control and Prevention (2011) *Gram-negative bacteria infections in healthcare settings [Internet]*. http://www.cdc.gov/hai/organisms/gram-negative-bacteria.html
6 Pitout, J.D.D., Nordmann, P. and Poirel, L. (2015) Carbapenemase-producing *Klebsiella pneumoniae*, a key pathogen set for global nosocomial dominance. *Antimicrob. Agents Chemother.* **59**, 5873–5884 doi:10.1128/AAC.01019-15
7 Willyard, C. (2017) The drug-resistant bacteria that pose the greatest health threats. *Nature* **543**, 15 doi:10.1038/nature.2017.21550
8 Soto, S.M. (2014) Importance of biofilms in urinary tract infections: new therapeutic approaches. *Adv. Biol.* **2014**, 1–13 doi:10.1155/2014/543974
9 Costerton, J.W., Stewart, P.S. and Greenberg, E.P. (1999) Bacterial biofilms: a common cause of persistent infections. *Science* **284**, 1318–1322 doi:10.1126/science.284.5418.1318
10 Lyczak, J.B., Cannon, C.L. and Pier, G.B. (2002) Lung infections associated with cystic fibrosis. *Clin. Microbiol. Rev.* **15**, 194–222 doi:10.1128/CMR.15.2.194-222.2002
11 Hammami, R., Fernandez, B., Lacroix, C. and Fliss, I. (2013) Anti-infective properties of bacteriocins: an update. *Cell Mol. Life Sci.* **70**, 2947–2967 doi:10.1007/s00018-012-1202-3
12 Micenková, L., Štaudová, B., Bosák, J., Mikalová, L., Littnerová, S., Vrba, M. et al. (2014) Bacteriocin-encoding genes and ExPEC virulence determinants are associated in human fecal *Escherichia coli* strains. *BMC Microbiol.* **14**, 109 doi:10.1186/1471-2180-14-109
13 Petkovšek, Ž., Žgur-Bertok, D. and Erjavec, M.S. (2012) Colicin insensitivity correlates with a higher prevalence of extraintestinal virulence factors among *Escherichia coli* isolates from skin and soft-tissue infections. *J. Med. Microbiol.* **61**(Pt_6), 762–765 doi:10.1099/jmm.0.037234-0
14 Holt, K.E., Thieu Nga, T.V., Thanh, D.P., Vinh, H., Kim, D.W., Vu Tra, M.P. et al. (2013) Tracking the establishment of local endemic populations of an emergent enteric pathogen. *Proc. Natl Acad. Sci. U.S.A.* **110**, 17522–17527 doi:10.1073/pnas.1308632110
15 Majeed, H., Gillor, O., Kerr, B. and Riley, M.A. (2011) Competitive interactions in *Escherichia coli* populations: the role of bacteriocins. *ISME J.* **5**, 71–81 doi:10.1038/ismej.2010.90
16 Nedialkova, L.P., Denzler, R., Koeppel, M.B., Diehl, M., Ring, D., Wille, T. et al. (2014) Inflammation fuels colicin Ib-dependent competition of *Salmonella* serovar typhimurium and *E. coli* in *Enterobacterial* blooms. *PLoS Pathog.* **10**, e1003844 doi:10.1371/journal.ppat.1003844

Emerging Topics in Life Sciences (2017) **1** 65–74
DOI: 10.1042/ETLS20160016

17 Francino, M.P. (2016) Antibiotics and the human gut microbiome: dysbioses and accumulation of resistances. *Front. Microbiol.* **6**, 1543 doi:10.3389/fmicb.2015.01543
18 Isaacs, D. (2006) Unnatural selection: reducing antibiotic resistance in neonatal units. *Arch. Dis. Child. Fetal Neonatal Ed.* **91**, F72–F74 doi:10.1136/adc.2005.074963
19 Cotter, P.D., Ross, R.P. and Hill, C. (2013) Bacteriocins — a viable alternative to antibiotics? *Nat. Rev. Microbiol.* **11**, 95–105 doi:10.1038/nrmicro2937
20 Joerger, R.D. (2003) Alternatives to antibiotics: bacteriocins, antimicrobial peptides and bacteriophages. *Poult. Sci.* **82**, 640–647 doi:10.1093/ps/82.4.640
21 Fields, F.R., Lee, S.W. and McConnell, M.J. (2016) Using bacterial genomes and essential genes for the development of new antibiotics. *Biochem. Pharmacol.* 1–13 doi:10.1016/j.bcp.2016.12.002
22 Rios, A.C., Moutinho, C.G., Pinto, F.C., Del Fiol, F.S., Jozala, A., Chaud, M.V. et al. (2016) Alternatives to overcoming bacterial resistances: state-of-the-art. *Microbiol. Res.* **191**, 51–80 doi:10.1016/j.micres.2016.04.008
23 Yang, S.-C., Lin, C.-H., Sung, C.-T. and Fang, J.-Y. (2014) Antibacterial activities of bacteriocins: application in foods and pharmaceuticals. *Front. Microbiol.* **5**, 241 doi:10.3389/fmicb.2014.00241
24 Cavera, V.L., Arthur, T.D., Kashtanov, D. and Chikindas, M.L. (2015) Bacteriocins and their position in the next wave of conventional antibiotics. *Int. J. Antimicrob. Agents* **46**, 494–501 doi:10.1016/j.ijantimicag.2015.07.011
25 Brown, C.L., Smith, K., McCaughey, L. and Walker, D. (2012) Colicin-like bacteriocins as novel therapeutic agents for the treatment of chronic biofilm-mediated infection. *Biochem. Soc. Trans.* **40**, 1549–1552 doi:10.1042/BST20120241
26 Kirkup, B.C. (2006) Bacteriocins as oral and gastrointestinal antibiotics: theoretical considerations, applied research, and practical applications. *Curr. Med. Chem.* **13**, 3335–3350 doi:10.2174/092986706778773068
27 Sassone-Corsi, M., Nuccio, S.-P., Liu, H., Hernandez, D., Vu, C.T., Takahashi, A.A. et al. (2016) Microcins mediate competition among Enterobacteriaceae in the inflamed gut. *Nature* **540**, 280–283 doi:10.1038/nature20557
28 Smith, K., Martin, L., Rinaldi, A., Rajendran, R., Ramage, G. and Walker, D. (2012) Activity of pyocin S2 against *Pseudomonas aeruginosa* biofilms. *Antimicrob. Agents Chemother.* **56**, 1599–1601 doi:10.1128/AAC.05714-11
29 Rendueles, O., Beloin, C., Latour-Lambert, P. and Ghigo, J.-M. (2014) A new biofilm-associated colicin with increased efficiency against biofilm bacteria. *ISME J.* **8**, 1275–1288 doi:10.1038/ismej.2013.238
30 Brown, C.L., Smith, K., Wall, D.M. and Walker, D. (2015) Activity of species-specific antibiotics against Crohn's disease-associated adherent-invasive *Escherichia coli*. *Inflamm. Bowel Dis.* **21**, 2372–2382 doi:10.1097/MIB.0000000000000488
31 Trautner, B.W., Hull, R.A. and Darouiche, R.O. (2005) Colicins prevent colonization of urinary catheters. *J. Antimicrob. Chemother.* **56**, 413–415 doi:10.1093/jac/dki228
32 Lorenz, A., Pawar, V., Häussler, S. and Weiss, S. (2016) Insights into host-pathogen interactions from state-of-the-art animal models of respiratory *Pseudomonas aeruginosa* infections. *FEBS Lett.* **590**, 3941–3959 doi:10.1002/1873-3468.12454
33 Cascales, E., Buchanan, S.K., Duché, D., Kleanthous, C., Lloubès, R., Postle, K. et al. (2007) Colicin biology. *Microbiol. Mol. Biol. Rev.* **71**, 158–229 doi:10.1128/MMBR.00036-06
34 Jacob, F. (1954) Biosynthèse induite et mode d'action d'une pyocine, antibiotique de *Pseudomonas pyocyanea*. *Ann. Inst. Pasteur.* **86**, 149–160 PMID:13158940
35 Fyfe, J.A., Harris, G. and Govan, J.R. (1984) Revised pyocin typing method for *Pseudomonas aeruginosa*. *J. Clin. Microbiol.* **20**, 47–50 PMCID:271243
36 Kleanthous, C. (2010) Swimming against the tide: progress and challenges in our understanding of colicin translocation. *Nat. Rev. Microbiol.* **8**, 843–848 doi:10.1038/nrmicro2454
37 McCaughey, L.C., Grinter, R., Josts, I., Roszak, A.W., Waløen, K.I., Cogdell, R.J. et al. (2014) Lectin-like bacteriocins from *Pseudomonas* spp. utilise D-rhamnose containing lipopolysaccharide as a cellular receptor. *PLoS Pathog.* **10**, e1003898 doi:10.1371/journal.ppat.1003898
38 Johnson, C.L., Ridley, H., Marchetti, R., Silipo, A., Griffin, D.C., Crawford, L. et al. (2014) The antibacterial toxin colicin N binds to the inner core of lipopolysaccharide and close to its translocator protein. *Mol. Microbiol.* **92**, 440–452 doi:10.1111/mmi.12568
39 Ghequire, M.G.K. and De Mot, R. (2014) Ribosomally encoded antibacterial proteins and peptides from *Pseudomonas*. *FEMS Microbiol. Rev.* **38**, 523–568 doi:10.1111/1574-6976.12079
40 Cutler, S.A., Lonergan, S.M., Cornick, N., Johnson, A.K. and Stahl, C.H. (2007) Dietary inclusion of colicin E1 is effective in preventing postweaning diarrhea caused by F18-positive *Escherichia coli* in pigs. *Antimicrob. Agents Chemother.* **51**, 3830–3835 doi:10.1128/AAC.00360-07
41 Walker, D. and Smith, K. (2015) Colicins for treating bacterial infections. United States; US20150164984A1
42 McCaughey, L.C., Ritchie, N.D., Douce, G.R., Evans, T.J. and Walker, D. (2016) Efficacy of species-specific protein antibiotics in a murine model of acute *Pseudomonas aeruginosa* lung infection. *Sci. Rep.* **6**, 1–8 doi:10.1038/srep30201
43 Scholl, D. and Martin, D.W. (2008) Antibacterial efficacy of R-type pyocins towards *Pseudomonas aeruginosa* in a murine peritonitis model. *Antimicrob. Agents Chemother.* **52**, 1647–1652 doi:10.1128/AAC.01479-07
44 Coetzee, H.L., De Klerk, H.C., Coetzee, J.N. and Smit, J.A. (1968) Bacteriophage-tail-like particles associated with intra-species killing of *Proteus vulgaris*. *J. Gen. Virol.* **2**, 29–36 doi:10.1099/0022-1317-2-1-29
45 Zink, R., Loessner, M.J. and Scherer, S. (1995) Charaterization of cryptic prophages (monocins) in *Listeria* and sequence analysis of a holin/endolysin gene. *Microbiology* **141**, 2577–2584 doi:10.1099/13500872-141-10-2577
46 Michel-Briand, Y. and Baysse, C. (2002) The pyocins of *Pseudomonas aeruginosa*. *Biochimie* **84**, 499–510 doi:10.1016/S0300-9084(02)01422-0
47 Köhler, T., Donner, V. and van Delden, C. (2010) Lipopolysaccharide as shield and receptor for R-pyocin-mediated killing in *Pseudomonas aeruginosa*. *J. Bacteriol.* **192**, 1921–1928 doi:10.1128/JB.01459-09
48 Kocíncová, D. and Lam, J.S. (2013) A deletion in the *wapB* promoter in many serotypes of *Pseudomonas aeruginosa* accounts for the lack of a terminal glucose residue in the core oligosaccharide and resistance to killing by R3-pyocin. *Mol. Microbiol.* **89**, 464–478 doi:10.1111/mmi.12289
49 Damasko, C., Konietzny, A., Kaspar, H., Appel, B., Dersch, P. and Strauch, E. (2005) Studies of the efficacy of enterocoliticin, a phage-tail like bacteriocin, as antimicrobial agent against *Yersinia enterocolitica* serotype O3 in a cell culture system and in mice. *J. Vet. Med. Ser. B* **52**, 171–179 doi:10.1111/j.1439-0450.2005.00841.x

PORTLAND PRESS

Emerging Topics in Life Sciences (2017) **1** 65–74
DOI: 10.1042/ETLS20160016

50 Bird, T.J. and Grieble, H.G. (1969) Pyocin antibiosis in chick embryos. *Antimicrob. Agents Chemother.* **9**, 495–498 PMID:4990372
51 Merrikin, D.J. and Terry, C.S. (1972) Use of pyocin 78-C2 in the treatment of *Pseudomonas aeruginosa* infection in mice. *Appl. Microbiol.* **23**, 164–165 PMID:4621792
52 Haas, H., Sacks, T. and Saltz, N. (1974) Protective effect of pyocin against lethal *Pseudomonas aeruginosa* infections in mice. *J. Infect. Dis.* **129**, 470–472 doi:10.1093/infdis/129.4.470
53 Riley, M.A., Robinson, S.M., Roy, C.M., Dennis, M., Liu, V. and Dorit, R.L. (2012) Resistance is futile: the bacteriocin model for addressing the antibiotic resistance challenge. *Biochem. Soc. Trans.* **40**, 1438–1442 doi:10.1042/BST20120179
54 Williams, R.J. (1976) Treatment of *Pseudomonas aeruginosa* infections with pyocins. *J. Med. Microbiol.* **9**, 153–161 doi:10.1099/00222615-9-2-153
55 Higerd, T.B., Baechler, C.A. and Berk, R.S. (1967) In vitro and in vivo characterization of pyocin. *J. Bacteriol.* **93**, 1976–1986 PMID:4960899
56 Lukacik, P., Barnard, T.J. and Buchanan, S.K. (2012) Using a bacteriocin structure to engineer a phage lysin that targets *Yersinia pestis*. *Biochem. Soc. Trans.* **40**, 1503–1506 doi:10.1042/BST20120209
57 Jakes, K.S., Davis, N.G. and Zinder, N.D. (1988) A hybrid toxin from bacteriophage f1 attachment protein and colicin E3 has altered cell receptor specificity. *J. Bacteriol.* **170**, 4231–4238 doi:10.1128/jb.170.9.4231-4238.1988
58 Qiu, X.-Q., Wang, H., Lu, X.-F., Zhang, J., Li, S.-F., Cheng, G. et al. (2003) An engineered multidomain bactericidal peptide as a model for targeted antibiotics against specific bacteria. *Nat. Biotechnol.* **21**, 1480–1485 doi:10.1038/nbt913
59 Dorit, R., Roy, S.M. and Riley, M.A. (eds) (2016) *The Bacteriocins*, 1st edn. Caister Academic Press, Norfolk, UK
60 Qiu, X.-Q. (2006) Methods and compositions for the treatment of infection, **vol. 1**. United States; US2006/0156009A1
61 Qiu, X.-Q., Zhang, J., Wang, H. and Wu, G.Y. (2005) A novel engineered peptide, a narrow-spectrum antibiotic, is effective against vancomycin-resistant *Enterococcus faecalis*. *Antimicrob. Agents Chemother.* **49**, 1184–1189 doi:10.1128/AAC.49.3.1184-1189.2005
62 Williams, S.R., Gebhart, D., Martin, D.W. and Scholl, D. (2008) Retargeting R-type pyocins to generate novel bactericidal protein complexes. *Appl. Environ. Microbiol.* **74**, 3868–3876 doi:10.1128/AEM.00141-08
63 Ritchie, J.M., Greenwich, J.L., Davis, B.M., Bronson, R.T., Gebhart, D., Williams, S.R. et al. (2011) An *Escherichia coli* O157-specific engineered pyocin prevents and ameliorates infection by *E. coli* O157:H7 in an animal model of diarrheal disease. *Antimicrob. Agents Chemother.* **55**, 5469–5474 doi:10.1128/AAC.05031-11
64 Olofsson, S.K. and Cars, O. (2007) Optimizing drug exposure to minimize selection of antibiotic resistance. *Clin. Infect. Dis.* **45**(Suppl 2), S129–S136 doi:10.1086/519256
65 Inglis, R.F., Scanlan, P. and Buckling, A. (2016) Iron availability shapes the evolution of bacteriocin resistance in *Pseudomonas aeruginosa*. *ISME J.* **10**, 2060–2066 doi:10.1038/ismej.2016.15
66 Hawlena, H., Bashey, F. and Lively, C.M. (2010) The evolution of spite: population structure and bacteriocin-mediated antagonism in two natural populations of xenorhabdus bacteria. *Evolution* **64**, 3198–3204 doi:10.1111/j.1558-5646.2010.01070.x
67 Gerardin, Y., Springer, M. and Kishony, R. (2016) A competitive trade-off limits the selective advantage of increased antibiotic production. *Nat. Microbiol.* **1**, 1–7 doi:10.1038/nmicrobiol.2016.175
68 Walker, D. and McCaughey, L. (2016) *Pulmonary Administration of Pyocins for Treating Bacterial Respiratory Infections*, World Property Organization, WO2016046218A1
69 Svetoch, E.A. and Stern, N.J. (2010) Bacteriocins to control *Campylobacter* spp. in poultry — a review. *Poult. Sci.* **89**, 1763–1768 doi:10.3382/ps.2010-00659
70 Desriac, F., Defer, D., Bourgougnon, N., Brillet, B., Le Chevalier, P. and Fleury, Y. (2010) Bacteriocin as weapons in the marine animal-associated bacteria warfare: inventory and potential applications as an aquaculture probiotic. *Mar. Drugs* **8**, 1153–1177 doi:10.3390/md8041153
71 Bycroft, N.L., Byng, G.S. and Good, S.R. (1986) Synergistic antimicrobial compositions, **vol. 104**. US pat. 5,043,176. p. 54–55
72 Shanks, R.M.Q. and Kadouri, D.E. (2015) *Citrobacter freundii* antibacterial agents and their use. United States; US9139622B2
73 Dorit, R. and Riley, M.A. (2006) Engineered bacteriocins and bacteriocin combinations and methods for treating bacterial based infections. United States; US20060229244A1
74 Lichter, J., Lebel, C., Piu, F. and Harris, J.P. (2011) Compositions and methods for the treatment of sinonasal disorders. World Intellectual Property Organization; WO2011050206A2
75 Scholl, D.M., Gebhart, D., Williams, S.R., Govoni, G.R. and Martin, J.R. (2011) Diffocin and methods of use thereof. United States; US20110293566A1
76 Scholl, D.M. and Williams, S.R. (2014) Recombinant bacteriophage and methods for their use. United States; US8673553B2
77 Scholl, D. and Williams, S.R. (2012) Recombinant P4 bacteriophage and methods for their use. World Intellectual Property Organization; WO2012064660A1
78 Gebhart, D. and Scholl, D.M. (2008) Inhibition of *Yersinia pestis*. United States; US20080286236A1
79 Scholl, D.M. and Williams, S.R. (2010) Modified bacteriocins and methods for their use. United States; US20100261258A1
80 Schulz, S., Stephan, A., Hahn, S., Bortesi, L., Jarczowski, F., Bettmann, U. et al. (2015) Broad and efficient control of major foodborne pathogenic strains of *Escherichia coli* by mixtures of plant-produced colicins. *Proc. Natl Acad. Sci. U.S.A.* **112**, E5454–E5460 doi:10.1073/pnas.1513311112
81 Fernández, L., Delgado, S., Herrero, H., Maldonado, A. and Rodríguez, J.M. (2008) The bacteriocin nisin, an effective agent for the treatment of staphylococcal mastitis during lactation. *J. Hum. Lact.* **24**, 311–316 doi:10.1177/0890334408317435

9. Bibliography

Adams PD, Afonine P V., Bunkóczi G, Chen VB, Davis IW, Echols N, Headd JJ, Hung LW, Kapral GJ, Grosse-Kunstleve RW, McCoy AJ, Moriarty NW, Oeffner R, Read RJ, Richardson DC, Richardson JS, Terwilliger TC, Zwart PH. 2010. PHENIX: A comprehensive Python-based system for macromolecular structure solution. *Acta Crystallogr Sect D Biol Crystallogr* **66**:213–221. doi:10.1107/S0907444909052925

Al-amoudi A, Dubochet J, Beveridge TJ. 2003. Cryo-Transmission Electron Microscopy of Frozen-Hydrated Sections of *Escherichia coli* and *Pseudomonas aeruginosa*. *J Bacteriol* **185**:6112–6118. doi:10.1128/JB.185.20.6112

Altschul SF, Gish W, Miller W, Myers EW, J.Lipman D. 1990. Basic Local Alignment Search Tool. *J Mol Biol* **215**:403–410.

Ankenbauer RG, Quan HN. 1994. FptA, the Fe(III)-pyochelin receptor of *Pseudomonas aeruginosa*: A phenolate siderophore receptor homologous to hydroxamate siderophore receptors. *J Bacteriol* **176**:307–319. doi:10.1128/jb.176.2.307-319.1994

Ankenbauer RG, Toyokuni T, Staley A, Rinehart KL, Cox CD. 1988. Synthesis and biological activity of pyochelin, a siderophore of *Pseudomonas aeruginosa*. *J Bacteriol* **170**:5344–5351. doi:10.1128/jb.170.11.5344-5351.1988

Arnold T, Zeth K, Linke D. 2009. Structure and function of colicin S4, a colicin with a duplicated receptor-binding domain. *J Biol Chem* **284**:6403–6413. doi:10.1074/jbc.M808504200

Atanaskovic I, Kleanthous C. 2019. Tools and Approaches for Dissecting Protein Bacteriocin Import in Gram-Negative Bacteria. *Front Microbiol* **10**:1–12. doi:10.3389/fmicb.2019.00646

Baboolal TG, Conroy MJ, Gill K, Ridley H, Visudtiphole V, Bullough PA, Lakey JHH. 2008. Colicin N Binds to the Periphery of Its Receptor and Translocator, Outer Membrane Protein F. *Structure* **16**:371–379. doi:10.1016/j.str.2007.12.023

Baty D, Lakey J, Pattus F, Lazkunski C. 1990. A 136-amino-acid-residue COOH-terminal fragment of colicin A is endowed with ionophoric activity. *Eur J Biochem* **189**:409–413. doi:10.1111/j.1432-1033.1990.tb15503.x

Behrens HM, Six A, Walker D, Kleanthous C. 2017. The therapeutic potential of bacteriocins as protein antibiotics. *Emerg Top Life Sci* **1**:65–74. doi:10.1042/ETLS20160016

Benedetti H, Frenette M, Baty D, Knibiehler M, Pattus F, Lazdunski C. 1991. Individual domains of colicins confer specificity in colicin uptake, in pore-properties and in immunity requirement. *J Mol Biol* **217**:429–439. doi:10.1016/0022-2836(91)90747-T

Benedetti H, Frenette M, Baty D, Lloubès R, Geli V, Lazdunski C. 1989. Comparison of the uptake systems for the entry of various BtuB group colicins into *Escherichia coli*. *J Gen Microbiol* **135**:3413–3420. doi:10.1099/00221287-135-12-3413

Bénédetti H, Lloubès R, Lazdunski C, Letellier L. 1992. Colicin A unfolds during its translocation in *Escherichia coli* cells and spans the whole cell envelope when its pore has formed. *EMBO J* **11**:441–447. doi:10.1002/j.1460-2075.1992.tb05073.x

Benkert P, Biasini M, Schwede T. 2011. Toward the estimation of the absolute quality of individual protein structure models. *Bioinformatics* **27**:343–350. doi:10.1093/bioinformatics/btq662

Bosák J, Laiblová P, Smarda J, Dedicova D, Smajs D. 2012. Novel colicin FY of *Yersinia frederiksenii* inhibits pathogenic *Yersinia* strains via YiuR-mediated reception, TonB import, and cell membrane pore formation. *J Bacteriol* **194**:1950–

1959. doi:10.1128/JB.05885-11

Bosák J, Micenková L, Doležalová M, Šmajs D. 2016. Colicins U and Y inhibit growth of *Escherichia coli* strains via recognition of conserved OmpA extracellular loop 1. *Int J Med Microbiol* **306**:486–494. doi:10.1016/j.ijmm.2016.07.002

Brandel J, Humbert N, Elhabiri M, Schalk IJ, Mislin GLA, Albrecht-Gary A-M. 2012. Pyochelin, a siderophore of *Pseudomonas aeruginosa*: physicochemical characterization of the iron(III), copper(II) and zinc(II) complexes. *Dalt Trans* **41**:2820–2834. doi:10.1039/c1dt11804h

Braun V, Patzer SI, Hantke K. 2002. Ton-dependent colicins and microcins: Modular design and evolution. *Biochimie* **84**:365–380. doi:10.1016/S0300-9084(02)01427-X

Brown CL, Smith K, McCaughey L, Walker D. 2012. Colicin-like bacteriocins as novel therapeutic agents for the treatment of chronic biofilm-mediated infection. *Biochem Soc Trans* **40**:1549–1552. doi:10.1042/BST20120241

Brown CL, Smith K, Wall DM, Walker D. 2015. Activity of Species-specific Antibiotics Against Crohn's Disease-Associated Adherent-invasive *Escherichia coli*. *Inflamm Bowel Dis* **21**:2372–2382. doi:10.1097/MIB.0000000000000488

Buchanan SK, Lukacik P, Grizot S, Ghirlando R, Ali MMU, Barnard TJ, Jakes KS, Kienker PK, Esser L. 2007. Structure of colicin I receptor bound to the R-domain of colicin Ia: implications for protein import. *EMBO J* **26**:2594–604. doi:10.1038/sj.emboj.7601693

Bullock J, Cohen FS, Dankert JR, Cramer WA. 1983. Comparison of the macroscopic and single channel conductance properties of colicin E1 and its COOH-terminal tryptic peptide. *J Biol Chem* **258**:9908–9912.

Bullock JO, Cohen FS. 1986. Octyl glucoside promotes incorporation of channels into

neutral planar phospholipid bilayers. Studies with colicin Ia. *BBA - Biomembr* **856**:101–108. doi:10.1016/0005-2736(86)90015-5

Bullock JO, Kolen ER, Shear JL. 1992. Ion selectivity of colicin E1: II. Permeability to organic cations. *J Membr Biol* **128**:1–16. doi:10.1007/BF00231866

Cascales E, Buchanan SK, Duché D, Kleanthous C, Lloubès R, Postle K, Riley M, Slatin S, Cavard D. 2007. Colicin Biology. *Microbiol Mol Biol Rev* **71**:158–229. doi:10.1128/MMBR.00036-06

CDC. 2013. Antibiotic Resistance Threats. *Centers Dis Control Prev* 22–50. doi:CS239559-B

Celia H, Noinaj N, Zakharov SD, Bordignon E, Botos I, Santamaria M, Barnard TJ, Cramer WA, Lloubes R, Buchanan SK. 2016. Structural insight into the role of the Ton complex in energy transduction. *Nature* **538**:60–65. doi:10.1038/nature19757

Chang C, Mooser A, Plückthun A, Wlodawer A. 2001. Crystal Structure of the Dimeric C-terminal Domain of TonB Reveals a Novel Fold. *J Biol Chem* **276**:27535–27540. doi:10.1074/jbc.M102778200

Charalampous T, Kay GL, Richardson H, Aydin A, Jeanes C, Rae D, Grundy S, Turner DJ, Leggett RM, Livermore DM, Building E, Ln Colney, Ln Colney, Road WB, Ln Conley, Technologies ON, Building G, Park OS, Halley E, Ln Conley. 2019. Nanopore metagenomics enables rapid clinical diagnosis of bacterial lower respiratory infection. *Nat Biotech* **37**. doi:10.1038/s41587-019-0156-5

Chen VB, Arendall WB, Headd JJ, Keedy DA, Immormino RM, Kapral GJ, Murray LW, Richardson JS, Richardson DC. 2010. MolProbity: All-atom structure validation for macromolecular crystallography. *Acta Crystallogr Sect D Biol Crystallogr* **66**:12–21. doi:10.1107/S0907444909042073

Chevalier S, Bouffartigues E, Bodilis J, Maillot O, Lesouhaitier O, Feuilloley MGJ,

Orange N, Dufour A, Cornelis P. 2017. Structure, function and regulation of *Pseudomonas aeruginosa* porins. *FEMS Microbiol Rev* **41**:698–722. doi:10.1093/femsre/fux020

Choi DS, Kim DK, Choi SJ, Lee J, Choi JP, Rho S, Park SH, Kim YK, Hwang D, Gho YS. 2011. Proteomic analysis of outer membrane vesicles derived from *Pseudomonas aeruginosa*. *Proteomics* **11**:3424–3429. doi:10.1002/pmic.201000212

Chorev DS, Baker LA, Wu D, Beilstein-Edmands V, Rouse SL, Zeev-Ben-Mordehai T, Jiko C, Samsudin F, Gerle C, Khalid S, Stewart AG, Matthews SJ, Grünewald K, Robinson C V. 2018. Protein assemblies ejected directly from native membranes yield complexes for mass spectrometry. *Science* **362**:829–834. doi:10.1126/science.aau0976

Church D, Elsayed S, Reid O, Winston B, Lindsay R. 2006. Burn wound infections. *Clin Microbiol Rev* **19**:403–434. doi:10.1128/CMR.19.2.403-434.2006

Clément E, Mesini PJ, Pattus F, Schalk IJ. 2004. The binding mechanism of pyoverdin with the outer membrane receptor FpvA in *Pseudomonas aeruginosa* is dependent on its iron-loaded status. *Biochemistry* **43**:7954–7965. doi:10.1021/bi049768c

Cobessi D, Celia H, Pattus F. 2005. Crystal Structure at High Resolution of Ferric-pyochelin and its Membrane Receptor FptA from *Pseudomonas aeruginosa*. *J Mol Biol* **352**:893–904. doi:10.1016/j.jmb.2005.08.004

Cobessi D, Célia H, Pattus F. 2004. Crystallization and X-ray diffraction analyses of the outer membrane pyochelin receptor FptA from *Pseudomonas aeruginosa*. *Acta Crystallogr Sect D Biol Crystallogr* **60**:1919–1921. doi:10.1107/S090744490401995X

Collarini M, Amblard G, Lazdunski C, Pattus F. 1987. Gating processes of channels

induced by colicin A, its C-terminal fragment and colicin E1 in planar lipid bilayers. *Eur Biophys J* **14**:147–153. doi:10.1007/BF00253839

Cornelis P, Bodilis J. 2009. A survey of TonB-dependent receptors in fluorescent pseudomonads. *Environ Microbiol Rep* **1**:256–262. doi:10.1111/j.1758-2229.2009.00041.x

Cowles KN, Moser TS, Siryaporn A, Nyakudarika N, Dixon W, Turner JJ, Gitai Z. 2013. The putative Poc complex controls two distinct *Pseudomonas aeruginosa* polar motility mechanisms. *Mol Microbiol* **90**:923–938. doi:doi:10.1111/mmi.12403.

Cox CD. 1980. Iron uptake with ferripyochelin and ferric citrate by *Pseudomonas aeruginosa. J Bacteriol* **142**:581–587.

Cox CD, Graham R. 1979. Isolation of an iron-binding compound from *Pseudomonas aeruginosa*. *J Bacteriol* **137**:357–364.

Cramer WA, Sharma O, Zakharov SD. 2018. On mechanisms of colicin import: the outer membrane quandary. *Biochem J* **475**:3903–3915. doi:10.1042/bcj20180477

Cutler SA, Lonergan SM, Cornick N, Johnson AK, Stahl CH. 2007. Dietary inclusion of colicin E1 is effective in preventing postweaning diarrhea caused by F18-positive *Escherichia coli* in pigs. *Antimicrob Agents Chemother* **51**:3830–3835. doi:10.1128/AAC.00360-07

Cystic Fibrosis Trust. 2013. UK Cystic Fibrosis Registry 2012 Annual Data Report. *Cyst Fibros Trust*.

DaCosta RS, Kulbatski I, Lindvere-Teene L, Starr D, Blackmore K, Silver JI, Opoku J, Wu YC, Medeiros PJ, Xu W, Xu L, Wilson BC, Rosen C, Linden R. 2015. Point-of-care autofluorescence imaging for real-time sampling and treatment guidance of bioburden in chronic wounds: First-in-human results. *PLoS One* **10**.

doi:10.1371/journal.pone.0116623

de Chial M, Ghysels B, Beatson SA, Geoffroy V, Meyer JM, Pattery T, Baysse C, Chablain P, Parsons YN, Winstanley C, Cordwell SJ, Cornelis P. 2003. Identification of type II and type III pyoverdine receptors from *Pseudomonas aeruginosa*. *Microbiology* **149**:821–831. doi:10.1099/mic.0.26136-0

Dean CR, Poole K. 1993. Expression of the ferric enterobactin receptor (PfeA) of *Pseudomonas aeruginosa*: involvement of a two-component regulatory system. *Mol Microbiol* **8**:1095–1103. doi:10.1111/j.1365-2958.1993.tb01654.x

Delano W. 2002. The PyMOL Molecular Graphics System. *DeLano Sci Palo Alto, CA*.

Dinc F, Akalin H, Özakin C, Sinirtas M, Kebabci N, Iscimen R, Kelebek Girgin N, Kahveci F. 2016. Comparison of blood culture and multiplex real-time PCR for the diagnosis of nosocomial sepsis Fatih. *Minerva Anestesiol* **82**:301–309.

Doring G, Parameswaran IG, Murphy TF. 2011. Differential adaptation of microbial pathogens to airways of patients with cystic fibrosis and chronic obstructive pulmonary disease. *FEMS Microbiol Rev* **35**:124–146. doi:10.1111/j.1574-6976.2010.00237.x

Dover LG, Evans LJA, Fridd SL, Bainbridge G, Raggett EM, Lakey JH. 2000. Colicin pore-forming domains bind to *Escherichia coli* trimeric porins. *Biochemistry* **39**:8632–8637. doi:10.1021/bi000160n

Duché D. 2002. The pore-forming domain of colicin A fused to a signal peptide: A tool for studying pore-formation and inhibition. *Biochimie* **84**:455–464. doi:10.1016/S0300-9084(02)01424-4

Duché D, Baty D, Chartier M, Letellier L. 1994a. Unfolding of colicin A during its translocation through the *Escherichia coli* envelope as demonstrated by disulfide bond engineering. *J Biol Chem* **269**:24820–24825.

Duché D, Parkere MW, Gonzalez-Manas J-M, Pattus F, Daniel B. 1994b. Uncoupled Steps of the Colicin A Pore Formation Demonstrated by Disulfide Bond Engineering. *J Biol Chem* **269**:6332–6339.

El Kouhen R, Pagès JM. 1996. Dynamic aspects of colicin N translocation through the *Escherichia coli* outer membrane. *J Bacteriol* **178**:5316–5319. doi:10.1128/jb.178.17.5316-5319.1996

Elfarash A, Dingemans J, Ye L, Hassan AA, Craggs M, Reimmann C, Thomas MS, Cornelis P. 2014. Pore-forming pyocin S5 utilizes the FptA ferripyochelin receptor to kill *Pseudomonas aeruginosa*. *Microbiol (United Kingdom)* **160**:261–269. doi:10.1099/mic.0.070672-0

Elkins P, Bunker A, Cramer W a, Stauffacher C V. 1997. A mechanism for toxin insertion into membranes is suggested by the crystal structure of the channel-forming domain of colicin E1. *Structure* **5**:443–458. doi:10.1016/S0969-2126(97)00200-1

Emsley P, Cowtan K. 2004. Coot: Model-building tools for molecular graphics. *Acta Crystallogr Sect D Biol Crystallogr* **60**:2126–2132. doi:10.1107/S0907444904019158

Evans LJA, Goble ML, Hales KA, Lakey JH. 1996. Different sensitivities to acid denaturation within a family of proteins: Implications for acid unfolding and membrane translocation. *Biochemistry* **35**:13180–13185. doi:10.1021/bi960990u

Farrell DJ, Flamm RK, Sader HS, Jones RN. 2013. Antimicrobial Activity of Ceftolozane-Tazobactam Tested against *Enterobacteriaceae* and *Pseudomonas aeruginosa* with Various Resistance Patterns Isolated in U.S. Hospitals (2011-2012). *Antimicrob Agents Chemother* **57**:6305–6310. doi:10.1128/aac.01802-13

Folkesson A, Jelsbak L, Yang L, Johansen HK, Ciofu O, Hoiby N, Molin S. 2012.

Adaptation of *Pseudomonas aeruginosa* to the cystic fibrosis airway: An evolutionary perspective. *Nat Rev Microbiol* **10**:841–851. doi:10.1038/nrmicro2907

Francino MP. 2016. Antibiotics and the human gut microbiome: Dysbioses and accumulation of resistances. *Front Microbiol* **6**:1–11. doi:10.3389/fmicb.2015.01543

Franke D, Svergun DI. 2009. DAMMIF, a program for rapid ab-initio shape determination in small-angle scattering. *J Appl Crystallogr* **42**:342–346. doi:10.1107/s0021889809000338

Geli V, Baty D, Pattus F, Lazdunski C. 1989. Topology and function of the integral membrane protein conferring immunity to colicin A. *Mol Microbiol* **3**:679–687. doi:10.1111/j.1365-2958.1989.tb00216.x

Gerding MA, Ogata Y, Pecora ND, Niki H, De Boer PAJ. 2007. The trans-envelope Tol-Pal complex is part of the cell division machinery and required for proper outer-membrane invagination during cell constriction in E. coli. *Mol Microbiol* **63**:1008–1025. doi:10.1111/j.1365-2958.2006.05571.x

Ghequire MGK, De Mot R. 2014. Ribosomally encoded antibacterial proteins and peptides from *Pseudomonas*. *FEMS Microbiol Rev* **38**:523–568. doi:10.1111/1574-6976.12079

Ghequire MGK, Dingemans J, Pirnay JP, De Vos D, Cornelis P, De Mot R. 2014. O serotype-independent susceptibility of *Pseudomonas aeruginosa* to lectin-like pyocins. *Microbiologyopen* **3**:875–884. doi:10.1002/mbo3.210

Ghequire MGK, Kemland L, Anoz-Carbonell E, Buchanan SK, De Mot R. 2017a. A Natural Chimeric *Pseudomonas* Bacteriocin with Novel Pore-Forming Activity Parasitizes the Ferrichrome. *MBio* **8**:1–12.

Ghequire MGK, Kemland L, De Mot R. 2017b. Novel Immunity Proteins Associated with Colicin M-like Bacteriocins Exhibit Promiscuous Protection in *Pseudomonas*. *Front Microbiol* **8**:1–9. doi:10.3389/fmicb.2017.00093

Ghequire MGK, Öztürk B. 2018. A colicin M-type bacteriocin from *Pseudomonas aeruginosa* targeting the HxuC heme receptor requires a novel immunity partner. *Appl Environ Microbiol* AEM.00716-18. doi:10.1128/AEM.00716-18

Ghequire MGK, Swings T, Michiels J, Buchanan SK, De Mot R. 2018. Hitting with a BAM : Selective Killing by Lectin-Like. *MBio* **9**:1–15.

Ghysels B, Dieu BTM, Beatson SA, Pirnay JP, Ochsner UA, Vasil ML, Cornelis P. 2004. FpvB, an alternative type I ferripyoverdine receptor of Pseudomonas aeruginosa. *Microbiology* **150**:1671–1680. doi:10.1099/mic.0.27035-0

Gillor O, Nigro LM, Riley M a. 2005. Genetically engineered bacteriocins and their potential as the next generation of antimicrobials. *Curr Pharm Des* **11**:1067–1075. doi:10.2174/1381612053381666

Gutiérrez-del-Río I, Marín L, Fernández J, Álvarez San Millán M, Ferrero FJ, Valledor M, Campo JC, Cobián N, Méndez I, Lombó F. 2018. Development of a biosensor protein bullet as a fluorescent method for fast detection of *Escherichia coli* in drinking water. *PLoS One* **13**:e0184277. doi:10.1371/journal.pone.0184277

Hahn-Löbmann S, Stephan A, Schulz S, Schneider T, Shaverskyi A, Tusé D, Giritch A, Gleba Y. 2019. Colicins and Salmocins – New Classes of Plant-Made Non-antibiotic Food Antibacterials. *Front Plant Sci* **10**:1–16. doi:10.3389/fpls.2019.00437

Hammami R, Fernandez B, Lacroix C, Fliss I. 2013. Anti-infective properties of bacteriocins: An update. *Cell Mol Life Sci* **70**:2947–2967. doi:10.1007/s00018-012-1202-3

Hancock RE. 1998. Resistance mechanisms in *Pseudomonas aeruginosa* and other nonfermentative gram-negative bacteria. *Clin Infect Dis* **27**:93–9. doi:10.1086/514909

Hancock REW, Mutharia LM, Chan L, Darveau RP, Speert DP, Pier GB. 1983. *Pseudomonas aeruginosa* isolates from patients with cystic fibrosis: A class of serum-sensitive, nontypable strains deficient in lipopolysaccharide O side chains. *Infect Immun* **42**:170–177. doi:10.1128/CMR.5.4.356.Updated

Heinrichs DE, Poole K. 1996. PchR, a regulator of ferripyochelin receptor gene (*fptA*) expression in *Pseudomonas aeruginosa*, functions both as an activator and as a repressor. *J Bacteriol* **178**:2586–2592.

Heinrichs DE, Young L, Poole K. 1991. Pyochelin-mediated iron transport in *Pseudomonas aeruginosa*: Involvement of a high-molecular-mass outer membrane protein. *Infect Immun* **59**:3680–3684.

Hickman SJ, Cooper REM, Bellucci L, Paci E, Brockwell DJ. 2017. Gating of TonB-dependent transporters by substrate-specific forced remodelling. *Nat Commun* **8**:14804. doi:10.1038/ncomms14804

Hilsenbeck JL, Park H, Chen G, Youn B, Postle K, Kang C. 2004. Crystal structure of the cytotoxic bacterial protein colicin B at 2.5 A resolution. *Mol Microbio* **51**:711–720. doi:10.1046/j.1365-2958.2003.03884.x

Hoa Tran EN, Papadopoulos M, Morona R. 2014. Relationship between O-antigen chain length and resistance to colicin E2 in Shigella flexneri. *Microbiol (United Kingdom)* **160**:589–601. doi:10.1099/mic.0.074955-0

Hoegy F, Lee X, Noel S, Rognan D, Mislin GLA, Reimmann C, Schalk IJ. 2009. Stereospecificity of the siderophore pyochelin outer membrane transporters in fluorescent peudomonads. *J Biol Chem* **284**:14949–14957.

doi:10.1074/jbc.M900606200

Hoegyt F, Celia H, Mislin GL, Vincent M, Gallay J, Schalk IJ. 2005. Binding of iron-free siderophore, a common feature of siderophore outer membrane transporters of *Escherichia coli* and *Pseudomonas aeruginosa*. *J Biol Chem* **280**:20222–20230. doi:10.1074/jbc.M500776200

Hohnadel D, Haas D, Meyer J-M. 1986. Mapping of mutations affecting pyoverdine production in *Pseudomonas aeruginosa*. *FEMS Microbiol Lett* **36**:195–199.

Housden NG, Hopper JTS, Lukoyanova N, Rodriguez-Larrea D, Wojdyla J a., Klein A, Kaminska R, Bayley H, Saibil HR, Robinson C V., Kleanthous C. 2013. Intrinsically Disordered Protein Threads Through the Bacterial Outer-Membrane Porin OmpF. *Science* **340**:1570–1574. doi:10.1126/science.1237864

Housden NG, Loftus SR, Moore GR, James R, Kleanthous C. 2005. Cell entry mechanism of enzymatic bacterial colicins : Porin recruitment and the thermodynamics of receptor binding. *Proc Natl Acad Sci* **102**:13849–13854. doi:10.1073/pnas.0503567102

Housden NG, Wojdyla J a, Korczynska J, Grishkovskaya I, Kirkpatrick N, Brzozowski a M, Kleanthous C. 2010. Directed epitope delivery across the *Escherichia coli* outer membrane through the porin OmpF. *Proc Natl Acad Sci U S A* **107**:21412–21417. doi:10.1073/pnas.1010780107

Howard SP, Herrmann C, Stratillo CW, Braun V. 2001. In vivo synthesis of the periplasmic domain of TonB inhibits transport through the FecA and FhuA iron siderophore transporters of *Escherichia coli*. *J Bacteriol* **183**:5885–5895. doi:10.1128/JB.183.20.5885-5895.2001

Hsueh PR, Tseng SP, Teng LJ, Ho SW. 2005. Pan-drug-resistant *Pseudomonas aeruginosa* causing nosocomial infection at a university hospital in Taiwan. *Clin*

Microbiol Infect **11**:670–673. doi:10.1111/j.1469-0691.2005.01196.x

Huang B, Ru K, Yuan Z, Whitchurch CB, Mattick JS. 2004. tonB3 Is Required for Normal Twitching Motility and Extracellular Assembly of Type IV Pili. *J Bacteriol* **186**:4387–4389. doi:10.1128/JB.186.13.4387

Isaacs D. 2006. Unnatural selection: reducing antibiotic resistance in neonatal units. *Arch Dis Child Fetal Neonatal Ed* **91**:F72–F74.

Jakes KS, Davis NG, Zinder ND. 1988. A Hybrid Toxin from Bacteriophage fl Attachment Protein and Colicin E3 Has Altered Cell Receptor Specificity. *J Bacteriol* **170**:4231–4238.

Jakes KS, Finkelstein A. 2010. The colicin Ia receptor, Cir, is also the translocator for colicin Ia. *Mol Microbiol* **75**:567–578. doi:10.1111/j.1365-2958.2009.06966.x

Johnson CL, Ridley H, Marchetti R, Silipo A, Griffin DC, Crawford L, Bonev B, Molinaro A, Lakey JH. 2014. The antibacterial toxin colicin N binds to the inner core of lipopolysaccharide and close to its translocator protein. *Mol Microbiol* **92**:440–452. doi:10.1111/mmi.12568

Joshi A, Grinter R, Josts I, Chen S, Wojdyla JA, Lowe ED, Kaminska R, Sharp C, McCaughey L, Roszak AW, Cogdell RJ, Byron O, Walker D, Kleanthous C. 2015. Structures of the Ultra-High-Affinity Protein–Protein Complexes of Pyocins S2 and AP41 and Their Cognate Immunity Proteins from *Pseudomonas aeruginosa*. *J Mol Biol* **427**:2852–2866. doi:10.1016/j.jmb.2015.07.014

Kageyama M, Kobayashi M, Sano Y, Masaki H. 1996. Construction and characterization of pyocin-colicin chimeric proteins. *J Bacteriol* **178**:103–110.

Karpiński TM, Szkaradkiewicz AK. 2013. Characteristic of bacteriocines and their application. *Polish J Microbiol* **62**:223–235.

Kirkup BC. 2006. Bacteriocins as Oral and Gastrointestinal Antibiotics: Theoretical

Considerations, Applied Research, and Practical Applications. *Curr Med Chem* **13**:3335–3350.

Klebba PE. 2016. ROSET model of TonB action in Gram-negative bacterial iron acquisition. *J Bacteriol* **198**:1013–1021. doi:10.1128/JB.00823-15

Klein A, Wojdyla JA, Joshi A, Josts I, McCaughey LC, Housden NG, Kaminska R, Byron O, Walker D, Kleanthous C. 2016. Structural and biophysical analysis of nuclease protein antibiotics. *Biochem J* **473**:2799–2812. doi:10.1042/BCJ20160544

Knirel YA, Prokhorov NS, Shashkov AS, Ovchinnikova OG, Zdorovenko EL, Liu B, Kostryukova ES, Larin AK, Golomidova AK, Letarov A V. 2015. Variations in O-Antigen Biosynthesis and O-Acetylation Associated with Altered Phage Sensitivity in *Escherichia coli* 4s. *J Bacteriol* **197**:905–912. doi:10.1128/jb.02398-14

Ködding J, Killig F, Polzer P, Diederichs K, Howard SP, Welte W. 2005. Crystal Structure of a 92-Residue C-terminal Fragment of TonB from *Escherichia coli* Reveals Significant Conformational Changes Compared to Structures of Smaller TonB Fragments. *J Biol Chem* **280**:3022–3028. doi:10.1074/jbc.m411155200

Koedding J, Howard P, Kaufmann L, Polzer P, Lustig A, Welte W. 2004. Dimerization of TonB Is Not Essential for Its Binding to the Outer Membrane Siderophore Receptor FhuA of *Escherichia coli*. *J Biol Chem* **279**:9978–9986. doi:10.1074/jbc.M311720200

Koh GCKW, Peacock SJ. 2012. Oxford Textbook of Medicine In: Warrell DA, Cox TM, Firth JD, editors. Oxford Textbook of Medicine. doi:10.1093/med/9780199204854.001.1

Krewulak KD, Vogel HJ. 2011. TonB or not TonB: is that the question? *Biochem Cell*

Biol **89**. doi:10.1139/O10-14

Krissinel E, Henrick K. 2004. Secondary-structure matching (SSM), a new tool for fast protein structure alignment in three dimensions. *Acta Crystallogr Sect D Biol Crystallogr* **60**:2256–2268. doi:10.1107/S0907444904026460

Kurisu G, Zakharov SD, Zhalnina M V., Bano S, Eroukova VY, Rokitskaya TI, Antonenko YN, Wiener MC, Cramer WA. 2003. The structure of BtuB with bound colicin E3 R-domain implies a translocon. *Nat Struct Biol* **10**:948–954. doi:10.1038/nsb997

Lakey JH, Baty D, Pattus F. 1991. Fluorescence energy transfer distance measurements using site-directed single cysteine mutants. The membrane insertion of colicin A. *J Mol Biol* **218**:639–653. doi:10.1016/0022-2836(91)90707-D

Lakey JH, Duché D, González-Mañas JM, Baty D, Pattus F. 1993. Fluorescence energy transfer distance measurements: The hydrophobic helical hairpin of colicin A in the membrane bound state. *J Mol Biol*. doi:10.1006/jmbi.1993.1218

Lam JS, Taylor VL, Islam ST, Hao Y, Kocíncová D. 2011. Genetic and functional diversity of *Pseudomonas aeruginosa* lipopolysaccharide. *Front Microbiol* **2**:1–25. doi:10.3389/fmicb.2011.00118

Lam M, McGroarty E, Kropinski A, MacDonald L, Pedersen S, Hoiby N, Lam J. 1989. Occurrence of a common lipopolysaccharide antigen in standard and clinical strains of *Pseudomonas aeruginosa*. *J Clin Microbiol* **27**:962–967.

Larsen RA, Postle K. 2001. Conserved Residues Ser16 and His20 and Their Relative Positioning Are Essential for TonB Activity, Cross-linking of TonB with ExbB, and the Ability of TonB to Respond to Proton Motive Force. *J Biol Chem* **276**:8111–8117. doi:10.1074/jbc.M007479200

Larsen RA, Thomas MG, Postle K. 1999. Protonmotive force, ExbB and ligand-bound

FepA drive conformational changes in TonB. *Mol Microbiol* **31**:1809–1824. doi:10.1046/j.1365-2958.1999.01317.x

Latino L, Patin D, Chérier D, Touzé T, Pourcel C, Barreteau H, Mengin-Lecreulx D. 2019. Impact of FiuA outer-membrane receptor polymorphism on the resistance of *Pseudomonas aeruginosa* towards peptidoglycan lipid II-targeting PaeM pyocins. *J Bacteriol*. doi:10.1128/jb.00164-19

Li G-W, Burkhardt D, Gross C, Weissman JS. 2014. Quantifying absolute protein synthesis rates reveals principles underlying allocation of cellular resources. *Cell* **157**:624–635. doi:doi:10.1016/j.cell.2014.02.033

Lin Y, Elias Y, Huang RH. 2005. Structural and Mutational Studies of the Catalytic Domain of Colicin E5 : A tRNA-Specific Ribonuclease. *Statistics* **44**:10494–10500.

Ling H, Saeidi N, Rasouliha BH, Chang MW. 2010. A predicted S-type pyocin shows a bactericidal activity against clinical *Pseudomonas aeruginosa* isolates through membrane damage. *FEBS Lett* **584**:3354–3358. doi:10.1016/j.febslet.2010.06.021

Llamas MA, Sparrius M, Kloet R, Jiménez CR, Vandenbroucke-Grauls C, Bitter W. 2006. The heterologous siderophores ferrioxamine B and ferrichrome activate signaling pathways in *Pseudomonas aeruginosa*. *J Bacteriol* **188**:1882–1891. doi:10.1128/JB.188.5.1882-1891.2006

Lloubès R, Cascales E, Walburger A, Bouveret E, Lazdunski C, Bernadac A, Journet L. 2001. The Tol-Pal proteins of the *Escherichia coli* cell envelope: An energized system required for outer membrane integrity? *Res Microbiol* **152**:523–529. doi:10.1016/S0923-2508(01)01226-8

Lukacik P, Barnard TJ, Buchanan SK. 2012. Using a bacteriocin structure to engineer a phage lysin that targets *Yersinia pestis*. *Biochem Soc Trans* **40**:1503–1506.

doi:10.1016/j.cmet.2012.08.002.

Luo W, Yao X, Hong M. 2005. Large structure rearrangement of colicin Ia channel domain after membrane binding from 2D 13C spin diffusion NMR. *J Am Chem Soc* **127**:6402–6408. doi:10.1021/ja0433121

Madeira F, Park YM, Lee J, Buso N, Gur T, Madhusoodanan N, Basutkar P, Tivey A, Potter S, Finn R, Lopez R. 2019. The EMBL-EBI search and sequence analysis tools APIs in 2019. *Nucleic Acids Res* **April**:epub. doi:10.1093/nar/gkz268

Madej T, Lanczycki CJ, Zhang D, Thiessen PA, Geer RC, Marchler-Bauer A, Bryant SH. 2014. MMDB and VAST+: Tracking structural similarities between macromolecular complexes. *Nucleic Acids Res* **42**:297–303. doi:10.1093/nar/gkt1208

Maki-Yonekura S, Matsuoka R, Yamashita Y, Shimizu H, Tanaka M, Iwabuki F, Yonekura K. 2018. Hexameric and pentameric complexes of the ExbBD energizer in the Ton system. *Elife* **e35419**:1–24. doi:DOI: https://doi.org/10.7554/eLife.35419

McCaughey LC, Grinter R, Josts I, Roszak AW, Waløen KI, Cogdell RJ, Milner J, Evans T, Kelly S, Tucker NP, Byron O, Smith B, Walker D. 2014. Lectin-Like Bacteriocins from *Pseudomonas* spp. Utilise D-Rhamnose Containing Lipopolysaccharide as a Cellular Receptor. *PLoS Pathog* **10**:1–15. doi:10.1371/journal.ppat.1003898

McCaughey LC, Josts I, Grinter R, White P, Byron O, Tucker NP, Matthews JM, Kleanthous C, Whitchurch CB, Walker D. 2016a. Discovery, characterisation and in vivo activity of pyocin SD2, a protein antibiotic from *Pseudomonas aeruginosa*. *Biochem J* **473**:2345–2358. doi:10.1042/BCJ20160470

McCaughey LC, Ritchie ND, Douce GR, Evans TJ, Walker D. 2016b. Efficacy of

species-specific protein antibiotics in a murine model of acute *Pseudomonas aeruginosa* lung infection. *Sci Rep* **6**:1–8. doi:10.1038/srep30201

Michel-Briand Y, Baysse C. 2002. The pyocins of *Pseudomonas aeruginosa*. *Biochimie* **84**:499–510. doi:10.1016/S0300-9084(02)01422-0

Michel L, Bachelard A, Reimmann C. 2007. Ferripyochelin uptake genes are involved in pyochelin-mediated signalling in *Pseudomonas aeruginosa*. *Microbiology* **153**:1508–1518. doi:10.1099/mic.0.2006/002915-0

Michel L, Gonzalez N, Jagdeep S, Nguyen-Ngoc T, Reimmann C. 2005. PchR-box recognition by the AraC-type regulator PchR of *Pseudomonas aerugionsa* requires the siderophore pyochelin as an effector. *Mol Microbiol* **58**:495–509.

Micreos. 2016. Staphefekt, the world's first product that selectively kills Staphylococcus aureus in cluding MRSA. https://www.staphefekt.com/en/

Molecular Probes Inc. 2006. Alexa Fluor® 488 Protein Labeling Kit. *ThermoFisher Sci*. https://www.thermofisher.com/document-connect/document-connect.html?url=https://assets.thermofisher.com/TFS-Assets/LSG/manuals/mp10235.pdf

Murphy K, Park AJ, Hao Y, Brewer D, Lam JS, Khursigaraa CM. 2014. Influence of O polysaccharides on biofilm development and outer membrane vesicle biogenesis in *Pseudomonas aeruginosa* PAO1. *J Bacteriol* **196**:1306–1317. doi:10.1128/JB.01463-13

Nardi A, Slatin SL, Baty D, Duché D. 2001. The C-terminal half of the colicin a pore-forming domain is active in vivo and in vitro. *J Mol Biol* **307**:1293–1303. doi:10.1006/jmbi.2001.4524

Nestorovich EM, Sugawara E, Nikaido H, Bezrukov SM. 2006. *Pseudomonas aeruginosa* porin OprF. Properties of the channel. *J Biol Chem* **281**:16230–16237.

doi:10.1074/jbc.M600650200

Nilsson IM, von Heijne G. 1990. Fine-tuning the topology of a polytopic membrane protein: Role of positively and negatively charged amino acids. *Cell* **62**:1135–1141. doi:10.1016/0092-8674(90)90390-Z

Nogueira RA, Varanda A. 1988. Gating properties of channels formed by colicin Ia in planar lipid bilayer membranes. *J Membr Biol* **105**:143–153. doi:10.1007/BF02009167

Noinaj N, Guiller M, Barnard TJ, Buchanan SK. 2010. TonB-dependent transporters: regulation, structure, and function. *Annu Rev Microbiol* **64**:42–60. doi:doi:10.1146/annurev.micro.112408.134247

Ochsner UA, Johnson Z, Asil ML. 2000. Genetics and regulation of two distinct haem-uptake systems, phu and has, in *Pseudomonas aeruginosa*. *Microbiology* **146**:185–198. doi:10.1099/00221287-146-1-185

Oeemig JS, Ollila OHS, Iwaï H. 2018. NMR structure of the C-terminal domain of TonB protein from *Pseudomonas aeruginosa*. *PeerJ* **6**:e5412. doi:10.7717/peerj.5412

Parker MW, Pattus F, Tucker AD, Tsernoglou D. 1989. Structure of the membrane-pore-forming fragment of colicin A. *Nature* **337**:93–96.

Parker MW, Postma JPM, Pattus F, Tucker AD, Tsernoglou D. 1992. Refined structure of the pore-forming domain of colicin A at 2.4 A resolution. *J Mol Biol* **224**:639–657. doi:10.1016/0022-2836(92)90550-4

Parret A, De Mot R. 2000. Novel bacteriocins with predicted tRNase and pore-forming activities in *Pseudomonas aeruginosa* PAO1. *Mol Microbiol* **35**:472–473. doi:10.1046/j.1365-2958.2000.01716.x

Paškevičius Š, Starkevič U, Misiūnas A, Vitkauskienė A, Gleba Y, Ražanskienė A.

2017. Plant-expressed pyocins for control of *Pseudomonas aeruginosa*. *PLoS One* **12**:e0185782. doi:10.1371/journal.pone.0185782

Pawlek PD, Croteau N, Ng-Thow/Hing C, Khursigara CM, Moiseeva N, Allaire M, Coulton JW. 2006. Structure of TonB in Complex with FhuA, E. coli Outer Membrane Receptor. *Science* **312**:1399–1402.

Penfold CN, Healy B, Housden NG, Boetzel R, Vankemmelbeke M, Moore GR, Kleanthous C, James R. 2004. Flexibility in the Receptor-Binding Domain of the Enzymatic Colicin E9 Is Required for Toxicity against *Escherichia coli* Cells. *J Bacteriol* **186**:4520–4527. doi:10.1128/jb.186.14.4520-4527.2004

Petoukhov M V., Franke D, Shkumatov A V., Tria G, Kikhney AG, Gajda M, Gorba C, Mertens HDT, Konarev P V., Svergun DI. 2012. New developments in the ATSAS program package for small-angle scattering data analysis. *J Appl Crystallogr* **45**:342–350. doi:10.1107/s0021889812007662

Pettersen EF, Goddard TD, Huang CC, Couch GS, Greenblatt DM, Meng EC, Ferrin TE. 2004. UCSF Chimera--a visualization system for exploratory research and analysis. *J Comput Chem* **25**:1605–12. doi:10.1002/jcc.20084

Pilsl H, Braun V. 1995. Evidence that the immunity protein inactivates colicin 5 immediately prior to the formation of the transmembrane channel. *J Bacteriol* **177**:6966–6972. doi:10.1128/jb.177.23.6966-6972.1995

Pilsl H, Šmajs D, Braun V. 1998. The tip of the hydrophobic hairpin of colicin U is dispensable for colicin U activity but is important for interaction with the immunity protein. *J Bacteriol* **180**:4111–4115.

Poole K, Mckay GA. 2003. Iron acquisition and its control in *Pseudomonas aeruginosa*: many roads lead to Rome. *Front Biosci* **8**:661–686. doi:10.1016/j.jchromb.2005.05.050

Poole K, Zhao Q, Neshat S, Heinrichs DE, Dean CR. 1996. The *Pseudomonas aeruginosa* tonB gene encodes a novel TonB protein. *Microbiology* **142**:1449–1458.

Postle K. 1990. TonB and the Gram-negative dilemma. *Mol Microbiol* **4**:2019–2025. doi:10.1111/j.1365-2958.1990.tb00561.x

Potter SC, Luciani A, Eddy SR, Park Y, Lopez R, Finn RD. 2018. HMMER web server: 2018 update. *Nucleic Acids Res* **46**:W200–W204. doi:10.1093/nar/gky448

Poulsen BE, Yang R, Clatworthy AE. 2018. Preprint Defining the core essential genome of *Pseudomonas aeruginosa*.

Prieto L, Lazaridis T. 2011. Computational studies of colicin insertion into membranes: The closed state. *Proteins Struct Funct Bioinforma* **79**:126–141. doi:10.1002/prot.22866

Pulagam LP, Steinhoff HJ. 2013. Acidic pH-induced membrane insertion of colicin A into E. Coli natural lipids probed by site-directed Spin labeling. *J Mol Biol* **425**:1782–1794. doi:10.1016/j.jmb.2013.01.037

Qiu X-Q. 2006. Methods And Compositions For The Treatment Of Infection. US 2006/0156009 A1.

Qiu X-Q, Jakes KS, Kienker PK, Finkelstein A, Slatin SL. 1996. Major transmembrane movement associated with colicin Ia channel gating. *J Gen Physiol* **107**:313–328. doi:10.1085/jgp.107.3.313

Qiu X-Q, Wang H, Lu X-F, Zhang J, Li S-F, Cheng G, Wan L, Yang L, Zuo J-Y, Zhou Y-Q, Wang H-Y, Cheng X, Zhang S-H, Ou Z-R, Zhong Z-C, Cheng J-Q, Li Y-P, Wu GY. 2003. An engineered multidomain bactericidal peptide as a model for targeted antibiotics against specific bacteria. *Nat Biotechnol* **21**:1480–1485. doi:10.1038/nbt913

Rambo RP. 2019. ScÅtter version 3.0. *Diam Light Source* **Didcot**.

Rasouliha BH, Ling H, Ho CL, Chang MW. 2013. A Predicted Immunity Protein Confers Resistance to Pyocin S5 in a Sensitive Strain of *Pseudomonas aeruginosa*. *ChemBioChem* **14**:2444–6. doi:10.1002/cbic.201300410

Raymond L, Slatin SL, Finkelstein A. 1985. Channels formed by colicin E1 in planar lipid bilayers are large and exhibit pH-dependent ion selectivity. *J Membr Biol* **84**:173–181. doi:10.1007/BF01872215

Rendueles O, Beloin C, Latour-Lambert P, Ghigo J. 2014. A new biofilm-associated colicin with increased efficiency against biofilm bacteria. *ISME J* **8**:1275–1288. doi:10.1038/ismej.2013.238

Ridley H, Johnson CL, Lakey JH. 2010. Interfacial Interactions of Pore-Forming ColicinsProteins: Membrane Binding and Pore Formation. pp. 81–90.

Rivera M, Chivers TR, Lam JS, McGroarty EJ. 1992. Common antigen lipopolysaccharide from *Pseudomonas aeruginosa* AK1401 as a receptor for bacteriophage A7. *J Bacteriol* **174**:2407–2411. doi:10.1128/jb.174.7.2407-2411.1992

Rocchetta HL, Pacan JC, Lam JS. 1998. Synthesis of the A-band polysaccharide sugar D-rhamnose requires Rmd and WbpW: Identification of multiple AlgA homologues, WbpW and ORF488, in *Pseudomonas aeruginosa*. *Mol Microbiol* **29**:1419–1434. doi:10.1046/j.1365-2958.1998.01024.x

Sano Y, Kobayashi M, Kageyama M. 1993a. Functional domains of S-type pyocins deduced from chimeric molecules. *J Bacteriol* **175**:6179–6185.

Sano Y, Matsui H, Kobayashi M, Kageyama M. 1993b. Molecular structures and functions of pyocins S1 and S2 in *Pseudomonas aeruginosa*. *J Bacteriol* **175**:2907–2916. doi:10.1128/jb.175.10.2907-2916.1993

Schalk IJ, Hennard C, Dugave C, Poole K, Abdallah MA, Pattus F. 2001. Iron-free pyoverdin binds to its outer membrane receptor FpvA in *Pseudomonas aeruginosa*: A new mechanism for membrane transport. *Mol Microbiol* **39**:351–360. doi:10.1046/j.1365-2958.2001.02207.x

Schauer K, Rodionov DA, de Reuse H. 2008. New substrates for TonB-dependent transport: do we only see the "tip of the iceberg"? *Trends Biochem Sci* **33**:330–338. doi:10.1016/j.tibs.2008.04.012

Schiessl KT, Janssen EML, Kraemer SM, McNeill K, Ackermann M. 2017. Magnitude and mechanism of siderophore-mediated competition at low iron solubility in the *Pseudomonas aeruginosa* pyochelin system. *Front Microbiol* **8**:1–11. doi:10.3389/fmicb.2017.01964

Schneck E, Oliveira RG, Rehfeldt F, Demé B, Brandenburg K, Seydel U, Tanaka M. 2009. Mechanical properties of interacting lipopolysaccharide membranes from bacteria mutants studied by specular and off-specular neutron scattering. *Phys Rev E - Stat Nonlinear, Soft Matter Phys* **80**:1–9. doi:10.1103/PhysRevE.80.041929

Schneider T, Hahn-Löbmann S, Stephan A, Schulz S, Giritch A, Naumann M, Kleinschmidt M, Tusé D, Gleba Y. 2018. Plant-made Salmonella bacteriocins salmocins for control of Salmonella pathovars. *Sci Rep* **8**:4078. doi:10.1038/s41598-018-22465-9

Schulz S, Stephan A, Hahn S, Bortesi L, Jarczowski F, Bettmann U, Paschke A-K, Tusé D, Stahl CH, Giritch A, Gleba Y. 2015. Broad and efficient control of major foodborne pathogenic strains of *Escherichia coli* by mixtures of plant-produced colicins. *Proc Natl Acad Sci U S A* **112**:5454–5460. doi:10.1073/pnas.1513311112

Sean Peacock R, Peter Howard S, Vogel HJ, Weljie AM, Price FD. 2005. The Solution Structure of the C-terminal Domain of TonB and Interaction Studies with TonB

Box Peptides. *J Mol Biol* **345**:1185–1197. doi:10.1016/j.jmb.2004.11.026

Sharma O, Datsenko KA, Ess SC, Zhalnina M V., Wanner BL, Cramer WA. 2009. Genome-wide screens: Novel mecnanisms in colicin import and cytotoxicity. *Mol Microbiol* **73**:571–585. doi:10.1111/j.1365-2958.2009.06788.x

Sharp C, Boinett C, Cain A, Housden NG, Kumar S, Turner K, Kleanthous C, Parkhill J. 2019. O-Antigen-Dependent Colicin Insensitivity of Uropathogenic *Escherichia coli*. *J Bacteriol* **201**:1–18. doi:https://doi.org/10.1128/JB .00545-18

Sharp C, Bray J, Housden NG, Maiden MDJ, Kleanthous C. 2017. Diversity and distribution of nuclease bacteriocins in bacterial genomes revealed using Hidden Markov Models. *PLOS Comput Biol* 1–24. doi:10.1099/mic.0.055459-0

Shirley M, Lamont IL. 2009. Role of TonB1 in pyoverdine-mediated signaling in *Pseudomonas aeruginosa*. *J Bacteriol* **191**:5634–5640. doi:10.1128/JB.00742-09

Shrivastava R, Jiang X, Chng SS. 2017. Outer membrane lipid homeostasis via retrograde phospholipid transport in *Escherichia coli*. *Mol Microbiol* **106**:395–408. doi:10.1111/mmi.13772

Shultis DD, Purdy MD, Banchs CN, Wiener MC. 2006. Outer Membrane Active Transport: Structure of the BtuB:TonB Complex. *Science* **312**:1396–1399.

Silhavy T, Kahne D, Walker S. 2010. The bacterial cell envelope. *Cold Spring Harb Perspect Biol* **2**:1–16. doi:10.1101/cshperspect.a000414

Sioud M. 2019. Phage Display Libraries: From Binders to Targeted Drug Delivery and Human Therapeutics. *Mol Biotechnol* **61**:286–303. doi:10.1007/s12033-019-00156-8

Skare JT, Ahmer BMM, Seachord CL, Darveau RP, Postle K. 1993. Energy transduction between membranes: TonB, a cytoplasmic membrane protein, can be chemically cross-linked in vivo to the outer membrane receptor FepA. *J Biol Chem*

268:16302–16308. doi:1471-2105-9-243 [pii]\r10.1186/1471-2105-9-243

Slatin SL, Duché D, Kienker PK, Baty D. 2004. Gating movements of colicin A and colicin Ia are different. *J Membr Biol* **202**:73–83. doi:10.1007/s00232-004-0720-9

Slatin SL, Finkelstein A, Kienker PK. 2008. Anomalous proton selectivity in a large channel: Colicin A. *Biochemistry* **47**:1778–1788. doi:10.1021/bi701900x

Smith K, Martin L, Rinaldi A, Rajendran R, Ramage G, Walker D. 2012. Activity of pyocin S2 against *Pseudomonas aeruginosa* biofilms. *Antimicrob Agents Chemother* **56**:1599–1601. doi:10.1128/AAC.05714-11

Sokol PA. 1986. Production and utilization of pyochelin by clinical isolates of *Pseudomonas cepacia*. *J Clin Microbiol* **23**:560–562.

Song HY, Cramer WA. 1991. Membrane topography of ColE1 gene products: The immunity protein. *J Bacteriol* **173**:2935–2943. doi:10.1128/jb.173.9.2935-2943.1991

Song Y, Gyarmati P. 2019. Optimized detection of bacteria in bloodstream infections. *PLoS One* **14**:e0219086. doi:https://doi.org/ 10.1371/journal.pone.0219086

Souli M, Galani I, Giamarellou H. 2008. Emergence of extensively drug-resistant and pandrug-resistant Gram-negative bacilli in Europe. *Eurosurveillance* **13**:19045.

Stevenson G, Neal B, Liu D, Hobbs M, Packer NH, Batley M, Redmond JW, Lindquist L, Reeves P. 1994. Structure of the O Antigen of *Escherichia coli* K-12 and the Sequence of Its rfb Gene Cluster. *J Bacteriol* **176**:4144–4156. doi:10.1016/0196-9781(83)90004-9

Svergun D. 1999. Restoring low resolution structure of biological macromolecules from solution …. *Biophys J* **76**:2879–2886.

Takase H, Nitanai H, Hoshino K, Otani T. 2000. Requirement of the *Pseudomonas aeruginosa* tonB gene for high-affinity iron acquisition and infection. *Infect*

Immun **68**:4498–4504. doi:10.1128/IAI.68.8.4498-4504.2000

Taylor R, Burgner JW, Clifton J, Cramer WA. 1998. Purification and characterization of monomeric *Escherichia coli* vitamin B12 receptor with high affinity for colicin E3. *J Biol Chem* **273**:31113–31118. doi:10.1074/jbc.273.47.31113

Turano H, Gomes F, Barros-Carvalho GA, Lopes R, Cerdeira L, Netto LES, Gales AC, Lincopan N. 2017. Tn *6350* , a Novel Transposon Carrying Pyocin S8 Genes Encoding a Bacteriocin with Activity against Carbapenemase-Producing *Pseudomonas aeruginosa*. *Antimicrob Agents Chemother* AAC.00100-17. doi:10.1128/AAC.00100-17

van der Goot FG, Gonzales-Manas JM, Lakey JH, Pattus F. 1991. A "molten-globule" membrane-insertion intermediate of the pore-forming domain of colicin A. *Nature* **354**:408–410. doi:10.1038/354408a0

Van Der Ley P, De Graaff P, Tommassen J. 1986. Shielding of *Escherichia coli* outer membrane proteins as receptors for bacteriophages and colicins by O-antigenic chains of lipopolysaccharide. *J Bacteriol* **168**:449–451. doi:10.1128/jb.168.1.449-451.1986

Vankemmelbeke M, Housden NG, James R, Kleanthous C, Penfold CN. 2013. Immunity protein release from a cell-bound nuclease colicin complex requires global conformational rearrangement. *Microbiologyopen* **2**:853–861. doi:10.1002/mbo3.122

Vetter IR, Parker MW, Tucker a D, Lakey JH, Pattus F, Tsernoglou D. 1998. Crystal structure of a colicin N fragment suggests a model for toxicity. *Structure* **6**:863–874. doi:10.1016/S0969-2126(98)00088-4

Waite RD, Curtis MA. 2009. *Pseudomonas aeruginosa* PAO1 pyocin production affects population dynamics within mixed-culture biofilms. *J Bacteriol* **191**:1349–

1354. doi:10.1128/JB.01458-08

Walker D, Smith K. 2015. Colicins For Treating Bacterial Infections. US20150164984A1.

Walsh CT, Wencewicz TA. 2014. Prospects for new antibiotics: A molecule-centered perspective. *J Antibiot* **67**:7–22. doi:10.1038/ja.2013.49

Wang H, Wu H, Ciofu O, Song Z, Høibya N. 2012. In Vivo pharmacokinetics/pharmacodynamics of colistin and imipenem in *Pseudomonas aeruginosa* biofilm infection. *Antimicrob Agents Chemother* **56**:2683–2690. doi:10.1128/AAC.06486-11

Waterhouse A, Bertoni M, Bienert S, Studer G, Tauriello G, Gumienny R, Heer FT, De Beer TAP, Rempfer C, Bordoli L, Lepore R, Schwede T. 2018. SWISS-MODEL: Homology modelling of protein structures and complexes. *Nucleic Acids Res* **46**:W296–W303. doi:10.1093/nar/gky427

White JC, Di Girolamo PM, Fu ML, Preston YA, Bradbeer C. 1973. Transport of Vitamin B12 in *Escherichia coli*. *J Biol Chem* **248**:3978–3986.

White P, Joshi A, Rassam P, Housden NG, Kaminska R. 2017. Exploitation of an iron transporter for bacterial protein antibiotic import. *PNAS* 0–2. doi:10.1073/pnas.1713741114

WHO. 2017. Prioritization of pathogens to guide discovery, research and development of new antibiotics for drug resistant bacterial infections, including tuberculosis. *Essent Med Heal Prod* 88. doi:WHO reference number: WHO/EMP/IAU/2017.12

WHO. 2014. Antimicrobial Resistance Global Report on Surveillance. World Health Organization.

Wiener M, Freymann D, Ghosh P, Stroud RM. 1997. Crystal structure of colicin Ia. *Nature*. doi:10.1038/385461a0

Wriggers W. 2012. Conventions and workflows for using Situs. *Acta Crystallogr Sect D Biol Crystallogr* **68**:344–351. doi:10.1107/S0907444911049791

Yang B, Hoegy F, Mislin GLA, Mesini PJ, Schalk IJ. 2011. Terbium, a fluorescent probe for investigation of siderophore pyochelin interactions with its outer membrane transporter FptA. *J Inorg Biochem* **105**:1293–1298. doi:10.1016/j.jinorgbio.2011.03.016

Yang SC, Lin CH, Sung CT, Fang JY. 2014. Antibacterial activities of bacteriocins: Application in foods and pharmaceuticals. *Front Microbiol* **5**:1–10. doi:10.3389/fmicb.2014.00241

Youard ZA, Mislin GLA, Majcherczyk PA, Schalk IJ, Reimmann C. 2007. *Pseudomonas fluorescens* CHA0 produces enantio-pyochelin, the optical antipode of the *Pseudomonas aeruginosa* siderophore pyochelin. *J Biol Chem* **282**:35546–35553. doi:10.1074/jbc.M707039200

Youard ZA, Wenner N, Reimmann C. 2011. Iron acquisition with the natural siderophore enantiomers pyochelin and enantio-pyochelin in *Pseudomonas species*. *BioMetals* **24**:513–522. doi:10.1007/s10534-010-9399-9

Zamri A, Abdallah MA. 2000. An improved stereocontrolled synthesis of pyochelin, siderophore of *Pseudomonas aeruginosa* and *Burkholderia cepacia*. *Tetrahedron* **56**:249–256. doi:10.1016/S0040-4020(99)00946-1

Zhang Y, Cramerz WA. 1993. Intramembrane Helix-Helix Interactions **268**:10176–10184.

Zhao Q, Poole K. 2000. A second tonB gene in *Pseudomonas aeruginosa* is linked to the exbB and exbD genes. *FEMS Microbiol Lett* **184**:127–132. doi:10.1016/S0378-1097(00)00036-7